MINING SUBSIDENCE : ITS EFFECTS ON THE SOUTH-EAST FIFE COASTLINE, SCOTLAND

Elisabeth Saiu

A Thesis Submitted for the Degree of PhD
at the
University of St Andrews

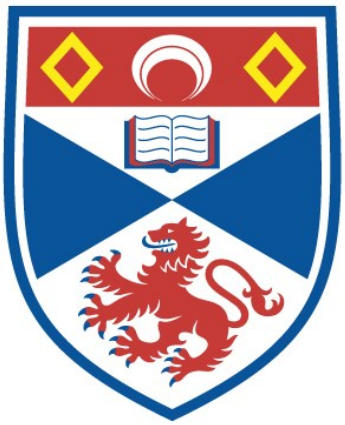

1999

MINING SUBSIDENCE: ITS EFFECTS ON THE SOUTH-EAST FIFE COASTLINE, SCOTLAND

by
Elisabeth Saiu
(B.Sc(Hons))

A Thesis Submitted for the Degree of Doctor of Philosophy
at the University of St. Andrews
May 1997

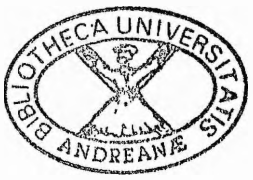

ProQuest LLC.
789 East Eisenhower Parkway
P.O. Box 1346
Ann Arbor, MI 48106 – 1346

Content of the Thesis

Declarations

I, E.M. Saiu, hereby certify that this thesis, which is approximately 50,000 words in length, has been written by me, that is the record of the work carried out by me and that it has not been submitted in a previous application for a higher degree.

Date 18.08.98 Signature of Candidate

E.Saiu

I was admitted as a candidate for the degree of Ph.D. in September 1993; the higher study for which this is a record was carried out in the University of St. Andrews between 1993 and 1997.

Date 18.08.98 Signature of Candidate

E.Saiu

In submitting this thesis to the University of St. Andrews I understand that I am giving permission for it to be made available for use in accordance with the regulations of the University Library for the time being in force, subject to any copyright vested in the work not being affected thereby. I also understand that the title and the abstract will be published, and that a copy of the work may be made and supplied to any bona fide library or research worker.

Date 18.08.98 Signature of Candidate

E.Saiu

Certification

I hereby certify that the candidate has fulfilled the conditions of the Resolution and Regulations appropriate for the degree of Ph.D. in the University of St. Andrews and that the candidate is qualified to submit this thesis in application for that degree.

Date Signature of Supervisor

Prof. John McManus

List of Publications

Saiu, E. McManus, J., & Duck R. W. (1994). Impact of industrial growth and decline on coastal equilibrium, eastern Scotland. *Coastal Zone Canada '94, Co-operation in the coastal zone: Confernece Proceedings.* 5, 2205-2219.

Saiu, E., & McManus, J. (1998). Impacts of coal mining on coastal stability in Fife. In J. Hooke (Ed). *Coastal Defence and Earth Science Conservation.* The Geological Society. The Alden Press Oxford. UK, 58-66.

Conferences Attended

Coastal Zone Canada 1994. Co-operation in the Coastal Zone. Halifax, Nova Scotia, Canada. September 20-23 1994.

Coastal Defence and Earth Science Conservation. University of Portsmouth. March 26-27 1996.

Acknowledgements

I am very grateful to my supervisor Prof. Graeme Whittington for his guidance and supervision. I am particularly thankful to him for his scientific advice and enthusiasm but also for his support during those tough times. I would like to thank Prof. John McManus for setting up the PhD and finding the necessary funding. During the late stages of the production of this thesis I am indebted to Dr. Jack Jarvis for his expert guidance and technical supervision including the technical help he provided together with Colin Cameron on surveying the coastline. Similarly I would like to thank Prof. Colin Ballantyne for his support and advice on the administrative matters relating to the thesis.

Thanks are also due to the following: Jim Malcolm at International Mining Consultants for all his technical advice on mining subsidence; Prof. Zach Agioutantis from the University of Crete for his technical support in using the SDPS software; Simon Hart, Keith Allen and Dave McRae at Fife Council for their technical advice on Smallworld GIS; Dr. John Walden for his computing advice and arranging the loan of the PC over the past year; Kathryn Miller for her friendly assistance during the trips down to the coast; and Dr. Alison Sanderman for all her moral support.

I gratefully acknowledge the financial support of Fife Regional Council. Also I am indebted to my employers, RMS, for their general support and particularly for allowing me study leave to finish the thesis.

Dedication

To my husband John, for his immeasurable patience and support.

(Speru che dottu su turmentu de sa mente siada finida

prima de candu cind'adessi tresi de nosu).

Abstract

This thesis is concerned with the impact of coal mining activities upon the coastal zone of south-east Fife. Coastal changes over a 100 year period from 1894 to 1996 have been evaluated by determining the plan variation of the High Water and Low Water datum recorded on different editions of large scale Ordnance Survey (O.S.) Plans of the area. Deposition and erosion implied by the movement of the tidal datum are related to the longshore dispersal of spoil deposition from the coastal bings[1] and to mining subsidence. Mining subsidence is evaluated using the Surface Deformation Prediction System (SDPS), previously used at sites in the United States, and now applied for the first time to a United Kingdom coalfield. A new technique is developed that enables the subsidence values to be generated along O.S. co-ordinates at 10m intervals. Subsidence values are recorded with an accuracy of ±20% along the tidal marks of 1894, 1914, 1960, 1994 and 1996. Between Buckhaven and Dysart the coastline is found to have subsided with only small pockets having been left unaffected. Indeed, in the West Sands Bay area a subsidence trough with a maximum of 5.7±1.1m is calculated. The extent of recent coastal erosion along the shore can be seen to correlate with predicted subsidence over different mining panels and thus confirms the importance of this factor upon the coastal process in south-east Fife. These results are reinforced by comparing bench-mark heights against subsidence values producing a correlation coefficient of 0.9.

The state of the pre-mining coastline is evaluated using historic documents and photographs. This provides a starting point for evaluating the changes wrought on the coastline by the large scale mining activities which commenced about 1898 and terminated with the closure of the Frances colliery in 1984. Following this, the extent of coastal change from the analysis of O.S Plans is presented. Subsequent chapters evaluate the possible factors which may have caused the observed coastal changes including long term changes, land uplift or subsidence following the last glaciation, mining activities and possible sea level changes due to global warming.

To ensure the greatest possible accuracy in the determination of coastal changes against subsidence data a rigorous GIS is employed to analyse both map and mining data allowing for registrations to be obtained between the different surveys. This involves the manipulation of both vector and raster data from the O.S. plans and the SDPS software requiring the laborious and time consuming transfer of data between different computer platforms. Despite this caveat this novel method is demonstrated, in the thesis, to be a flexible and precise method which can be applied to any given site for the accurate prediction of mining subsidence.

[1] Bing is the Scottish phrase for slag heap.

Contents

Figures

[1] RC= Figure is held in the rear cover.

Plates

Tables

Chapter 1. Introduction

1.1 Background

Although many sections of the coastline in Fife have been subject to erosion or deposition in the last 100 years, no other area has experienced such a rapid transformation of the coast as the Buckhaven to Dysart shoreline which lies within the East Fife Coalfield (Figure 1.1). Here, shoreline progradation during the latter part of the last century and the first half of this century has given way to erosion and shoreline retreat. Causes of this erosion have never been identified, although the former Fife Council commissioned several coastal investigations to propose solutions to the erosion of the coast (Ove Arup & Partners 1991, Gowans 1994).

These coastal changes have caused public concern and have generated an ongoing campaign by the local press, highlighting the current erosion which threatens the ancient Wemyss Caves at East Wemyss (Arrol 24.10.96, Carins 10.10.96, Courier 01.04.96, Donald 23.10.96, Lironi 09.09.96 and Rankin 09.09.96). Speculation on the causes of the current phase of erosion along the south-east Fife coastline has ranged from global warming to the creation of the Methil docks. These suggestions have, however, not been reinforced with studies to support the arguments, and it is apparent that a detailed investigation of the area is required to identify the causes of the current erosion.

1.2 Aims

This thesis is concerned with coastal changes between Buckhaven to Dysart in Fife, with special emphasis on some environmental impacts of mining activity on the coastal zone of the East Fife Coalfield (Figure 1.1). A principal aim is to substantiate whether mining subsidence has played a significant role in altering the coastal equilibrium. Due to the dumping of colliery waste over the cliffs, the extraction of coal has resulted in the accumulation of this material in the coastal zone resulting in shoreline progradation. Subsidence following the collapse of the working and abandoned galleries has led to shoreline recession and coastal erosion. In the areas where detailed sequential surveys are available, this interplay between accumulation and erosion can be evaluated through the analyses of map evidence. In Fife, such surveys are limited to the various editions of the Ordnance Survey maps of the coastal zone; these have restricted information on ground elevations beyond the normal contour data. However, the Ordnance Survey maps do define the extent of the intertidal zone by identifying the locations of both High Water Mark (HWM) and Low Water Mark (LWM) for Ordinary Spring Tides (OST). Accordingly, with some qualifications which will be investigated later these liminal markers can be used to explore patterns of accretion and erosion related to waste disposal and mining subsidence.

The bings of the coastal zone in Fife and the exotic rocks on the beaches clearly signal an environmental impact of coal mining activities, whereas subsidence may not leave such a visual impact on the landscape, especially in the coastal zone where its effects have been counteracted by waste deposition. However, mathematical modelling of subsidence attributable to the exploitation of coal seams beneath the ground surface is possible and can provide an independent determination of ground lowering through coal extraction. In this thesis an American Model 'The Surface Deformation Prediction System' (SDPS), not previously used in this country, has been calibrated and used to assess subsidence in the coastal fringes of the East Fife Coalfield. SDPS is capable of calculating mining subsidence for multiple irregular workings. Combined with shoreline migration information, this model allows the impact of mining on the coastal zone to be more fully analysed.

The spatio-temporal data used in this study have been collated into the Smallworld and Idrisi Geographical Information Systems (GIS). This ensures excellent registration between different surveys at different scales carried out for different purposes. This approach represents a major investment of time within the restricted period of this research investigation. It has also limited some avenues that might have been explored in order to support and amplify this investigation of mining subsidence in the coastal zone. Both GIS and the SDPS are powerful tools in their separate subject areas. By integrating the results from these different applications and, in the process, overcoming complex technical problems relating to the data formatting and manipulation, the detailed understanding of some environmental impacts in the coastal zone has been achieved. Furthermore, the GIS database established by this research forms a model study which can be carried forward by Fife Council to record and analyse future changes in the East Fife Coalfield and the methodology employed here can be developed to examine areas beyond the coastal zone.

1.3 Study Area

The coast of the East Fife Coalfield lies on the southern shore of the Firth of Forth which extends for some 100km eastwards from Stirling into the North Sea. Flanking the Firth are rocks predominantly of Carboniferous age while much of the geomorphology of the estuary owes its origin to the successive glaciations which flowed from the Highlands into the North Sea Basin during the Quaternary (Sissons 1974). In the estuary, which for the greater part is less than 20 metres deep (Admiralty Chart 734), this glacial legacy is reflected by the extensive cover of soft sediments, whereas, the margins of the Firth of Forth are characterised by rocky headlands, drift filled embayments and tidal flat environments. The East Fife shoreline between Buckhaven and Dysart is dominated by small rocky headlands with intervening pebbly beaches fronted by wave cut platforms (Ritchie 1979) (Figure 1.1). The solid geology of the cliffs and the rock platform are composed of cyclic sequences of Carboniferous sedimentary rocks consisting of red and brown micaeous sandstones, intercalated with siltstones, shales and coals.

These rocks form part of the Upper Coal Measure Sequence, and the coal seams formed the basis of the economic wealth of the area. The coastal zone functioned both as a convenient repository for dumping waste material from the coal mines and as a recreational area for miners and visitors.

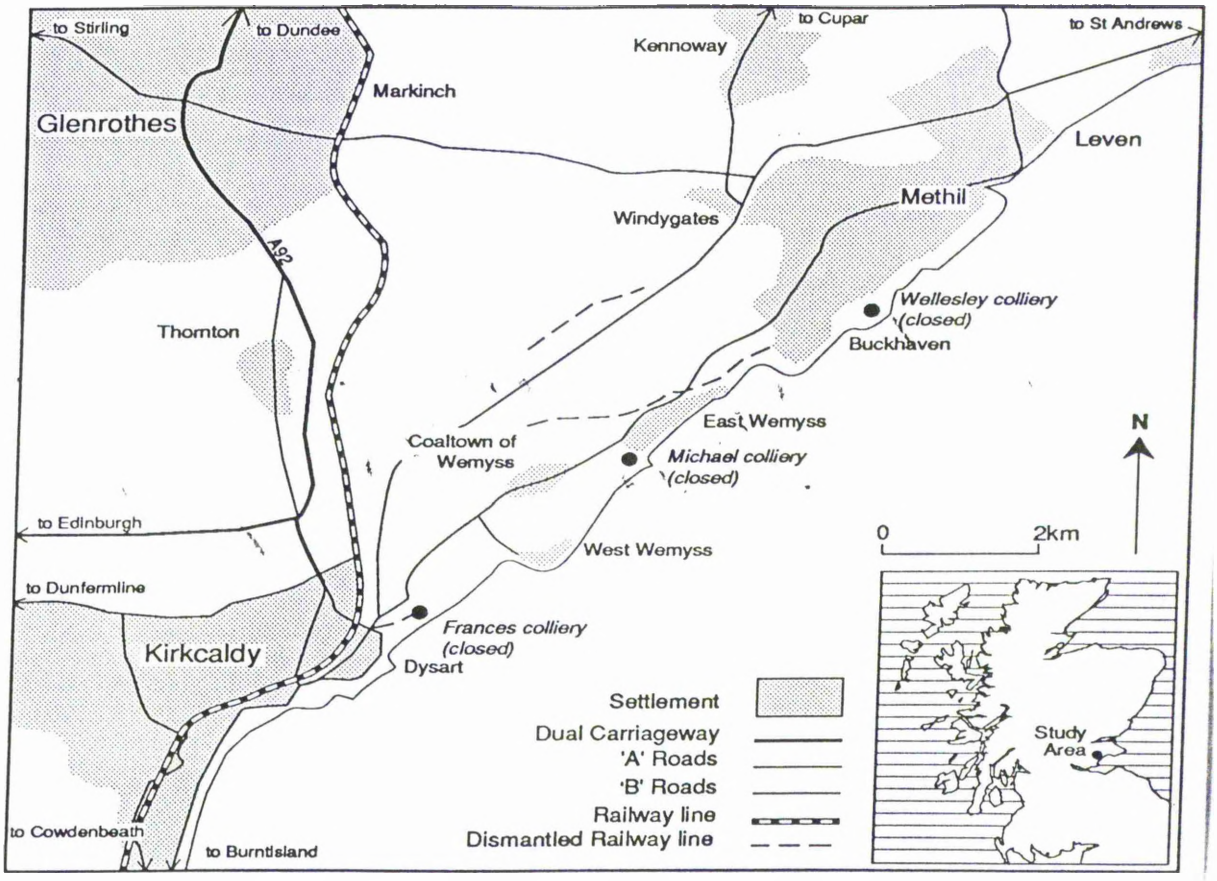

Figure 1.1: Location of the south-east Fife coastline (After Saiu 1992).

In the study area, the beaches have few natural backshore expressions in the form of dunes or links and tend to be narrow, while the forward margins are characterised by rock platforms extending to the LWMOST. Natural headlands at Buckhaven and Dysart define the east and west limits of the study area while the intervening rocky headlands at West Wemyss and Blair Point sub-divide the area into 3 shallow embayments. The embayment between Buckhaven and West Wemyss is further divided by a promontory developed through the dumping of material from the Michael Colliery. The shoreline has been much modified by anthropogenic factors during the last few hundred years. This has resulted in changes to the planform of the beaches as well as to the beach profile; consequently, it is now difficult to define the exact nature of the pre-industrial shoreline which ideally would form the starting point for this study. Coastal forms to the East e.g. at St Monans, suggest that the shallow embayments, characteristic of the Fife Coast (Ritchie 1979), are often backed by a degraded cliffline which was at least modified at the maximum of the postglacial transgression and the embayments partially infilled during

the transgression to an elevation of some 5-8m O.D. Coastal processes since that time have cut back the unconsolidated infill and in places reactivated the former cliffline.

At Buckhaven the present coastline lies some 100m in front of a former cliffline; the backshore area is protected by a rip-rap wall, constructed of blocks up to 1m across, which rests upon a wave cut platform. These coastal defences extend westwards to Buckhaven Harbour. It is now infilled and abandoned. Further east and as far as Wemyss Caves the coast is exposed to waves from a southerly and south-westerly direction. Here the upper beach is eroding into material from a former bing which partially obscures a former cliff line. A rock platform defines the seaward limit of much of the intertidal zone along this stretch of the coast although a break in the platform occurs at the head of the embayment. The Wemyss Caves were probably formed during the postglacial transgression and are part of the stranded cliff consisting of pinkish-red, fine to coarse grained sandstone with occasional fine gravel layers. Today these are partially protected from erosion by coarse dumped material although in the recent past this protection was afforded by postglacial deposits. A low terraced coast, facing south-east and largely formed in reclaimed material, extends from East Wemyss to West Wemyss. Just west of East Wemyss a promontory marks the location of the former Michael Colliery and projects to the HWM where the colliery waste is being reworked by wave activity. The beach materials are mainly derived from industrial waste but local erosion of outcrops of the Upper Coal Measures Sequence and of glacial drift contribute to a wide variety of rock types on the beach. This material frequently covers the intertidal rock platforms with a veneer of sand. These rock platforms, either exposed or thinly covered with sediment, do not prevent relatively high energy waves from reaching the shore. As a result, given the presence of an abundant source of erodable material in the bings, considerable movement of sediment can occur along the beach and possibly also offshore across the platform. West Wemyss is located on a rocky promontory, although much of the village is also protected by coastal defences. Beyond West Wemyss the orientation of the coastline changes and the embayment which extends to Blair Point is open to waves from the south. The HWM is defined initially by a vertical wall supporting a road and further west by a coarse cobble beach separating a narrow terrace from the cliffline behind. Coarse cobbles are found close to the LWM by Wemyss Harbour but these give way to a wave cut platform as Blair Point is approached. The former shoreline is again buried west of Blair Point by the waste material from the Frances colliery. At the seaward margins of the beach a rock platform emerges from beneath the dumped material while the landward limit of the beach is defined by a steep cliff cut into the old bing. A cliffed and rocky shoreline at Dysart marks the limit of the study area.

A number of recent studies have contributed to our understanding of the natural and anthropogenic factors affecting the study area (Inglis 1951, Saiu 1992, and Gowans 1994). The undergraduate dissertation by Inglis (1951) focused on how the mining activities were influencing the coastline. Likewise, Saiu (1992) explored the coastal changes which had taken

place during the past 100 years by comparing 1:10 000 Ordnance Survey maps. The scale of the plans used, restricted the accuracy of measurements which could be taken, and the technique used to compare the results by merely overlying the HWM of different years using tracing paper, was prone to generating large errors. However, the study concluded that trends in the coastal changes were linked to the mining activities. Both Inglis (1951) and Saiu (1992) describe how three coal mines, the Wellesley, Michael and Frances Collieries, located close to the shoreline, dumped the excess waste from the mining activities over the cliff edge and onto the beach. The redd[1] slowly built-up on the shoreline and the waves rapidly reworked the material along the coastline in both directions. The former beaches of the 1890s were covered by a blanket of colliery waste (Saiu 1992). This new landscape was maintained throughout the mining era, but when the mines were abruptly closed in the 1960s, the shoreline was thrown into a phase of disequilibrium and the beaches experienced phases of erosion. Saiu (1992) concludes that the main cause of this changing landscape was due to a combination of the cessation in the supply of sediment and the human interference which was occurring along segments of the coastline, especially at Buckhaven. Mining subsidence was proposed as a possible cause of the current phase of erosion, but this idea was not explored in any detail.

Work by Gowans (1994) focused on the current coastal processes and addressed the coastal changes by comparing old editions of the OS plans. Two segments of the coastline at East Wemyss and Dysart provided valuable information on coastal change and sediment movement (these will be discussed in more detail in chapter 2). Gowans (1994) concluded that without special protection measures being undertaken it is anticipated that a great deal of land reclaimed and developed over the last 100 years will be at risk. This literature provides a foundation for building a more detailed picture of what has happened along this coastal stretch, and for exploring the causes of the events. Coal mining has played a dominant role in the area, in particular the dumping of the waste onto the shoreline. None of the previous investigations take this subject further nor do they attempt to quantify the actual effects of the mining subsidence - another consequence of coal mining.

1.4 Structure of thesis

The structure of the thesis is designed to ensure that the reader is provided initially with a detailed understanding of the historical changes which have occurred along the coast before investigating in chronological order the possible causes for the coastal changes. The discussions then allow for a detailed critical appraisal of the findings from the previous chapters.

The prime objectives of each chapter are outlined so that the reader understands how each segment of the thesis fits together. In Chapter 2 a brief review of the mining industry will

[1] Redd is Scots for colliery waste generated from coal mining.

outline the main events which influenced the Fife area. The photographic evidence collected for this coastal stretch provides a graphic illustration of the major changes that have occurred over the past 100 years. It will become apparent later, that these visual changes provide only a simplistic view of the changing coastal equilibrium, and other mechanisms were occurring at the same time that need to be considered, in order to understand the causes of the coastal disequilibrium.

In Chapter 3, the coastal changes which occurred between Buckhaven and Dysart, Site 1, and south of Kirkcaldy to Kinghorn, Site 2, during the past 100 years are quantified. The coastal changes recorded at Site 2 are used as a control zone to explore not only the quality and accuracy of the OS data available but also to identify whether these historical coastal movements are unique to the Buckhaven to Dysart coastal zone. Geomorphological descriptions of the shoreline and a discussion of coastal processes are provided to reinforce the core analytical work performed: the determination of the movements of the HWM and LWM. The historical data available documenting the coastal changes recorded during the past 100 years will be thoroughly analysed using a Geographic Information System. Having identified the coastal changes, the thesis then focuses on the potential causes. Chapter 4 reviews the effects of isostatic uplift on the south-east Fife coastline, and discusses the role of isostasy in the coastal equilibrium. This chapter explores the question of whether isostasy has played a significant role in the changing equilibrium of the south-east Fife coastline during the past 100 years.

The effects of the mining activities are quantified in Chapter 5, in order to establish whether the extraction of coal along the coast has influenced the coastal equilibrium. Human interaction along the coastal zone has manifested itself through the extraction of coal in the East Fife Coalfields. All coal workings located within the coastal zone are identified and mining subsidence calculated for each panel[2] in order to assess the effects of the workings on the land surface. Mining subsidence is a well recognised phenomenon; while its effects on buildings have been studied, it has been neglected in relation to the coastal zone. The comparison of measurements resulting from mining subsidence and coastal changes has never been undertaken, and a new method for combining these data sets has been established in the present work. Hindman & Treworgy (1989) used GIS to ensure coincidence of mine panels with urban settlements in order to estimate the number and total value of housing units exposed to subsidence risk. This basic technique of using GIS to locate the relative positions of the two features has been developed further to allow for the precise positioning of subsidence troughs, generated from the East Fife mine workings, directly over the relative positions of the HWM and LWM from the OS plans. It is important to highlight from the outset the significant amount of time which was invested in the data manipulation required to generate these final results. Taking the possible causes for the coastal changes in chronological order means that in Chapter

6 the more recently recognised phenomenon of global warming is investigated, questioning whether one effect of global warming - namely sea level change has or will have a significant effect on the coastal equilibrium of south-east Fife. In particular limitations surrounding the current predictions are identified. The final discussions, in Chapter 7, explore the relationships between the changing positions of the tide marks and the coal mining activities; the results of the main analytical chapters are compared in an attempt to identify the most likely cause for the coastal disequilibrium. Finally, in Chapter 8, conclusions are presented, where the significance of this study, in the wider context, is evaluated.

1.5 Methodology

This thesis examines a new area of investigation which falls on the boundaries of several research fields. An in-depth knowledge of a broad spectrum of subjects, viz. mining subsidence, isostatic uplift, global warming and coastal dynamics, is required. The approaches used to investigate the individual topics vary. However, there is a common aim in the exploration of each subject which is to quantify the effects of the relevant parameters (within each subject) on the coastal equilibrium of south-east Fife. The final analyses of results for each topic, in relation to the south-east Fife coastline, will enable a greater understanding of the causes of the coastal erosion in the south-east Fife region. Schumm & Lichty (1965) highlight how the factors that determine the characters of landforms can be either dependent or independent variables as the limits of time and space change. Therefore, within this investigation which is examining the coastal environment of south-east Fife, given a short time span (i.e. days or weeks), the coastal equilibrium will be dependent on the coastal dynamics. For longer time scales (years or decades) the coastal environment will be dependent on the climatic and human environment, and the coastal dynamics will become an independent variable, classified as being in a state of dynamic equilibrium. In order to investigate the changing characteristics of the south-east Fife coastline since 1894, the climatic and human influences are investigated in detail, and the coastal dynamics are classified as independent variables. The multiple working hypothesis (Chamberlain 1897), an alternative approach to a scientific investigation, is chiefly a way of determining facts allowing for the guidance of lines of inquiry within a complete framework (Schumm 1991). It allows for a range of explanations to be investigated and the consequent development of the respective hypotheses. This approach not only eliminates the chances of missing crucial evidence but also provokes increased analytical thought and allows for an unbiased and fair analysis of all the data collected (Haines-Young & Petch 1983). It is this approach which will be adopted in this thesis, in an attempt not to overlook any possible element of information which may hold the key to understanding the coastal system. The methodologies used to investigate individual areas of this thesis will be discussed in the separate chapters.

---

[2] A panel is defined as a section of a coal seam which has been extracted.

Chapter 2. Historical overview of the south-east Fife coastline

2.1 Introduction

The Fife coastline has undergone significant coastal changes over the past 100 years and this chapter provides a description of those features. The evidence is presented in pictorial format to provide a visual understanding of the coastal changes which occurred, before a detailed technical investigation into the changing equilibrium of the south-east Fife coast is made.

In section 2.2 a short description of the Buckhaven to Dysart coastline is provided. Section 2.3 outlines the history of the coal mining industry in south-east Fife, together with the most significant coastal changes which occurred along the coastline during the mining era. Section 2.4 provides photographic evidence describing the coastal changes between Buckhaven and Dysart. The reader is informed of the most important historical mining events. However, for a detailed review of the mining industry and the economic growth in the area see Cunningham (1905, 1912, 1913 and 1922), Goodwin (1959), Duckham (1970) and Halliday (1990).

2.2 Description of the Buckhaven to Dysart coastline in 1894

A detailed description of the coastline as it was perceived to be over 100 years ago is presented below, to highlight the main features along this coastal stretch in 1894. It is important to appreciate the extent to which the shoreline has changed over a relatively short time scale; this is best achieved by using photographic evidence.

In 1894 the coastal area between Buckhaven and Dysart was characterised by flat wide beaches, which consisted of pockets of sand overlying a rock platform. Small villages fronted directly onto the beach at Buckhaven (Plate 2.1), East Wemyss, West Wemyss and Dysart. The coast between West Wemyss and Dysart consisted of large headlands with small intervening sandy bays. A coastal path ran along the back of the beach from Buckhaven as far as Dysart harbour.

The West Sands of Buckhaven was a local attraction for the townsfolk. There was a tidally linked swimming pool with three buildings located close to the HWM (Plate 2.2). The coastal path ran from Buckhaven to East Wemyss passing the gasworks, situated to the east of the Well Cave (Figure 2.1). A small wall at the back of the beach extended from Court Cave to the gasworks and a footpath ran parallel to the wall, passing along the outside perimeter of the works (Plate 2.3). A 16th century dovecot was situated behind the sea wall, located below the ruins of Macduff's Castle (Plate 2.4) (Figure 2.1). Four houses were located at the site providing accommodation for the employees of the gasworks. A Rifle Range was sited to the east of the gasworks with the targets positioned just beyond the Well Cave. There were also two golf courses - the Buckhaven Links and East Wemyss Links.

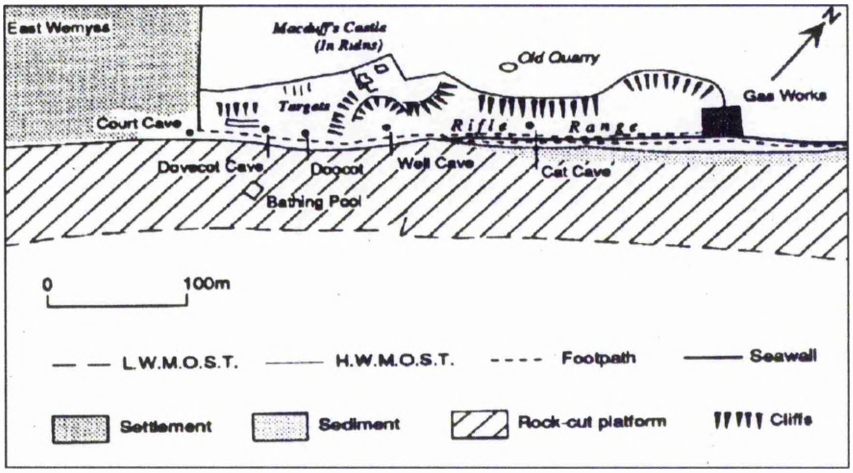

Figure 2.1 The Wemyss Caves, 1894. (After OS Plan, 1:2500).

Plate 2.1 Looking west along Shore Street, Buckhaven, towards Buckhaven harbour, 1894. The houses were situated directly at the back of the beach behind the seawall. The beach consisted of small fines and pebbles over a rocky platform which extended to LWM.

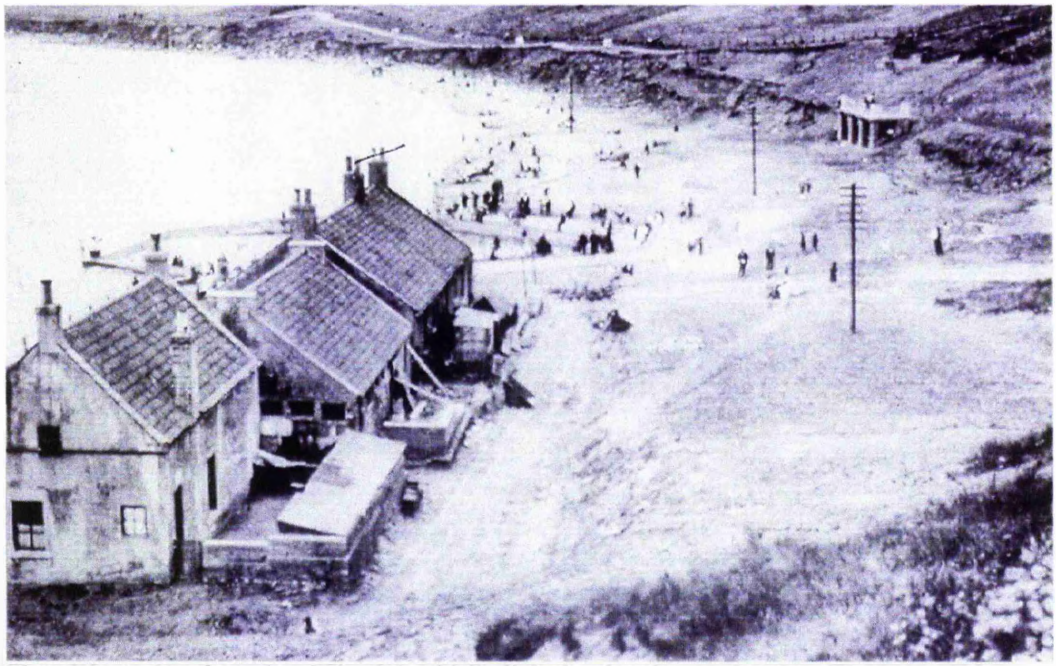

Plate 2.2 A view from the cliffs of the tidally linked swimming pool at East Wemyss together with the three houses sited close to the HWM.

The Wemyss Caves (which are noted for their prehistoric drawings), are located between East Wemyss gasworks and West Wemyss. Originally there were 12 caves and the beach extended close to the opening of most of the caves. For centuries the caves were places of shelter and working places for many local people. In 1610, for example, a glass works was established within the cave to the south of East Wemyss, later known as Glass Cave (Cunningham 1905).

The narrow beach extended as far as West Wemyss, a small fishing village which also traded with northern Europe. The beach consists of small rock headlands as far as Dysart harbour. Beyond Blair Point, a large sandy bay existed, together with houses backing onto the shoreline, where the gasworks of Panhall was located (Plate 2.5). Small pitheads were located near to the shoreline and these will be referred to later in the text.

2.3 Brief history of the coal industry

Records suggest that coal was being mined in the West Wemyss and Dysart area as far back at the 13th century (Wemyss Coal Company 1908). There were three pits at West Wemyss: Victoria Pit, Blind Pit and Lady Pit. The Dysart area contained many small shafts including the Lady Blanche Pit and Given Pit, located on the foreshore close to Dysart harbour. All of these smaller pits were active from a very early date, using primitive extraction methods. It was from these shallow mines that coal was mined by day level methods, involving naturally draining the coal before it was extracted. By 1649-1679 the Second Earl of Wemyss had sunk long levels inland from the sea and the workings were kept dry by means of horse-gins and water mills. Steam pumps were finally introduced to lift the water from the pit bottom, at Dysart in 1791 and at Wemyss in 1838 (Cunningham 1905, Goodwin 1959). The NCB 1:2500 mine plans

indicate that coal was being actively mined in the mid 1800s at these sites. Once the Michael and Frances Collieries were well established, the coal was extracted through the larger mine shafts, leaving the smaller pit heads at West Wemyss and Dysart abandoned.

Plate 2.3 A view from the gasworks towards East Wemyss, and West Wemyss beyond (circa 1890). Court Cave and the coastal path are situated just at the back of the beach. The beach is made up of pebbles and rocky platform, and there is a small wall separating the path and the beach. Note how the edge of the cave signifies the back of the beach.

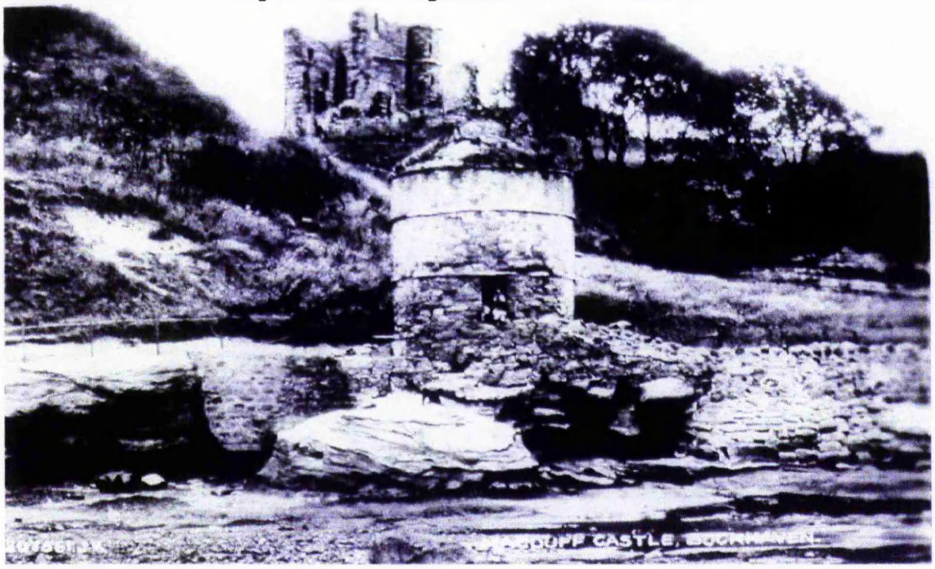

Plate 2.4 The 16th century dovecot at East Wemyss, located behind the seawall, sited just below Macduff Castle (circa 1900s).

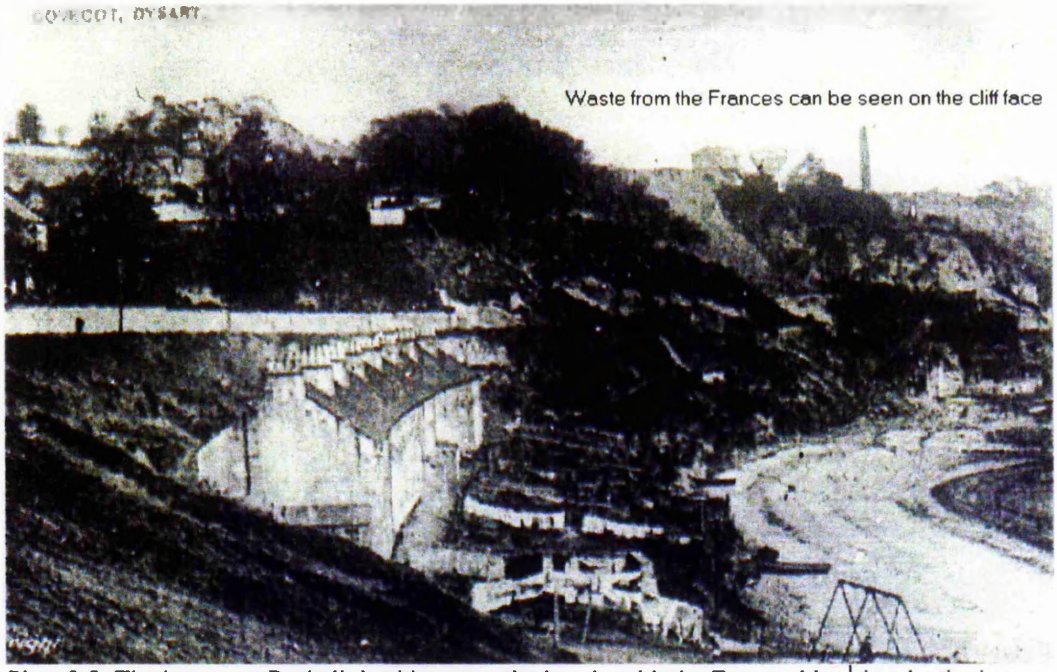

Plate 2.5 The houses at Panhall, backing onto the beach, with the Frances bing[1] just beginning to develop over the cliffs (circa 1890s).

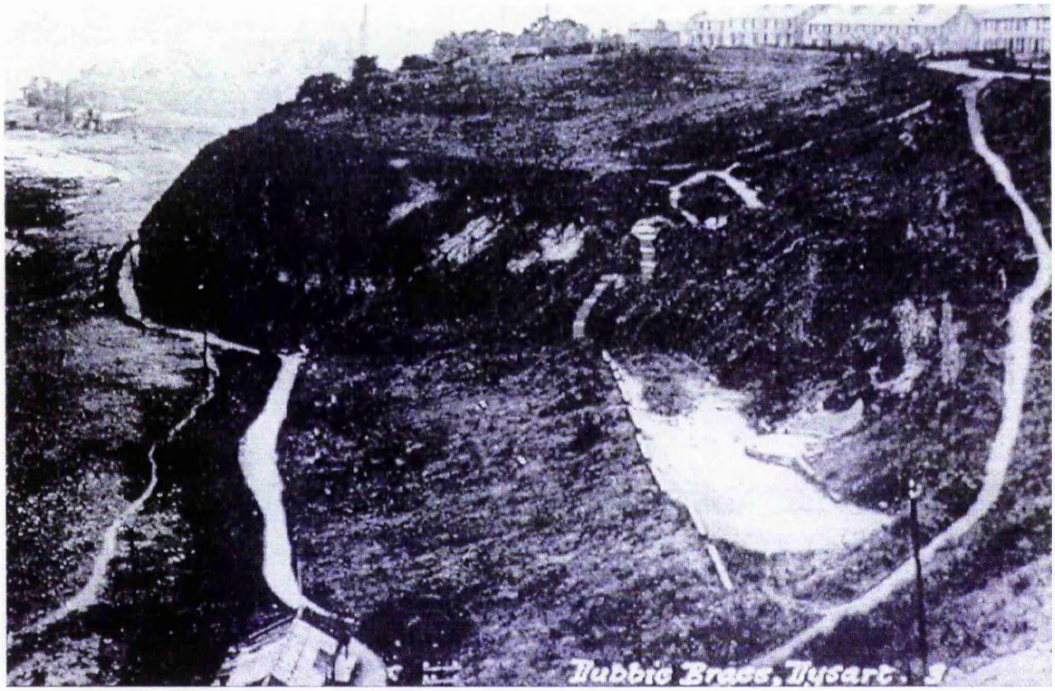

Plate 2.6 The Frances Colliery locally known at the Dubbie (circa 1890s). A view from the Dubbie looking down over the embayment. Note the houses were located close to the shoreline and the steep cliff over which all the colliery waste was dumped.

[1] Bing is the Scottish phrase for slag heap.

The Frances Colliery opened in 1850 and from it the Productive Coal Measures could be exploited. The mine shaft was located high on the cliffs allowing colliery waste to be conveniently dumped over them onto the shoreline (Plates 2.6, 2.7). At East Wemyss, the Michael Colliery opened in 1898. The Michael shafts were positioned on the higher ground (11m above sea level) about 50m away from the sea. The former Denbeath Colliery at Methil, which opened in 1691 (Brister 1972), was taken over by the Wemyss family in the late 1890s. By 1905 the bing from the Denbeath Colliery had grown to such an extent that the Links of Buckhaven were acquired by the Laird of Wemyss for the dumping of redd and used as sidings for the Wellesley Colliery (Cunningham 1922). The colliery was refurbished and reopened as the Wellesley in 1908 (Plates 2.8). The mine shafts were sunk close to the shoreline. At the three coastal collieries, waste was deposited on the shoreline, directly fronting the pit heads; this rapidly polluted the sea and killed off inshore fish along the Fife coastline. After 1910 the houses on the Buckhaven Links which were located close to the shoreline were buried by the bing. Many of the fishermen turned to the mines for a more stable source of income, as the fishing industry fell into decline. In 1898, at Buckhaven, there were just 40 fishing boats, in 1908 20 boats and in 1914 only 5 boats remained (Third Statistical Account). The village of Buckhaven also switched its focus from being a small fishing village to becoming an industrial mining town. In 1932 the old fishing harbour was rendered unusable. The 1946 aerial photograph clearly shows the colliery waste which has completely filled the harbour at Buckhaven and submerging the entire coastline in a blanket of redd (Plate 2.9).

The area occupied by the Michael Colliery expanded from 8 hectares in 1914, to 10.5 hectares in 1938 and by 1965 it had expanded to 22 hectares, thus leading to an increase in the size of the bings which developed as a result of the mining activities (Wemyss Estate Records). A second smaller waste heap was developed to the south of the Michael buildings in an attempt to reclaim land for railway sidings and workshops. This feature is visible on the 1946 aerial photographs (Plate 2.10).

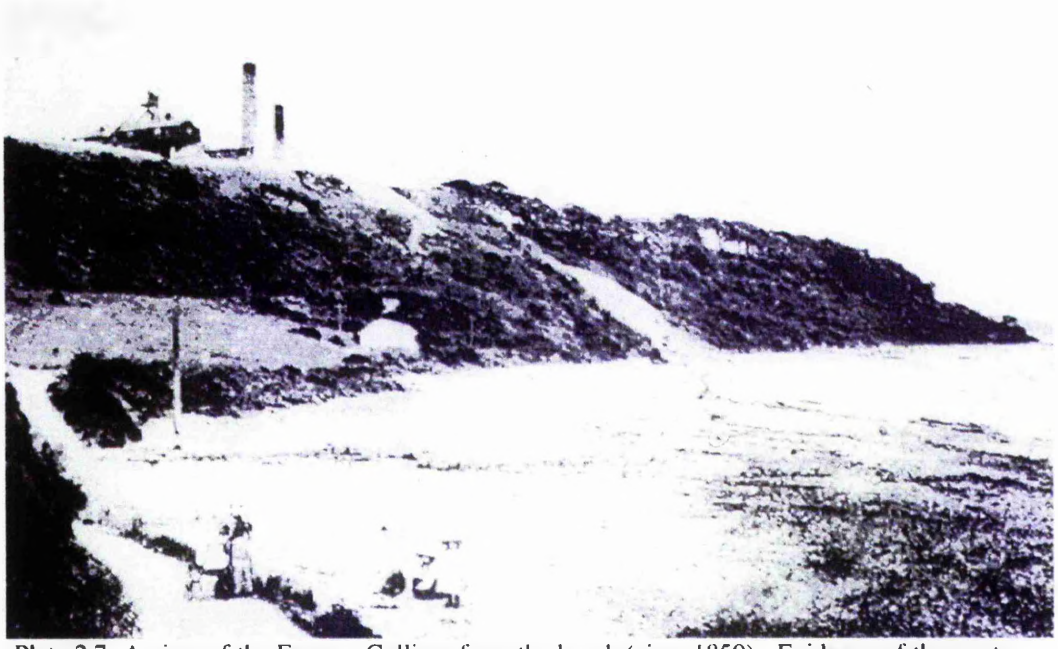

Plate 2.7 A view of the Frances Colliery from the beach (circa 1850). Evidence of the waste can be seen on the cliff face with the pit shaft located on the top of the cliff. This large sandy embayment was eventually completely filled by colliery waste.

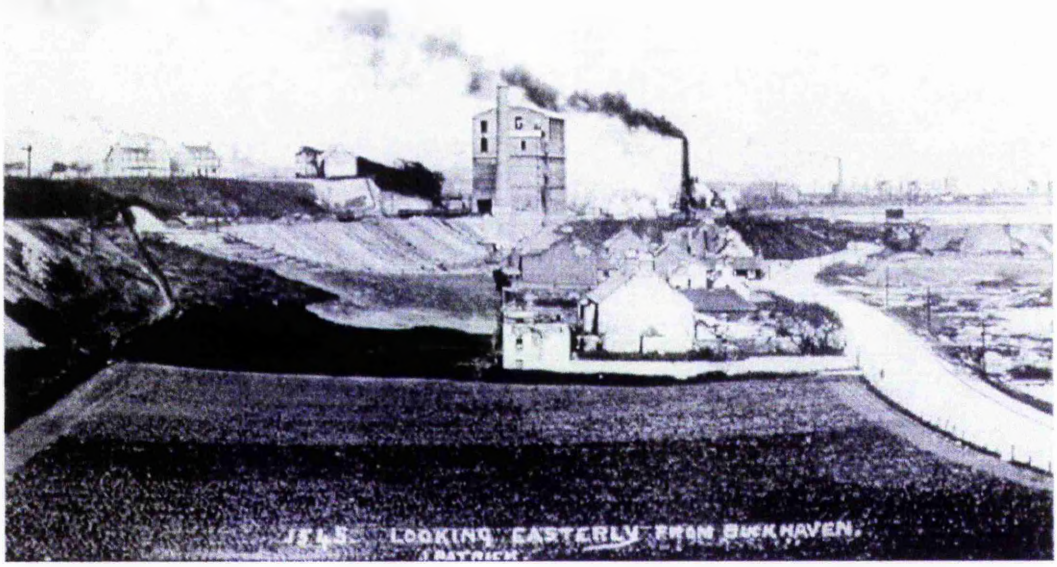

Plate 2.8 A view looking east from Buckhaven, the Denbeath is visible in the background and the small bing is already evident. The two houses sited in the foreground were eventually submerged by the colliery waste.

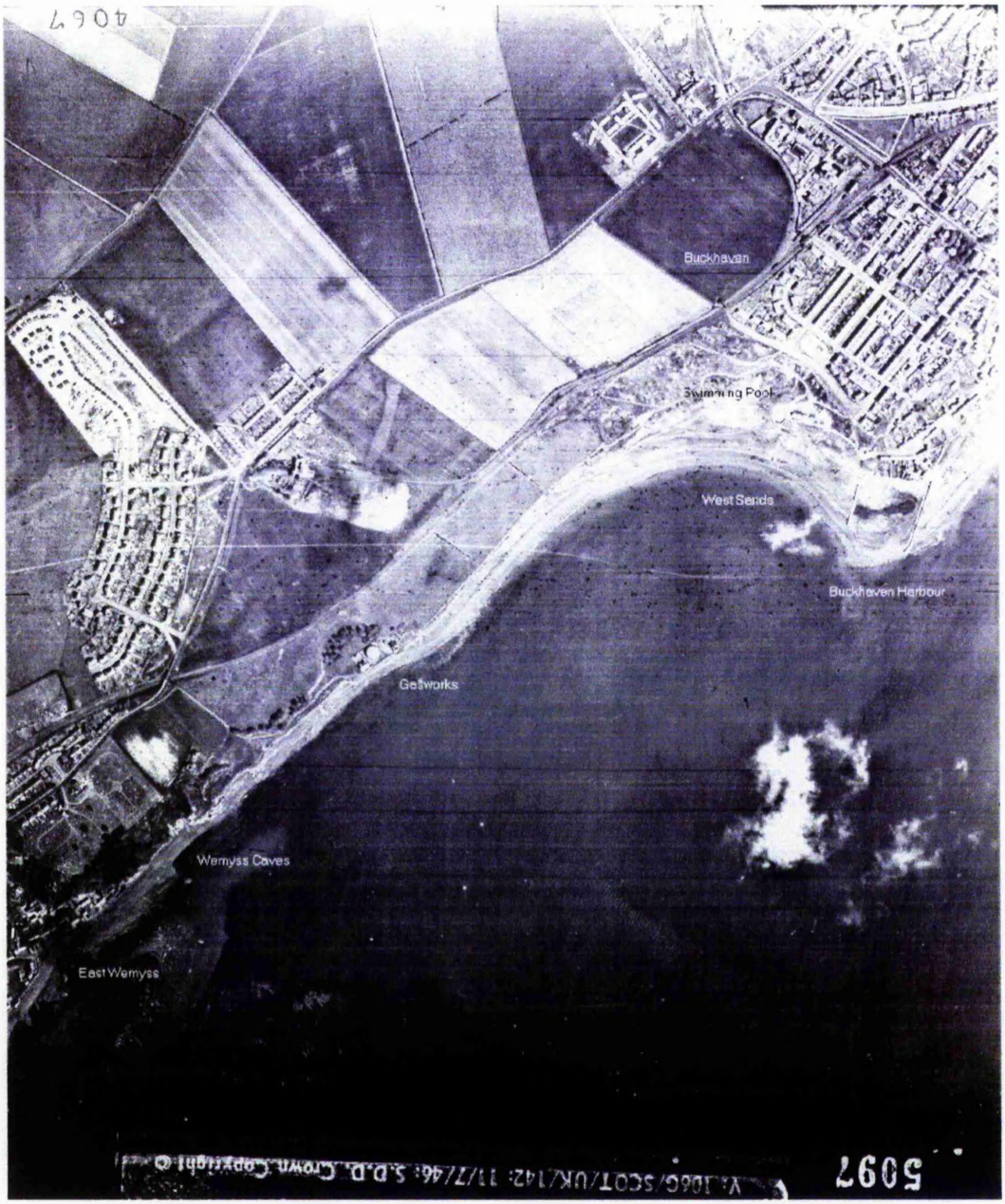

Plate 2.9 Buckhaven to the Wemyss Caves: 1946 aerial photograph. The former houses at Shore Street, Buckhaven are now much further away from the beach. The harbour at Buckhaven is completely silted up and the disused swimming pool sits high and dry above the water mark. The coastal walk is visible running at the back of the fields towards the gasworks. The gasworks was no longer located close to the shoreline. The build up of colliery waste along the entire coastal stretch is clearly evident in the image.

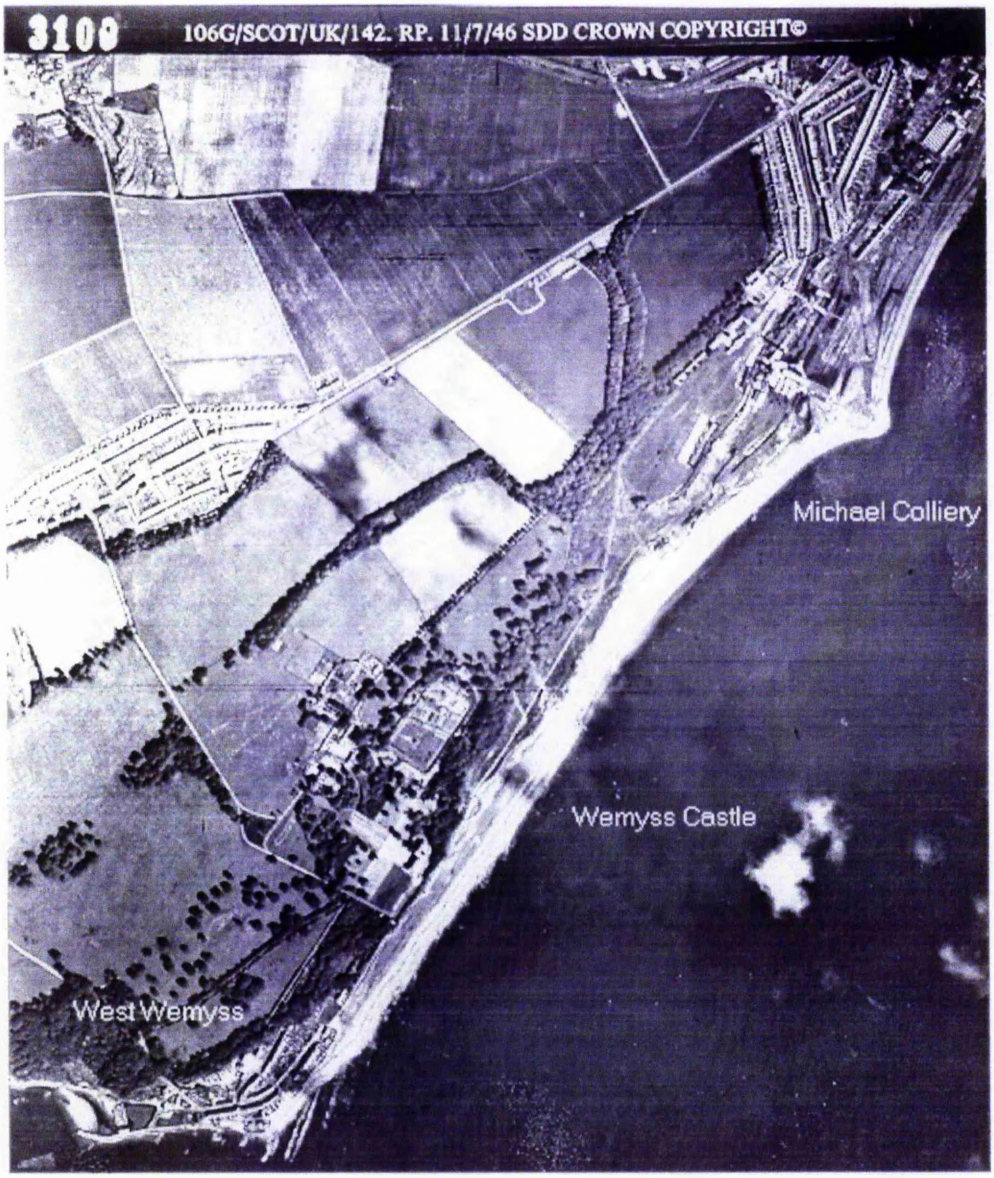

Plate 2.10 The Michael Colliery to West Wemyss: 1946 aerial photograph. The two bings of the Michael Colliery are evident building forward on the foreshore. The large build-up of colliery waste along the coastal strip has caused the West Wemyss harbour to silt up.

Plate 2.11 The Frances Colliery to Dysart Harbour: 1946 aerial photograph. The extremely large bing of the Frances Colliery dominates the coastal zone in this photograph. The sediment has been transported down coast as far as Dysart Harbour.

At East Wemyss, the original beach, characterised by small pockets of sand and large boulders, became submerged beneath a blanket of colliery waste (Plate 2.10). The two photographs taken at East Wemyss (Plates 2.12, 2.13), one in 1926 and the other in 1951 illustrate how the beach was transformed in less than 20 years. Such photographic evidence suggests that there was a build up of over 2.5m of colliery waste. By 1951, at East Wemyss, the reclaimed foreshore, consisting of deposited redd, extended half way towards West Wemyss (Inglis 1951) and at Dysart the former sandy embayment had been completely infilled by waste from the Frances Colliery (Plate 2.11). During the 1950s when the mining industry was reaching its peak in productivity, the bing had grown to such an extent that it had completely filled the bay. The beaches had built forward along the entire coastal stretch between Buckhaven and Dysart.

The entire community celebrated the new wealth in the area; the previously rural area was transformed into a primary producing region for coal. The resulting features, bings and blackened coastlines characteristic of the mining activities, were an accepted part of the Fife scenery.

The coal industry was nationalised on the 1st January 1947. At this point the three coastal collieries were the largest in Scotland, with the Michael Colliery topping the coal production output (Halliday 1990). The mine shafts (from all three collieries) were approximately 600m deep with the whole vertical range of Productive Coal Measures accessible to them. By the early 1960s most of the coal seams inland and close to the shoreline were exhausted, forcing coal mining out under the Forth over a kilometre in distance.

The Wellesley Colliery closed in 1967 due to a bad fire. Shortly afterwards at the Michael an explosion caused a fire which killed nine men. The mine shaft was damaged so badly that it was beyond repair, and the colliery closed in January 1968 (NCB records). The Frances Colliery also closed due to a fire in 1984, but it was maintained in working order for over 10 years, only to be closed permanently in 1993. Despite the complete closure of these mines substantial reserves remain un-exploited beneath the Forth.

When the Wellseley closed, the supply of new sediment onto the bing ceased; however, due to the fact that the bing extended into the Forth estuary, the removal of material continued. At this time, in the early 1970s, a new housing estate at Shore Street, Buckhaven was built on part of the reclaimed land created from the mining waste. The foreshore area directly in front of the houses was dressed off and sown down with top soil and grass. The scheme later won a Saltire Society Housing Award for the Regional Council. This development can be seen on the 1974 aerial photographs (Plates 2.15).

Plate 2.12 East Wemyss in 1924. The beach is made up of boulders and pebbles. To the far left of the photograph, steps lead down to the beach, and the people on the beach are dwarfed by the tall seawall behind - which appears to be over twice their height.

Plate 2.13 East Wemyss in 1951. The beach, by this date, has been submerged beneath a blanket of colliery waste. Note how the large seawall to the left, is now merely a 'step' away from the beach. The steps leading to the door in the wall have also been completely covered in sediment. The colliery waste appears to have grown to over 3m in depth indicated by the complete submergence of the seawall to the left of the image where previously (in Plate 2.12) people were standing.

2.4 Methil to Buckhaven

After the closure of the Wellesley Colliery, the site was obtained by Redpath Dorman Long (R.D.L.) for the development of an offshore construction yard at Methil. A graving dock was constructed for the launching of oil rigs. To enable the use of the reclaimed land and to prevent the dock from being filled by sediment, the seaward margin of the bing was protected by a coarse boulder rip-rap apron. Almost immediately after the protection work had been completed erosion began downstream of the bund wall, situated just south of the R.D.L. site. The main outfall sewer had to be concreted and the bund wall extended eastwards beyond it. However, this pattern of fresh erosion was merely deflected to the end point of the protection. The new housing estate began to be threatened by the coastal erosion. Fife Council were called into monitor the situation and within a 6 month period from spring 1976 erosion lowered the beach level by 5m vertically and the sea had encroached onto the land by approximately 30m (Fife Council Report, 1977) (Plate 2.17).

Macaferri stone filled baskets were put out to extend from the bund wall to the Buckhaven harbour. Erosion inland was halted, but erosion downwards towards the bedrock underlying the old beach continued at an alarming rate. In addition, stone armouring from the bund wall and rocks were tossed up on to the baskets causing abrasion of the baskets with many of them bursting open. Drawdown was occurring with the baskets and mattresses being undermined, destabilising the entire coastal defence scheme. Running repairs had to be carried out constantly during the contract and it soon became evident that stronger protection of the coastal strip was required. The erosion of the beach was caused by a combination of wave action at high tide and littoral drift in a westerly direction, where the replenishment material from the bing was now protected by rip-rap. It had been estimated that if further work was not carried out along the coast, erosion would continue and reach the road by 1978.

The Scottish Development Department was finally approached and consultant engineers advised protection of the rip-rap at R.D.L. dock yard to be extended along to the Buckhaven harbour. This proposal was accepted and, since completion, only a small amount of maintenance work has been required (Plate 2.18).

Plate 2.14 Buckhaven, 1974 aerial photograph. The RDL yard is sited on the former Wellesley bing. One area of the bing remains, and some areas of this have been colonised by grasses. The land reclaimed close to the beach and the site of the swimming pool at Buckhaven are clearly identifiable, as is the former site of the swimming pool at Buckhaven, now more than 150m above HWM. The former Buckhaven harbour is visible, but has been completely filled, and is now visible only in outline.

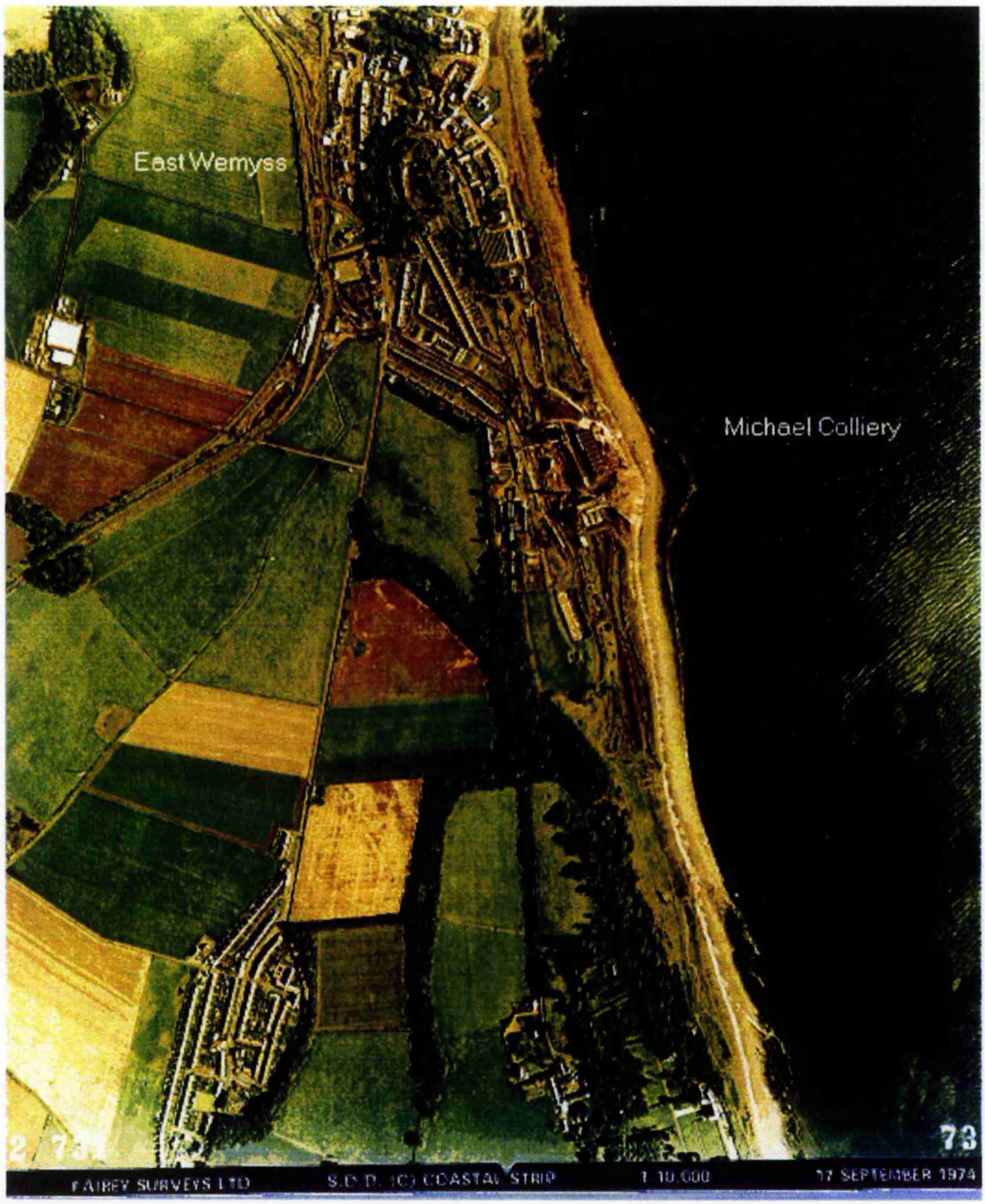

Plate 2.15 East Wemyss, 1974 aerial photograph. The black waste on the beaches has almost disappeared and, at the back of the beach, much of the grassed area running parallel to the beach is reclaimed land. The railway sidings to the south of the Michael Colliery are sited on reclaimed land. The sea close to the shoreline is blackened by the colliery waste, which has been reworked from the remains of the former Michael bing.

Plate 2.16 West Wemyss to the Frances Colliery, 1974 aerial photograph. West Wemyss harbour has almost silted up completely. Note how the water close to the beach has been blackened by the transportation of colliery waste in the water. A collection of bings, within the former embayment at the Frances Colliery, has developed over the years from the waste produced from the coal mining. The bings extend parallel to the beach for over 600m.

Plate 2.17 The erosion at Shore Street, Buckhaven, in 1974.

Plate 2.18 The riprap protection laid down to protect the houses at Buckhaven, 1990.

2.4.1 West Sands to East Wemyss

The colliery waste which had formed a blanket covering the West Sands area towards East Wemyss remained a feature of the landscape until the mines closed in the 1960s after which the waste was slowly removed by the wave action (Plates 2.9, 2.13, and 2.15). The exact dates when the old houses at the West Sands swimming pool were abandoned and later demolished are unknown; but no evidence of them exists on the 1960 OS plans. The tidally linked swimming pool which was separated from the water during the mining activities is evident in the aerial photographs of 1946 and 1974 (Plates 2.9 and 2.14). The removal of sediment along the West Sands bay area, during the 1970s, was of less concern because no new buildings had been constructed on the reclaimed land. No action was taken by local townsfolk to protect the eroding land as it was felt that the sea was merely reclaiming what was formerly its own.

The gasworks, originally sited at the back of the beach, had become distanced from the sea (Plate 2.9) due to the dumping of the waste onto the beach during the mining era. By the late 1970s however, most of the redd had been removed, and the gasworks was again closer to the HWM. The wave action destroyed much of the gasworks and only their foundations remained by the late 1980s; by the 1990s the sea wall which ran along the front of the gasworks was dislodged and lay horizontal on the shoreline (Plate 2.19). Close to the gasworks, the 16th century dovecot situated behind the sea wall became exposed to the waves after a large storm in 1945 destroyed the sea wall. Over the years the dovecot suffered damage and it finally collapsed in July 1986 (Rankin 1989).

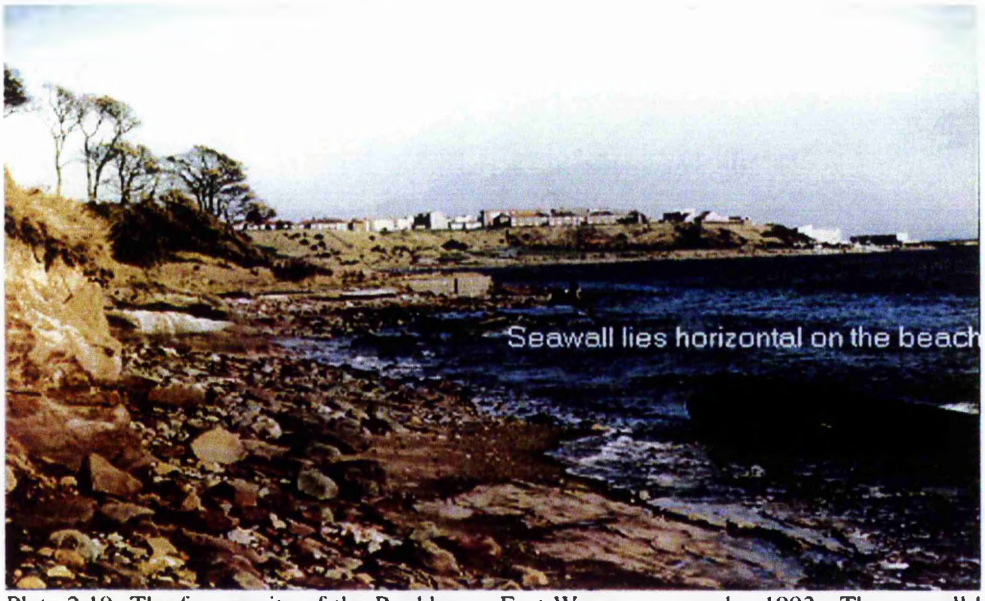

Plate 2.19 The former site of the Buckhaven East Wemyss gasworks, 1993. The seawall has collapsed and lies on the shore. The HWM now reaches further inland beyond the seawall. In the late 1800s four houses were located in this coastal area. Now however, these houses have been demolished and the sea has encroached landward beyond their former position.

Plate 2.20 Court Cave 1990s. Note the build up of colliery waste in front of Court Cave, compared to Plate 2.3, p.10. It was possible to drive along to Jonathan's Cave in the early 1990s.

Plate 2.21 Looking towards the site of the gasworks from East Wemyss, 1992. The riprap boulders were positioned on the shoreline along with the dismantled sea wall which was repositioned on the beach. The boulders were not secured properly, and within a year this protection work was undermined. Fresh erosion was taking place behind the boulders and as the photograph shows the protection work proved to be ineffective as some of the boulders can be seen in the foreground. Within a year severe erosion was re-initiated.

To the east end of East Wemyss, as a result of the reworking of the redd along the beaches, some of the wasteland had become established as a small car park and a track at the back of the beach. It was not until the late 1980s that rapid erosion threatened the Wemyss Caves and track road to the former gasworks (Plate 2.20); storms during the winter were thought to have triggered this new attack on the coast. Since early 1989 Fife Council has been attempting to protect Jonathan's Cave and the sewer directly in front as there was a strong possibility that tidal action would erode the material in front of the cave and flood it. In March 1989 large boulders and concrete slabs were placed in front of Jonathan's Cave; very little further

maintenance was required thereafter. In October 1991, however, large whin boulders had to be imported and placed immediately to the west of the original protection as the path to the caves was now being eroded. By the end of 1991 the sea wall had to be extended to protect the old live sewer as far as Court and Dovecot Caves, but yet again almost immediately afterwards, heavy storms in March 1992 severely undermined the new protection works.

Further remedial work was carried out on the sea wall to protect the sewer, but eventually it was decided to redirect it to the other side of East Wemyss. The rate of erosion had increased further and the 10m of waste land in front of Court Cave was rapidly being eroded away. Fife Council attempted an assortment of cheap protection schemes, all of which failed during subsequent large storms. The eroding sea wall was dismantled and laid at an angle on the beach and large boulders were positioned above, in an attempt to dissipate the energy of the waves and protect the land behind. This protection was extended to the end of the caves (Plates 2.21, 2.22). The boulders, however, were quickly undermined and erosion of the sediment behind the protection rapidly occurred (Plate 2.23). Further attempts were made to protect the caves, but each time new storms caused further erosion.

In 1995, in front of Dovecot Cave, a soft-engineering approach was adopted to protecting the caves from the encroaching sea. A form of meshing was laid down in order to catch the longshore transportation of sediment, thus encouraging the natural development of a sandy beach in front of the caves. This scheme has worked surprisingly well, although concerns are rising about the side effects of the protection measures down coast towards East Wemyss.

Riprap protection was also laid down along the front of the East Wemyss village (Plate 2.24). The riprap forms a wall at the back of the beach over 2m in height. The difference in height between the beach and village appear to be similar to those features of the 1926 photograph (Plates 2.12, 2.25), where steps are visible leading down to the shoreline. The newly positioned live sewer at East Wemyss has already been undermined and is now exposed to further attack from the waves. The rock platform in front of the riprap has been freshly exposed; this has been made apparent by the lack of micro-organisms on it. More recently the old sea wall, evident in old photographs which became submerged in colliery waste during the mining era (Plates 2.2 and 2.4) has been exposed once more.

Plate 2.22 East Wemyss Caves, 1993. The orange pipe became exposed by over 2m in less than 6 months and the unconsolidated material around it was being rapidly removed by the sea. The sediment was made up of rubble and colliery waste which was easily washed away at high tide and during severe storms.

Plate 2.23 Remedial work was carried out by Fife Council to protect the live sewer and track road to the gasworks in 1993. Erosion of the material behind the riprap is visible in the lighter coloured areas on the left of the picture, where the sediment has been washed away. This picture highlights how some of the actions carried out by Fife Council encouraged further instability of the coastline as opposed to stabilising it.

Plate 2.24 East Wemyss 1997, looking towards Buckhaven. The riprap protection scheme dominates the coastline. Note the height of the caravan to the left compared to the height of the wall of boulders towards the back of the picture.

Plate 2.25 Height of beach in relation to the East Wemyss village, in 1997. The roofs of the houses at the East End are just visible behind the riprap protection, to the right of the picture. This picture contrasts significantly with those taken in 1924 and 1951 (Plates 2.12 and 2.13).

Plate 2.26 A view from the sea of the Michael headland, 1992. Note how the cliff line has been eroded and there is considerable slumping of the cliff. The mine shaft has now been dismantled.

Plate 2.27. The Michael headland in 1993 (the remains of the Michael bing). The slag heap is over 5m in height, and the large concrete slabs have fallen from the upper level of the cliff, showing the extreme instability of this headland.

2.4.2 East Wemyss to West Wemyss

To the west of the Michael Colliery headland, land was reclaimed to create a tarmac road. In 1974 this road, running parallel to the sea for about 420m, was visible on the aerial photographs (Plate 2.15). Within 20 years of the colliery closing the reclaimed land had washed away. The protruding land mass, made up of unconsolidated colliery waste was subject to constant wave attack causing severe landslipping (Plates 2.27, 2.28). Today, the headland is significantly smaller and for the first time in 100 years it is possible to see West Wemyss along the coast from East Wemyss.

By the late 1940s the West Wemyss harbour had silted up and was cited as a health hazard and thus was partly filled during the 1960s. The area in front of West Wemyss has remained slightly more stable than the surrounding areas. Some erosion of the coastal stretch towards East Wemyss has taken place, but at a slower rate (Plate 2.28).

Plate 2.28 Looking towards West Wemyss from the Michael Colliery, 1992. The small cliff face at the back of the beach shows some evidence of being eroded during high tide and severe storms.

2.4.3 Blair Point to Dysart Harbour

The local walk from West Wemyss to Dysart around Blair Point has undergone change since the 1950s (Plates 2.11, 2.16). When the mines were open, the miners would walk from the Frances pit towards West Wemyss; some locals were known to have carved drawings in the

cliff face along the walk. One such carving was popularly known at the 'Man in the Rock' (Cunningham 1912.). This was originally sited high above the water mark. Today however, the sculpture is being eroded by the action of the waves. The Frances bing has dominated the coastal landscape in the Dysart area for over 60 years. Some time after the Frances closed in 1984, work was carried out on the Dysart harbour to remove the build up of waste which had accumulated (Plate 2.29, 2.31, 2.32). A new recreation harbour was completed; the problem of silting up was now less severe than before due to the closure of the mines and the reduction in the supply of sediment coming from the bings.

At Dysart the beach splits into two parts separated by the Panhall Rocks. From the Fishermens' Huts to Panhall Rocks the storms of 1992 and 1993 were of sufficient magnitude as to require the Council to provide emergency armouring revetment along a substantial stretch of this section to protect the existing sewer. From Panhall Rocks to the harbour quay wall, the reclaimed land has been used to establish a car park and local amenities, all of which are now threatened by erosion due to the lack of re-nourishment by sediment from the bings.

Plate 2.29 The Frances Colliery (1992), is located at the top of the cliff; the bing dominates the foreground of the picture. This is in strong contrast to Plate 2.7, p.13.

Plate 2.30 A view of the Frances bing looking towards Dysart (1992). The bing material extends as far as Dysart harbour. The grass area, in the far left of the picture, is reclaimed land from the bing material. Again this contrasts strongly with Plate 2.6.

Plate 2.31 The Frances bing looking towards West Wemyss (1992). The Frances bing has been retained with strong mesh in an attempt to prevent any further erosion and the transfer of the material down coast.

2.5 Summary

The photographic evidence provided in this chapter illustrates the significant amount of change this coastline has undergone during the past 100 years. The coastline of traditional fishing village communities has been permanently scarred by the effects of the coal mining activities from the three mines located close to the shoreline. Methil and Buckhaven are now dominated by the RDL yard. The beaches at East Wemyss and Dysart remain unstable and exposed to further erosion. This thesis will now explore in detail those changes which have taken place, attempting to quantify the coastal changes and investigate the impact of the coal mining on the coastline.

Chapter 3. Changes in the positions of the HWM and LWM, between the years 1894-1996, along the south-east Fife coastline

3.1 Introduction

Having provided the reader with pictorial evidence of the coastal changes which have occurred between Buckhaven and Dysart, this chapter will now quantify those changes, as reflected in the positions of the HWM and LWM along the coast. The coastal changes to the south at Kinghorn where no coal mining took place, will also be investigated; this will be used as a 'control section' to the analyses. In order to understand what has caused the current phase of erosion, it is necessary to describe in considerable detail the changes which have occurred, after which the possible causes will be investigated.

The methods used to examine the coast will be outlined, together with a discussion on the GIS software used. For an introduction and discussion on the principles of GIS, relevant information can be found in Bourrough (1986). The historical development of data analysis and GIS are reviewed in detail in Bernhardsen (1992).

3.2 Method

The largest possible scaled data available, in the form of Ordnance Survey (OS) 1:2500 plans - editions[1] 1894, 1914, 1960 and 1994, were chosen to investigate the changes in the coastline. In order to compare the data between the plans, a GIS was used to manipulate the data. GIS is a tool for the collection, management and display of spatial information (Burrough 1986). The advantages of using a GIS are that it allows for the manipulation of large volumes of data as precisely as possible. Initially the inputting of data is time consuming beyond which the system becomes a fast and flexible tool (Frank & Egenhofer 1992).

The GIS provides complete control over the entire data set. It does not guarantee that the source maps themselves are perfect, with uniform levels of data quality over the whole area. The data must be treated with care, to ensure that errors generated in the processing are identified and quantified before the results are analysed. Errors can result from natural variations or from original measurements including positional inaccuracy, observational bias and mistakes generated during the data entry.

Smallworld GIS is a UNIX system capable of handling large volumes of raster and vector data. Already established by Fife Council, Smallworld GIS contained the current 1994 HWM and LWM digitised data. Thus the comparison of the historical data sets with the

[1] A list of OS plans used in this thesis is held in Appendix 1.

most recent data was easily performed. The system allows the operator to determine which attributes are to be viewed at any given time. Once the OS plans from 1894, 1914 and 1960 were scanned and digitised into the system it was possible to compare different features and collect results. The setting up of the system was a very time consuming task.

All the plans were scanned, (using an A0 scanner attached to a PC [486-DX, IBM compatible]) into Smallworld GIS and snapped[2] into the real world. For the older plans not based on the current co-ordinate system, it was necessary to locate at least four or five points on extant buildings on the digitised 1994 data within Smallworld GIS. Having located the points in the current data set, the co-ordinates of the points were noted and used as real co-ordinates to snap the old plans into the real world (See Appendix 1). The best results were generated from plans where the fixed points were evenly distributed across the entire plan. This is because the image was evenly stretched in all directions. The error created from this method did not exceed ±1m. The process of sending the plans to the real world produces average displacement values. These were recorded for each sheet and are also held in Appendix 1. The mean displacement for all plans was estimated to be 0.3m.

Features on the plans were then digitised in point and line format. The coastal features include HWM, LWM, the benchmarks and surface points. On completion of the digitised work, any combination of HWM and LWM from any year could be overlaid in order to quantify the variations in the coastline between the plans. Presentation of the benchmark evaluation study will be discussed in Chapter 5.

Changes in the relative positions of the HWM and LWM, over the 100 year period, were measured using the HWM and LWM of the 1894 coastline as the baseline. No evidence exists describing the stability of the coast in 1894, thus no assumptions can be made about the state of the equilibrium at that time. Despite this limitation, the OS plans for 1894 remain the most reliable and largest scale data source available prior to the exploitation of the coal from the deep mines, and are therefore a valuable baseline from which to identify any coastal changes.

Between Buckhaven and Dysart and Kirkcaldy and Kinghorn, points were selected along the 1894 HWM line at 100m intervals. At each point, a line perpendicular to the 1894 HWM was taken. If the coastline was curved a tangent was drawn to the curve, and the normal was taken. Where the perpendicular line or normal intersected the HWM for the given year, the distance between the point and the intercept was recorded. This procedure was repeated for the LWM. Each point on the 1894 HWM was numbered and co-ordinates

[2]This method ensures that the plans are positioned in their correct locations (i.e. real world location). The system uses the actual O.S. co-ordinates on the plans and they are then located in their correct relative positions. Within the system any co-ordinate can then be identifed by the computer.

noted to enable re-visitation and the checking of the results. The measurements allowed for further calculations to be made on the movements of the HWM and LWM during the intermediate years. Thus the appendices include the basic measurements of the movement of the HWM and LWM from 1894 to 1914, 1894 to 1960, 1894 to 1994, and also 1914 to 1960 and 1960 to 1994. The width of the beach at each point along the coastline for the respective years was also taken.

The dates when the coastline was surveyed for different plans are recorded on individual O.S. sheets. It is emphasised that the date of publication is different from the date of survey and accordingly the calculation of shoreline displacements between different maps is based upon the survey dates, but for convenience, in the following text the displacements are quoted from publication date. The first detailed survey of the coastline was taken for the publication of the 1894 1:2500 plans. The coast was re-surveyed in 1913 for the publication of the 1914 1:2500 editions. In 1928 the policy changed on the revision of the OS plans and it became standard practice to re-survey only urban areas (Oliver 1993). The next full survey release was not published until 1960 after the whole coastline had been re-surveyed between 1945 and 1955 (See Appendix 1 for further details). The data used to compile the 1994 OS plans were extracted from the 1960 plans; only the sections of the Methil to West Sands coastline, and the Dysart coastal section were re-surveyed. For the intervening coastal stretches, between East Wemyss and West Wemyss the coast was re-surveyed in 1996. The coastal changes are held separately for the changes recorded in 1996 as different co-ordinates were used along the coast for the survey. As before, the co-ordinates were used within the GIS and the changes in the HWM and LWM recorded for the dates between 1984 and 1996. (For the 1996 data the co-ordinates of the points along the coast are held in Appendix 2, and the movements of the HWM are held in Appendix 11 [1996]).

According to the natural breaks in the direction of the coastline, the investigation has been divided into six sections; Methil Docks to Buckhaven harbour; West Sands to the Michael Headland at East Wemyss; the Michael Headland to West Wemyss; West Wemyss to the Blair Point; Blair Point to Dysart harbour and to the south the control section, Tyrie Works to Kinghorn. For information on the exact values recorded see Appendices 2 and 3. (Appendix 2 lists co-ordinates from which all measurements were taken. Appendix 3 documents changes in the postion of the HWM and LWM for the respective years). This section documents the recorded changes in the HWM and LWM and provides explanations where possible on the causes of these changes. Figures (3.1-3.9) illustrating the coastal changes are provided in the envelope at the back of the thesis.

3.3 Coastal Changes in the control section - Tyrie Works to Kinghorn

The plan position of the HWM and LWM depends upon the location of the coastline combined with tidal heights at the time of survey. It has not proved possible to examine the notebooks of the surveyors who mapped the limits of the various editions of the Ordnance Survey Maps. Thus there is an element of uncertainty about the comparability between the different surveys and thus to what extent any observed map displacements of the HWM and LWM do in fact represent 'on the ground' movement. However examination of the coastline between Kinghorn and Tyrie Works, which has not been affected by mining subsidence, can give some insight into the accuracy and reproducibility of the mapping. This will allow some quantification of the possible errors associated with the measured displacements of the tidal indicators between Dysart and Methil.

Between Kinghorn and Tyrie Works (Figure 3.1) a cliffed coastline is fronted by an intertidal area which is characterised by a number of small sandy embayments separated by fragments of rock platform which trend obliquely across the beaches. Over the 100 year period from 1894 -1994 repeated surveys show apparent displacements of the HWM of up to 5 metres with many parts of the coast showing negligible movement. The LWM does not reflect the same degree of stability that is noted with respect to the HWM. Where the rock platform extends to the LWM subsequent surveys in general show a total movement of less than 5 metres between 1894-1994. However in the sandy embayments, where unconsolidated sediments extend below the intertidal zone, movements of up to 90 metres have been recorded although the mean amount of movement is much less than this (10 metres).

The area between Kinghorn and Tyrie works is largely cliffed and it is not thought to have undergone significant retreat or collapse during the last 100 years. Accordingly the map evidence, which confirms this presumed stability, gives confidence that the HWM has been mapped with accuracy between the different surveys. Likewise the LWM on the intertidal rock platform is mapped with little variation between surveys. Not only does this repeatability affirm the accuracy of survey, it also suggests that, because the plan location of the LWM on the intertidal rock platform varies with tidal range, the different surveys were carried out on similar tidal ranges. The greater displacements noted on the sandy beaches, however, may be interpreted as reflecting either erosion/sedimentation or surveys conducted with different tidal heights. It is not easy to resolve these possibilities without further information about the surveys. If differing tidal heights are important the apparent stability of the intertidal rock platform may be explained because of its greater gradient, compared to the sandy beaches, which would result in smaller plan displacements of the tidal mark for a given change in tidal height.

3.3 Coastal Changes in the control section - Tyrie Works to Kinghorn

The plan position of the HWM and LWM depends upon the tidal heights at the time of survey. It has not proved possible to examine the notebooks of the surveyors who mapped the limits of the various editions of the Ordnance Survey Maps. Thus there is an element of uncertainty about the comparability between the different surveys and thus to what extent any observed map displacements of the HWM and LWM do in fact represent 'on the ground' movement. However examination of the coastline between Kinghorn and Tyrie Works, which has not been affected by mining subsidence, can give some insight into the accuracy and reproducibility of the mapping. This will allow some quantification of the possible errors associated with the measured displacements of the tidal indicators between Dysart and Methil.

Between Kinghorn and Tyrie Works (Figure 3.1) a cliffed coastline is fronted by an intertidal area which is characterised by a number of small sandy embayments separated by fragments of rock platform which trend obliquely across the beaches. Over the 100 year period from 1894 -1994 repeated surveys show apparent displacements of the HWM of up to 5 metres with many parts of the coast showing negligible movement. The LWM does not reflect the same degree of stability that is noted with respect to the HWM. Where the rock platform extends to the LWM subsequent surveys in general show a total movement of less than 5 metres between 1894-1994. However in the sandy embayments, where unconsolidated sediments extend below the intertidal zone, movements of up to 90 metres have been recorded although the mean amount of movement is much less than this (10 metres).

The area between Kinghorn and Tyrie works is largely cliffed and it is not thought to have undergone significant retreat or collapse during the last 100 years. Accordingly the map evidence, which confirms this presumed stability, gives confidence that the HWM has been mapped with accuracy between the different surveys. Likewise the LWM on the intertidal rock platform is mapped with little variation between surveys. Not only does this repeatability affirm the accuracy of survey, it also suggests that, because the plan location of the LWM on the intertidal rock platform varies with tidal range, the different surveys were carried out on similar tidal ranges. The greater displacements noted on the sandy beaches, however, may be interpreted as reflecting either erosion/sedimentation or surveys conducted with different tidal heights. It is not easy to resolve these possibilities without further information about the surveys. If differing tidal heights are important the apparent stability of the intertidal rock platform may be explained because of its greater gradient, compared to the sandy beaches, which would result in smaller plan displacements of the tidal mark for a given change in tidal height.

Between Dysart and Methil the data from the control section would suggest that movements of HWM or LWM between surveys are likely to reflect true displacements if they exceed about 5 metres and might be attributed to erosion, subsidence, emergence or rockfall. Where the intertidal area is formed of sediment, it is noted that the beach is steep (on average about 8 degrees) near the HWM and thus the plan location of the HWM is relatively insensitive to small variations in tidal height. Accordingly it is suggested that although the HWM may not refer to exactly the same tidal level on different surveys a displacement of greater than 10 metres is likely to represent a movement of the shoreline due to erosion or accretion. The more gentle slopes of the beaches close to the LWM indicate that greater circumspection is necessary to interpret apparent displacements of the LWM and perhaps 20 metres variation could result from methodological difference between surveys.

3.4 Methil Docks to Buckhaven Harbour

This section encompasses the area from the Methil docks (currently the Redpath Dorman Long (R.D.L.) yard), to the former Buckhaven harbour. Over a total distance of 3.3km, 23 points were identified and measurements taken from the 1894 HWM to the respective HWMs from the other OS plans, along the coast. The coastal changes can be subdivided into 3 distinctive zones of movement: points 1-6 which encompass the Methil Docks area; points 7-15 which include the area in front of the Wellesley Colliery (Figure 3.2) and points 16-23 (Figure 3.3) which extend along to Buckhaven harbour and encompass the area formerly known as Shore Street (Figure 3.2).

Between 1894 and 1914, directly south of the Methil Docks (points 1-6), the HWM moved seaward by an average of 54m; this trend is reflected in front of the colliery (points 7-15) with an average movement of 33m seaward. This change in the location of the HWM has been caused by dumping the waste material from the Wellesley Colliery directly on to the shoreline. The waves then redistributed material down coast. Towards Shore Street (points 16-23) the build up of the sediment (between 1894-1914) from the Wellesley Colliery had less impact on the coast and the HWM migrated seaward by 13m.

During the same period, the LWM reacted differently to the changes in the coastal environment. It migrated landward, by as much as 158m at Methil (on average 120m), narrowing the beach from a mean width of 220m in 1894 to 39m in 1914. To the west of the Wellesley (points 7-15) the beach was 70m wide in 1914, and the LWM migrated landward by only 71m. In contrast, at Shore Street (points 16-23) the width of the beach narrowed by only 20m; here the LWM was more stable, migrating only 8m landward by 1914. These landward migrations are difficult to interpret in terms of dumping of material on the beaches since this would lead to seaward migration of the LWM. Subsidence caused by mining, dredging for Methil harbour, errors in survey, or mapping of the LWM

at different tidal elevations are the potential reasons for the anomalous movement of this datum.

Between 1914 and 1960, at Methil (points 1-6), the beach widened to approximately 46m, from its previous width of 39m. During the same period at the Wellesley (points 7-15), the beach narrowed from 69m to 33m, and at Shore Street (points 16-23) the beach reduced from 148m to 43m width. This period saw a rapid expansion of the mines together with an increase in the amount of waste being deposited on the coast. The HWM was forced to move seaward, as the sediment built up along the coast. A radical change in the make-up of the beach environment was occurring as the colliery waste, including many exotic materials such as coal and ironstones, was added to the beach and submerged the natural coastal sediments. In contrast to the landward migration of the LWM between 1894 and 1914, a seaward migration was recorded between Methil and the Wellesley bing (points 1-15), of up to 50m, which is consistent with the dumped material prograding below LWM. However, a landwards shift in the LWM by an average of 28m at Shore Street (points 16-23) was also observed.

The 1994 data for this coastal stretch are known to be accurate, since the coastline was re-surveyed to monitor the rapid erosion that took place close to the housing development in the 1970s. (See Chapter 2 for more information). Changes in the HWM and LWM during the period between the surveys of circa 1960 and 1994 conflate the impact of continued dumping from the Wellesley Colliery up to its closure in 1967 and subsequent coastal changes. At Methil (points 1-7) the HWM migrated seaward, on average by a further 99m (between 1960 and 1994); the LWM also migrated in a seaward direction. In front of the colliery the average movement of both the HWM and LWM was approximately 130m seaward. However, towards Shore Street between 20 and 50m of net erosion occurred between 1960 and 1994. This erosion was known to have been initiated after the closure of the Wellesley and the cessation of the sediment deposition, together with the creation of riprap protection for the RDL yard. Such erosion may well be attributed to the starvation of beach material from the Shore Street coastal section caused by the coastal protection measures at the RDL yard.

In summary between Methil and Shore Street, during the 100 year period (1894-1994), the HWM and LWM both shifted seaward. The beach has built forward by approximately 250m. The narrowing of the intertidal zone caused by landward migration of the LWM is difficult to explain, although a steep gradient in the intertidal area might be expected where material is dumped onto the shore and is either much coarser than the original beach material or has not been redistributed by longshore sediment transport. Despite the erosion which occurred at Shore Street (points 16-23), following closure of the Wellesley colliery, the 1994 HWM did not migrate beyond the original position of the 1894 HWM. Here

some of the colliery waste which built-up over the past 90 years is now protected behind the coastal defences. This coastal stretch was not re-surveyed in 1996, because it is believed that the riprap protection installed along this stretch of coastline has provided stability.

3.5 West Sands to the Michael Headland, East Wemyss

In planform this stretch of the coastline is a shallow embayment which approaches the equilibrium (cycloid) form predicted by Bird (1993) for waves predominantly derived from the south west. In order to determine shoreline shifts Orthogonals were taken at 100m intervals, from the west of the Buckhaven harbour at West Sands (point 24) to the Michael Headland (point 60) and changes on those lines measured. The coastline breaks down into 3 sub-sections: West Sands to the gasworks (points 24-34); the gasworks to East Wemyss (points 35-51); and East Wemyss to the Michael bing (points 52-60) (Figures 3.2, 3.4, 3.5).

Between 1894 and 1914 the coastline underwent a significant amount of erosion. At West Sands to the East Wemyss Caves (points 24-42), the HWM migrated landward by approximately 14m. At Court Cave (point 43), however, which is not signified by a break in the coastal stretch, the data show a sudden reduction in the movement of the HWM. From Court Cave to the Michael Colliery (points 43-52), a distance of approximately 1km, there was an insignificant movement of the HWM whereas the 1914 OS plans indicate that directly in front of the Michael Colliery a small bing was developing. The sediment built forward approximately 25m to the west of the Michael Headland (points 54 and 56).

The LWM during the same period (1894-1914) was relatively stable; movement ranged between 0.5 and 9m landwards, from West Sands along to the Michael Colliery (points 24-60). As a result of the stability of the LWM and the landwards movement of the HWM, the intertidal area increased marginally in width over much of its length. Since the prevailing direction of sediment transport is eastwards along this coastline, the erosion observed here may well be related to a reduction of sediment supply from Shore Street. Such a reduction can be explained by the construction of Buckhaven harbour which would have intercepted longshore sediment transport and caused accumulation on the updrift side and starvation of sediment to West Sands. The harbour clearly did not allow material to move onto the West Sands prior to 1914.

Sediment bypassing the harbour would take place when the updrift accumulation extended seaward of the harbour walls and feed into the West Sands area from the east. This pattern of change is reflected in the shoreline migration between 1914 and 1960 (points 24-31), where there was a build-up of sediment causing the HWM to move seaward approximately 77m. There was a maximum movement of 28m between points 27 and 28. This supply of sediment, probably from the Wellesley bing 3km to the east, shows maximum

accumulation just to the east of Buckhaven Harbour and by 1960 this westwards drift of sediment appears to have not extended much further west than point 36; at the gasworks (point 37) erosion was still occurring and the HWM had moved landwards by approximately 7m.

West of the gasworks deposition and seaward migration of the HWM is again recorded. The amount of deposition gradually increases towards the Michael's bing; thus at the Cat Cave (point 39) 15m of shore advance is recorded which increases to 81m advance just east of the Michael headland (point 51). This gradual build-up of material in a westerly direction most probably reflects the eastwards drift of spoil from the Michael's bing rather than supply from the east. Accordingly, the build up here reflects longshore drift caused by the prevailing south-westerly waves rather than the dominant waves from the North Sea. This counter drift is obvious here because of the massive inputs of material onto the shore at the Michael Colliery. Directly in front of the Michael Colliery (points 52-60), the growth of the bing caused the HWM to move seaward by 120m. During this period the bing was so large that it extended across the former intertidal area to form a cliff of unconsolidated material, allowing the waves to constantly rework sediment at all states of the tide along the beaches in both directions.

The LWM during 1914-1960, as at Methil between 1894 and 1914, shows potential deepening of the embayment reflected in the landward migration of the LWM by as much as 153m in some places, although, beyond the East Wemyss village, at the Michael Colliery, there was a switch in the direction of the movement of the LWM to a more seaward position than previously. Most movement of the LWM is at the head of the embayment (West Sands) where the LWM is formed in unconsolidated sediments but, as with the control section, the LWM shows little movement where it is located on the rock platform, as at the gasworks (point 37). The impact of the sediment supply from the Michael's bing has caused seaward migration of the LWM. At the bing face (points 52-60), the build up of detritus caused the movement of the LWM seawards, by up to 100m. The mapping of the LWM at the bing and on the rock platforms imply a degree of accuracy in the survey work and thus suggests that the erosion /subsidence noted in the Bay at West Sands does represent lowering of the sea-bed in this area.

By 1960 Buckhaven Harbour had been completely infilled with sediment and a beach had built up in front of it. The 1994 survey shows the disused harbour re-emerging from the spoil but without maintenance the structure has begun to collapse. In the lee of the harbour there has been little change in the position of the HWM over the 34 year period up to 1994, but dramatic retreat commenced 200 metres west of the harbour and within 400 metres west of the harbour the HWM was now located some 20-30m landwards of its 1894 position. Thus, at point 29, 102 metres of erosion was recorded. Westwards the extent of

erosion diminishes and at the gasworks 39 metres of erosion occurred resulting in the shoreline being some 20m landwards of the 1894 HWM. These varying extents of erosion are the result of distance down drift from the sediment supply source, exposure to wave activity, and more importantly a reflection of limited retreat following the excavation of the cliffed coastline west of the gasworks in comparison to the retreat through the unconsolidated deposits at the head of the embayment of the West Sands.

For the coastal stretch between the East Wemyss Caves and the Michael Headland the 1996 survey showed that the position of the current HWM has changed considerably from the 1960s. Erosion in front of the Wemyss Caves which began in the 1980s has continued and the HWM now sits landward of its former position in 1894. Maximum erosion has taken place at the gasworks and less erosion has occurred in front of the loom factory at East Wemyss. In 1994 Gowns estimated that the rate of erosion was 5m/year directly in front of the East Wemyss village. These latter areas are now protected by rip-rap but west of the loom factory (point 58) the unprotected HWM is still retreating both at East Weymss and the Michael Headland.

3.6 The Michael Colliery to West Wemyss

Twelve measurement sites are located in the linear coastal segment between the Michael Headland (point 61) and West Wemyss (point 73) which is characterised by a low rock platform in the intertidal zone, particularly near to West Weymss. The surveys of 1894 and 1914 show the development of a small bing at the Michael Colliery but otherwise the HWM is fairly stable in position. The fact that there is little change in width of the beach over this time would suggest that the coast was in near equilibrium prior to the dumping of spoil. (Figure 3.5).

Increasing spoil deposition clearly upset this equilibrium in the following years as is evidenced by the extent of coastal change between 1914 and 1960. At the Michael Colliery the HWM prograded by at least 65m. Longshore movement of the spoil from the bing caused shoreline advance all the way to West Weymss and partially covered the rock platform. The source and transport path of the material responsible for the progradation are clearly indicated by the westwards tapering wedge of material from the bing. The overall beach gradient steepened during this period, reflecting a landward movement of the LWM. Near West Weymss the LWM still appears to be defined by a rock platform in 1960 and the movement of the LWM shorewards would seem to imply some subsidence of the rock platform.

The most recent survey in 1996 shows that erosion has dominated coastal processes in this area following closure of the Michael Pit in 1967. Towards West Wemyss (points 61-73) the HWM has migrated landward at between 5 and 20m; to the west of the Michael

Colliery, (points 56-62) it is now located beyond the original position of the 1894 HWM, between 5 and 20m and wave activity on spring tides penetrates to the village at West Wemyss.

3.7 West Wemyss to Blair Point

The coastal section from West Wemyss to Blair Point is defined by the harbour and sea wall at West Wemyss and the rocky headland at Blair Point (points 74-87) (Figures 3.5 and 3.6). These features at the extremities of this coastline inhibit the free transfer of beach material by longshore drift from the adjacent sections of coast. As a result coastal responses here may be little affected by the major sediment inputs to the coastline from the Frances and Michael Collieries. Erosion and retreat of the HWM is apparent from the 1894 and 1914 surveys and, as with the West Sands, this may in part be related to the impact of the West Wemyss Harbour on sediment throughput from the east. In particular, movements of between 11 and 20m were recorded in front of the Chapel Gardens and at Blair Point (points 76-78 and 83-87 respectively). The LWM, during the same period (1894-1914) migrated landward at a higher rate, on average by 46m, with the maximum movement occurring at Chapel Gardens Bay (points 77-85).

Beach aggradation to the west and sedimentation in the harbour between 1914 and 1960 surveys may be associated with the shadow area of the harbour piers or with the dumping of spoil onto the coast from the Lady Pit area. However the remainder of the coast shows only minor changes such that from West Wemyss to Blair Point (points 74-87) the HWM prograded by a mean value of 4m in a seaward direction and eroded by up to 10m around Blair Point (points 80-86). Considerable modification of the intertidal zone continued through this period with a landwards displacement of 80m at point 76, although, near Blair Point, the recorded changes are within the possible survey errors established for the control section at Kinghorn.

The more recent survey of the coastline in 1994 suggests that the beach has stabilised. Results suggest that the HWM between 1960-1994 remained stable, with only a small amount of movement occurring in the LWM of approximately 9m.

3.8 Blair Point to Panhall

The coastline between Blair Point and Panhall formed a shallow embayment in 1894 with prominent rocks at Panhall forming a partial barrier to longshore sediment movement (points 88-93) (Figure 3.8). However, it is the Frances Colliery that has dominated coastal processes on this stretch of coastline and has been responsible for the radical transformations of the shoreline over the past 100 years. There is little impact of mining activity on the coastline prior to the 1914 survey since this map shows that erosion forced

the HWM landward between 3 and 27m and, in common with the coastal segment to the east, the LWM was also mapped at a more landward position than that for the 1894 survey. The following 46 years saw the HWM migrate seaward between 20 and 153m at the Frances Colliery (points 89-91). The LWM also moved seaward, by as much as 62m, as a result of the build-up of sediment from the dumping of waste onto the shore.

In 1894 the flat sandy beach measured 128m in width; this was reduced to 116m by 1914 and by 1960 the beach was only 66m wide. The supply of material from the growing bing exceeded the rate of removal by longshore processes and this resulted in a steepening beach gradient which was clearly not in equilibrium with the coastal processes. The small bay (Plates 2.7) was completely infilled with colliery waste but by 1994 the beach was only 16.2m wide.

Mobilisation of the sediment from the bing by wave activity caused longshore transport westwards and aggradation of the beaches towards Panhall between 1914 and 1960. Of note is the fact that little counter drift appears to have taken place here and there are only minor changes in shoreline alignment to the east of the bing. At Panhall (points 99-100) there is only a small seaward movement of the HWM shown in 1960 in comparison to the bing face although the progradation at Dysart (see below) would suggest that much material bypassed this area. This beach is one of the few zones along the coast which does show accumulation of material between the 1960 and 1994 surveys.

3.9 Panhall to Dysart Harbour

Prior to the 1890s there were numerous pits located between Panhall, to the west of the Frances bing, and Dysart harbour (Knox 1954) (points 94-102) (Figure 3.9). Thus, in 1894 when the initial OS plans were established, it is unlikely that this coastline was in a stable equilibrium, as the previous coal mining activities in the area would have already disrupted the natural stability of the coastline. Between 1894 and 1914 the HWM migrated seaward by 16m; this trend of deposition continued over the 100 years, progressively building forward another 24m between 1914 and 1960 and a further 7m between 1960 and 1994. The LWM, during the 100 year period however, progressively migrated landward. Initially the LWM retreated by an average of 20m by 1914, followed by 9m by 1960 and then finally stabilising in 1994.

A detailed survey of the beach at Panhall, Dysart carried out by Gowans (1994) included 5 profiles of the beach. The rate of erosion was estimated to be occurring at 2-3m per year. By 1993 the car park, constructed on reclaimed colliery wasteland (points 94-100), was being severely undermined. By 1994 emergency temporary revetments were constructed (Gowans 1994). Although the survey of the HWM taken in 1996 has shown that it has not

retreated as far back as the former position of 1894, the current erosion continues and it is likely that the position of the 1894 HWM will be reached soon.

In summary, over the past 100 years the coastal stretch between West Wemyss and Dysart has been transformed by the coal wastes dumped on the beach at the Frances and Michael Colliery. The sheltered inlet at West Wemyss has undergone irregular phases of erosion and deposition. This contrasts with the bay at the Frances Colliery which has been completely filled with redd. At Dysart there has been a constant trend of progradation over the 100 years, unlike anywhere else along the coast.

3.10 Conclusions

The results show that the former coastline in 1894 between Buckhaven and Dysart has radically changed over the 100 year period. In general this coast has undergone a phase of deposition, with the dumping of colliery waste on the coastline, followed by a phase of erosion, after the closure of the mines.

The 1896 coastline was characterised by a narrow coastal zone, dominated by rocky platform at LWM and small pockets of shingle and finer grained material along the HWM. The opening of the deep mines along the edge of the Firth of Forth marked a significant change in the coastal equilibrium. From then on, colliery material was consistently dumped on to the foreshore of the Fife coastline, at the three sites between Methil and Dysart. The unconsolidated detritus was reworked along the coastline in both directions.

In 1914 the OS data indicate that the areas immediately surrounding the colliery pit heads were most affected by the sediment influx. The changes in the 1914 HWM and LWM indicate that the coastal zone adjacent to the main collieries where the waste was dumped on the coast underwent a period of aggradation. These effects, overtime, were fed into the whole coastal system, affecting the entire beach.

Between 1914 and 1960 the beaches consistently narrowed along the entire coastal zone from Buckhaven to Dysart. The movements of the HWM and LWM were often not concordant. There were however, some erratic changes in the relative positions of the high and low water marks, where abrupt movements in the tidal positions cannot be explained by the changing sediment variable.

The LWM, mainly situated on rocky platform, migrated landwards, despite the fact that this period signifies an increase in sediment along the coast; the LWM would have been expected to move with the direction of sediment build up. By the 1960s, however, the photographic evidence, together with the OS data discussed in this chapter, demonstrate that the original coastline had been completely submerged in a blanket of colliery waste. A phase of deposition was experienced along the entire coastline.

With the closure of the collieries the raised coastline was thrown into a new phase of disequilibrium caused by the halt in the supply of sediment to the bings. The unconsolidated beach material on the shoreline quickly disappeared, including those locations where the reclaimed land had been developed. Almost immediately human intervention was required to protect the eroding coast. Where the sea was able to reclaim the coal detritus, the beach returned to its former position of 1894. The results from the 1996 data, indicate that in some locations the HWM has receded beyond the 1894 position, and the LWM also sits landward of its original location.

The results from this chapter raise many questions. Why have different sections of the beach reacted differently to the increase in sediment along the beach? Were there any other processes at work which could have influenced the coastline to such an extent? What caused the differential movements of the HWM and LWM during the early phases of coal mining? It is difficult to explain the results purely by the influx in sediment during the mining era. If sediment supply was the only changing variable in the coastal equation then the coast would have returned to its former positions of 1894, and the former equilibrium would be re-established. Instead the process of erosion dominates segments of the coastline. Further investigations are required into all the other possible processes which could have influenced this coastal zone and to cause such variations in tidal movements.

In conclusion, general trends have been identified, some of which can be attributed to the result in the increase in sediment on the beaches. However, this evidence suggests that there are multiple processes at work influencing the coastal environment, and these will now be explored in detail. The succeeding chapters will investigate the following processes considered to be possible influences on the nature of the coastline: the effects of isostatic uplift; the effects of mining subsidence; and the effects of climatic change and global sea levels.

Chapter 4. A review of the causes and effects of isostatic uplift on the south-east Fife coastline

4.1 Introduction

Isostatic and eustatic adjustments of land and sea-level are known to have affected Scotland following the decay of the Late Devensian Ice Sheet some 14,000 years ago. This Chapter investigates the possible impact of these factors on the coastline of south-east Fife today and their possible role in the coastal erosion that is taking place currently. More recent concerns about sea-level changes associated with possible global warming are evaluated in Chapter 6.

Although this thesis is concerned with a small geographical area, many aspects of relative sea-level change are global in nature and are best examined with reference to world-wide models of eustasy and isostasy before focusing on a small area. In this chapter the local evidence of sea-level changes since the decay of the Late Devensian ice sheet in the coastal area of south-east Scotland is first presented. However, isostasy and eustasy reflect regional and global changes that result from large scale processes. Global changes of water volume in the oceans, during the Quaternary, are principally the result of changing ice volumes locked up in Quaternary ice sheets. These eustatic changes of sea level are best examined in areas remote from the centres of glaciation. Understanding the isostatic component of sea-level change requires a basic knowledge of the geophysics of the earth. A rebound model can then be formulated which predicts isostatic changes following the imposition and removal of an ice burden and provides a context for a review of the estimates of isostatic uplift in Fife. In fact, several models of isostatic uplift are available for the field area. These are discussed and through an understanding of the constraints of the various models a critical assessment can be made of the literature on isostatic uplift in south-east Fife.

4.2 Sea-level changes in Fife

Field data have been used in the construction and validation of rebound models covering the research area. In order to assess the credibility of isostatic uplift models for the UK and in particular for the Forth Valley it is necessary to investigate the data available in south east Fife.

At the maximum of the Late Devensian glaciation, between 25 000 and 18 000 yr. BP, virtually the whole of Scotland, Wales and northern England was covered by an ice sheet (Bowen *et al.* 1986; Huddart *et al.* 1977). This ice sheet was small in global terms but sufficiently large to cause differential crustal warping due to ice loading. Little is known concerning the early stages of ice retreat from its maximum positions but a major climatic improvement occurred from about 14 000 - 13 500 yr. BP, which led to the collapse of the Late Devensian ice sheet. The ice sheet probably came to an end by about 12 500 yr. BP but was followed by a gradual

climatic cooling, culminating with the Loch Lomond Stadial in Scotland between 10 800-10 300 yr. BP (Price 1983, Sissons 1974, Whittington *et al* .1996). Many models of the Scottish ice sheet suggest that the North Sea was largely ice free during the Late Devensian time (c. 18 000 - 10 000 yr. BP) and that the British Ice Sheet terminated at the Wee Bankie Moraine off the coast of eastern Scotland (Sutherland 1984). In eastern Scotland the sea flooded the proglacial area as the ice withdrew onto the present land surface and laid down glaciomarine sediments both on and off-shore whilst marginal sediments were emplaced by glacial outflows at the ice front. (Lambeck 1993b, p.964). Seaward of the margin, erosional and depositional shorelines were formed on the isostatically depressed land surface and subsequently uplifted.

Shorelines formed during ice sheet decay ('Lateglacial') in Fife are recognised primarily as morphological benches. Individual benches although small can be linked into a shoreline sequence by plotting onto a shoreline diagram (Cullingford and Smith 1966). Stratigraphic investigations more firmly constrain the identification and location of shoreline features formed during the Holocene. Sea-level changes can be deduced from the analysis of cores showing marine or freshwater sediments intercalated with aquatic and herb flora of peats. Past sequences relating to freshwater and marine transgressions correspond to a level near mean high water spring tide, although formation range about this level may be quite large. Along the east coast of Scotland indications of Holocene changes in sea-level are primarily in the form of marine deposits, peat beds intercalated with marine or brackish clastic sediments (Lambeck 1993b).

The Lateglacial East Fife shorelines (EF1-6) were initially mapped by Cullingford and Smith (1966) (Figure. 4.1) where they identified 6 separate beaches in sequence, each of which terminate in outwash plains with a break in slope between the beach or terrace. The six shorelines were formed during the early stages of retreat of ice, where the ice margins were thought to have retreated across the low grounds of eastern Fife, Kincardine and eastern Lothian and locally may have retreated up the Forth and Tay valleys (Lambeck 1993a). The shorelines become progressively younger in age at lower elevation and extend further in a westerly direction, indicating a westward retreat of the ice sheet margin. The oldest shoreline of the six identified, the EF-6 is thought to correlate with the Errol Beds (a glaciomarine clay) found at up to 35m OD in the Tay estuary and the St Abbs Beds, the lateral equivalent to the Errol beds, found offshore in St Andrews Bay and the Forth estuary, as far west as Inverkeithing (Paterson *et al* .1981). Using dating from these clays, the EF-6 Shoreline has been tentatively dated to 14 750 yr. BP (Browne 1980).

In the Lateglacial sequence one shoreline, the Main Perth Shoreline (MPS), is more continuously developed than the other features and was formerly related to a supposed readvance of the ice sheet (Sissons 1976). This lies at a lower elevation than the EF-6

shoreline, although this is not based on quantitative evidence, (Smith *et al.* 1969; Lambeck 1993b) (Figure 4.1). By the time of the MPS, about 13 500 yr. BP, ice had retreated up the Forth and Tay River valleys and areas such as the upper Teith valley and west Stirling were ice free (Gray and Lowe 1977).

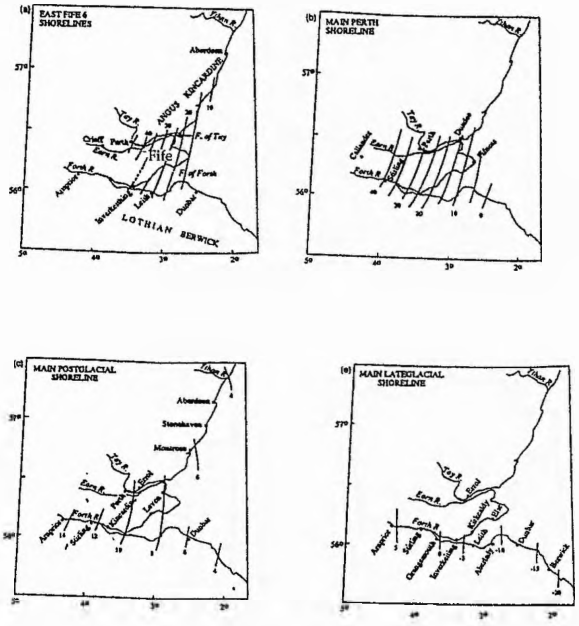

Figure 4.1 Isobases of the major shorelines identified in eastern Scotland. (a) the East Fife 6 Shorelines, (b) the Main Perth Shoreline, (c) the Main Postglacial Shoreline, (d) the Main Late glacial Shoreline (After Lambeck 1993b, p.968).

Another prominent feature the 'Main Late Glacial Shoreline' post-dates the Main Perth Shoreline, but pre-dates the Holocene shoreline sequence and the overlying sediment deposited at about 10 300 yr. BP (Sissons 1967) (Figure 4.1). This shoreline slopes down the Firth of Forth at c.0.17m km^{-1} and appears to represent a major erosional event cutting across both solid rock and unconsolidated sediments (Sissons 1983). The extent of the erosion suggests that sea-level may have stood at this height for a considerable duration.

Relative sea-level rose during the early part of the postglacial and laid down a series of 'carse' clays in the shallow water of the Firth of Forth which are characterised by a much warmer fauna than the preceding St Abbs beds laid down during the Lateglacial. These carse clays were thought to have been deposited in the estuarine environment during the time of relative sea-level rise; the clays are overlain by peat, carbon dated to 6500 yr. BP (Lambeck 1993b). The end of the transgressive phase is marked by the formation of a prominent coastal feature:- the Main Postglacial Shoreline (Sissons 1967). This transgression marked the point in the Forth at which the rate of eustatic sea-level rise exceeded that of isostatic uplift of the area following the decay of the glaciers of the Loch Lomond Stadial. Intermittent regression from the Main Postglacial shoreline to present sea-level is indicated by 3 shorelines identified in the Forth valley (Smith 1968), where extensive mudflat deposition continued in the more sheltered areas.

Changes in relative sea-level over the last two millennia, prior to documentary evidence, are not well dated, although recorded data since the last century allow recent movements to be evaluated (See Chapter 6).

For the Forth Valley the relative sea level curve from Lambeck (1991) corresponds with the geomorphological evidence described above, with the present MHWS (Mean High Water Spring) tides occurring at 2-3m above mean sea-level and the predicted heights of past shoreline features lie above mean sea-level by this amount (See Figure 4.2) for more details.

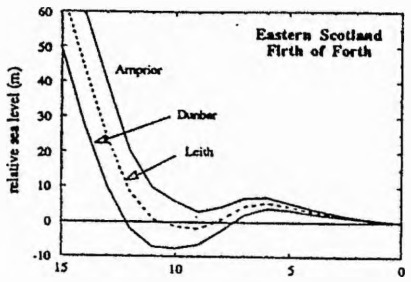

Figure 4.2 Predicted mean sea-level in the Forth Estuary. Note the predicted relative low stand at about 9000-10 000 yr. BP corresponding to the Main Lateglacial Shoreline whose depth and time varies systematically from east to west (Lambeck 1991, p386).

4.3 Eustasy and sea-level changes

Relative sea-level changes, which are directly determined in the field, include the combined effects of all factors that may have affected the level of the oceans and crustal land level. Isostasy and eustasy are two physical processes which affect the earth's lithosphere and hydrosphere, involving vertical motions which can be monitored specifically by mean sea-level (Fairbridge 1983). Eustatic effects account for the changes in the volume of the sea; they can be estimated only from relative sea-level data (Mörner 1969, 1987a, Chappell 1974). Isostatic changes are caused predominately by the radial displacement of the surface of the solid earth, caused by melting of ice sheets (Devoy 1987).

In order to calculate relative sea-level changes it is necessary to separate and identify movements attributable to isostasy and eustasy. However, for a global system, which historically has undergone phases of complete or partial glaciation, affecting the ocean floor, ocean surface and land masses, there remains no stable region where eustatic sea-level changes alone can be measured since any addition of water to the ocean basin will deform the earth and change the observer's point of reference (Clark *et al.* 1978). In some areas local evidence is available giving an insight into past sea-levels, but in many regions data are limited or non-existent. Isostatic changes, like eustatic changes, cannot be treated as an independent variable since loading of the crust by an ice sheet will generate a gravitational attraction on the local oceans which will, in itself, cause sea-level changes independent of the withdrawal of water from the oceans into the ice sheet (Clark *et al.* 1978). Thus, to develop an understanding of

sea-level changes associated with glacial phases recourse is made to models of the earth's response to glaciation, which incorporate both isostatic and eustatic factors.

Isostatic and Eustatic responses to glaciation vary across the globe Lambeck (1993b). In areas within former ice limits (*a near field site*) relative sea level changes are dominated by isostatic uplift whereas in areas remote from glaciation (*a far field site*) eustatic sea level changes predominate over isostatic changes. In simple terms a *near field* relative sea level curve would show an exponential fall in sea level with time following deglaciation while a *far field* site would show a gradual rise of sea level with global deglaciation (Pirazzoli 1996). Scotland, although glaciated during the Late Devensian, was at an intermediate distance from the Scandinavian and Laurentide Ice sheets and thus shows a sea level response reflecting both *near field* and *far field* responses. Sea level changes in Scotland are further complicated by the growth of glaciers during the Loch Lomond Stadial introducing a *near field* response at sites close to that ice mass compared to more remote sites (Sutherland 1984).

Few reliable relative sea level curves are available for *far field* sites (Pirazzoli 1996). Fairbanks (1989) obtained a continuous and detailed record of sea-level change for the geographical area of Barbados during the last deglaciation period. Barbados (like the UK) is described by Pirazzoli (1996) as being located in Zone II an intermediate field site which corresponds to the peripheral bulge around a former ice margin which tends to subside in late and post-glacial times, to compensate the uplift in nearby formerly glaciated areas. This may occur long after the period of deglaciation is over. A curve was constructed for eustatic sea-level rise after adjustments were made for an uplift rate of 0.34mm/yr for the south coast of Barbados. The results show a rise in sea-level of 121±5m since 18 Ka BP with two periods of more rapid rise around 12 and 10 Ka BP (Pirazzoli 1996, p.88) (Figure 4.3). According to Pirazzoli (1996) these data provides some of the best evidence of relative sea-level change on a global scale although glacio-isostatic and hydro-isostatic effects are not included..

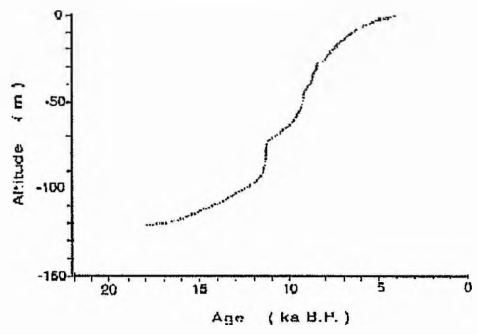

Figure 4.3 Deglacial relative sea-level changes in Barbados (After Pirazzoli 1996, p. 88).

4.4 Isostasy

This section describes the basic principles involved in isostatic movement and the development of an isostatic rebound model. The theory of isostasy suggests that all large portions of the Earth's crust are in balance as though they were floating on a denser underlying layer; thus areas of less dense crustal material rise topographically above areas of more dense material (Pirazzoli 1996). Hence, loading of Scotland by an ice sheet will cause a depression of the land surface, which is accommodated by the flow of material from deeper in the earth into the peripheral regions. When the ice sheet melts, the surface beneath the ice sheet is uplifted but in the peripheral regions the land may sink as the material flows back under the area which was ice covered thus re-establishing isostatic equilibrium.(Figure. 4.4) (Clark *et al.* 1978).

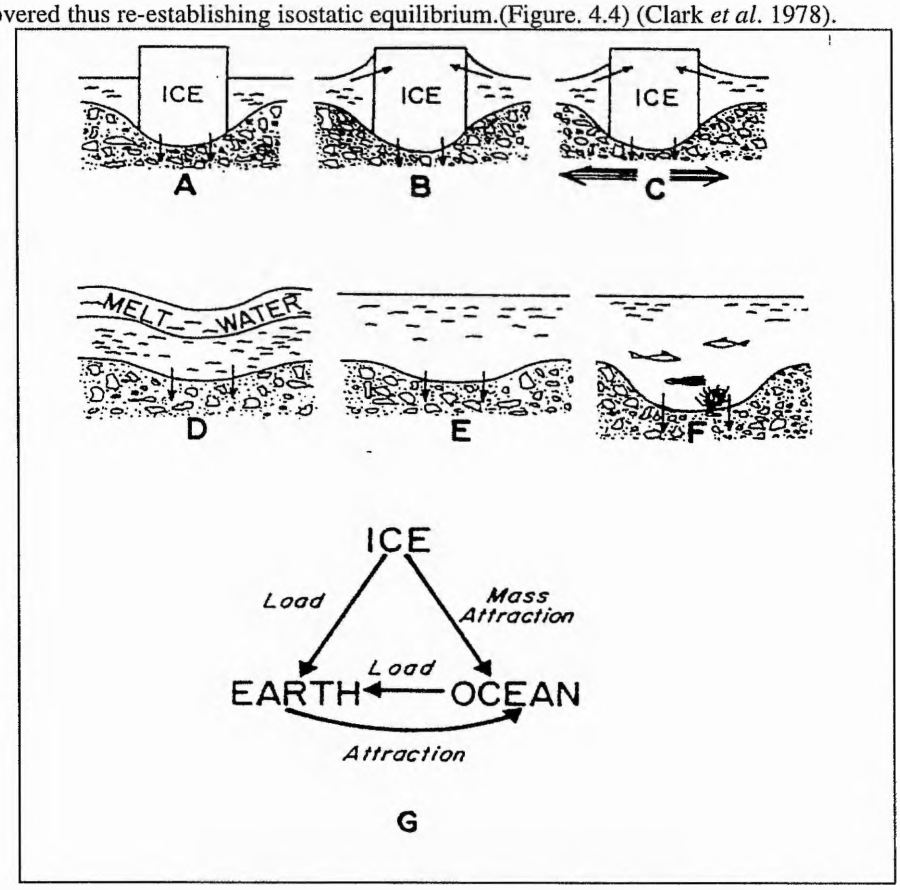

Figure 4.4 Interactions among ice loads, water loads and the deformable Earth: (A) The weight of the ice deforms the Earth and (B) the ice mass attracts the water. (C) The transfer of matter within the Earth distorts the geoid. Similarly, (D) the weight of meltwater depresses the Earth differentially and (E) more water flows into this depression, increasing the water load and (F) causing added deformation of the ocean floor. These processes are interrelated as indicated in (G), and all are included in the numerical model proposed by Clark *et al.* (1978, p.266).

Isostasy also effects the free ocean surface because of density and structural differences in the earth's surface beneath the oceans. Models of the geoid show that the surface of the non-perturbed sea, or geodetic sea-level, to be irregular in form, having a spatially varied pattern of

swells and depressions and with a range in relief of up to 200m (Marsh & Martin 1982, Mörner 1976). Tectono/glacio-eustatic and isostatic factors will also affect the geoid surface, particularly through the influence of material flows within the earth, in response to changes in surface mass distribution (Devoy 1987). Changes in the geoid can be of the same order of magnitude as the eustatic rise resulting from the meltwater increase of the ocean volume. Consequently, possible changes in the geoid must be considered in any model of sea-level changes during glacial phases.

The earth's mantle responds directly to glacial loading which will change the shape of the planet's surface. The rate at which the deformed mantle will return to its gravitational equilibrium is determined by the viscosity of the lithosphere. The exact processes involved in the response produced by the earth's mantle are not fully understood. Variations in the earth's rheology, geologic structure, tectonic and loading history may lead to important modifications of the uplift pattern for post glacial time (Cathles 1980, Lambeck & Nakada 1985). However, a limited understanding of the rheological characteristics suggests that the upper and lower layers of the earth respond at different rates. Lambeck (1990, p.5), for example, characterised the response to surface loading by an initial elastic deformation followed by stress relaxation, such that the load - induced stresses in the body ultimately vanish (Lambeck 1990, p.5). But, any simplistic models such as that proposed by Cathles (1980) where the earth's mantle shows a uniform mantle viscosity of about 10^{22} P does not take into account any of the variables listed previously. This model can not be applied to areas of crustal bulge peripheral to loading, as in the UK, where the earth's rheology demonstrates behaviour in a linear-non-linear fashion.

In order to model isostatic changes due to glacial phases it is necessary to determine former ice loads as well as knowing the earth's rheology. In the estimation of ice thickness the simplest approach is to estimate values for a static ice model; this assumes that the ice volume is in a constant state of equilibrium. However, Budd and Smith (1987) argue that ice sheets are driven by external climatic forcings and feedback mechanisms; therefore the ice volumes may differ significantly from those estimated with static models. Peltier and Andrews (1976), for example, check the volume of ice in their model by comparing it with the position of sea-level at approximately 18 000 years ago, which they assume to be 80 to 100m below the present level. However, if that assumption is wrong, the ice volume will be inaccurately estimated. This point is reinforced by Peltier (1987) who highlights the fact that the ice sheets are not circular discs with parabolic cross-sections which are applied and removed instantaneously. Furthermore, a critical unknown is the amount of isostatic compensation that has occurred beneath the load, particularly when the ice sheet geometries are complex. Thus, in estimating ice thickness, the effect of delay in isostatic response means that the ice models are not free from assumptions about the earth's response.

Geomorphological field data have been used to indicate glacial limits and ice thickness in Scotland from which ice volumes can be computed. Nevertheless, there are conflicting estimations of the British ice field. Models of maximum ice growth proposed by Denton and Hughes (1981) and Boulton *et al.* (1977) suggest that the ice sheet merged with that of Fennoscandiavia to form a thick ice sheet coverage over the North Sea in the Late Devensian time, with the ice thickness exceeding 1800m, covering the peaks of the highest mountains. The ice limits of this model, however, do not correlate with the field evidence. Ballantyne (1984), for example, identified geomorphological evidence in Scotland to suggest the existence of nunataks, trimlines and striae. Sutherland (1984), argues for a model where thinner ice coverage, providing nunataks and producing trim lines suggests that the ice thickness is unlikely to have exceeded more than 1300m. This latter model correlates with the evidence of ice limits terminating at the Wee Bankie Moraine off the east coast of Scotland. Lambeck (1993b) reinforces Sutherland's argument, and believes that the maximum values of ice thickness are unlikely to have exceeded 1500m.

This brief outline highlights some of the complexities of attempting to develop a model of Scotland's response to an ice sheet burden. These complexities extend to the melting of the glaciers, where the processes of hydro-isostasy, tectono-isostasy and glacio-isostasy occur at different rates in a non-linear fashion. Further complications have been suggested by Mörner (1987a, 1987b) who argues that earth movements will automatically cause deformations of ocean basin volumes which in turn will lead to tectono-eustatic sea-level changes, involving the redistribution of mass that will simultaneously lead to deformations of the geoid configuration. Meltwater produced by ice sheet disintegration cannot be added uniformly to the ocean basins since this violates the equilibrium constraint that the geoid remains an equipotential surface (Peltier 1987). Walcott (1980) illustrates how relative sea-level at great distances from glaciated regions is affected by meltwater loading of the ocean floor. Assuming that the effect of glacial unloading is negligible at great distances from ice, Walcott (1980) found that continents should rise slightly relative to the ocean floor. This is significant for Scotland, suggesting that the Laurentide and Fennoscandian ice sheets will have affected the loading of the ocean floors and must therefore be taken into account in any rebound model developed for Scotland.

In conclusion, the creation of an accurate rebound model must attempt to quantify the earth's response to earth rheology, ice volumes and the ocean configurations, all of which contain parameters that are poorly known (Lambeck 1990). As the research has developed the subject has been shown to become increasingly more complicated with interrelationships being identified across the spectrum of variables. As a result the geomorphological evidence collected remains important within the field of relative sea-level change.

4.5 Models of isostatic uplift

For a number of decades differential crustal movements within the UK have been estimated based on geologic, geodetic and tide gauge data. All agree that glacio-isostatic processes have resulted in uplift in northern England and mainland Scotland (Shennan 1989). Longer term isostatic processes have been estimated by a number of workers using models which vary in complexity, depending on the methodology adopted.

Flemming (1982) developed a basic model, with known limitations. The latter were justified by arguing that the spatial and temporal distribution of data points precluded a more complex numerical model. Although geological theory of isostatic recovery shows a curvilinear function, the model clearly stated that it would assume a linear model of uplift. Few assumptions were made about global sea-level curves or known geological corrections for faulting and subsidence. The results show a range from 2.5 mm/yr. over the Highlands and west coast of Scotland to -0.5 mm/yr. over the extreme south-west of England. Despite the simplistic nature of the model, the results correlate with observed data and other more complex models.

Peltier (1987), using relative sea-level data, models of sheet ice disintegration and a model of earth rheology, estimates that the present day rates of relative sea-level change in the UK show relative uplift ranging from -0.4 - 0 mm/yr. from south-west to north-west Scotland. The advantages of Peltier's model are that it combines the effects of both glacial and hydro-isostasy, and the ice water attraction. However, Shennan (1989) also argues that a disadvantage of this type of model is that, because the results are based on global criteria, the final estimations need to be refined to take into account regional features.

Within the Firth of Forth, Shennan (1989) subtracted a eustatic from a relative sea-level value to give an estimate of uplift/subsidence (including glacio-isostatic, hydro-isostatic and tectonic components) combined with the effect of more local scale factors, such as sediment compaction, and oceanographic and hydrological effects, including palaeo-tidal changes. The computed value also accounted for the effects of ice-water gravitational attraction (Peltier 1987) and localised neo-tectonic activity. There are currently only 11 data points for the Forth Valley. The scatter points reveal differential uplift in the estuary, with both upper and lower valley sites revealing exponential declines in the respective rates of uplift. The maximum values for current uplift are 2.0mm/yr. for the upper Forth Valley and 1.0mm/yr. for the outer estuary (Shennan 1989, p.86) (Figure 4.5).

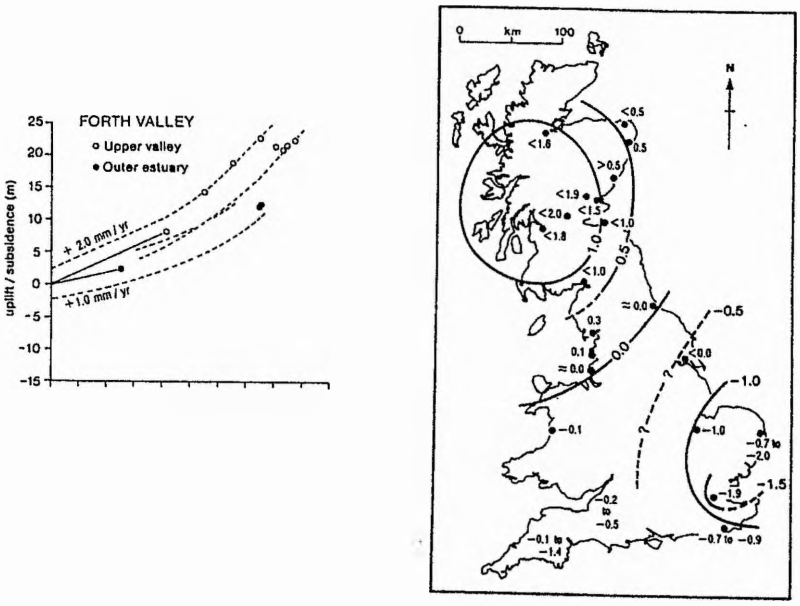

Figure 4.5 The pattern of Holocene uplift/subsidence inferred from individual sea level index points from the site in the Forth Valley, and a map of crustal movement in mm/yr (After Lambeck 1993b, p967).

In order to achieve a factor of precision better than 1m in uplift at British sites, Lambeck (1993b) incorporates in his model Fennoscandian and other distant ice sheets in order to include their far-field effects. As discussed previously, Walcott (1972) showed how relative sea-level at great distances from glaciated regions is affected by meltwater loading of the ocean floor. Further, the introduction of earlier load cycles for the ice sheets must also be included, because the past events will have a major effect on the planet. If a higher spatial resolution and smaller time steps can be introduced in the rebound models then it will be easier to identify the effects of glaciations such as that of the Loch Lomond Stadial.

The Scottish evidence outlined describes the relative sea-level changes from the Late Devensian era to the present day. Rates of uplift decreased in a curvilinear fashion throughout the Holocene until today, where estimates range from zero in south Lancashire and Tees Estuary, to over 1mm/yr. in central Scotland (Shennan 1989). The data have allowed for a range of estimates of isostatic uplift from 0.4 mm/yr. for North Scotland (Peltier 1987), to 1-2 mm for specific areas within the Forth (Shennan 1989). The range of values raises the question of the accuracy of these calculations, depending on whether the models are based on global criteria or local scale parameters.

4.6 Conclusions

This chapter illustrates that isostasy and eustasy are two highly complex processes that can individually and simultaneously induce changes in relative sea-level.

On a local scale, changes in sea-level can be identified by two methods; directly from index points, using sea-level indicators such as high water mark, and raised beach shorelines, or inductively by analysing marine organism features. Where sea-level changes have been investigated globally, *a priori* knowledge of deglaciation chronologies, the mantle viscosity profile and observed relative sea-level data for different areas allow a model testing methodology to be used (Peltier 1982), compared with the inductive approach used in local sea-level studies (Sissons 1966, 1967, Sissons & Brooks 1971, Sissons *et al.* 1969).

There are a number of fundamental factors which need to be addressed before global models of sea level changes can be applied to small areas and over restricted time scales as covered by this study. Inherent problems underlie the global theories on sea-level change, relating for example to inconsistency in quality of data across the globe and knowledge of earth rheology. More work must be undertaken on the geomorphological evidence at a local and regional scale. This opinion is confirmed by Clark *et al.* (1978) who argue that by considering relative sea-level changes throughout the world and comparing observations, it will be possible to 'infer' sea-level changes. Shennan (1987) proposed the aim for the future should be to combine the rigour of data verification in tidal analysis, with better regional scale models for ice sheet retreat and global models of earth rheology, in order to achieve a fully integrated approach to sea-level changes, at all scales.

In the Forth Valley the evidence collected by Smith (1968) has been used for numerous models on sea-level changes. These data for example have been used without critical examination by Lambeck (1993a, 1993b), in the development of complex glacial rebound models generated for the North Sea region. The field data collected by Sissons *et al.* (1966) relies heavily on a surveyor's level and visual observation. On visiting the East Fife shorelines, the visible 'breaks in slope' identified and surveyed by Sissons *et al.* (1966) proved difficult to locate. Since the period of active surveying in the 1960s and 1970s there have been few follow-up field investigations, despite significant advancements in technology which would allow for more accurate dating and positioning of palaoeshorelines. Such geomorphological evidence needs to be challenged as it is clearly influencing the generation of current global theories on isostatic rebound and sea-level change.

Within the UK, rates of differential crustal movements all show similar patterns of movement with relative uplift in Scotland and subsidence in the south of England. At present, work carried out by Shennan is the most detailed research available for the Forth Valley. However, the results are generated by subtracting a eustatic value from a relative sea-level. His results of 1-2mm/yr. of uplift occurring suggest that there is scope for a large margin of error to have been overlooked; the margin of error is not discussed in the paper. This result assumes that eustatic change will be constant. This chapter has shown that the evidence collected in

Barbados suggests that the eustatic changes will not remain constant over a given time period and that it is also difficult to assume that the relative sea-level, used in the calculation, will be sufficiently accurate at any level of confidence.

In conclusion, given the current data available, the estimations for isostatic uplift are likely to remain at the present level, as proposed by Shennan (1989) whose approach appears to be more precise in relation to the Forth Valley, given that he has used local geomorphological data. The rate of uplift along the south-east coast of Fife, is estimated to be 1-2mm/yr. (Shennan 1989). It is doubtful that such land movements would have triggered the rapid phase of erosion along the Buckhaven to Dysart coastline. Thus isostatic uplift, although an ongoing process, does not appear to be the underlying cause of the problems identified today.

Chapter 5. Estimating the effects of mining subsidence along the Buckhaven to Dysart coastline

5.1 Introduction

Mining subsidence is a well established specialist field. The aim in this chapter is to apply the techniques used in that field to the coastal environment, in an attempt to quantify the effects of the coal mining on the coastal equilibrium and then to present the field evidence of known subsidence movements to allow for a detailed discussion on coastal changes later in Chapter 7.

The comparison of measurements resulting from mining subsidence and coastal changes has never been undertaken, and a new method for combining these data sets has been established. GIS technology has been used to evaluate the risk of damage to structures from mine subsidence in Illinois (Hindman & Treworgy 1989). The investigation showed the coincidence of underground mines with urban areas and estimated the number and total value of housing units exposed to subsidence risk. The techniques used to scan the plans into the GIS system have been adapted here, although the aim here is to further develop the techniques outlined by Hindman and Treworgy (1989) and also quantify the amount of subsidence which has occurred. The initial techniques of scanning the mine plans into a GIS system to identify the exact location of the mine workings relative to the land surface was fundamental to relating coastal changes to mining subsidence. The use of the Surface Deformation Prediction System (SDPS) to quantify the mining subsidence ensured maximum accuracy. However, it became immediately apparent that Smallworld GIS was not ideal for overlaying grids of data for the production of a subsidence contour image. IDRISI GIS, a raster based GIS system, was more suitable for this type of data manipulation. The preparation of the mine plans for calculating subsidence values and then overlaying the results required preparing the data and taking it through three different software packages: Smallworld GIS, SDPS and IDRISI. The flow of data through each piece of software had to be repeated for each individual mine panel identified as influencing the coastal zone; a labour intensive task but one which ensured that the accuracy of the results was not reduced.

The major characteristics of the coal mining area in south-east Fife are outlined and the coal seams which underlie the coastal zone are briefly described. The methods of coal extraction will be explained. Principles of mining subsidence will be outlined, followed by a review of the main methods of calculations for mining subsidence. The influence function methods adopted in this thesis for calculating subsidence will be discussed along with details of the computing software used for the subsidence analyses, and the errors and limitations incurred in this procedure. The subsidence results will be presented in a summary format. Finally, field evidence in the form of benchmark evaluation supporting the results generated from the model analysis will be presented. Further analyses of the subsidence results will take place in Chapter 7.

5.2 The Fife coalfields

The south-east region of Fife is underlain by coal bearing rock successions, with the most productive coals occupying a 30km long by 5km wide strip between Largo and Cowdenbeath. These coal bearing strata which are known to extend over at least 35km^2 beneath the sea are divided into two groups, the Productive Coal Measures and the Limestone Coal Group (Goodwin 1959). The lower members of the group occupy the centre of the Thornton-Balgonie Syncline southwards from the Leven Fault, and the entire group extends north east in a broad belt as far as the Durie Fault (Figure 5.1). Dipping east beneath the Barren Red Measures in the centre of the Leven syncline, the Productive Coal Measures come to the surface again between the Durie Colliery and Lower Largo.

The Productive Coal Measures include the Lower Dysart Coal up to Skipsey's Marine Band. Its maximum development occurs to the south, towards Dysart, where the total thickness is of the order of 510-540m. North east, along the strike, the thickness diminishes to about 480m in the Michael Colliery, and to around 370m at the Wellesley Colliery. The lower members of the Productive Coal Measures have historically been of great economic value. The maximum exploitation occurred to the south-east where it contained up to 20 workable seams of coal, around Dysart and East Wemyss. Northwards and north eastwards from these points there is a steady decrease in thickness and coal content.

The list shows the stratigraphic names of coal seams found in the Productive Coal Measures and their depths:

1.	Skipsey's Marine Band	Surface level
2.	Pilkembare	71.4m
3.	Wall	88.0m
5.	Barncraig	100.0m
5.	Coxtool	129.5m
6.	Den	148.0m
7.	Chemiss	181.8m
8.	Bush	219.1m
9.	Wemyss Parrot	275.0m
10.	Wood	290.5m
11.	Earl David's Parrot	317.1m
12.	Bowhouse	340.3m
13.	Branxton	355.2m
15.	More	375.2m
15.	Boreland	398.4m
16.	Sandwell	408.4m
17.	Victory	435.1m
18.	Dysart Main	486.4m
19.	Lower Dysart	507.0m

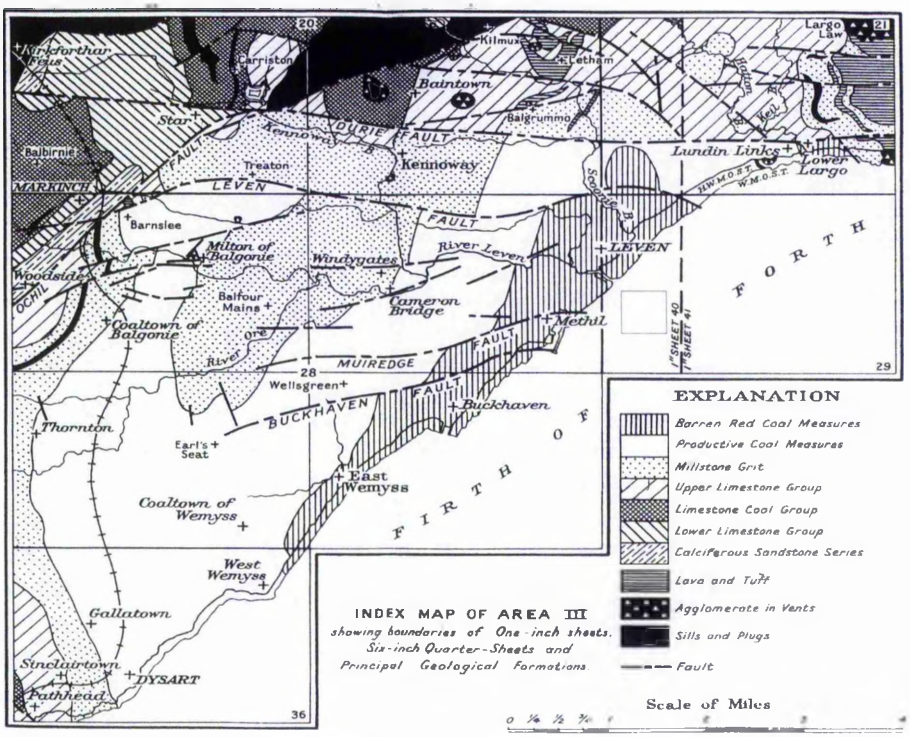

Figure 5.1 Geology of south-east Fife (After Knox (1954)).

There are 19 seams which are worked within the coastal area between Buckhaven and Dysart. Of these, 14 seams directly influence the coastal zone, and it is these which will be described in detail. Since the 1900s, along or near to the coastline, the coal was extracted from four main collieries, the Wellesley, Michael, Frances and Rosie mines. During the 1800s coal was worked from smaller individual pits such as Lady Pit and Victoria Pit at West Wemyss. The specific depths at which coal has been found at each colliery is noted in the mine shaft depths. These range from the shallowest seam, Pilkembare at approximately 70m below ground, to the Lower Dysart seam lying over 500m below the surface level. This summary does not attempt to document the full extent of the workings but merely identifies those panels which have influenced the coastal zone. Knox (1954) complied maps for each coal seam, illustrating the extent of the mining at that time, although the mine workings extended far beneath the Forth by the late 1960s. The figures (Figures 5.2-5.12), based on these maps, provide the reader with an indication for the locations of the different seams and their positions with respect to the coastline.

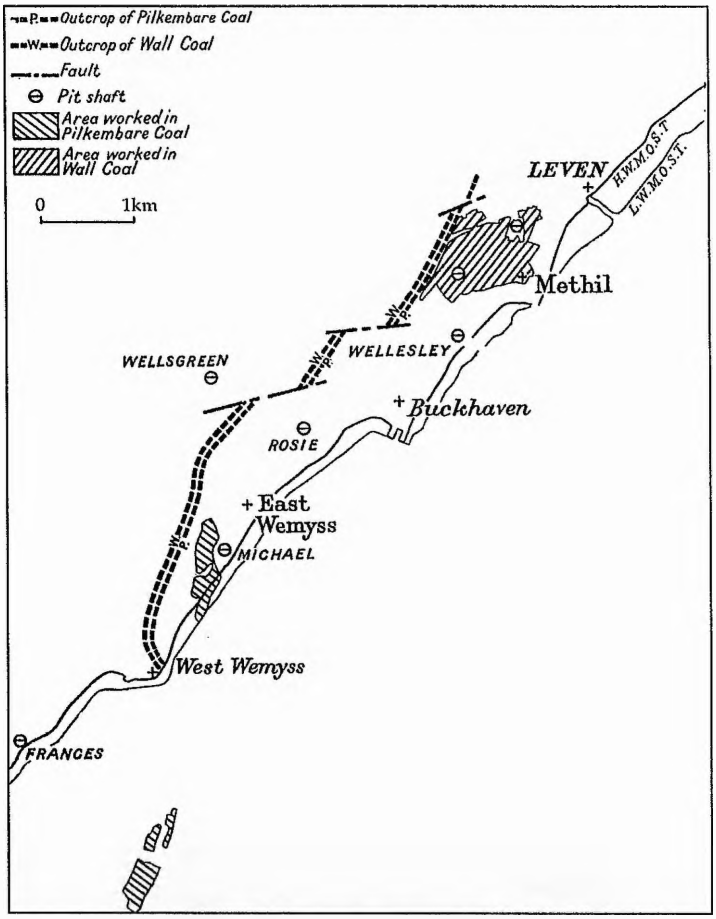

Figure 5.2 Pilkembare and Wall Coal: areas of coal worked along the Leven Dysart coastline until 1954. Adapted from Knox (1954 p.112).

The Pilkembare Coal or Wall Coal is the shallowest seam in the Productive Coal Measures. This coal seam was worked to a very limited extent in the coastal zone between the Michael and Frances Collieries. It was worked inland at Methil, and to the south of East Wemyss, landward of the 1914 HWM (Figure 5.2). Only the panel to the south of East Wemyss was of relevance to this thesis as it was a steeply dipping panel, whose subsidence trough was estimated to influence the coastal zone. Further north inland beyond the Wellesley Colliery the Pilkembare Coal was exploited to a greater extent. The coal lay at a depth of between 91m and 172.7m, dipping in a south-easterly direction by 18°. The coal at East Wemyss was worked out by 1923.

The Barncraig Coal was extensively worked within the south-east Fife coalfields especially along the coastline between West Wemyss and Methil (Figure 5.3). A total of 15 individual panels have been identified in this area, three of which were old stoop and room workings[1] at West Wemyss. The coal was taken out via the Michael, Rosie and Wellesley pitheads. Barncraig Coal was worked between 1851 and 1931. The coal dipped south-eastwards by

[1] Extracting coal by stoop and room method involves leaving pillars of coal to support the roof. For more information see section 5.3.

approximately 11°. The thickness of the coal extracted ranged from 0.84 to 2.29m, and it was mined between depths of 82m to 302m.

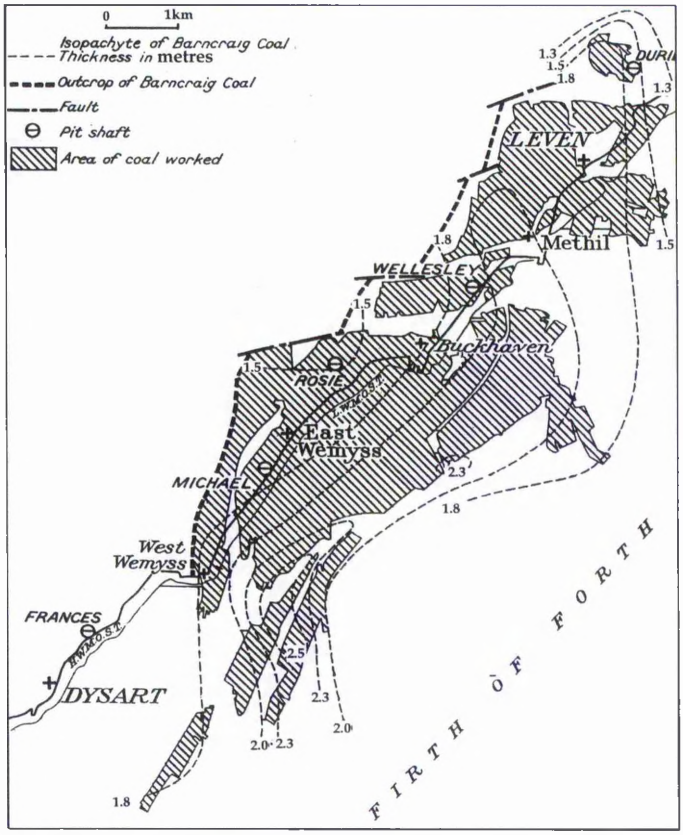

Figure 5.3 Barncraig Coal: areas of coal worked (until 1954) and isopachytes of seam. Adapted from Knox (1954 p.111).

The Lower and Upper Coxtool Coals were first mined in the Michael Colliery and were later exploited from the Rosie and Wellesley pits. At the Michael Colliery the Coxtool leaves[2] were worked separately. Further north in the Rosie and Muiredge collieries the coal was worked as a single unit. The map shows that the coal was mainly exploited between East Wemyss and West Sands of Buckhaven (Figure 5.4). Five large panels were identified as having influenced the coast. These were worked between 1914 and 1945. The coal was extracted between depths of 124m to 323.7m. The coal dipped in a south-easterly direction by approximately 7°. The thickness of the seam ranged from 0.5 to 2.3m.

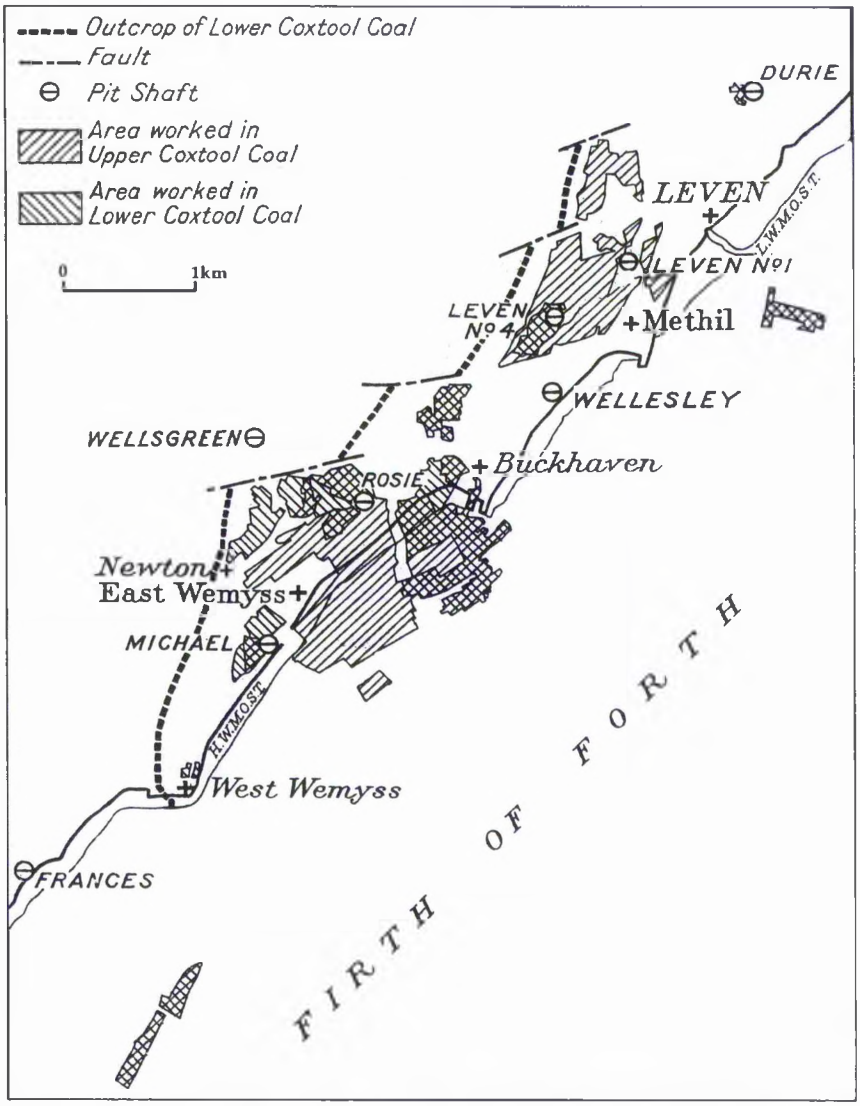

Figure 5.4 Lower and Upper Coxtool Coal: areas of coal worked until 1954. Adapted from Knox (1954).

[2] A single coal seam may be made up of multiple 'leaves' of coal, whereby layers of coal are interspersed with partings of unusable material.

The Den Coal was not mined along the coastal fringes and so was less relevant to this current study. It will not be referred to in this discussion; it was worked from the Leven Pits where its thickness varied between 0.5m and 1.02m. For more information see Knox (1954, p106).

The Chemiss Coal was extensively worked in the south-east Fife area; from the Wellesley Colliery to West Wemyss, where the oldest workings are found (Figure 5.5). The seam increases in thickness seawards, and southwards from Methil towards East Wemyss. A fourfold division of the seam is recognised. A total of 16 panels was identified as being of importance to the coastline. Older workings identified on the plans are too old for subsidence analyses to be performed due to the lack of recorded data. The seam dips on average by 11° in a south-easterly direction. The Chemiss Coal was taken out in the coastal zone between 1889 and 1918.

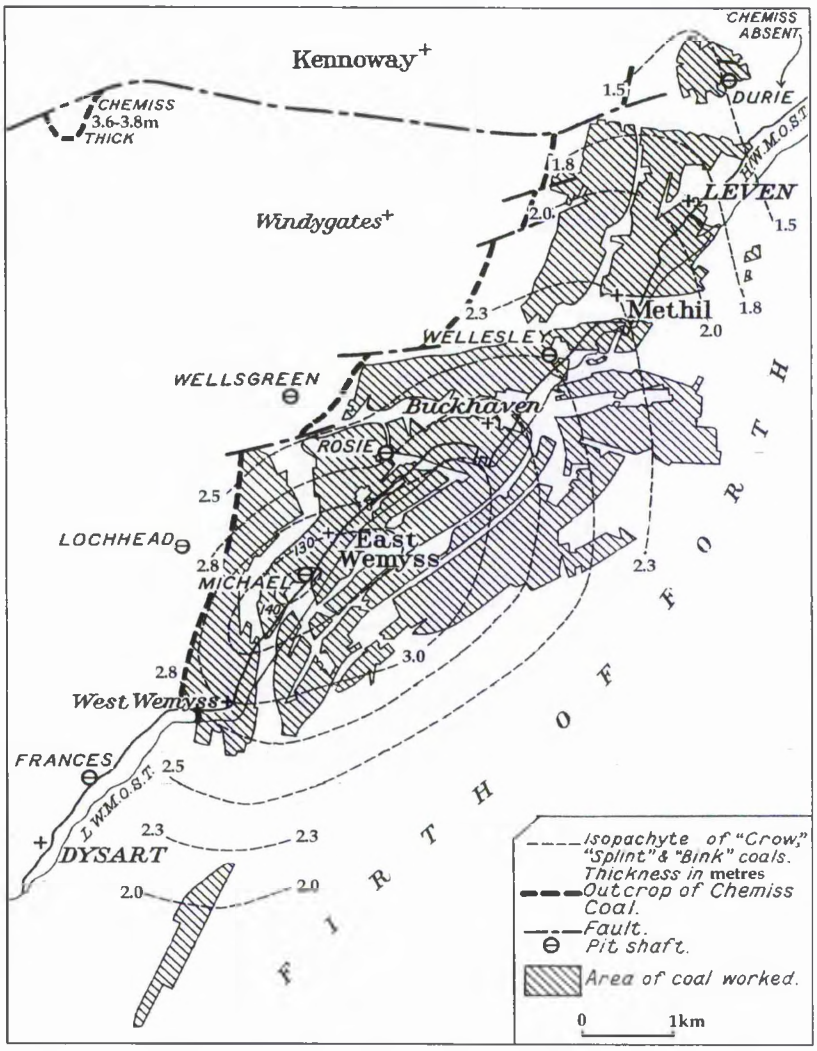

Figure 5.5 Chemiss Coal: areas of coal worked until 1954, and isopachytes of seam. Adapted from Knox (1954).

The main occurrence of the Bush Coal is in the Dysart area. It has been worked also, to a small extent in the Rosie and Michael Collieries. None of the workings influences the coastal zone. For more information on this seam see Knox (1954, p102).

The Wemyss Parrot Coal was recognised as an exceedingly inconsistent seam worked in only two limited areas; Newton and West Wemyss towards the Frances Colliery (Figure 5.6). Only one panel was recorded on the NCB 1:2500 plans. Knox (1954) states that the Wemyss Parrot Coal was mainly worked from the Lady Pit to a thickness of 1m, but was subject to numerous wants[3] revealed in the old workings. These wants are recognised to be the result of contemporaneous erosion during the early stages in the deposition of this overlying sandstone. Eastwards from West Wemyss the coal appears to deteriorate; records in the Michael Colliery indicates a thickness of 0.3m which was too narrow to justify working.

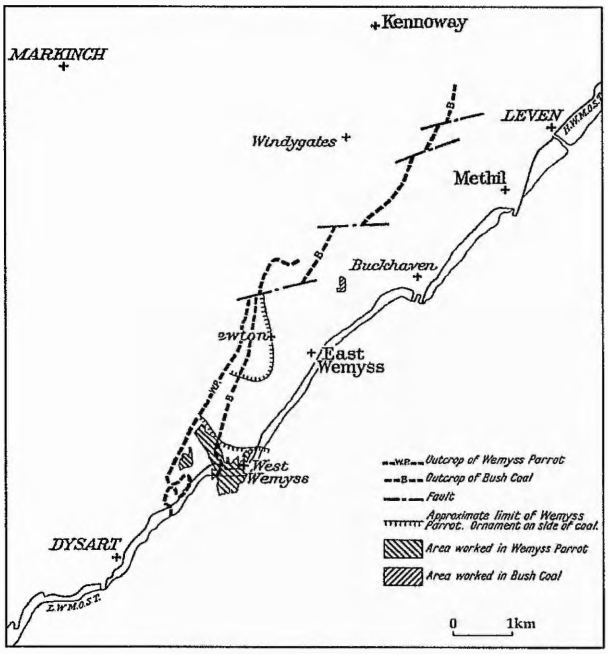

Figure 5.6 Wemyss Parrot Coal: areas of coal worked until 1954. Adapted from Knox (1954, p.101).

Four Feet Coal also known as Wood Coal, was mainly exploited in the West Wemyss area (Figure 5.7). Those worked panels identified provided no information, the only data available on the mine plans were the dates of extraction, in 1842. The location of the stoop and room workings offshore indicate that the subsidence will have been deflected away from the coast, and as a result, the subsidence caused by these older workings has been ignored. Knox (1954, p100) indicates that this coal varies in thickness considerably across the coal fields, being less than 0.3m in the north to over 1.8m to the south in the undersea region of the Michael Colliery.

[3] A want is defined as a small fault running through the coal, preventing the coal from being extracted.

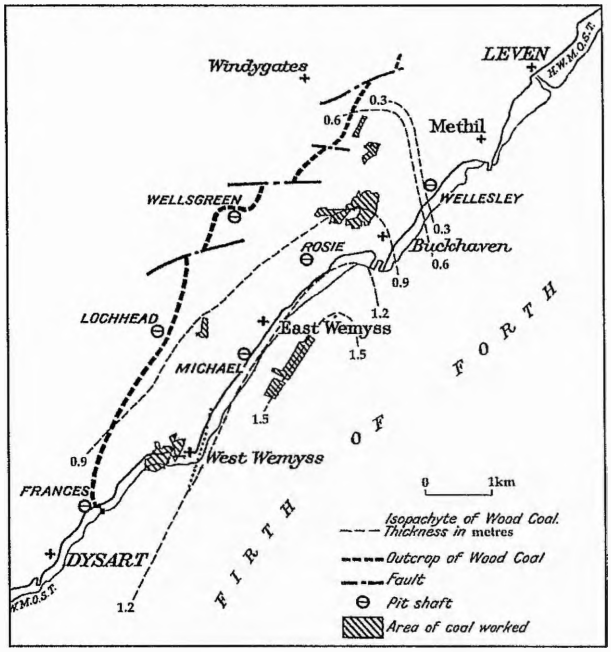

Figure 5.7 Four Feet Coal: areas of coal worked and isopachytes of seam. Adapted from Knox (1954 p.100).

The Earl David Parrot Coal was worked mainly in the Methil area, thus making it of no significance to this study. For more information see Knox (1954, p.97-99).

The Bowhouse Coal was extensively worked in the East and West Wemyss region (Figure 5.8). Nine panels have been identified for further investigation in this thesis. Workings in West Wemyss are characterised by predominantly stoop and room methods of extraction, two old panels have been identified but not included in the subsidence calculations. The coal was worked between 1891 and 1958. Mined between depths of 137.6m to 540.5m, the coal dipped steeply in a south-easterly direction, ranging in thickness between 0.91m and 2.74m.

The Branxton Coal was found inland towards Thornton as well as along the coastline between West Wemyss and West Sands of Buckhaven (Figure 5.9). Large extensive workings existed close to the Michael Colliery. One such panel which lies over 110m beyond the LWM of 1945, dips seaward by 18°, causing the subsidence to be deflected out to sea by more than 140m.

Another Branxton panel, located in the West Wemyss region is over 518m long and 107m wide. This is an old working, such that the mine plans provide only limited information on the date the coal was extracted; no information is available on the depth of working or the size of the remaining pillars produced from the stoop and room extraction method. These limitations on information make it difficult to produce an accurate result. The outline of these workings was included, although subsidence calculations were not performed for the panels in question. Four other panels have been identified, for which further analyses were performed, these were worked between 1873 and 1962. The thickness of coal ranged between 0.9m to the south of the

Michael Colliery to as much as 3.6m at West Sands of Buckhaven. The coal was extracted between depths of 255-540m.

The More Coal was worked in some areas of south-east Fife, but was not exploited within the coastal zone and thus is of no significance to the present thesis. See Knox (1954, p.93) for more information on this coal seam.

The Boreland Coal was found inland at Wellsgreen as well as in the Dysart region, surrounding the Frances Colliery (Figure 5.10). There were 3 main panels influencing the shoreline, one seam lies in the Frances area, and the other two panels lie close to the Michael Colliery pit head. The coal was worked between 1925 and 1960. It was approximately 0.9m in thickness and dipped steeply seaward at between 27° and 11°.

The Sandwell Coal was made up of two main large panels together with offshore workings which were identified as not influencing the shoreline (Figure 5.10). There is also one large panel at the Given Pit where coal was extracted during the 19th century. The coal seam ranges between 0.6 and 1.2m in thickness. The coal dips steeply seaward ranging from 7° and 22°. The workings were completed by 1939.

The Dysart Main Coal makes up one of the largest coal seams which has been exploited from all of the collieries fronting the estuary (Figure 5.11). The Dysart Main Coal consists of 3 leaves, two larger coal leaves and a third leaf also known as Coronation Coal. A total of 21 panels underlie the coastal zone between Buckhaven and Dysart. The workings located landward beyond the Wemyss Castle were estimated not to affect the coastal zone and have not been included in this analysis. The Dysart Main coal is extremely thick in the south-east Fife region, varying between 6m and 1.1m. It was mined to a depth of over 639m at the Michael to 109.1m to the south of the Frances Colliery. The coal was worked from 1881, at the Frances Colliery, until 1967. Beyond this date, the coal beneath the Forth was exploited; these workings will not have affected the shoreline and are not included in the present work.

The Lower Dysart Coal was extensively worked in the Dysart area (Figure 5.12). A total of 12 panels have been identified, 4 of which consist of two leaves. The coal was mined between 1915 and 1960, ranging from a depth of 156m to 556m. It again dips steeply towards the Forth, between 7° and 27°. Its thickness increases from the northern coal field towards the south-eastern area of Dysart.

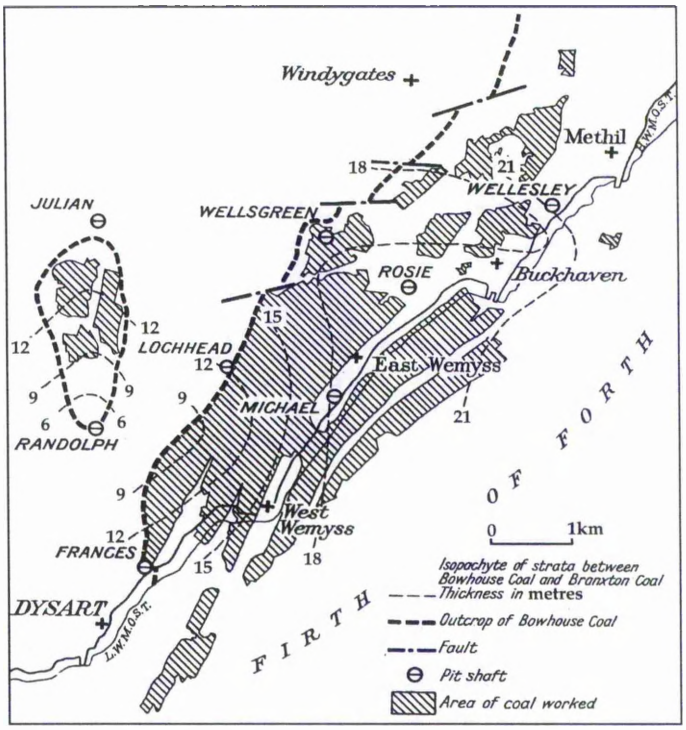

Figure 5.8. Bowhouse Coal: areas of coal worked and isopachytes of seam. Adapted from Knox (1954, p. 96).

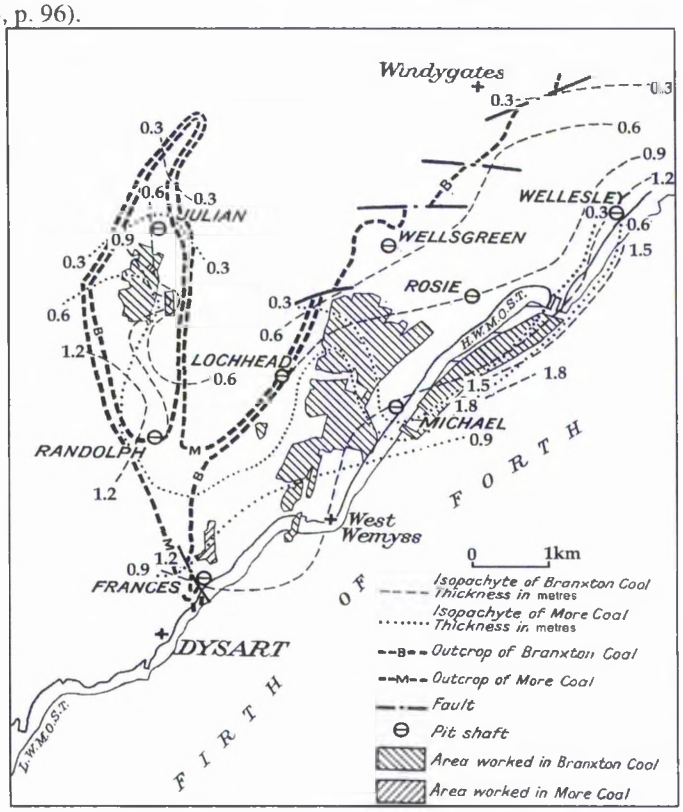

Figure 5.9 Branxton Coal: areas of coal worked and isopachytes of seam. Adapted from Knox (1954).

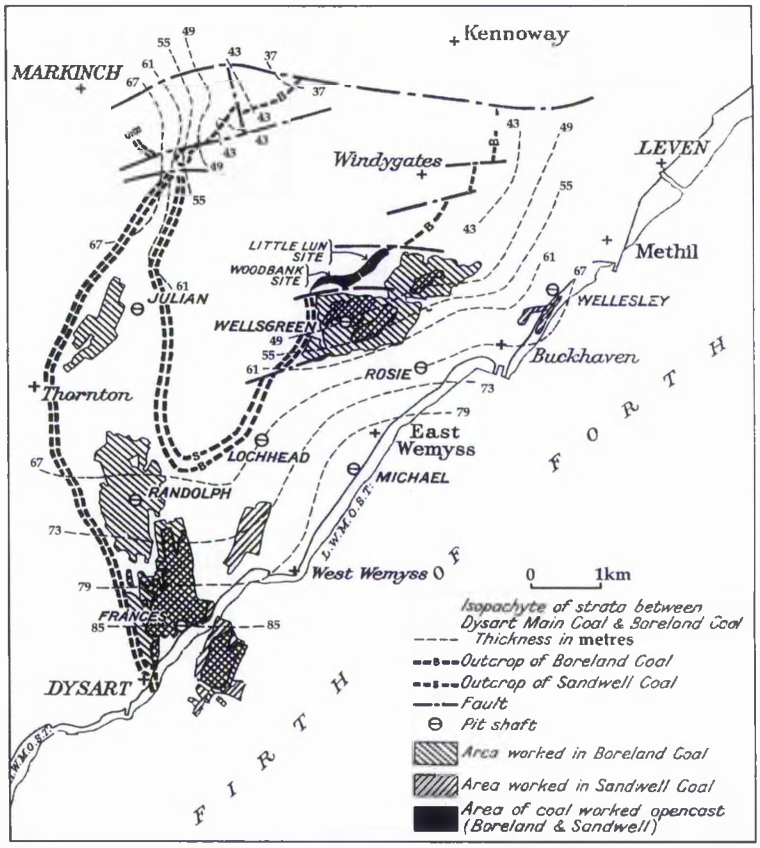

Figure 5.10 Areas of coal worked in the Boreland and Sandwell seams. Adapted from Knox (1954, p. 92).

Finally, Lethemwell seam had its coal extraction focused around the Frances Colliery. Six panels underlie the shoreline. The coal which was mined between 1964 and 1968, at depth of 277 m to 484m, ranged in thickness between 1.3m and 3.2m. It dipped in a southerly direction between 18° and 10°.

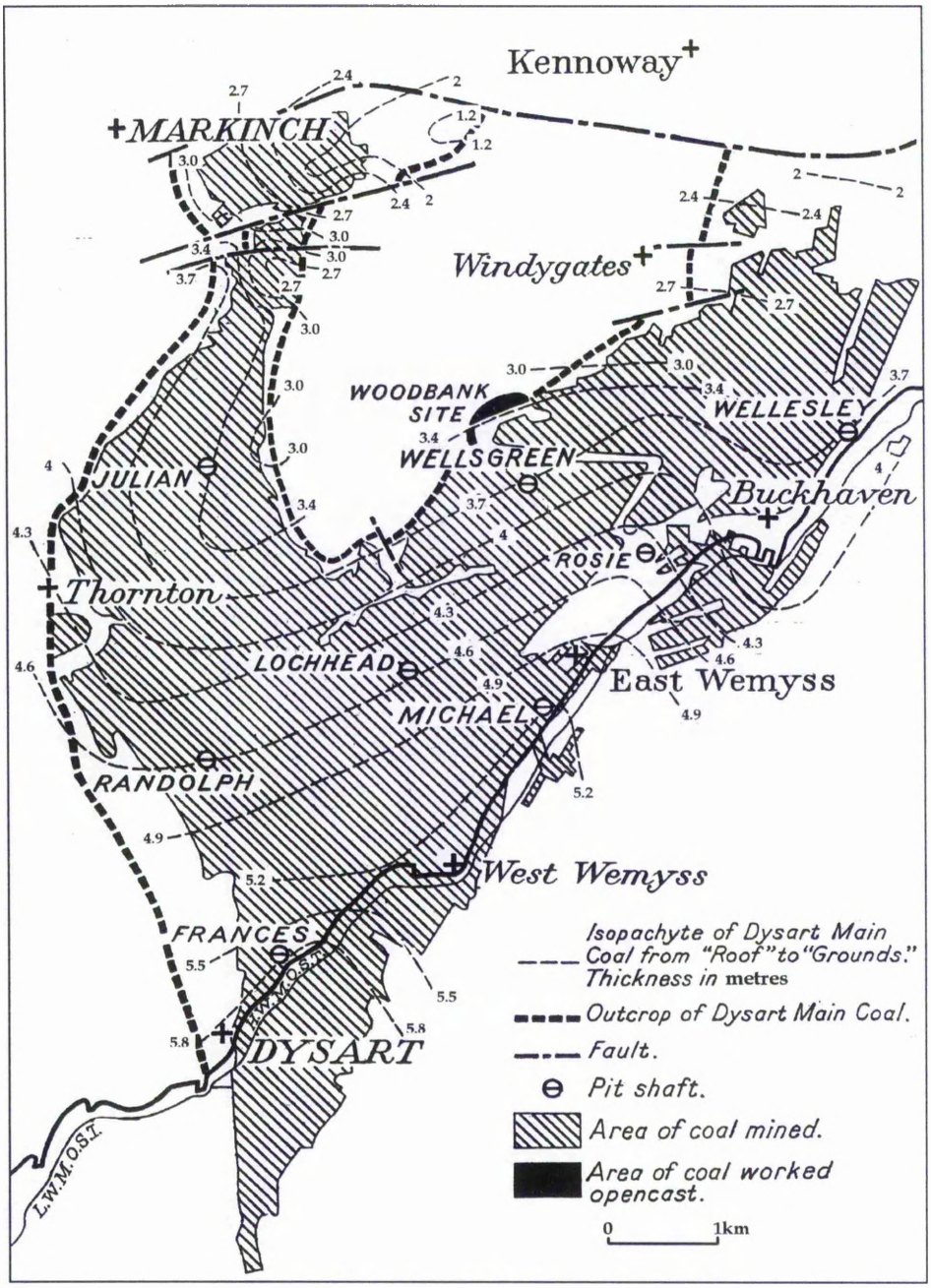

Figure 5.11 Dysart Main Coal isopatches of coal and areas of coal worked until 1954. (After Knox 1954).

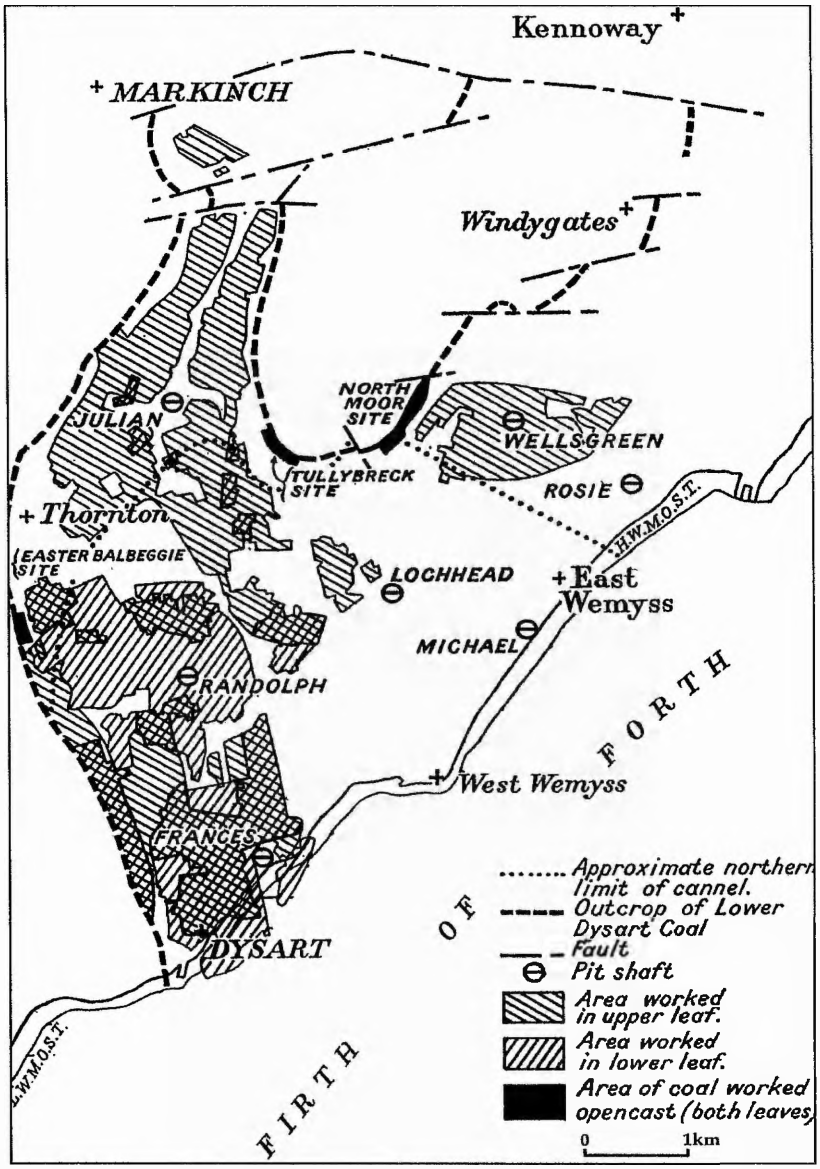

Figure 5.12 Lower Dysart Coal: areas of coal worked until 1954. Adapted from Knox (1954).

5.3 Coal mining techniques

Room and pillar workings, a method of partial extraction was the most common form of mining during the last century, especially where shallow seams were being worked (Malcolm 1996). Pillars of coal would remain in the working seam, in order to support the upper strata and overlying surface and would be created either at right angles to each other, or irregularly, depending on the thickness of the coal and the depth of the seam. It was common practice to leave these pillars unworked to give support to the roof of the mine until such time as they could be removed by a secondary system of mining called 'broken working' (Figure 5.13). Local mining conditions dictated how much coal could be removed by this secondary system of mining. Unfortunately, this secondary working is not always recorded on the mine plans, which can make it exceedingly difficult to identify areas which may be prone to sink-hole type of subsidence.

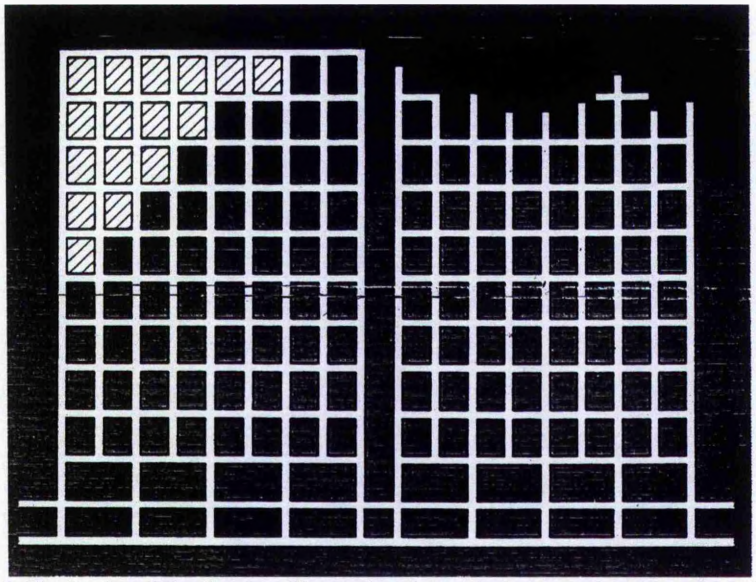

Figure 5.13 A schematic diagram illustrating the technique used to extract coal in stoop and room workings. Note how the pillars (black areas) are left to support the roof of the panel. The black areas indicates the unworked coal (After NCB Records). The white areas indicate where the coal has been extracted (roads). On some occasions the remaining pillars may have been removed at a later date - indicated by the hatched zone in the left of the image. The size of the pillars and roads would have been determined by the characteristics of the coal being worked.

In the case of room and pillar workings, the following two common forms of subsidence occur: sink-holes develop from collapsed mine junctions, whereby the roof above the area between pillars collapses producing localised holes. Sinkholes can occur at any time but are less likely where the rock cover above the seam is approximately 10 times the seam thickness. Pillar collapse is where one pillar with a factor of safety of around unity reduces in size as a result of weathering and can no longer sustain its load (Malcolm 1996). Collapse occurs transferring increased load onto surrounding pillars which may also collapse. The second form of subsidence, the saucer shaped depression is more common. Subsidence of the latter form can occur immediately, although it is governed by different parameters from those which control longwall workings.

Longwall workings were developed in the late seventeenth century and are generally the modern method of mining in the UK. The initial longwall mining system produced irregular workings where a number of tunnels advanced behind the coal face, or longwall, providing access to the coal face as shown in Figure 5.14. This technique was later superseded by the current highly mechanised longwall method of extraction producing rectangular mine plans (Figure 5.15). Longwall mining has the advantages of being economical and allowing for a high productivity capacity as well as controlling the amount of subsidence which develops. The panels are developed from an initial drivage within the seam, and as the face advances supports are withdrawn, which allows the roof to collapse behind the current working face (active subsidence). The system of longwall workings is based on either longwall advancing, where coal is worked away from the shafts and towards the boundaries, or by longwall retreat where

the coal is extracted back from the boundaries towards the shafts. The geotechnical conditions in the area and the dip of the seam will significantly affect which system is used. In areas where the seams are steeply dipping, the main extraction method involves working along the strike of the seam. The caving of the roof strata above a longwall working along the strike of a steeply inclined coal seam will give rise to an asymmetrical form of subsidence trough (Ren *et al.* 1989, Yao *et al.* 1991)

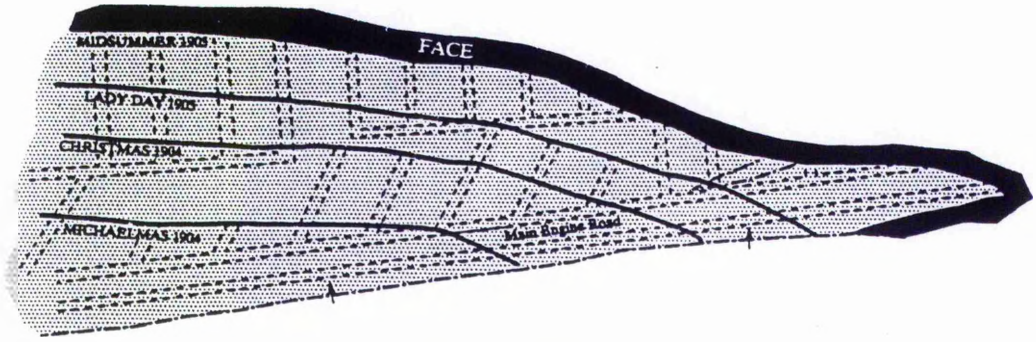

Figure 5.14 This method of mining 'hand filled longwall mining system' enabled miners to extract all the coal without leaving any pillars supporting the roof (After NCB Records).

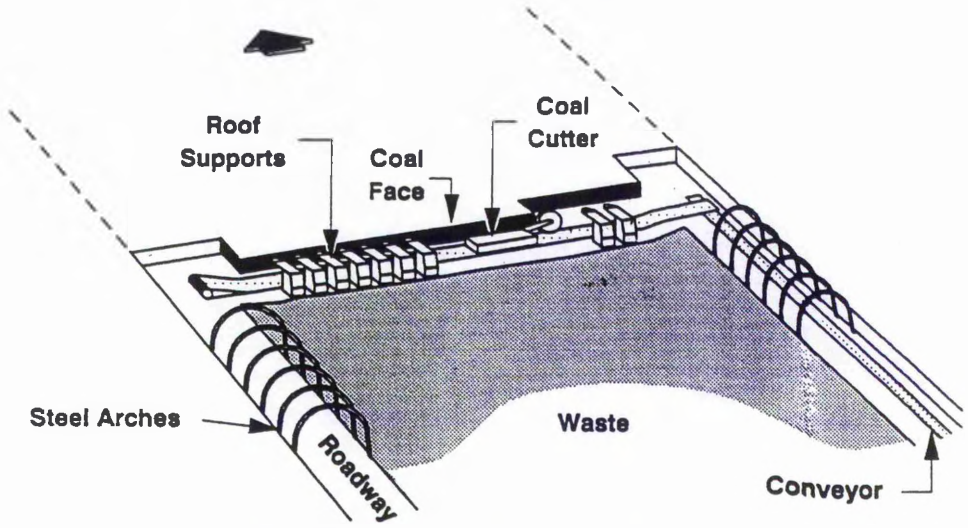

Figure 5.15 The longwall mining system. This mechanical technique meant that panels became more regular in shape (After NCB Records).

The amount of subsidence which occurs as a result of longwall extraction is dependent on the size and geometry of the mine plan, and whether any void-filling is incorporated in the operation. A certain amount of surface subsidence is associated with most large scale underground mining operations. The degree of effect ranges from no subsidence to highly localised features with destructive effects on the surface. The main cause of damage at the surface is due to ground strain, either tensile or compressive, which accompany subsidence (NCB 1975). The greatest damage is not always located at the point of maximum subsidence, but occurs where the greatest curvature is encountered.

5.4 Principles of mining subsidence

Subsidence will normally occur directly over the extracted coal panel in a trough-like shape that depends on the characteristics of the individual workings (Figure 5.16). A fundamental assumption of all prediction methods is that the surface subsidence cannot exceed the extraction thickness and that the maximum value of surface subsidence appears to be 0.9M, where the extraction conditions permit the development (Whittaker & Reddish. 1989, p.52).

The magnitude of full potential subsidence is a linear function of the extracted seam thickness. The following general expression is commonly employed in subsidence prediction assessments

$$S = a\,M \qquad (5.1)$$

where:

S= maximum value of subsidence

M= extracted seam height

a= subsidence factor.

The subsidence factor, *a*, is dimensionless and is dependent upon the nature of the overburden and type of goaf[4] treatment such as total caving or some form of stowing. In the UK the subsidence factor corresponds to 0.9, whilst stowing results in the factor being lowered to around 0.4 to 0.5 (Whittaker & Reddish. 1989). Solid stowing was introduced in the UK after 1960 (NCB 1975).

The amount of subsidence which will develop over a given seam is determined by the depth, width and length of the seam, the thickness of the coal extracted and by the operational techniques used.

The characteristics of the mining subsidence trough produced at the surface are influenced by the width to depth (w/h) ratio (Figure 5.17). Where the w/h<1.4, a subcritical panel is said to exist; maximum subsidence will not be achieved because the ribsides of the panel allow for the development of natural arching across the extraction. This is especially common in deep mining conditions (Whittaker & Reddish 1989). A critical extraction situation arises where the width/depth =1.4 which is just sufficient to allow the development of full potential subsidence. Full subsidence will develop at only one surface point. A supercritical situation exists where the w/h >1.4 allowing for the development of full potential subsidence at multiple surface points. The extraction width is too great in relation to the depth to allow for natural arching across the ribs on each side of the extraction.

[4] empty space left behind the working which can be utilised for the stowage of rubbish.

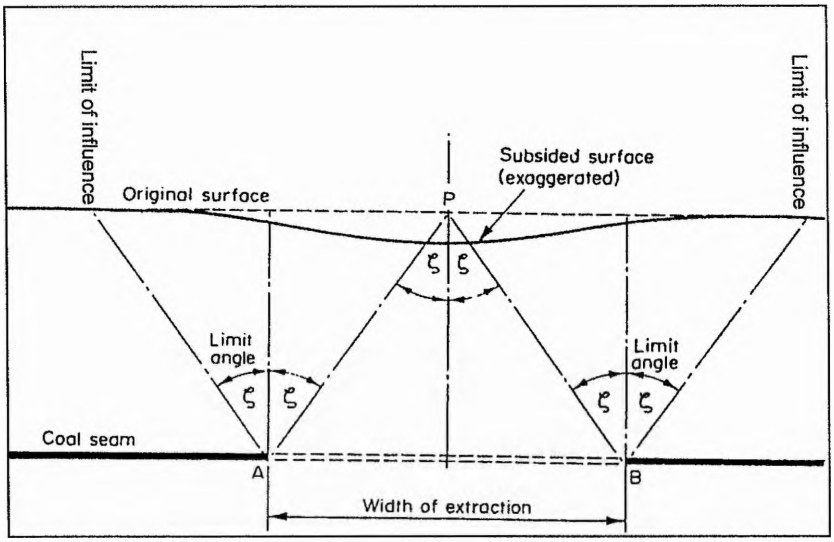

Figure 5.16 The main characteristics of the subsidence trough created from a coal panel. Note how the limits of the subsidence profile are determined by the angle of influence also known as the limit angle (After Whittaker & Reddish 1989).

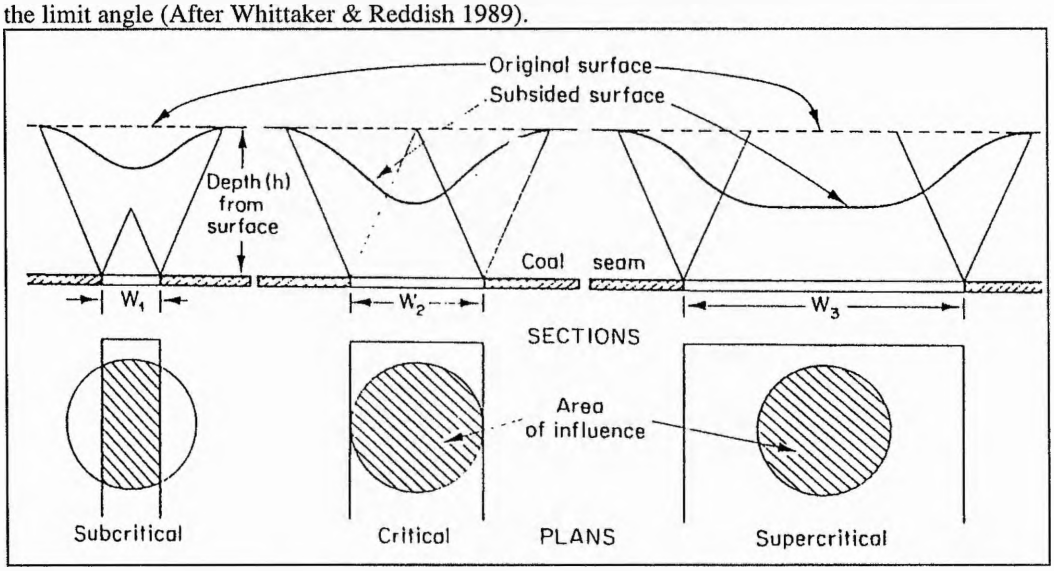

Figure 5.17 The change in surface subsidence by variation of the width working (w=width of panel extracted) (After Brauner 1973).

The shape of a subsidence curve will be determined by the factors above, along with parameters describing the local rock structures, including the rock properties in the overburden, the stratigraphy of the overlying layers and the surface topography. The limit of the effect of subsidence on the surface is defined by the angle of influence which has been determined by observations in British coalfields to average 35° to the normal of the seam. It indicates the limit of measurable movement and varies in different countries depending on the overlying strata conditions. The angle of influence or the limit angle, affects not only the maximum subsidence value, but also the shape and area of the subsidence trough generated from a particular panel extracted. Hence, the larger the angle, the larger the area of influence which the excavation has on the surface (in terms of the horizontal influence), but at the same time the maximum subsidence will be less. The gradient of the seam will also affect the limit angles. The subsidence trough will be tilted in the direction of the dip. A simple and reliable method for

adjusting the dip of the seam is to take the height of a given point and divide it by the gradient at that location (Malcolm 1996). This will generate the 'distance of throw' created by the gradient. The dip of the seam will affect the panel limits differently, depending if one is looking at the rise or limit side of the working (Figure 5.18). The limit angle does vary between sites and it is also affected by the thickness of the seam, so that a more accurate parameter for determining the limit of subsidence is the critical radius value, which is a distance parameter referring to certain percentages of full subsidence (Brauner 1973). The radius of the critical area, R, is the product of the extraction depth (h) and the tangent of the limit angle ($\tan \beta$) and is given by;

$$R = h \tan \beta \qquad (5.2)$$

where: R = radius of critical area

h = depth below surface of workings

β = angle of draw / limit angle: the angle subtended between the vertical and the line joining the extraction edge to the limit of subsidence.

Ground movements which occur at the surface are not confined to vertical lowering. Points on the surface, in addition to subsiding vertically, move laterally. Horizontal strain is proportional to the subsidence and inversely proportional to the depth (NCB 1975). The amount of strain which develops over a subsidence trough, is defined in terms of the change in length over a given piece of ground. The point of inflection which also signifies half maximum subsidence, indicates the point at which the ground extension changes to compression. On a critical panel, on a horizontal plane, the point of inflection will occur directly over the edge of the panel or ribside. For all other panels, i.e. subcritical and supercritical, the location of the point of inflection will be located beyond or within the ribside, depending on the panel geometry. This is also known as the edge effect, where the strength of the ribside and overlying geology determine the exact location of the half maximum subsidence (See Figure 5.16). This can be determined on an individual basis using empirical charts created in the SEH (Subsidence Engineer's Handbook). If the seam is dipping, the point of inflection will be shifted in the direction of throw.

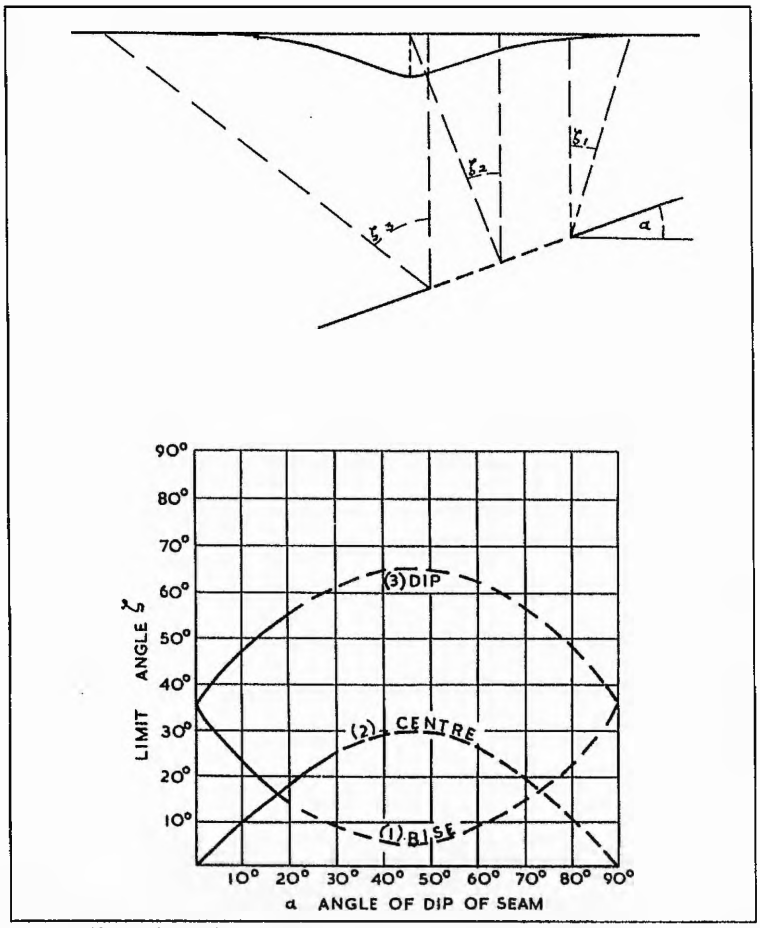

Figure 5.18 The effect of gradient on the resultant subsidence trough (After NCB 1975, p.18).

The principle of undisturbed super-position can be applied to the calculations of mining subsidence in multiple seam workings. This principle assumes that the displacement due to any extraction is not affected by the existence of displacements due to other extractions. Therefore the displacements which result from more than one extraction area are simply the sum of the displacement that would occur if each area was mined alone. This is only approximately true as every subsidence process will change the consistency of the rock mass above and the response of that rock mass to further mining extraction may become different; however, this variation is negligible and so the effects of each working are calculated separately and then summed (Brauner 1973).

Active subsidence will occur during extraction of the coal and the continued advance of the face. In addition to active subsidence there is time-dependent subsidence which continues after the active subsidence has ceased. This is called residual subsidence and its magnitude varies according to the distance from the face. Subsidence begins at the surface as soon as the face reaches a distance where the seam horizon begins to relax. The slumping of the ground above the extracted panel occurs immediately, with the effect being felt on the ground surface almost instantaneously. Identifying the time period of residual subsidence is more difficult. Sometimes it is claimed that damage has occurred several months after the workings passed, but

it is possible that the damage has only just been identified. Under some circumstances where open gate roads could close after a lapse of time, or in shallow workings there could, theoretically, be delayed subsidence. Strong strata in the overburden can also delay the residual subsidence, but these are the exception. When assessing mining subsidence which has occurred over 30 years ago, one can assume when dealing with longwall mining methods that vertical movement of the overlying strata will be complete (NCB 1975).

5.5 Methods for calculating mining subsidence

There are several methods for calculating subsidence based on either empirical data (e.g. Subsidence Engineer's Handbook (SEH), NCB 1975), or mathematical models (e.g. the influence function method). Attention will focus on the three main methods most commonly used; the profile function method, the influence function method and the SEH. Other methods include the analytical models which are based on treating subsidence as a problem which can employ the laws of elasticity, plasticity and visco-elasticity, and physical models which use small scale models to represent different mining situations for the purpose of observing the resulting subsidence behaviour.

5.5.1 Subsidence Engineer's Handbook (SEH)

The British SEH is based on the collection of a large number of observations throughout the UK, producing a level of accuracy greater than 10% for the prediction of the amount of resulting subsidence (NCB 1975 p.8). The subsidence values generated within the SEH are based on multiple workings where the overlying geology has been previously disturbed from other workings. The empirical data were collected from horizontal or gently inclined seams. For shallow dipping seams the SEH method provides satisfactory answers. For seams inclined at angles greater than 30°, the accuracy of the SEH method breaks down (Ren *et al.* 1989). The empirical curves were developed from actual cases in certain limiting conditions. These conditions are: a) where the total length of the panel is >1.4h; b) where the working panels have no centre gates[2] or other zones of special packing, apart from those at the main and tail gates; c) where the sides of the panel are not parallel, in which case the average panel width must be determined (NCB 1975, p.8). If a panel has not exceeded a length of 1.4h, then the maximum subsidence must be partially reduced using correction factors found in the SEH.

The SEH empirical method refers to longwall mining operations with fairly consistent mining extraction dimensions. It is assumed that the width of the longwall extraction (w) is fairly constant throughout the area of influence and the same applies to the extraction height (m). Irregular longwall extractions are not considered by the SEH prediction charts, nor are different thicknesses of extraction. The SEH contains several graphs of subsidence data. Important

[2] A small reinforced roadway which exists in the goaf area, which is supported by wooden or steel props and bars.

relationships were presented graphically, especially the dependence of subsidence on principal extraction dimensions. The generalised relationship between the principal variables is given by the equation (Whittaker & Reddish 1989, p. 56):

$$\frac{S}{M} = f\left(\frac{w}{h}\right) \tag{5.3}$$

where:

S = maximum subsidence

h = depth below surface

w = width of extraction

M = thickness of extraction

The ground strain values produced by the development of the subsidence trough can be calculated using the empirically derived formula below, to determine the maximum values of compressive and tensile strains:

$$E = f\left(\frac{S}{h}\right) \tag{5.4}$$

E = maximum value of ground strain.

The following worked example illustrates the basic procedures discussed above. Elements of this method are used at a later stage when preparing local mine plans for further analysis.
Example 1: L = 150m, depth(h) = 300m, width(w)= 180m, seam thickness = 1.5m. From Appendix 4, S/m= 0.61. Hence S= 0.61*1.5=0.915m. This is maximum subsidence for an extraction length L=1.4h (i.e. 420m). The correction for the limited face advance is :

$$\frac{advance}{h} = \frac{150}{300} = 0.5$$

Referring to Appendix 5 this value of 0.5 on the bottom scale gives an s/S value which is 0.51. Therefore the reduced S for the limited face advance = 0.915m x 0.51= 0.467m. This is the maximum subsidence over the centre of the of the rectangle of goaf (NCB 1975, p.10). It is then possible to identify the position of half maximum subsidence, and the shape of the subsidence trough by using Table 1 from the SEH to construct a profile of the subsidence (Appendix 6). This has been produced in the Table 5.1 overleaf, together with a simple graph illustrating the shape of the subsidence trough (Figure 5.19).

The results overleaf, illustrate the shape of the subsidence trough and the subsidence values at specified points along the profile, which have been specified via table 1 (NCB 1975, p14) (Appendix 6). This technique is easy to apply to simple rectangular troughs. The procedure for identifying the position of half maximum subsidence will be used in the preparation of the mine plans of south-east Fife; this will be discussed in more detail later.

s/S	0	0.05	0.1	0.2	0.3	0.4	0.5	0.6	0.7	0.8	0.9	0.95	1.00
S(m)	0	-0.023	-0.0467	-0.0934	-0.1401	-0.187	-0.234	-0.280	-0.3269	-0.3736	-0.4203	-0.4436	-0.467
Distance (h)	1.00	0.59	0.47	0.36	0.3	0.26	0.22	0.19	0.16	0.13	0.09	0.06	0
Distance (m) from panel centre	300	177	141	108	90	78	66	57	48	39	27	18	0

Table 5.1: Example 1 relationship between w/h (=0.6) and d/h for various points on the subsidence profile

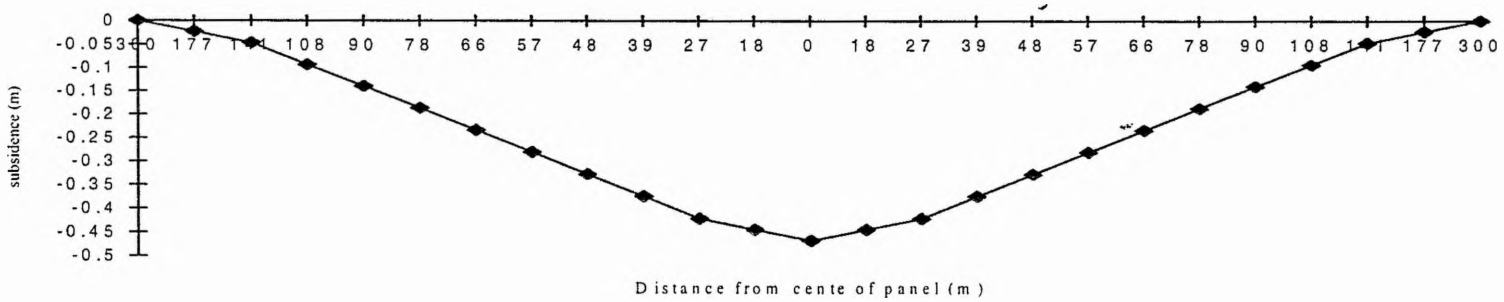

Figure 5.19: Plotted subsidence profile, using data from Example 1.

5.5.2 The profile function

The profile function defines the distribution of the subsidence and strain values on the surface along a profile perpendicular to the boundary, for a theoretically infinitely long panel; this is to eliminate the effect of the length of the panel when calculating subsidence for seams where L<1.4h. The parameters are empirically based. The function is applicable to panels of rectangular shape. The geometry of the excavation together with equations or tables of data are used to predict a longitudinal or transverse profile for subsidence or strain (Whittaker & Reddish 1989). Its advantages are that it can be easily applied to subcritical workings and produces accurate results. On the other hand, the profile function is unable to cope with irregular mine workings. The profile function has been used extensively throughout the world because it is relatively easy to apply to new situations. For a detailed review on the state of the art profile functions see Brauner (1973) and Kratzsch (1983).

5.5.3 The influence function

This method for calculating subsidence focuses on predicting subsidence at particular surface points. A typical influence function looks at annular zones around a point and uses equations to relate the percentage extraction in each area to the subsidence of that point. The formula used is based either on empirically derived functions which use arbitrary constants to produce the desired value and form of subsidence or it will include parameters which describe the rock properties and mechanics of the extracted area.

The influence function is based on the concept that the distribution of ground movement, either subsidence or strain values, is caused above an underground excavation. The principle of superposition is applied to allow for the calculation of subsidence over any mining geometry. The subsidence trough is imagined to be composed of infinitesimal troughs which are produced by the extraction elements (Figure 5.20). The trough is broken down into an infinite number of parts, and the individual elements of the trough are added together to produce subsidence for the point P on the surface. Therefore each extraction area dA will make a contribution to the overall subsidence of the surface.

$$K_Z = f(r) \qquad (5.5)$$

where:

K_Z = magnitude of influence of dA on P

r = horizontal distance between position of P and the infinitesimal element dA.

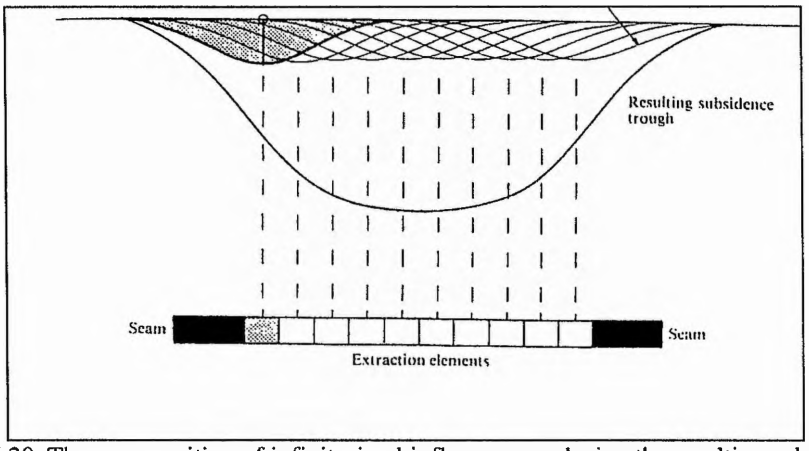

Figure 5.20 The superposition of infinitesimal influences producing the resulting subsidence trough. (After Whittaker & Reddish 1989).

The equation above is the standard form of an influence function as related to subsidence prediction. The product of dA and the influence function K_Z gives the contribution which that element makes to subsidence of a surface point. This principle is illustrated in Figure 5.21 (Whittaker & Reddish 1989, p.63).

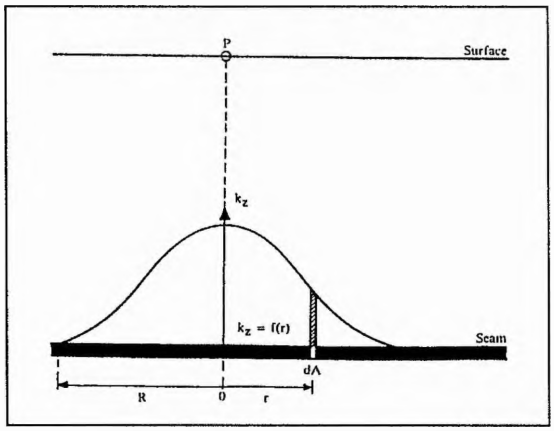

Figure 5.21 The influence of the subsidence for a given point on the surface. (After Whittaker & Reddish 1989).

The area of influence around a point P above a seam working is considered circular in shape. The radius of the circle of influence is defined by the depth of the working at that point and the angle of draw (which will be the same in all directions because it is a horizontal seam).

The actual location of P on the surface will affect how many individual elements will influence the subsidence value. When P is positioned in the centre of a critical width of an extraction, then P is influenced by all the elements within the range, governed by the function and resulting in full subsidence at P. When P is located over the extraction edge (of a critical width) then it experiences only half of the possible influence, resulting in half of the full subsidence. The point of inflection coincides with S/2.

The influence function is based on the principle of superposition and thus can be applied to multiple seam workings. It can be adapted to any mining situation because the function

depends mainly on the radius of influence (R). It can also take into account the effect of the coal pillar remaining within the coal seams (Marr 1975). The influence function uses more rigorous mathematical methodology compared with the methods used in the profile function. However, because the influence function can cope with more complex workings some of the accuracy is reduced at a cost of its added flexibility (Whittaker & Reddish 1989, p.75). Ren *et al.* (1987) demonstrated that the influence function method is capable of giving reasonably accurate predictions of subsidence in steeply dipping seam situations, with the greatest accuracy evident with gently dipping seams. One of the major drawbacks of the influence function is that it is considerably more difficult to apply than profile functions and much more difficult to check and calibrate (Whittaker & Reddish 1989, p55).

Selected influence functions include Keinhorst's, Bal's and Knothe's methods. For a detailed review of these different techniques see Whittaker & Reddish. (1989 p.63-76).

5.5.4 The Surface Deformation Prediction System (SDPS)

Ren *et al.* (1989) discussed the flexibility of using the influence function for subsidence prediction. The subsidence profiles which they produced using the afore mentioned protocol showed favourable comparison with NCB (1975); an accuracy of generally better than 5% when compared to the standard subsidence data. As a result of these published results, it was decided to purchase a suitable subsidence prediction program capable of performing subsidence calculations. An American Surface Deformation Prediction System (SDPS) which had been developed by Karmis & Agioutantis (1989, 1992), was able to monitor subsidence in the USA and it boasted the ability to apply the influence function method to any coal mining environment in the world.

The SDPS package is able to calculate subsidence, surface slope, horizontal displacement, horizontal strain and surface curvature in any given direction at individual surface control points, using either the profile function or influence function method. This software has been developed for US coalfields where the empirical parameters differ from the UK experience.

The accuracy of the SDPS system when dealing with irregular workings arises from its ability to calculate any combination of ground movement in any direction, which allows for the simple determination of the cumulative subsidence effect.

The influence function method in the SDPS package is able to calculate superposition of the subsidence calculated, from a number of excavated areas having different mining characteristics. The function utilised in the SDPS is the bell-shaped Gaussian function (Knothe 1957). This method assumes that the influence function for the two dimensional case is given by:

$$g(x,s) = \frac{S_o(x)}{r}\exp\left[-\pi\frac{(x-s)^2}{r^2}\right] \quad (5.6)$$

where

r = the radius of principle influence = $h/\tan\beta$

h = the overburden depth

β = the angle of principle influence

s = co-ordinate of point P, where subsidence is considered

x = co-ordinate of the infinitesimal excavated element

$S_O(x)$= convergence of the roof of the infinitesimal excavated element

Subsidence at any point P(s) therefore can be expressed by the following equation:

$$S(x,s) = \frac{1}{r}\int_{-\infty}^{+\infty} S_o(x)\exp\left[-\pi\frac{(x-s)^2}{r^2}\right]dx \quad (5.7)$$

where

$S_O = m(x)\,a(x)$

$m(s)$= extraction thickness

$a(x)$ = roof convergence (subsidence) factor.

If $m(x)$ and $a(x)$ are constants with respect to x, then $S_O(x)$ is a constant:

$$S_O(x) = S_{max} = ma = constant\ for\ x_1 \le x \le x_2 \quad (5.8)$$

where x_1 and x_2 are the limits of the excavation and :

$$S(x,s) = \frac{S_{max}}{r}\int_{x1}^{x2}\exp\left[-\pi\frac{(x-s)^2}{r^2}\right]dx \quad (5.9)$$

The data required to generate subsidence values include: the geometry of the mine plan and the associated properties (extraction thickness, subsidence factor for supercritical conditions); the co-ordinates of the points on the surface for which prediction of the deformation indices (subsidence, strain, slope, curvature and horizontal displacement) is to be performed; and the numerical parameters which represent the behaviour of the overburden (Karmis *et al.* 1994, p35). This enables the system to reflect the subsidence characteristics of the area in question.

The geometry of the mine plan can be either rectangular or an irregularly shaped panel. Similarly the surface prediction points can be specified as a grid, by cell size in both the x and y direction or as scattered prediction points. The scattered prediction points are more relevant if the investigation was to be focusing on a single line of subsidence. The program would assume that half maximum subsidence would occur over the ribside unless the user informed the system otherwise. The user has complete control on adjusting the program to reflect the subsidence characteristics of a particular area.

5.6 The Fife coalfields: method adopted for calculating subsidence

This section lists the reasons for selecting the chosen method of calculating mining subsidence and then outlines the procedure required to prepare the raw data from the basic mine plans through to the stage where they were ready for calculating the final subsidence values using the appropriate software.

The area for which mining subsidence is to be calculated relates only to the coastal strip between Buckhaven and Dysart. The area has been extensively mined, using both mining extraction methods of stoop and room and longwall mining. Many of the older seams consist of highly irregular workings. Section 5.2 outlines the complexities of the multiple seams which are common along the entire coastal stretch. The coal dips gently in the direction of the Forth, with the majority of seams dipping in the region of 11-20°. It is most appropriate to use the influence function method for the calculation of subsidence values as this method is able to cope with gently dipping seams, multiple workings and irregular panels. Finally, as the principle of superposition is applicable to multiple seam workings, a summation of subsidence values can be used to produce total values of movement for the area in question.

Using the influence function within the SDPS, it allows for a more accurate and detailed analysis of subsidence values than could be generated by using the profile function or SEH manual. This was of particular importance to the present thesis where the many simplifications of the mine workings necessary for the latter two methods would lead to a reduction in the accuracy of results along the coastal strip of south-east Fife. Adjustments to the SDPS were required so that it conforms to the British geological conditions, and not to the American situation. Karmis *et al.*(1989, 1992)) confirmed that the package was easily adjusted to become site specific without introducing any loss of accuracy. The best approach would have been to fix the SDPS against local data reflecting the subsidence characteristics in south-east Fife. However, this was not feasible due to an absence of actual subsidence measurements; thus the aim was to ensure that the SDPS results corresponded with those from the SEH.

With stoop and room workings the pillars which remain within the panels have the effect of increasing the stability of the extracted area and reducing the possible maximum subsidence. Hence the maximum subsidence generated will be significantly less than the subsidence produced from long-wall workings. As discussed previously, the second form of subsidence associated with stoop and room are sink holes which tend to lead to unpredictable catastrophic collapse. The general slumping of the trough associated with these workings can be estimated through a combination of empirically and mathematically based techniques. The width and length of the individual pillars, together with the total width and depth of the panel, are used to generate a factor of safety, based on the empirically based UK data set (Wilson 1990). This result translates directly into a maximum subsidence value which can then be used in the

influence function method within SDPS software. For a simple worked example to create the factor of safety see Appendices 8 and 9.

5.6.1 Adjustments of the SDPS to fit the empirically based SEH

The standard method for the calibration of different subsidence techniques is to compare the results for specified points along a subsidence profile ranging from maximum subsidence at the centre of the panel with zero subsidence beyond the panel ribside. This approach has been used to calibrate the SDPS influence function with the SEH empirical results. Four specific, but hypothetical panels (subcritical, critical, supercritical and stoop and room) were created to reflect the different workings most commonly found within the south-east Fife area. The influence angle was initially set at 35°, and the tangent of the angle of influence was 1.4. For each given panel, subsidence values were calculated using the SEH method. The SDPS method was then applied and the overburden parameters were adjusted to yield subsidence values that best fitted those results using the SEH method along the entire subsidence curve. The overburden characteristics within SDPS were adjusted to a varying extent for the different characteristic subsidence troughs (so as to reflect the SEH results). As a result the tangent of influence angle was adjusted to 3.1 for subcritical and all stoop and room workings. For these panels the maximum subcritical subsidence value was manually generated using the SEH tables and the results were fed into the SDPS software. For all critical and supercritical panels the tangent influence angle was estimated at 1.95, and the maximum supercritical subsidence factor (of 90%) was input in to SDPS. This value was based on the NCB (1975) which states that for supercritical panels maximum subsidence was estimated to be 90% in the UK. For those panels worked after 1960 when solid stowing was practised, the maximum subsidence for supercritical and critical seams was reduced to 45%. The SDPS was capable of adjusting for the edge effect, but required the empirical parameter, i.e. the percentage of overlying hard rock in the area; this information proved more difficult to obtain. Hence, the edge effect was adjusted manually using the SEH empirical data set. The co-ordinates fed into the system were already adjusted to reflect the edge effect; the program assumes that the inflection point is over the rib of the excavation.

For each example outlined below, subsidence was first calculated using the SEH manual; this was then repeated using the SDPS program. The points along the profile where comparisons of subsidence values were made, were determined by Table 1 of the SEH (1975, p.14) (Appendix 6). Detailed information on each of the examples can be found in Appendix 8. These examples are the results from a collection of tests performed to establish the correct parameters for the subsidence calculations. The parameters used here for the different classified panels were later used in the production of the subsidence values for the south-east Fife coastline. All of the subsidence results shown in the examples fall within the accepted error range as discussed by Karmis *et al.* (1989).

5.6.2 Example 1: subcritical panel

The degree to which the two curves conform to each other is illustrated in Figure 5.22, with most of the variation occurring at the outermost points of the subsidence trough. Note, however, that the SDPS underestimates the possible subsidence values which means that the overall values produced at the end will be a conservative estimate of the total subsidence. Maximum subsidence was estimated to be 67%. A comparison of the subsidence values generated from the SEH and SDPS methods suggests that most discrepancies occur at the outer edges of the profiles, where there are significant variations in subsidence values. As a percentage of the maximum subsidence, the difference in subsidence values at these outer points is very small. For example at 85m from the centre of the panel, the SEH predicts 0.2m subsidence whereas the SDPS software predicts 0.054m of subsidence. As a percentage of the maximum subsidence the difference between the two values works out to be 7.4%. In contrast, at the centre of the panel the error difference is 1% and at half maximum subsidence the subsidence values are identical.

Point	Distance along profile (m)	SEH results(m)	SDPS results (m)	σ %
1	172.5	0	0	0
2	102	-0.1	-0.005	95
3	85.5	-0.201	-0.054	73
4	69	-0.402	-0.278	30.8
5	60	-0.603	-0.537	10.94
6	54	-0.804	-0.760	5.47
7	48	-1.005	-1.005	0
8	43.5	-1.206	-1.19	1.33
9	37.5	-1.407	-1.421	1.0
10	30	-1.608	-1.657	3.05
11	21	-1.809	-1.847	2.1
12	15	-1.909	-1.921	0.63
13	0	-2.01	-1.985	1.24

Table 5.2: Comparison of SEH and SDPS subsidence values along a cross section of a subcritical panel. The measured distances from the centre of the panel are based on the SEH empirical calculations using table 1 (SEH 1975 p.14) (Appendix 6).

Where: σ, the error is given by: $\sigma = \left(\frac{S_{SEH} - S_{SDPS}}{S_{SEH}} \right) x100\%$.

Mean error = 17.3%

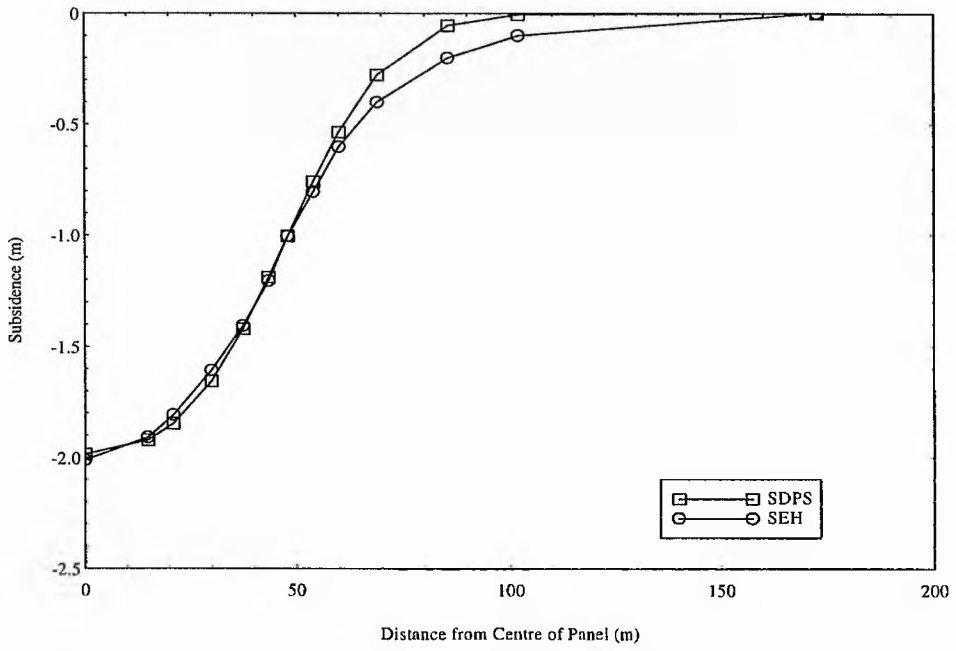

Figure 5.22 Subsidence trough for a hypothetical subcritical panel, using the influence function method and SEH method.

5.6.3 Example 2: stoop and room panel

Maximum subsidence equals 15% using the empirical formula by Wilson (1990). The SDPS influence function over-estimates the subsidence values at the centre of the panel by between 22 and 11%, whereas it underestimates the subsidence values beyond the half maximum value (Figure 5.23). The shapes of the two troughs are concordant, with the minimum and maximum values for each curve being identical. (Mean error =17.2%).

Point	Distance along Profile(m)	SEH Results (m)	SDPS Results (m)	σ %
1	0	0	0	0
2	57	-0.023	-0.002	91.3
3	75	-0.045	-0.014	68.9
4	99	-0.09	-0.062	31.1
5	114	-0.135	-0.128	5.2
6	126	-0.18	-0.17	5.6
7	138	-0.225	-0.216	5.0
8	150	-0.27	-0.262	3.0
9	162	-0.315	-0.306	2.9
10	180	-0.36	-0.377	5.7
11	210	-0.405	-0.42	3.7
12	243	-0.428	-0.442	3.3
13	390	-0.45	-0.45	0

Table 5.3: Comparison of SEH and SDPS subsidence values along a cross section of a stoop & room panel.

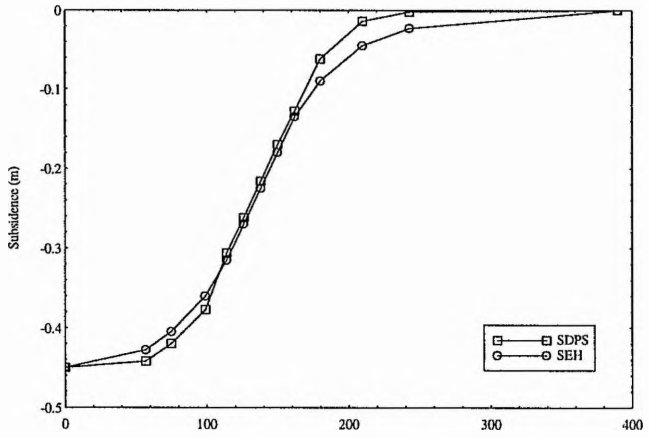

Figure 5.23: Subsidence trough for a hypothetical stoop and room panel, using the influence function method and SEH method.

5.6.4 Example 3: critical panel

Critical maximum subsidence = 87%, w/h=1.5. Both the SEH and SDPS subsidence profiles demonstrate similar characteristics (Figure 5.24). The maximum value of subsidence is located at the same point. The maximum value of subsidence generated by SEH is 1.65m compared to 1.70 for SDPS, a 2.80% error margin. For half maximum subsidence there is a differential error of 3.5% between the subsidence values. Towards the edge of the subsidence profile the SDPS tends to underestimate the subsidence values in the region of 24%, quantifying this in terms of subsidence on the surface equals 8.2cm against 7.5cm. (Mean error = 8.35%)

Point.	Distance. along profile	SEH results (m)	SDPS results (m)	σ% error
1	420	0	0	0
2	273	-0.0827	-0.075	9.3
3	240	-0.1653	-0.206	25.6
4	210	-0.3306	-0.422	27.6
5	192	-0.4959	-0.595	19.98
6	180	-0.6612	-0.722	9.20
7	168	-0.8265	-0.855	3.45
8	156	-0.9918	-0.988	0.38
9	144	-1.157	-1.115	3.63
10	129	-1.3224	-1.261	5.64
11	105	-1.4877	-1.449	2.6
12	81	-1.57035	-1.576	0.36
13	3	-1.653	-1.699	2.78

Table 5.4: Comparison of SEH and SDPS subsidence values along a cross section of a critical panel

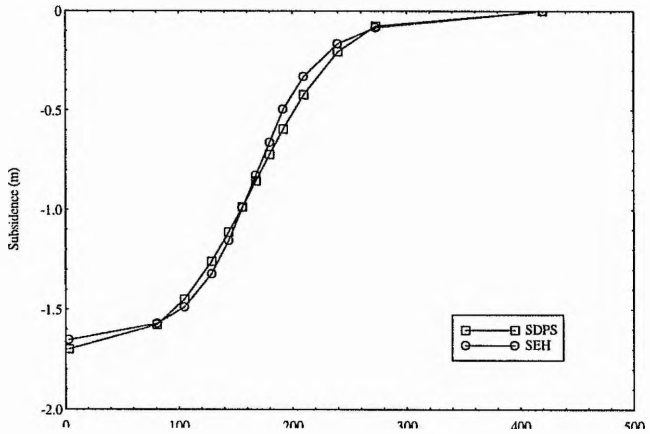

Figure 5.24: Subsidence trough for a hypothetical critical panel, using the influence function method and SEH method.

5.6.5 Example 4: supercritical panel

Maximum subsidence = 95%, w/h=1.5. The tangent of influence angle is estimated to be 1.95. The minimum and maximum values of the subsidence profile generated by the 2 methods are in the same location and are of equal heights (Figure 5.25). The shapes of the two curves vary slightly; in particular the location of the half maximum subsidence is different. Over a distance of 50m beyond the point of inflection, the SDPS curve has higher values of subsidence in the region of 16.8%. Inside the point of inflection the SDPS underestimates the subsidence values by 2.4%, which falls within the accepted error range, as discussed by Karmis *et al.* (1977). The mean subsidence error between the SEH and the SDPS values generated results is 9.5%. The greatest variation occurs at the outer limits of the trough.

Point	Distance along profile	SEH results (m)	SDPS results(m)	σ% error
1	375	0	0	0
2	252.5	-0.0895	-0.089	0.55
3	225	-0.179	-0.239	33.5
4	200	-0.358	-0.478	33.5
5	185	-0.537	-0.666	25.02
6	175	-0.716	-0.802	12.0
7	165	-0.895	-0.942	5.25
8	155	-1.074	-1.081	0.65
9	145	-1.253	-1.212	3.27
10	132.5	-1.432	-1.361	5.96
11	112.5	-1.611	-1.55	3.79
12	92.5	-1.7	-1.674	1.53
13	12.5	-1.79	-1.798	0.45

Mean error = 9.5%

Table 5.5: Comparison of SEH and SDPS subsidence values along a cross section of a supercritical panel

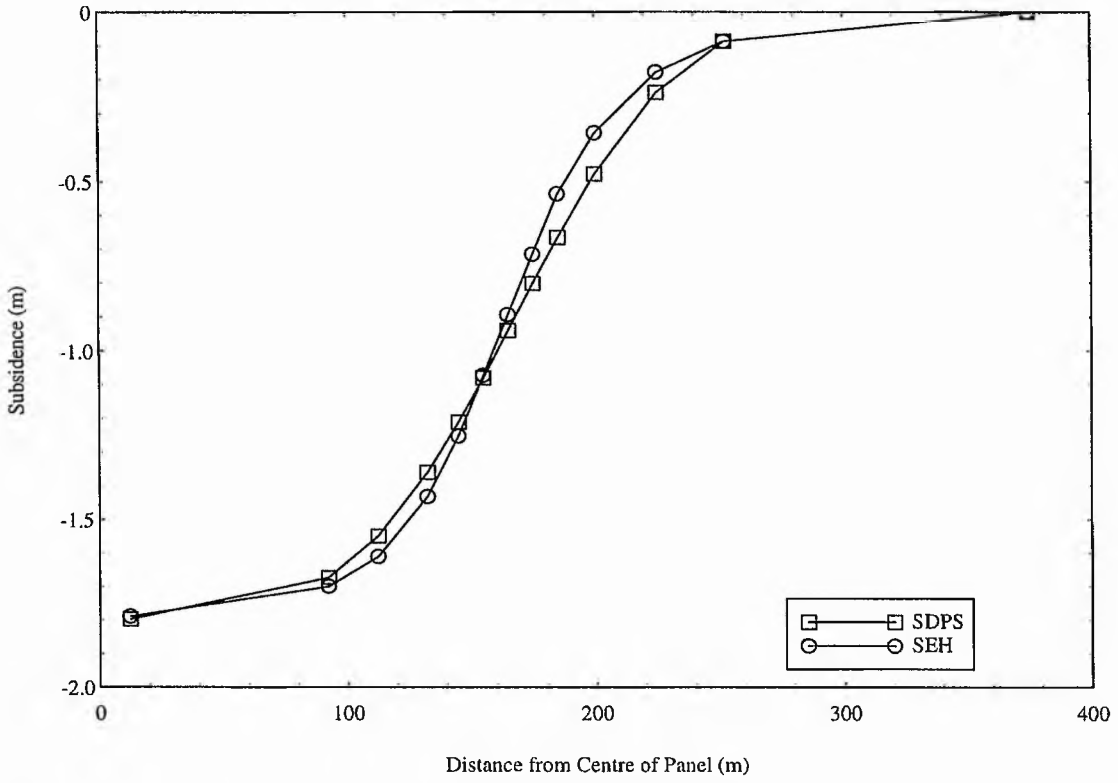

Figure 5.25: Subsidence trough for a hypothetical supercritical panel, using the influence function method and SEH method.

5.7 The preparation of the mine plans

The flow chart (Figure 5.26) outlines the preliminary stages of analyses required before the mining subsidence calculation can be produced. The fourteen coal seams which influence the coastal zone between Buckhaven and Dysart have previously been discussed. The 1:2500 mine plans collected from the NCB include surface information which facilitated the identification of those workings which underlie the HWM and LWM. A zone approximately 100m either side of the high and low water marks was used as a guide from which panels were selected for analysis. Those workings which 'skimmed' the coastal boundary were assessed on an individual basis, to estimate whether subsidence generated from the panel would affect the coastal zone. If the maximum subsidence (which would not occur directly over the coastal zone) was estimated to be less than 10cm, then the panel was omitted.

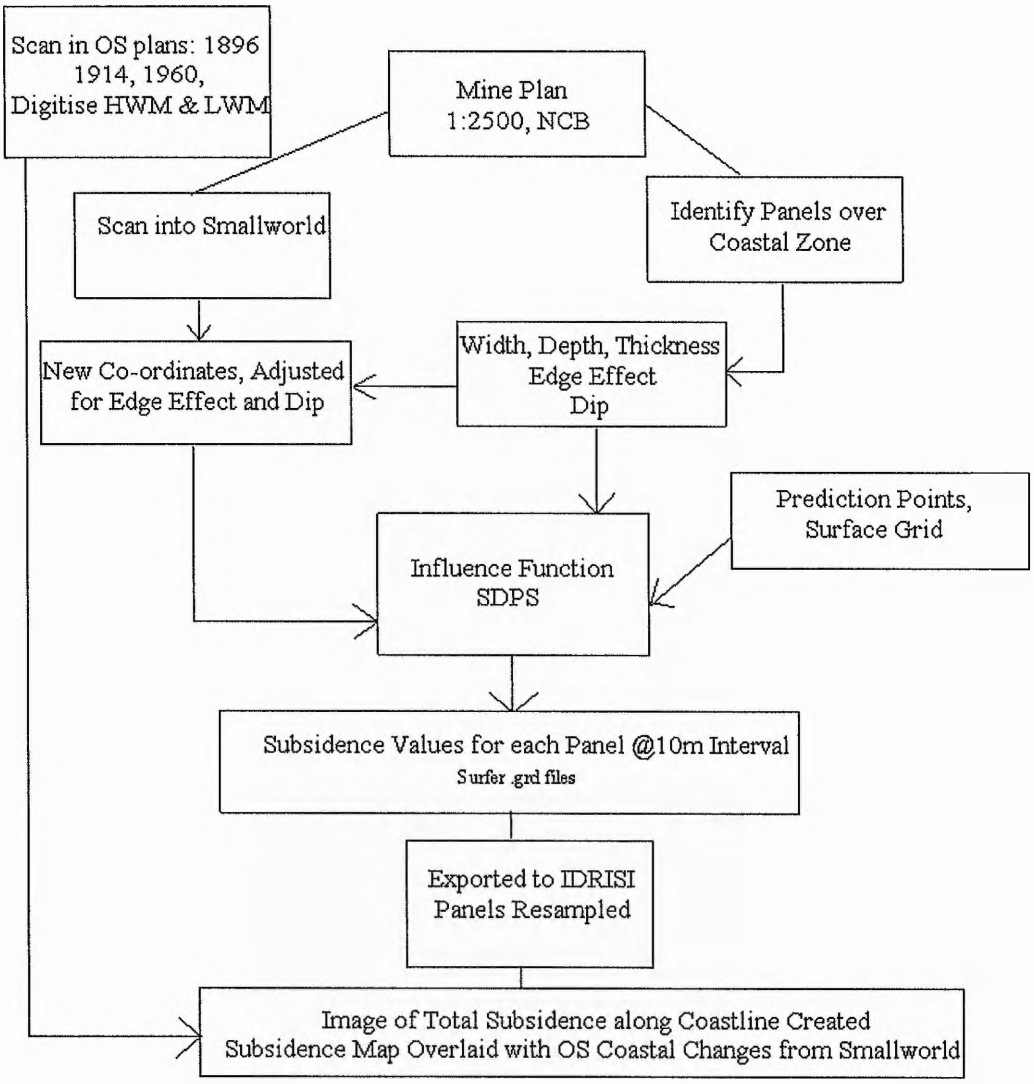

Figure 5.26 The stages of preparation required to calculate a subsidence image for the south-east Fife coastal zone.

The mine workings in their raster format were scanned into GIS Smallworld and snapped into the real world. This procedure involves digitising four real co-ordinates on each mine plan and then 'sending' the sheet to the real co-ordinates in the system; using the technique described in chapter 3. This enabled the exact co-ordinates on any point of the mine plans to be located.

For every seam the workings were divided into panels. These were selected by following the natural breaks such as roadways found in the coal seam. For each panel, the height (taken at 10 000ft below OD plus the height above surface), width of the panel (mean width if the panel was irregular) and thickness of coal extracted were recorded. The width to depth ratio was calculated. Not only did this indicate how the panel would react, (i.e. whether it was supercritical, critical or subcritical) but this information was also used to locate the half maximum subsidence in conjunction with the use of Table 1 (NCB 1975, p.14) (Appendix 6).

If the panel was critical then the half maximum subsidence would occur directly over the ribside; however, many of the panels identified here were subcritical and thus the edge effect had to be taken into account. Many of the seams were dipping in an irregular fashion. Each point of the panel was adjusted for the effect of dip separately. Having previously scanned the mine plans into Smallworld GIS, it was possible to revisit these rasterised seams, and by locating the individual points in the GIS system, and shifting the point in relation to the edge effect and effect of dip, new co-ordinates were produced which could then be fed into SDPS (Figures 5.27, 5.28, 5.29). These new points were then used to produce accurate subsidence values at real OS grid points. (See Appendix 10 for details on individual points of panels).

In order to calculate subsidence values using the influence function, co-ordinates on the ground surface are also required. The spatial distribution of points needed to reflect the changes in subsidence in the coastal zone had to be as dense as possible. Some of the panels identified on the mine plans were extremely large, over 500m in length. Due to the limitations of the PC system used, it was evident that assessing the total amount of subsidence produced for some panels in one process using the influence function, limited the density of prediction points on the surface grid. Consequently the prediction points were divided into sections across a given panel, to ensure that prediction points were produced at constant 10m intervals.

The prediction point grid represents the exact locations on the surface where the corresponding subsidence values were calculated. Due to the irregular shape of the majority of workings, grids larger than these panels were created in order to encompass the entire subsidence troughs generated. The surface level for all the panels has been assumed to be identical to the surface level of the mine shaft. This is a safe assumption as the study area is along a low-lying coastal stretch. Work by Frank and Geddes (1986) indicates that plane ground strain values and horizontal movements are significantly affected by surface slope, whereas the vertical movements are not. This relationship is of importance to the present thesis as, in some locations, close to the Frances Colliery several workings underlie the steeper ground. However, as Frank and Geddes (1986) illustrate, the subsidence values will have an insignificant affect on the slope.

On completion of the data preparation, the manual inputting of data into the SDPS software could proceed. A total of 14 seams and 92 panels were identified as influencing the coastal zone (Appendix 9).

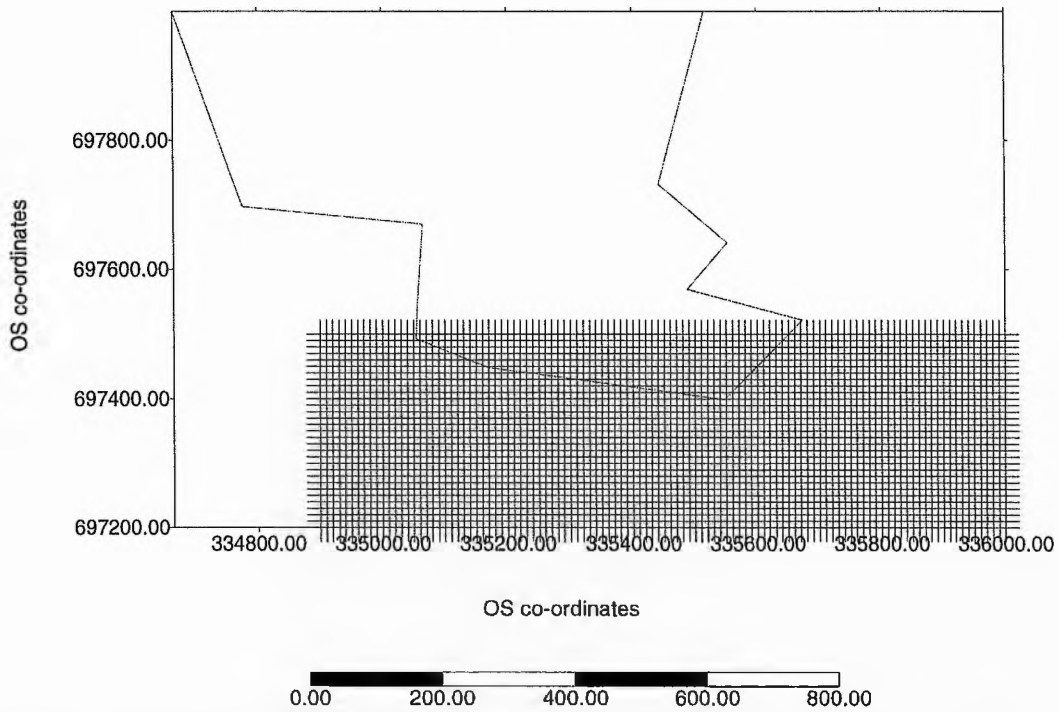

Figure 5.27 Panel Barncraig A, with subsection of the prediction point grid overlying the panel co-ordinates. Note how the grid is significantly larger than the panel itself, this is to ensure that the entire subsidence trough is recorded within the grid. Barncraig A consisted of three such prediction grids. The south of this particular panel overlies the West Sands of Buckhaven and Buckhaven harbour.

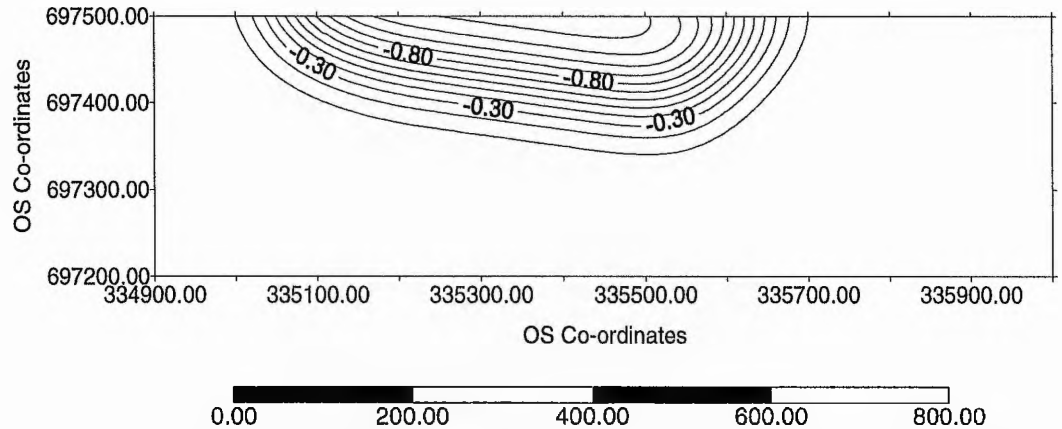

Figure 5.28 A 2D image of the subsidence trough produced for the prediction point illustrated in Figure 5.27. Barncraig A panel. Note how the sub-section of the whole subsidence image shows the edge of the trough.

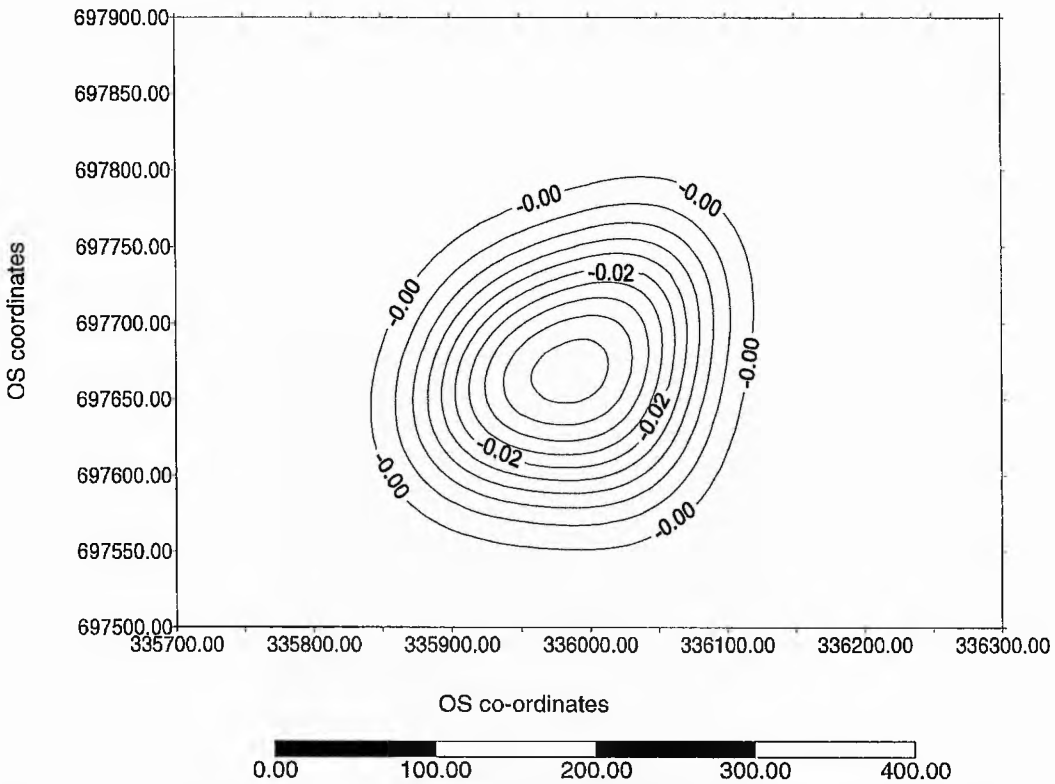

Figure 5.29 A 2:D subsidence trough generated from a small panel in the Barncraig seam. The maximum subsidence was estimated to be 3.5% (5cm). This panel was located close to Shore Street, Buckhaven.

Seam	Long Wall Panels	Stoop & Room Panels	Old Panels	Mean dip	Mean Thickness (m)	No. of Leaves.
Pilkembare	1	0	0	1-5	1.2	1
Barncraig	16	4	2	3-6	1.5	1
Coxtool	5	0	0	4-8	1.19	2
Chemiss	18	3	1	3-7	2.15	2
Wemyss Parrot	1		1	2.5		1
Branxton	4	0	1	3-5	1.6	1
Bowhouse	8	0	2	2-16	1.5	2
Boreland	3	0	0	2-14	1.0	1
Sandwell	2	0	1	3-8	0.9	1
Dysart Main	14	8	0	3-11	2.9	4
Lower Dysart	14	4	1	4-7	1.6	2
Lethemwell	6	0	0	3-6	2.5	1

Table 5.6: Summary of coal seams and relevant panels underlying the coastal zone between Buckhaven & Dysart.

The individual co-ordinates of each panel together with the thickness of the coal extracted, depth of the working at each point of the panel were fed into the computer. The subsidence values were produced on 10m grids over individual panels, where some larger panels were

divided into 5 sections. The results were saved as surfer .grd files, which were immediately imported into IDRISI.

The next stage involved resampling the subsidence files and, using the principle of superpositions, all the individual subsidence troughs were overlaid, in order to produce a single image of subsidence.

Once in IDRISI, the data were converted into individual raster grid files, to produce regularly spaced pixel images of each panel (mine panel). Each pixel was approximately 10mx10m in size and was assigned a subsidence value, the z co-ordinate. In order to create a single map of the amount of subsidence which had occurred along the coastal zone, every panel generated in the SDPS package needed to be standardised and then overlaid. This procedure involved formatting all the individual files to contain the same number of columns and rows. The resampling involved creating a new raster image from the original file, where the co-ordinates were large enough to encompass the whole coastline.

5.8 Errors and limitations

Although some of the errors generated within this procedure can be quantified, there remains an element of uncertainty in the accuracy of the raw data used. There is no guarantee that all the mine workings have been documented on the mine plans; more subsidence may have occurred than suggested in this investigation. For the majority of workings dated earlier than the 1860s at West Wemyss (Victoria Pit) and at the Frances Colliery (Given Pit), the plans provide only an outline of the coal worked, with no indication of the depth of the panels, the dip of the seams or the thicknesses of coal extracted. The 1872 Act made the keeping of mine plans a statutory obligation from the 1st January 1873. In these early cases, for which there is no information on the coal extracted, the areas of workings have been stored for the creation of the outline of these panels within IDRISI. Mining subsidence calculations have not been generated for these workings. Thus the final results will be a conservative estimate of the total subsidence which has occurred.

The overall aim of this chapter has been to generate a subsidence contour plan (created from apparently chaotically arranged coal workings), for the south-east Fife coast, illustrating the cumulative effects of multiple workings at the surface. From the subsidence value produced, at a given surface point, it is more difficult to know inherently the exact location of that point in relation to the multiple workings on which it may be situated; the point will overlie the edges of some panels and/or the centre of other panels.

As previously discussed, the subsidence values have been calibrated against the empirical data sets held within the SEH. Thus a confidence level has been assigned to the different categories of mining panels. Thus the total estimated margin of error on any given subsidence value

generated in this thesis is estimated to be between 9.5 and 17.3%. This value is in addition to the margin of error of 10% from the use of the SEH. Hence the total margin of error, estimated by summing the two errors in quadrature (taking the maximum error of 17.3% and the SEH error of 10%) is ±20%. It is important at this stage to emphasise that this result expresses the worst possible scenario (in terms of the inaccuracy of the method) and has been disproportionately weighted by the larger errors found at the edge of the trough where the actual values of subsidence are less significant.

5.9 Results

Fourteen seams were mined along the coastline between Buckhaven and Dysart. Ninety-two panels of mining extraction were identified as having influenced the coastline. Coal was mined between depths of approximately 80m to over 600m. The results from overlying the subsidence images in IDRISI suggest that over 5m of subsidence have occurred in the West Sands region of the coastline. On closer inspection of the mine plans and subsidence image, it can be seen that 6 seams of coal have been worked in the area extracting a total of more than 11m of coal.

These features are reflected in other pockets along the coastline. Directly south of the Michael Colliery total subsidence equates to 5.6m, here over 8m of coal were worked from six different seams. Subsidence extends as far as the East Wemyss village. There are also areas along the coast which have not been affected by the mining. These include a small area surrounding Wemyss Castle and the area directly underlying the Michael Colliery. For detailed results on the amounts of coal extracted from each panel see Appendix 10.

The results show that virtually the entire coastline has been affected by mining subsidence (Plates 5.1, 5.2, 5.3, 5.4). The irregular contours of the subsidence image reflect the complex nature in which the coal was extracted from this area. The seaward area of West Sands and south of the Michael Colliery have also undergone significant subsidence. Many more worked panels extend far into the Forth, all of which have not been included for the analysis in this thesis. The areas of maximum subsidence are found at West Sands, to the west of the Michael Colliery, and at points close to Blair Point. The exact values of subsidence have been recorded where coastal changes have also been measured. These results are held in Appendix 11.

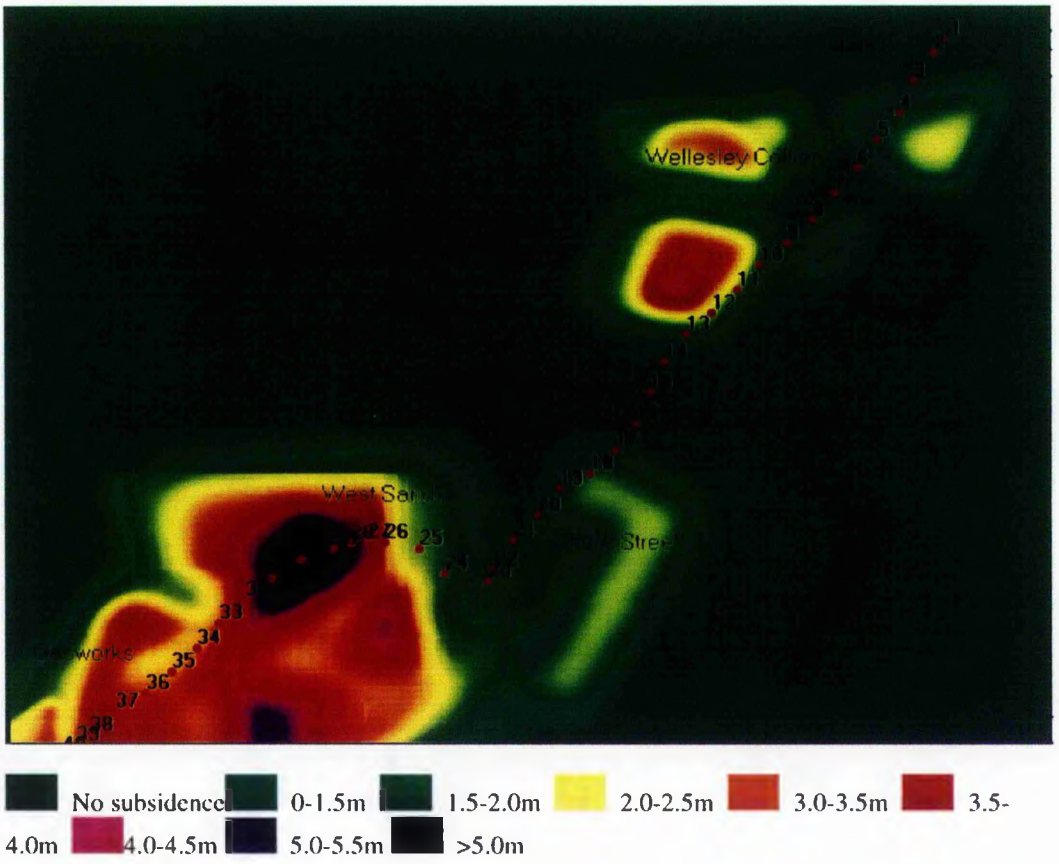

Plate 5.1 Mining subsidence experienced between Buckhaven and West Sands, for the period between 1894 and 1994. The numbered points indicate the location of the HWM for the year 1894, from which measurements in the changes in the HWM were taken. The darker coloured troughs indicate where greatest subsidence occurred. Deep subsidence (up to 5.7m) has occurred in the West Sands area (points 29-31) and this subsidence extends along to the gasworks and beyond. To the north at Shore Street, the subsidence generated from the mine workings is significantly lower (maximum of 1.9m), although one panel is clearly influencing the coastal zone. There is a coastal stretch where no subsidence has occurred (points 14-17). Close to the Wellesley Colliery (points 3-13) a collection of mine panels again influence the coastal zone (maximum subsidence =4m, landwards of the HWM). The olive green areas to the top left of the picture and the bottom right, away from the coastline are areas where subsidence calculations were not carried out; these areas were classified as not influencing the coastline.

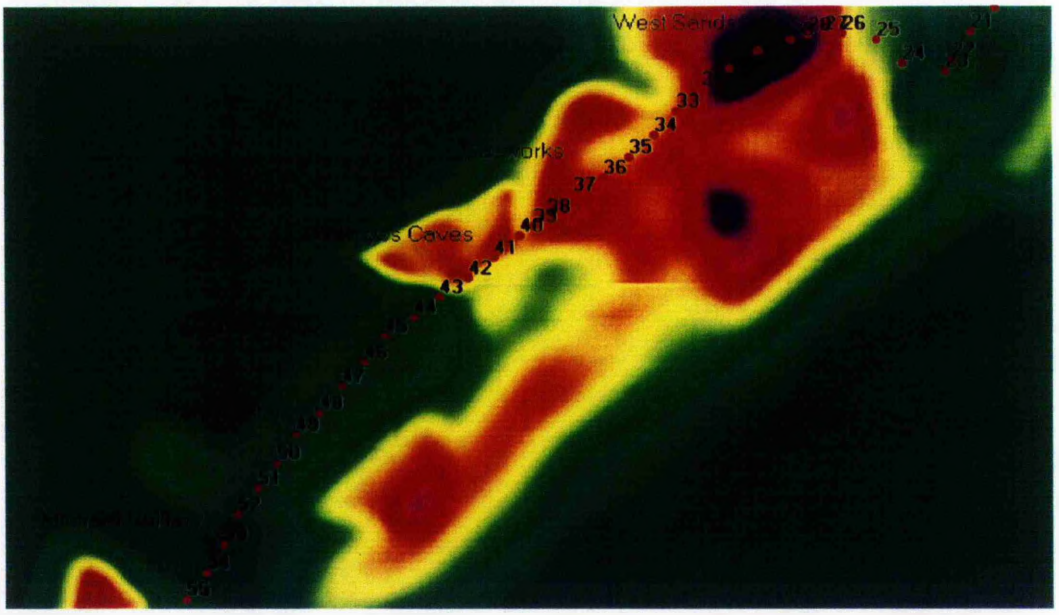

Plate 5.2 Total subsidence generated from the extraction of coal along the East Wemyss coastline. The subsidence troughs at the Wemyss Caves are greater (maximum subsidence=3m here) than in the local vicinity of the loom factory (maximum subsidence =0.3m). Note how points 41 and 43 signify the edges of different panels. The exact location of the Michael Colliery pithead is clearly identified as no coal has been worked here.

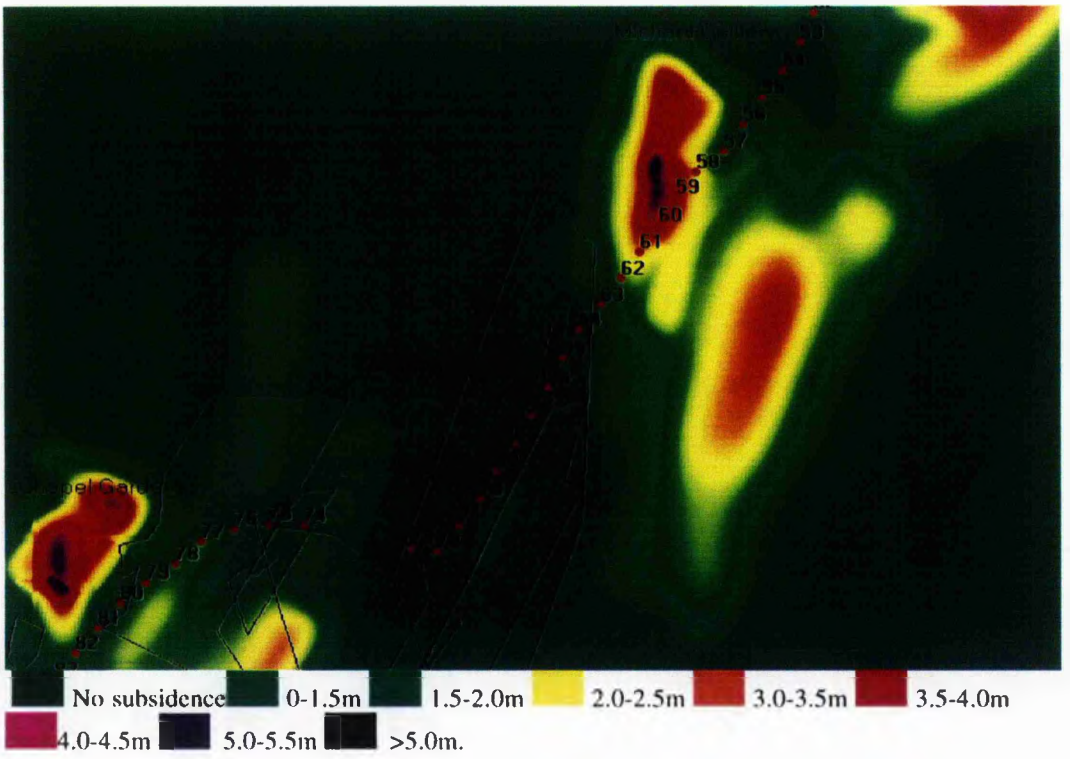

Plate 5.3 Total subsidence generated from the extraction of coal between the Michael Colliery and West Wemyss. The subsidence troughs to the south of the Michael Colliery are extremely deep between points 56 and 62 (maximum subsidence=4.7m). Point 64 signifies the edge of the coal workings where the subsidence toughs have been estimated, beyond this point, although the image indicates that no subsidence has taken place, the polygons indicate that coal has been worked in this area too. The polygons are the outlines of coal workings dating back prior to 1852, for which no data are available.

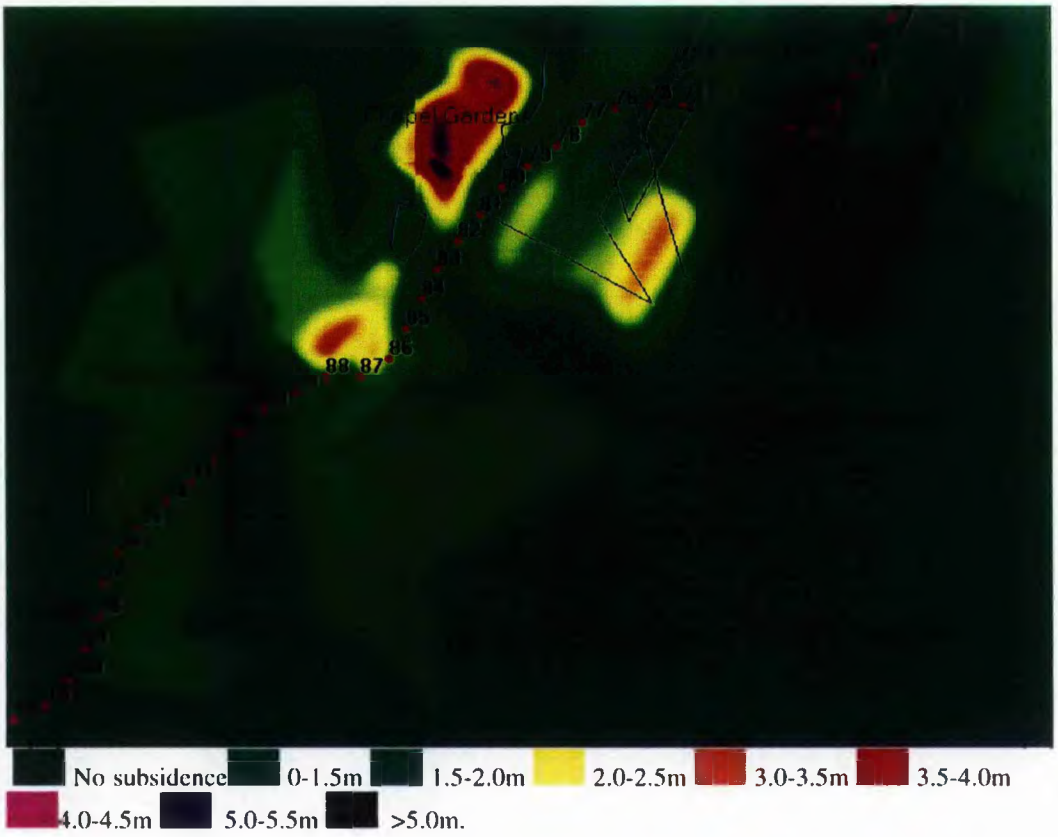

Plate 5.4 Total subsidence and location of the HWM from West Wemyss (point 71) to Dysart (point 102). Around West Wemyss (points 72-76) the polygons indicate those panels which were worked before 1852, for which no data is available to calculate subsidence. Large pockets of subsidence have occurred around Chapel Gardens and at Blair Point. (Values of between 2.5-4.7m of subsidence was generated). In particular around West Wemyss the calculated subsidence values may be significantly lower than the actual subsidence generated, as up to 3 panels (pre 1852 workings) overlie each other. Around the Frances Colliery only a limited amount of subsidence has occurred (subsidence <0.5m), as illustrated towards Dysart too. However, although only one polygon has been identified to the south of the Frances Colliery, undoubtedly more coal was worked in this region prior to 1850.

5.10 Field evidence: benchmark evaluation

Attention will now focus on the field evidence to support the modelling results generated from the use of the influence function. An investigation into the changing benchmark heights was made by comparing the different editions of the 1:2500 OS plans (editions: 1894, 1914, 1960, 1994). Movements of benchmarks and surface point heights, overtime, can give an indication of any ground subsidence which has occurred in the area. All benchmarks were identified along the coastline and digitised so that a comparison of benchmark changes could be made against the estimated subsidence values. Benchmarks were initially levelled to the Liverpool Datum in 1894 and 1914. In the 1950s Ordnance Survey switched to the Newlyn Datum. All the benchmarks in this thesis have been adjusted to the Newlyn Datum. Ordnance Survey advised that for the coastal strip between

Buckhaven and Kirkcaldy +0.03m should be added to the old Liverpool value, to give the Newlyn value. Caution has been advised by OS, (Southampton) regarding spot heights, stating that the maximum error at any given location is in the range of $\pm$ 0.3m.

Only a limited number of benchmarks and surface heights exist along the coastal strip between Buckhaven and Dysart. This is due to a combination of factors which include the fact that benchmarks and surface points tend not to exist in areas with no settlements or roads. Many original benchmarks from the 1900s have been abandoned, especially where the area has not been developed. Valuable data have also been lost where houses on which the benchmark was sited have been abandoned or demolished. Unfortunately, this is the case for many of the benchmarks sited close to the shoreline. Benchmarks were originally located on the buildings at Buckhaven, adjacent to the West Sands swimming pool, at the gasworks and on the dovecot at East Wemyss, all of which have been demolished. Consequently, along a coastline, the only long standing benchmarks, or surface heights can be found in the populated areas close to the sea.

All the benchmarks and spot heights located close to the beach were digitised on Smallworld GIS. The co-ordinates and height of every benchmark were recorded (Appendix 12); this allowed for the comparison of benchmark values from different dates. Seventy-nine benchmarks and spot heights were identified adjacent to the coastline between Buckhaven and Dysart, however many were later abandoned leaving only a small sample of heights available for further analysis. Sixteen of the identified heights demonstrated a decrease in the benchmark height greater than 0.3m, they are listed below.

Table 5.7 Changes in the heights of benchmarks and spot heights along the south-east Fife coastline.

ID code	Location	x co-ordinate	y co-ordinates	1894	1914	1960	1994	Change in height (m)
2	Wellesley Colliery	335882.4	697874.5	9.2		8.2		-1
8		336226.3	698284.9	6.4	6.1			-0.3
10	West Sands	335684.8	697846.0	26.6		25.9		-0.7
11	Buckhaven	335715.2	697829.9	25.3	25.2	24.7		-0.6
12		335718.3	697807.5	23.5		23.2		-0.3
13		335818.2	697788.5	7.4	6.7			-0.7
16		335698.3	697712.4		7.4	7.3	7.0	-0.4
50		333506.7	695951.0			8.2	7.4	-0.8

51		333173.2	695671.4		30.2	28.2		-2.2
57		332995.7	695406.7			28.5	28.2	-0.3
66	West Wemyss	332795.1	694878.9	6.0	5.9	5.6	5.4	-0.6
67		332755.7	694821.2	5.1	4.9	4.9	4.6	-0.5
71		332464.3	694708.6	16.5	14.1	14.3	14.3	-2.2
72		332422.3	694786.5		22.3	21.0		-1.3
74	Frances	330701.5	693608.9			43.6	43.0	-0.6
76		330595.3	693464.2			31.7	31.4	-0.3

Those surface points and benchmark values which do exist throughout the O.S. editions suggest a dominant trend of subsidence occurring locally within the area. The results suggest that there has been some significant slumping of the ground in some areas of the Wemyss coastline; the causes of which will be discussed in detail in Chapter 7.

5.11 Conclusions

The influence function proved to be the most flexible method for calculating mining subsidence in the south-east Fife region. The increased volume of work in preparing the coal seams for the subsidence calculations ensured maximum accuracy possible. Calibration of the SDPS for the Fife coalfields was performed for the first time adjusting the necessary parameters to reflect the British environment. One of the key strengths of the SDPS was its ability to deal with irregular workings, a major characteristic of the Fife coalfields. IDRISI GIS proved to be an effective tool for completing the superposition of all the relevant mine panels to generate the final subsidence contour image. However, the functionality within the system limited further detailed analysis of the results to be performed. For example it was extremely difficult to zoom into precise co-ordinates.

The results from the SDPS indicate that subsidence greater than 5m occurred at West Sands and to the south of the Michael Colliery. The results collected independently via the benchmark evaluation correlate well with the subsidence results. More precisely, the locations of the greatest movements of benchmark heights correspond to those areas where large volumes of coal have been extracted.

For 12 points where benchmark evaluation has been compared with the subsidence values calculated at the same co-ordinates, a correlation coefficient has been used to assess the relationship between subsidence and the lowering of the land surface. The coefficient was calculated to be 0.96.

The benchmarks and surface points identified between the Michael Colliery and West Wemyss (points 66 and 67) have been lowered in height by a significant amount, between 1894 and 1960. However, these points overlie the areas of the polygon data for which only a limited amount of information exists and cannot be used in the correlation equation. Using the best fit line equation from the graph (Figure 5.30) it is estimated that 0.5-0.6m of subsidence occurred in this area.

There is strong correlation between subsidence values and benchmark heights despite the limitations in obtaining accurate values for both parameters. Although most subsidence occurs immediately after the coal has been extracted, in some cases residual subsidence can develop up to a few months later. If residual subsidence was a process present along this coastal stretch then it would hinder any direct comparison of bench mark heights with subsidence values for particular dates. The correlation value generated provides sufficient evidence to propose that mining subsidence has occurred along this coastal stretch between Buckhaven and Dysart, and is the main cause of the land subsidence in the area.

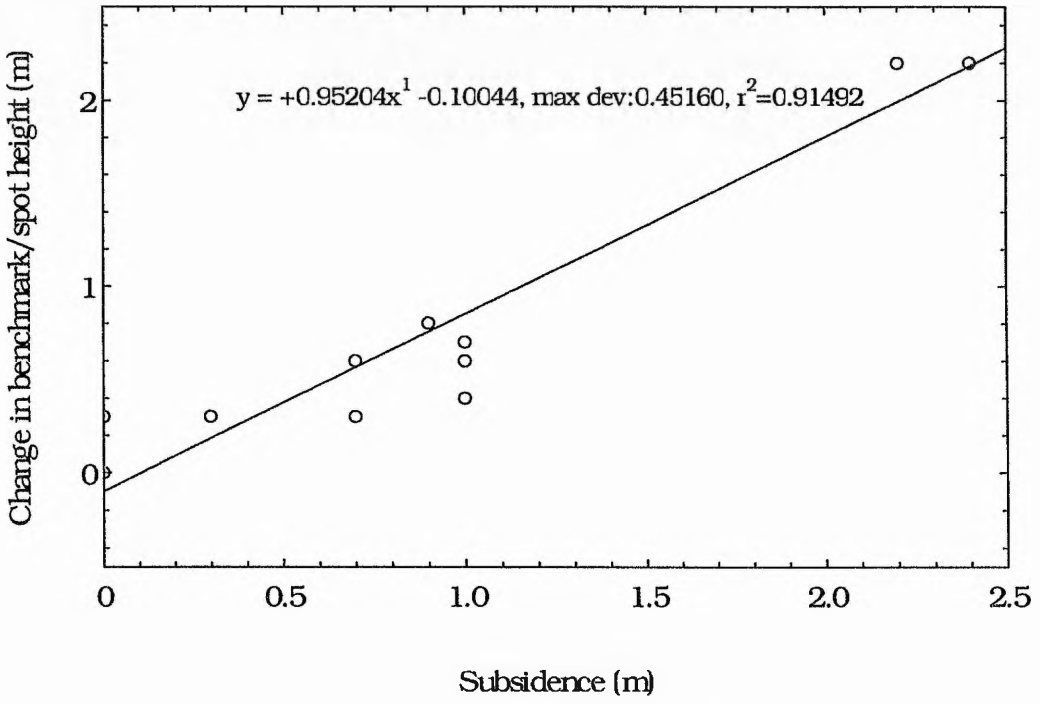

Figure 5.30 Changes in the benchmark/spot heights plotted against the subsidence values at the same location demonstrate a strong correlation of 0.91. The table below shows those values used to generate the graph above.

ID Code	Change in Benchmark/spot height (m)	Subsidence(m)
8	0.0	0.0
11	0.6	0.7
10	0.7	1.0
12	0.3	0.7
16	0.4	1.0

50	0.8	0.9
51	2.2	2.4
57	0.3	0.0
71	2.2	2.2
72	2.2	2.2
74	0.6	1.0
76	0.3	0.3

Limitations in the accuracy to which the benchmarks have been recorded is subject to numerous external forces. If for example, the trig point used to fix these benchmarks has also shifted, as a result of subsidence, all the results would be incorrect; as this entire area has been extensively mined this is a strong possibility. Due to the limitations in the accuracy of the benchmark data the calibration of the benchmark changes against subsidence values cannot be performed. However, the changes in the bench mark values strongly suggest that the land surface really has been lowered by an alternative process.

Further analysis of the subsidence results is carried out in Chapter 7 where the precise movements of sea level change and subsidence values are compared and discussed. Prior to exploring the implications of the mining subsidence results in terms of the coastal changes identified in Chapter 3, it is necessary to complete the investigation by examining the present sea level height predictions and their significance in terms of determining the future stability of the south-east Fife coastline. The role sea level rise may play on the Fife coastline can then be addressed.

Chapter 6. A review of the effects of global warming on the sea level heights for the south-east Fife coastline

6.1 Introduction

Earlier chapters in this thesis have demonstrated the impact of mining activities on the coastline of south-east Fife. Accretion and seaward migration of the HWM following spoil disposal have given way to erosion consequent upon subsidence and depletion of the dumped spoil bings by alongshore and offshore sediment transport. Along most of the coast this has resulted in beach lowering and landward migration of the HWM. Mean sea level provides the datum from which these coastal changes are measured. Superimposed upon this water level are periodic and non periodic fluctuations of the water surface which determines the vertical extent of the coastline. Clearly then, coastal development is intimately related to mean sea level and any changes in this datum will impact upon future coastal change.

Global warming is predicted to cause a rise in sea level of up to 86cm by 2100 (IPCC WGI 1995, p.364). Estimates of annual rate of sea level rise range from 1.2mm/yr (Fairbridge & Krebs 1962), 3.0mm/yr (Emery 1980) to 2.4 ±0.9mm/yr (Peltier & Tushingham 1989, 1991). The Brunn rule of erosion enables the quantification of a rise in sea level on a given coastal zone (Brunn 1962, 1985, 1988). For example, a sea level rise of 0.003m/yr equates to a shoreline recession of between 1.5-2m/yr (Brunn 1954, 1988). The impact of such change in the height of sea level could be catastrophic to some coastal areas.

This chapter will explore the validity of the present sea level height predictions and their significance in terms of determining the future stability of the south-east Fife coastline. What is the future impact of the predicted increases in sea level height as suggested by Gornitz *et al.* (1982) and Trupin & Wahr (1990)? Are these predictions valid and what are the assumptions on which they are based? A detailed investigation on global warming and sea level rise will allow a critical assessment to be made of the estimations of sea level change and to query the validity of these estimations at a global scale. Sea level rise is inherently linked with global warming; thus any uncertainties in global warming predictions have a knock-on effect for sea level change. For this reason the chapter explores both areas in detail. Thus, by critically examining the uncertainties which surround sea level change, the role sea level rise may play on the Fife coastline can be addressed.

An understanding of the dynamic features including the atmosphere, cryosphere, biosphere and geosphere are required to assess whether sea heights are changing, and if so, to explore how these parameters are affecting and will alter sea level. Projecting sea level rise requires the means to estimate future changes in atmospheric composition, to relate these changes to global warming, and then to determine how the warming can cause land based snow and ice to enter the sea and the oceans to expand thermally (Hoffman 1984).

There follows an examination of how the predictions for sea level changes and global warming have been established. The chapter will be divided into five sections. First, the individual elements which make up climate will be outlined, to give the reader an insight into the complexities which arise in attempting to simplify a phenomenon like climate. A review of the greenhouse effect, and the predicted carbon dioxide (CO_2) emissions will lead on to a discussion on general climatic models. The International Panel on Climate Change (IPCC) document will then be outlined and a critical assessment of the predictions made by the IPCC for global warming and sea level changes will be made. Attention can then focus on sea level changes so that a comprehensive assessment of the implications for the south-east Fife coastline can be made.

6.2 What is climate?

Climate can be defined as the total experience of weather at any place over a specific time period (Lamb 1995). Climate statistics relate to 30 years of data so as to include extremes and frequencies of every element (Lamb 1995, p.8). The interactions between the atmosphere, biosphere, cyrosphere, geosphere and oceans create the climate. The processes driving the global climate system are heating by incoming short wave solar radiation (i.e. shorter wavelength infra-red) and cooling by long wave radiation. The latitudinal gradient of heating drives the atmosphere and ocean circulations, providing the heat transfer necessary to balance the whole system (IPCC 1992 p.75). Any intervention by man in any of the elements listed above will alter the climate. The quantification of such human activities altering the climate is proving difficult to achieve due to the complex relationships which exist between the elements which make up the global environment.

The ocean circulations which are generated from wind stress at the sea surface redistribute heat, fresh water and dissolved chemicals around the globe. The oceans also absorb CO_2 and exchange it with the atmosphere. The volume of the oceans and sea level will vary with changes in the density of sea water. Density is a function of its temperature and salinity (Van de Veen 1988), and differences in density are also a driving mechanism for ocean circulations. In order to estimate ocean expansion one must take into account changes in the interior temperature, salinity and density of the oceans. However, any increase in atmospheric temperature will not raise the temperature of all the ocean layers immediately. The surface layers respond more quickly, essentially raising the air temperature in synchrony with the atmospheric temperature, whereas the transport of the heat downwards through the ocean layers is significantly slower (IPCC 1990).

The cryosphere encompasses the Greenland and Antarctic glacier systems and the mountain glacier regimes across the globe. The glacier systems directly affect the predictions of sea level rise, because any change in temperature will alter the natural equilibrium of individual glacier

systems resulting in the addition or withdrawal of water from the oceans. A great amount of uncertainty exists as to the reaction of the Greenland ice sheet system to global warming (Oerlemans 1993). Warrick & Oerlemans (1990) conclude that the contribution from the Greenland ice mass to past sea level rise appears to be somewhat less than that from glaciers and thermal expansion. The Antarctic ice sheet is even less well understood, due not only to its size, but also because it reacts slowly to atmospheric changes, and is presently thought to be still adjusting to the past glacial-interglacial transition (Warrick & Orlermans 1990). For a detailed discussion on the roles of the ice sheets on sea level change see IPCC WGI (1995, p.359-406), Oerlemans (1993).

The geosphere directly influences the hydrological cycle and the atmosphere. The geosphere encompasses soil moisture deficits, the location of aquifers, along with runoff and evapotranspiration rates. The soil interacts with the atmosphere due to its moisture content and the rate of evaporation or groundwater throughflow, which in turn is affected by vegetation cover (Fairbridge & Jelgersma 1990). Changes in the surface albedo through deforestation, or the extension of desert areas will affect the temperature of the surface of the earth and its ability to absorb heat. These will ultimately cause consecutive feedback mechanisms on the hydrological cycle and atmospheric system. The effects of these processes in relation to the other aspects of climate are not well understood (Melillo *et al.* 1996).

The geosphere also includes events such as volcanic eruptions which are capable of altering the atmospheric wind circulations and temperature through the ash ejected from volcanoes. Tectonic activities also influence the ocean volumes through the arrival of juvenile waters from the earth's interior (Bird 1993) and ocean basin topography alters as a result of tectonic movement (Fairbridge & Jelgersma 1990). Tectonic movements also include secular isostatic responses of the earth's crust to loading or unloading. In deltaic areas for example, regional downwarping has occurred as a result of the accumulation of a large sedimentary load and the coasts of major deltas such as the Mississippi have sectors that show a sea level rise because the level of the subsiding land has not been maintained by sedimentation (Bird 1993). An example of sea level changes resulting from earthquakes followed the Alaskan earthquake of 1964 when parts of the Homer Spit in Kachemak Bay sank nearly 2m (Bird 1993). All of these events need to be eliminated if global warming and sea level rise are to be asserted as resulting from one cause such as human activities.

The atmospheric contribution to climate is determined by numerous processes which also interact with the other formative elements. These processes include the turbulent transfer of heat through the momentum and moisture at the surface of the earth. The albedo of the surface will determine how much incoming solar radiation is absorbed and reflected. The clouds produced from the condensing of water play an important role in reflecting incoming solar short wave radiation and in absorbing and emitting long wave radiation. Although individual

elements of the climate system are relatively well understood, the interactive mechanisms which trigger changes in the overall equilibrium are far more difficult to quantify. These uncertainties over the interactions between the atmosphere, cyrosphere and oceans mean that many questions relating to feedback mechanisms remain unanswered.

This section has attempted an overview of the complex nature of the major elements which make up climate, an understanding and the ability to simplify these complex elements is required to allow for the modelling and future prediction of climate change (Figure 6.1).

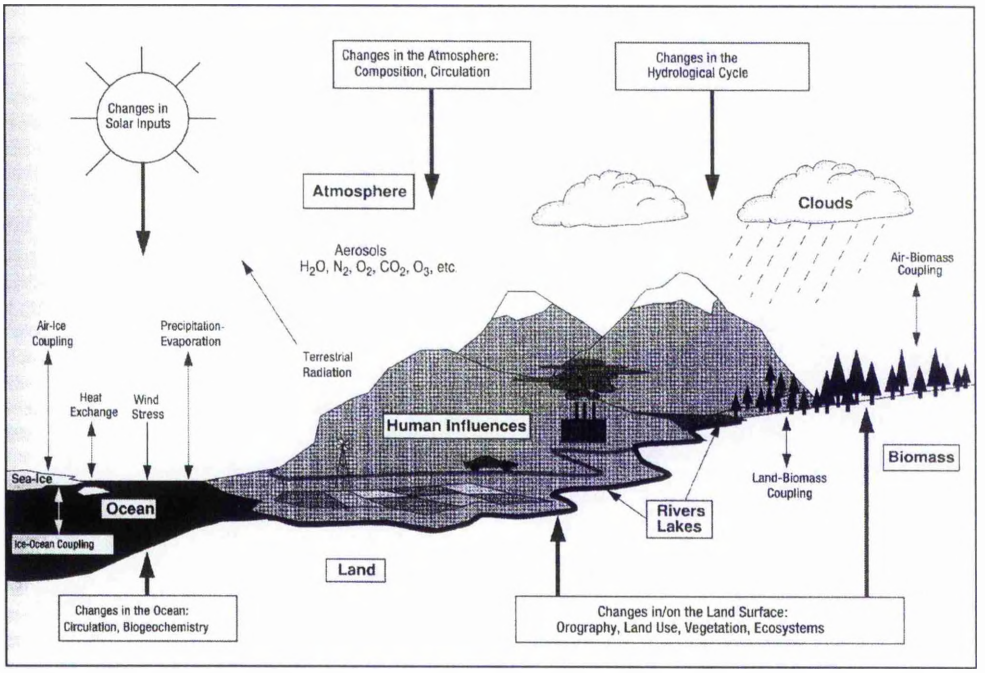

Figure 6.1 Schematic view of the components of the global climate system (bold), their processes and interactions (thin arrows) and some aspects that may change (bold arrows). (After IPCC WGI 1995, p.55).

One aspect of the global system, the greenhouse effect, will now be discussed in more detail, with particular reference to the balance of greenhouse gas emissions which are thought to have caused climatic changes in more recent years. A discussion on the causes of global warming will follow, highlighting the problems involved when attempting to quantify and predict climatic change.

6.3 Basic Principles of Greenhouse Effect

In 1827, the French physicist Fourier, proposed the term 'greenhouse effect', the analogy being between the glass panels of a greenhouse which prevent convectional cooling and the 'greenhouse gases' which inhibit radiational cooling (Ramanathan 1988). This natural warming of the climate is fundamental to the living forms on earth. On Mars where the greenhouse effect does not exist, the average temperature on the surface of the planet is -47^{O}C. If the

natural greenhouse gases were not present the average temperature of the earth would be -18^{O}C (Whyte 1995, p.65).

Short wave solar radiation passes easily through the atmosphere; some is reflected by clouds and dust back into space, while some is reflected away by the earth's surface. Approximately 48% of short wave radiation is absorbed by the earth's surface, and 21% is absorbed by the atmosphere. The heat absorbed by the earth is re-radiated as infra-red long wave radiation with only a fraction escaping back into space (as terrestrial radiation) (See Figure 6.2). Greenhouse gases absorb most of the long wave radiation and this contributes to the heating of the atmosphere. Over short time scales the inputs and outputs of heat are roughly in balance, so that the earth's atmospheric system has an average constant temperature of 15^{O}C. The greenhouse gases which enable the system to maintain this equilibrium are water vapour, carbon dioxide, methane, nitrous oxide and chlorofluorocarbons.

The contribution of a gas to the greenhouse effect depends on the wavelengths at which it absorbs infra-red radiation. If the gas overlaps with the window area of water vapour (4-7 micrometers) and carbon dioxide (13-19 micrometers), then it will have little effect on global warming. There is a 'window' between 7 and 13 micrometers through which more than 70% of the radiation from the earth's surface eventually escapes into space (Gribbin & Gribbin 1996). Most other greenhouse gases, methane, nitrous oxide, CFCs and tropospheric ozone, absorb in this window region.

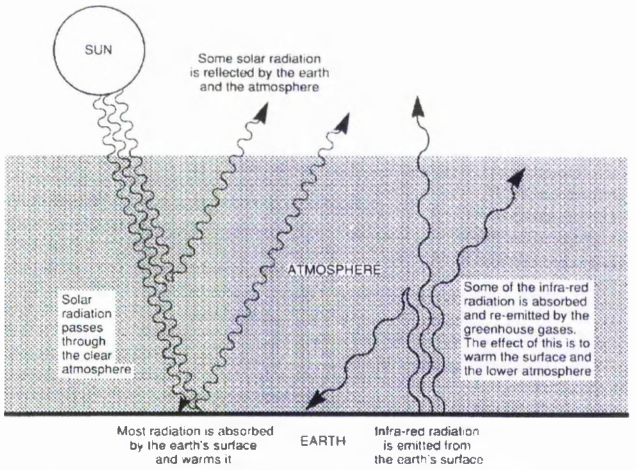

Figure 6.2 Some of the energy radiated at infrared wavelengths from the ground is absorbed and re-radiated downwards by the atmosphere - the greenhouse effect (After IPCC 1990, p.*xiv*).

6.3.1 Carbon Dioxide

Carbon dioxide is a naturally occurring gas, produced primarily from the respiration of animals, the combustion of organic material and the decay of vegetation. It is absorbed and transformed into oxygen by photosynthesis in living plants, the most effective agents being young trees and

phytoplankton in oceans upper layers. Human activity has now caused the release of locked up CO_2 with the burning of fossil fuels and thus upset the natural balance.

The atmospheric CO_2 concentration at 353 ppmv in 1990 is now about 25% greater than the pre-industrial (1750-1800) value of about 280 ppmv, and higher than at any time in at least the last 160 000 years (Whyte 1995, p.71). The earth responds slowly to any increase in CO_2 emissions which is determined mainly by the slow exchange of carbon between surface waters and the deeper layers of the ocean. Hence the CO_2 which is emitted into the atmosphere today will influence the atmospheric concentration of CO_2 for centuries into the future. Man-made CO_2 emissions however, are influenced by the economic growth and technical ability of individual countries. Developed countries currently produce electricity from coal, oil and natural gas accounting for 75% of the current CO_2 emissions. However, as political leaders in the rich developed countries call for a reduction in the CO_2emissions, so the less developed countries are just reaching the 'industrial growth period' and with the increase in world population in similar areas so the production of CO_2 is predicted to continue to rise.

6.3.2 Methane

The production of methane is also increasing as a result of human activity. Historically, it has been shown to vary markedly with temperature changes which suggests a strong feedback between the biosphere and climate on a time-scale of centuries. It occurs naturally with the decaying of organic matter in swamps and marshes, as well as being generated by cattle. Human activity has increased the production of methane from rice cultivation, landfill sites, the burning of fossil fuels and gas leaks. If temperatures increase and permafrost areas melt, so vast amounts of methane will be released. The pre-industrial concentration of methane in the eighteenth century is thought to have been around 700 ppbv. By 1988 this had more than doubled to 1720 ppbv with growth rates of around 1% per annum. Although its atmospheric concentration is less than 1% of that of carbon dioxide, its contribution to the man-enhanced greenhouse effect may be as much as 17-20% (Whyte 1995).

6.3.3 Nitrous Oxide

The main sources of nitrous oxide are from the burning of fossil fuels and the breaking down of chemical fertilisers in soils. The pre-industrial level of around 280 ppbv, which had been stable for about 2000 years began to rise from the early nineteenth century and now stands at about 310 ppbv, a rise of around 10%, currently increasing by about 0.3% per annum. This level represents a higher concentration than at any time within the last 45 000 years (Levenberger & Siegenthaler, 1992). Nitrous oxide has a long atmospheric life of 150 years, and its destruction occurs in the stratosphere by ultraviolet light in the photochemical reactions which contribute to the depletion of ozone (O_3) through the production of nitric acid (HNO_3). Its potential as a

greenhouse gas is about 230 times that of carbon dioxide molecule for molecule, so despite its far smaller presence, it is potentially significantly more important as an agent of global warming.

6.3.4 Chlorofluorocarbons (CFCs)

CFCs, solely a man-made product, are associated with the depletion of the ozone layer. They are generated from aerosol spray propellants, foam packaging, cleaning solvents and refrigerants. Their recent rate of increase in the atmosphere has been up to 5-6.5% per annum, faster than any other greenhouse gas (Whyte, 1995, p.82). The concentrations of the two main gases, CFC11 and CFC12 are 280 and 480 pptv (parts per trillion volume), with atmospheric lives of 55 years and 116 years respectively. Molecule for molecule they are extremely powerful being several thousand times more effective than carbon dioxide. CFCs are inert in the troposphere; in the stratosphere however, they are broken down by UV radiation which results in the decomposition and release of chlorine molecules which attack O_3 molecules converting them into O_2 molecules and thus reducing the O_3 concentration.

6.3.5 Halocarbons

Halocarbons are carbon compounds containing fluorine, chlorine, bromine or iodine, of which human activities are the source of emissions. Halocarbons which contain chlorine and bromine cause ozone depletion, and their emissions are controlled under the Montreal Protocol and its Adjustments and Amendments. Consequently the rates of emissions have fallen since 1990. Halocarbons are effective in two ways; by contributing directly to the concentration increases of CFCs and HCFCs and indirectly and by exerting a negative radiative force via the depletion of stratospheric ozone. Perfluorocarbons (PFCs), are removed very slowly, and have estimated long lifetimes, greater than 1000 years; as a result all current emissions will continue to affect the atmosphere well into the future.

6.3.6 Ozone

Ozone plays a fundamental role in the interception of incoming ultraviolet radiation. It is naturally self-regulating and is of primary importance in maintaining the temperature structure of the stratosphere. Since the 1970s it appears that human activity has produced gases which attack the O_3 layer causing it to thin, removing the protective UV screening. As a result more solar radiation is allowed to reach the earth's surface, further enhancing global warming. The two groups of gases responsible for reducing the balance of O_3 in the atmosphere are CFCs and oxides of nitrogen. The depletion of the stratospheric ozone, as a result of reactions involving CFCs, will lead to reduced absorption of incoming radiation and the cooling effect (Whyte 1995).

6.3.7 Human Influences

With the increase in population and the onset of industrialisation of first the developed counties, and now the third world countries, emissions of greenhouse gases such as CO_2, methane, nitrous oxide, CFCs and tropospheric ozone have substantially increased. Table 6.1 highlights the greenhouse gas emissions for the pre-industrial era and 1994. The increase in CO_2 is having the most profound effect, although quantifying this effect is difficult due to the combination of positive and negative feedback which occur.

	CO_2	CH_4	N_2O	CFC-11	HCFC-22	CF_4
Pre-industrial concentration	~280 ppmv	~700 ppbv	~725 ppbv	0	0	0
Concentration in 1994	358 ppmv	1720 ppbv	312 ppbv	268 ppbv	11 pptv	72 pptv
Rate of concentration change	1.5 ppmv/yr. 0.4%/yr.	10 ppbv/yr. 0.6%/yr.	0.8 ppbv/yr. 0.25%/yr.	0 pptv /yr* 0%	5. pptv/yr. 5%/yr.	1.2×10^{-6} pptv/yr. 2%/yr.
Atmospheric lifetime (yrs)	50-200	12	120	50	12	50,000

Table 6.1 A sample of greenhouse gases affected by human activities (IPCC WGI Technical Summary 1995,p.19)

*1 pptv = I part per trillion (million million) by volume

Scientists remain unsure of the various sources and sinks relating the two processes which link the levels of emissions of greenhouse gases to their atmospheric concentrations. The predictions of anthropogenic greenhouse gas emissions do not incorporate the possibility that there may be substantial indirect effects through changes in the natural sources and sinks such as the release of methane from high latitude wetlands. The impact of man's activities through the burning of fossil fuels has had the effect of increasing the amount of CO_2 which is produced within the atmosphere, upsetting the natural equilibrium and setting up a chain reaction of global warming, which is yet to be fully understood. It is proving extremely difficult to reproduce the global climate within the laboratory due to the complex interrelationships between elements of the global system. It is also difficult to directly verify quantitative predictions of greenhouse warming on the basis of purely historical events, due to insufficient data available on past events. Instead numerical equations based on physical laws have been used to create global climatic models which are then used to simulate the effects of changes in different greenhouse gases.

The calculation of future greenhouse gases, given certain emissions, involves modelling processes which transform and remove different gases from the atmosphere. It is crucial that the global carbon cycle and atmospheric chemistry can be understood and modelled, as these emissions are used to project the atmospheric concentrations of greenhouse gases and aerosols.

In turn these projections are used to generate climate models from which scientists can explore and predict changes in future climates.

6.4 General Climate Models (GCMs)

General climatic models (GCMs) are used to forecast future global climates. GCMs have also been used to simulate rises in global temperature resulting from the increase in greenhouse gas concentrations since the nineteenth century. They allow scientists to examine the relative importance of various elements such as different greenhouse gases and aerosols in influencing the climate, permitting the improvement in our knowledge of the relationships which cause climatic change.

GCMs are based on the physical conservation laws which describe the redistribution of momentum, heat and water vapour by atmospheric motions. The governing equations are non-linear partial differential equations whose solutions can only be obtained by numerical methods (IPCC 1992). The models can simulate the mass and energy transfers in the atmosphere and the vertical layer exchange in the uppermost 50-65m of the ocean.

These models, through numerical analysis, attempt to reproduce the global climate and then simulate climate changes by a series of steps that involves altering different parameters within the system. The models represent the climatic processes on three dimensional grids of points at the earth's surface and at a number of levels upwards through the troposphere and in the stratosphere. The horizontal resolution of the grid ranges between 300-1000km with many more layers included. For each grid box a range of climatic data is input including temperature, precipitation, wind, humidity and pressure. Limitations of the models' abilities lie in the interactive relationships between the climatic elements. For example, the majority of models do not allow for any changes from the present conditions in the horizontal and deep vertical heat and mass transfer in the oceans; thus the winds can change, but the ocean circulation will not in turn adjust. The models appear unable to represent the precipitation variations although their representation of real temperatures appears to be considerably better (Whyte 1995 p.95). Temperature rise tends to be over-predicted by about 1.0-1.8^{o}C, when in real terms the rise has been approximately 0.5^{o}C. Another limitation is that the incorporation of extreme events is also poor (Smith 1993). Validating GCMs is fundamental to climatic research, as future sea level predictions often include climatic forecasts based on these models. Different GCMs tend to contain errors which have a family resemblance due to the methods by which they are constructed; for example, a tendency to exaggerate coldness of the lower stratosphere in polar regions.

Many limitations exist on the actual applications of the results generated from the GCMs especially when focusing in at a regional scale. Even if conditions at a particular time in the

future were identical to those built in the model, it still might not represent the resulting climate accurately because of its oversimplifications (Whyte 1995, p.98). As Pearman (1986) highlights, despite the improvements in the performance of GCMs, these developments have raised the confidence of the predictions only marginally. The important issue remains the question of climate variations at a regional scale, and how they will affect communities. The predictions of mean global warming have little reference to the question of the viability of natural or cultivated ecosystems at a regional scale. Because the horizontal resolution is poor, no individual climate type can be represented with any confidence. Those models which have opted for higher resolution at a horizontal scale have done so at the expense of reducing the number of vertical layers. Parameterization is used to quantify the climatic processes which operate at a smaller scale. This involves taking the average of the distribution for each given phenomenon at grid square level, and using the averages as substitute data (Whyte, 1995 p.97). However, the simplification by parameterization means that many feedback mechanisms such as those related to cloud variations are completely overlooked. Soil moisture and albedo of the earth's surface are also crudely represented in the GCMs.

The problems of dealing with feedback mechanisms can be explained in the example which explores the water vapour feedback mechanism. A doubling of carbon dioxide will cause increased global warming. This warming will, in turn, automatically cause more water vapour, itself a greenhouse gas, inducing further warming, amplifying the initial increment. Furthermore, the interactions between elements do not all occur over similar time scales. Mikolajewicz & Maier Reimer (1990) highlighted the fact that within the climate system there exist 'slow components' (e.g. ocean circulation) which are altered by the 'fast components' (e.g. atmosphere) which in turn are influenced by slow components (e.g. oceans, cryosphere).

Kukla (1990) tested five general circulation models using the three following techniques: the degree of success in simulating the correct observed climate; the degree of mutual agreement among the models in the prediction of the increased carbon dioxide impact; and the degree of success in the simulation of past climates particularly the initiation of past climates and a glacial period.

The five models included in the analysis were those of Hansen *et al.* (1984), Schlesinger & Mitchell (1985), Wilson & Mitchell (1987), Wetherald & Manabe (1986) and Schlesinger & Zhao (1989). The models did not provide reliable results for any of the tests. Although the general mean global increase in precipitation is predicted by all the models, the differences among the individual predictions of regional precipitation rates in the carbon dioxide enriched atmosphere are such that none can be trusted (Kukla 1990). Kukla also indicated that the models consistently overestimate current precipitation in low latitudes, which raises fundamental questions about the significance of such inaccuracies on further predictions for carbon dioxide. There are also disturbing suggestions that the past insolation input was unable

to increase the precipitation rates in areas where the ice started to build up at the onset of the last glaciation. If the GCMs are unable to predict accurately these past events, how can any carbon dioxide forecasts be accepted with any confidence?

The palaeoclimatic evidence strongly illustrates that the oceans play a fundamental role in redistributing the solar energy received within the earth's system, with only a small amount being absorbed in the atmosphere. In the current climate models, it is presumed that the pattern of ocean circulation would not change in response to a major insulation shift or that it would not react to a major radiative perturbation such as carbon dioxide doubling. It is obvious from Kukla's work that the models need to be improved significantly and incorporate the intimate links between atmosphere and ocean circulation before any predictions can be confidently accepted. The greatest concern is that the predictions from these models are blindly incorporated into the predictions of global sea level changes, highlighting the potential margin of error available on any final forecasts for sea level change.

Having identified all of the elements which produce global climate together with a discussion on the problems of modelling these elements in any model, attention will now focus on the results generated from the IPCC group.

6.5 IPCC Predictions

In the 1980s it became apparent that there were significant problems for the global environment arising from human activities. In 1988 the World Meteorological Organisation and the UN Environmental Programme established the Intergovernmental Panel on Climate Change (IPCC). This group consisted of almost 400 scientists whose aim was to assess and summarise the current knowledge on climatic change, particularly the likelihood of global warming. The initial IPCC report was published in 1990 (IPCC 1990) with a further update in 1992 and 1995. The IPCC report which will be outlined in detail below, had initially been heavily criticised for not including more controversial aspects, as well as failing to address the limitations of the project (Whyte 1995). However, it remains an important yardstick against which new research findings are assessed and the latest edition attempts to tackle some of the original criticisms from the first publication in 1990.

The original aims as outlined in the IPCC report (1990) p.xiii were to:

1) Identify the factors which may affect climate change during the next century, especially those which are due to human activity.
2) Assess the responses of the atmosphere - ocean- land - ice system.
3) Assess the current capabilities of modelling global and regional climate changes and their predictability.
4) Assess the past climate record and presently observed climate anomalies.

The IPCC report has generated four scenarios for the emissions of both greenhouse gases and aerosol precursors from which projected global mean temperature changes, relative to 1990, were calculated for the 21st century. For all the scenarios the growth of the economy and population was taken into account. (For further details on the economic variables used for the scenarios see IPCC 1990 p.xxxiv).

The original scenarios for the emissions of greenhouse gases have been modified since the first publication in 1990. These scenarios are used to determine the temperature predictions and sea level change predictions. The IS92 scenarios extend to the year 2100 and include emissions of CO_2, CH_4, N_20 and halocarbons, precursors of tropospheric ozone and sulphate aerosols and aerosols from biomass burning. Since 1990, the inclusion of the effects of aerosols has caused a negative feedback, reducing the temperature effects and sea level rise predictions. The revised use of the carbon cycle means that the uptake of carbon through CO_2 was underestimated. GCMs have also become more advanced, and now it has been possible to include the spatial variations in climate sensitivity and effects of the changing strength of thermohaline circulation. The global average temperature and sea level projections presented between 1990 and 2100 (IPCC WGI 1995), taking into account the changing aerosol emissions, are significantly lower than the corresponding predictions in 1990 (from IPCC 1990). Whereas in 1990, there were 5 scenarios ranging from best-estimate to the low estimate, in the edition published in 1995 there are 6 scenarios (IS92a-f) which are based on assumptions concerning the population, economic growth, technology changes, and land use during the period 1900 to 2100. With the understanding of the global carbon cycle and atmospheric chemistry, these emissions can then be used to project the atmospheric concentrations of greenhouse gases and aerosols, which in turn can be used to generate climate models to understand and predict future climates.

For the mid-range IPCC emission scenario IS92a, assuming the 'best estimate' value of climate sensitivity[1] the models predict an increase in the global mean surface air temperature relative to 1990 of about $2^{o}C$ by 2100 (IPCC, Technical Summary 1995, p.11) The corresponding projection for the highest IPCC scenario (IS92e) combined with high value of climate sensitivity gives a warming of about $3.5^{o}C$.

Global mean sea level has risen 10-25cm, over the last 100 years, which is higher than reported in 1990. The IS92a prediction is that sea level will rise 50cm (with a range of 20-86cm of uncertainty) by 2100 (IPCC WGI 1995, p.364); this compares with the best estimate in 1990 of 66cm. For the range of emission scenarios IS92a-f using the best-estimate model parameters,

[1] In the IPCCreports, the climate sensitivity refers to the long term change in global mean surface temperature following a doubling of atmospheric $C0_2$ equivalent concentration. More generally it refers to the equilibrium change in surface air temperature following a unit change in radiative forcing ($^{o}C/Wm^{-2}$) (IPCC, Technical Summary, 1995, p.11).

sea level is projected to be 38-55cm higher than today by the year 2100. The extreme range of projections taking into account both emission scenarios and model uncertainties is 13-94cm. Most of the projected rise in sea level is due to the thermal expansion, followed by increased melting of glaciers and ice caps, a prediction which remains fraught with uncertainty.

The IPCC group have extended their knowledge base significantly since the 1990 and are becoming more aware of their limitations. These weaknesses are being tackled by numerous groups who are covering the following technical areas: estimating the future emissions and biogeochemical cycling of greenhouse gases; accurately modelling the effects of feedback mechanisms on all climate processes; and collecting data on all of the climate variables to allow for genuine model testing. Since 1990, the basic understanding of the climate-sea level relationships has not changed significantly. The reason why the best estimates for sea level rise are lower than in 1990, is that the estimates of global temperature change, which drive the projections of sea level rise, are also lower.

The IPCC report documents that the climate has changed over the past century with global mean surface temperature having increased between $0.3^{o}C$ and $0.6^{o}C$ since the late 19th century. The mid latitude continents in winter and spring are where the greatest warming has taken place, with precipitation increasing overland in high latitudes of the Northern hemisphere (IPCC 1990). The evidence available suggests that global sea level has risen between 10-25cm over the past 100 years, with much of that rise relating to the increase in global mean temperature.

Little confidence exists in the predictions of regional climatic changes, although confidence is higher for hemispheric-to-continental scale projections of coupled atmospheric-ocean climate models. All the models demonstrate greater surface warming of the land than of the sea and increased precipitation and soil moisture in high latitudes, in winter. The predictions also include a maximum surface warming in high northern latitudes in winter, with little surface warming over the Arctic in summer. More severe droughts and/or floods are expected in some places, and less severe droughts or floods will occur in other areas. Several models indicate an increase in precipitation intensity, suggesting the possibility for more extreme rainfall events. However, insufficient knowledge allows for any prediction in the geographical distribution of severe storms (Warrick *et al.* 1996, p.365).

The IPCC report has undoubtedly enabled the scientific community to unite in its attempt to forward research in relation to understanding and predicting global warming and the consequences of alternative scenarios. Despite the progress made by the IPCC group over the past 6 years, the results produced remain limited in their application and provide only a limited insight into how climate will change on a regional scale. It is clear that sea level rise is driven by increases in global temperature. How will a rise in temperature alter the natural equilibrium

of the atmosphere, cryosphere, geosphere and hydrosphere not only at a global scale, but regionally too? How will a rise in sea level of between 38-55cm be translated across the geoid, where there are variations in height of up to 200m? Could there be a fall in sea level in some regions, whilst other areas could experience significant rises in sea level? Will the rise in sea level changes occur as a catastrophic event, as the result of a sudden release of water from a glaciated region, or will the rise occur gradually over a number of years?

Kukla has already illustrated that most GCMs are inadequate at predicting correctly the effects of any change in climate, so how can we be confident about the IPCC predictions? It appears that with the solution to one problem, such as quantifying greenhouse gas emissions, a more complex set of questions is created which needs to be answered. Until the links between regional and global environmental systems are clearly understood, not only will the GCMs be unreliable but they will also be virtually redundant when attempting to solve the critical questions of the consequences of climate changes at a regional scale. A call for more information at a regional scale has already been made; this is fundamental to the further development of creating realistic solutions to the current global problems. As a result the confidence of many scientists will grow allowing for the further development of current knowledge in relation to the implications of man's activities on the global climate.

6.6 Sea level changes

Having reviewed the effects of increased greenhouse gas emissions on the global climate, as well as the limitations of the predictions, it is now possible to address the consequences of the climatic forecasts on the global and regional sea level. The mean sea level values generated from any of the research projects are merely averages of the heights of sea level across the globe, but in order to gain a more realistic understanding of what is happening, further data are required on sea level behaviour and its history together with the factors affecting changes in ocean volumes. An assessment of how sea level has changed over longer time scales and over decades is also required. The former need to be carried out in an attempt to understand how the oceans reacted to past climatic events and the latter are needed to assess the current changes which are occurring, thus enabling the creation of a full picture of past climatic events in an attempt to predict current variations.

The assessment of sea level changes can be achieved through different sources of data. The analogue approach involves reconstructing past climates and then, from an understanding of how climate varies, it is possible to proceed and estimate future climate and sea level changes (Titus 1987, Plag 1992). On a geological time scale the review of morphological features such as ancient strand lines and raised beaches should be used. With shorter time scales over decades, variations in sea level heights can be monitored in relation to benchmarks on land

although the collection of tide gauge data for assessing recent sea level changes is heavily dependent on the quality of the data set analysed.

Tide gauges measure sea level variations in relation to a fixed benchmark and thus record 'relative sea level' change due to both vertical land movements and real (eustatic) changes in ocean levels (Warrick & Oerlemans 1990). Many techniques exist for the collection of tide gauge data sets, but with no consensus on the correct method or length of record required for analysis, a lack of consistency exists between investigations and this makes it difficult to directly compare results from alternative sources.(Groger & Plag 1992). When evaluating global trends, estimates are obtained from either a global sea level curve or by determining an average of local trends. A summary of recent determinations of Global Sea Level Rise is presented in Table 6.2

Table 6.2 Studies of global sea level rise based on tide gauge data. From Groger and Plag (1992).

Author	Data Source	No. of Stations	Global Sea Level Rise in mm/yr	Methods
Gutenberg (1941)	AdOP	71	1.1±0.8	RA
Fairbridge and Krebs (1962)	?	?	1.2	SA
Lisitzin (1974)	?	6	1.1±0.4	SA
Emery (1980)	PSMSL	247	3.0	SA
Gornitz *et al.* (1982)	PSMSL	a)193 b)86	1.2 1.0	RA RA + GD
Barnett (1983)	PSMSL	9	1.5±0.2 1.8±0.2	EOF EOF
Barnett (1984)	PSMSL +NORPAX	155	1.4±0.1 2.3±0.2	EOF + RA EOF + RA
Gornitz and Lebedeff (1987)	PSMSL	a)286 b)231 c)130	0.6±0.4 1.7±0.3 1.2±0.3 1.0±0.1	SA SA SA + GD RA + GD
Peltier and Tushingham (1989; 1991)	PSMSL	40	2.4±0.9	EOF + GM
Trupin and Wahr (1990)	PSMSL	a) 120 b)97 c)84	1.2±0.1 1.6±0.1 1.75±0.1	SA + GM SA + GM SA + GM
Douglas (1991)	PSMSL	21	1.8±0.1	RA + GM

AdOP = Association d' Oceanographie Physique, Liverpool
PSMSL = Permanent Service for Mean Sea Level, Bidston Observatory, Birkenhead
NORPAX = North Pacific Experiment

SA= mean of all station trends
RA = regional averages used
EOF = empirical orthogonal functions
GD = correction by geological data
GM = correction by geophysical model

These data, after collection have been edited to remove a number of disturbing factors all of which have a degree of uncertainty about either their measurement or their impact upon the tidal record. Tectonic movements are corrected by using geological data about crustal movements. Geophysical models are used to calculate vertical movements of land associated with post-glacial rebound (see Chapter 4). Mid-latitude data sets are also susceptible to effects from sedimentation, ground water and oil extraction (Fairbridge & Jelgersma 1990). The characteristics of the tidal record on a given coastline are also modified by lithology, landform, wave climate, longshore currents and storm frequencies (Gornitz 1995), all of which must be eliminated when comparing tide gauges at a global scale. Further, tide gauging stations are not uniformly distributed across the globe, being more common in the northern hemisphere than in the southern hemisphere, with Africa, Asia, ocean islands and polar regions sparsely represented.

However, all the investigations reported in Table 6.2 find a positive mean rise in global sea level. Is this a robust finding as suggested by Warrick & Orlermans (1990) or is it merely a reflection of the fact that all the investigations are based on the same data set supplied by the Permanent Service for Mean Sea Level (PSMSL) (Woodworth 1990)? Given the facts that the surface of the ocean bodies is not a uniform surface and that the ocean masses are made up of layers which respond at different rates to changes in temperature, one may question the feasibility of generating values of mean sea levels based on a few limited gauging stations on the edges of these large water bodies. Indeed, Plag (1992) argues that one cannot use coastal relative sea level changes to deduce climate related signals in sea level. He suggests that the coastal observations of relative sea level do not give sufficient information to evaluate the integral over the ocean surface required to determine a global sea level curve or a global trend (Plag 1992, p.728). Gornitz (1995) highlights the fact that the effects of a world wide sea level rise will be spatially non-uniform. Where the global changes are superimposed on local vertical crustal movements, the sea level changes will either cancel out or be exaggerated. Barnett (1984), Pirazzoli (1986) and Emery & Aubrey (1991) are also all sceptical about the possibility of determining a global sea level rise from existing data.

The average rate of rise (Table 6.2) over the last 100 years has been 1.0-2.0 mm/yr. There is no firm evidence of an acceleration in global mean sea level rise during this century (although there is some evidence that sea level rose faster in this century than in the previous two centuries). There exist inherent problems when identifying where the changes have come from. The evidence suggests that the Greenland ice sheet has contributed positively to the rise in sea

level, whereas the Antarctic ice sheet remains insignificant in the estimations. The analyses of the tide gauge data all conclude that there has been a globally coherent secular rise in sea level and that the causes are most likely to be related to climatic change. One underlying fundamental limitation of these findings, however, is that all the investigations are based on the same data sets, so they may all be systematically flawed.

Although all the research studies indicate that globally sea level is rising, when these results are considered together with the list of limitations, outlined previously, it becomes apparent just how potentially inaccurate all of the results may be. In particular, in higher latitudes the signal of isostatic readjustment will be great i.e. Scandinavia and Peltier & Tushingham (1989) argue that relative sea level trends recorded on tide gauge records of sufficiently temporal duration are significantly contaminated by ongoing processes such as glacial isostatic adjustment and that these will be significant at sites well removed from centres of deglaciation.

Accordingly, is it really surprising that many researchers (eg. Pirazzolli 1986, 1989) are asking whether an average of tide gauge measurements can really represent any eustatic trend? There are techniques available for removing some of the factors which generate noise in the tidal data set. Peltier & Tushingham (1989) removed the effects of long wave crustal movements by geophysical modelling, whereas, Gornitz & Lebedeff (1987) used ^{14}C dated palaeosea level indicators to remove glacio-isostatic variations. However, any of these techniques will introduce new elements of errors, as the adjustments themselves will not be perfect, rendering many of the global estimates of limited value.

Looking to the future, scientists agree that global warming will cause sea level to rise, but by how much remains to be answered. The scale of past changes is equivocal for the reasons outlined above but estimates of future trends are difficult to compare because of the variation in methodologies used, the time scales over which the data are analysed, and the different models used to quantify certain aspects of global warming.

Despite all the data and research suggesting that sea levels are rising, there remain many inherent weaknesses in relation to aspects of the methodology. One of the most fundamental problems with sea level predictions, is the lack of data on a global scale, in relation to the ocean masses. A few tide gauges non-uniformly scattered across the globe provide insufficient data on which to generate sound conclusions. The IPCC predictions are not only based on fundamentally and poorly specified GCMs, but also on predictions for greenhouse gas emissions. The report predicts a global rise in sea level, which again is inherently incorrect, as global eustasy as formerly defined by Morner (1969), is now obsolete and of historical interest only (Tooley 1993, p.103).

6.7 Physical consequences of sea level rise: the effects of sea level rise in south-east Fife

The IPCC WGI (1995) projections suggest that there will be greater warming in higher latitudes than in the tropics. These temperature changes will induce changes in the wind patterns and distribution of precipitation. It is currently thought that for the British Isles the cyclonic migration paths will be displaced further northwards (CCIRG 1996). Although in Fife, local surface air temperatures are unlikely to rise by much more than 1-2^{o}C, the world-wide warming will lead to greater evaporation of water from the oceans and increased rainfall along the western and northern coastlines.

Other investigations into changes in tide gauge data across the UK show that northern Britain appears to have had slower rates of sea level rise than the south of Britain, and that the UK tide gauge data most probably do contain a contribution of the same order as the estimated global eustatic rise. Estimates of regional sea level changes by Shennan and Woodworth (1992) can be compared preferably to Gornitz and Lebedeff (1987). Although Woodworth (1985, 1987) believes the changes in the UK are comparative to the global estimates, given the previous discussions, this conclusion is open to criticism.

A fundamental question remains of how to apply an estimated sea level change to a specific coastline. The Brunn rule of erosion (Brunn 1962, 1985, 1988) based on the long term budget of onshore/offshore movement of material is a 2D model which attempts to predict changes in the beach profile and thus could be used in quantifying the effects of sea level rise. Fundamentally the Brunn rule adjusts a given profile based on a shift in the sea level height in terms of the area of deposition offshore to the zone of erosion in the zone of onshore sediment motion. It remains limited in its applications as it is merely a 2D model being applied to a 3D phenomenon together with the fact that it is based on the assumption of a closed material balance system between the beach and near shore and offshore bottom profile. In terms of applying this to south-east Fife the input in material from the mines onto the shoreline over a long time period falls in direct conflict with the assumption described above. Thus the application of the Brunn rule to this coastline would be inappropriate.

In more general terms, along the south-east Fife coastline, with the anticipated encroaching sea levels, the constant attack of waves will cause the profile of beaches to become dominantly erosive in nature. The changes in the climate, and atmospheric pressure, may cause increased storm surges, with the water level in certain areas rising temporarily, bringing new areas into the flood zones. Although the mean sea level may be higher, the tidal range should not change greatly from today. Areas such as Dysart Panhall and East Wemyss may be threatened by increased flooding where today's high water allows little freeboard flooding. Dock and harbour installations such as those at Dysart and Methil, which rise little above present high water will have less clearance at high water in the future. If there are increases in sea level heights as

predicted by the IPCC report, then this rise in sea level may in turn raise the local ground water levels and begin a weakening of the remaining pillars in the stoop and room workings, with a possible increase in collapse of old workings. No predictions of such catastrophic events can be made due to the lack of knowledge on the current stability of the pillars remaining. However the zones known to have been worked using the stoop and room technique can be identified, subject to the completeness of the NCB plans which were used.

Waves formed in the North Sea basin could reach higher levels at the coasts. Wave energies released upon beaches, cliffs and protection walls will lead to damage at sites higher than experienced today. The long term rise of sea level will mean that the area of peak wave activity will be gradually transferred landward from its present position on all beaches. There will be a need to establish equilibrium conditions at progressively higher levels which will inevitably lead to changes in the beach profiles. Changes on any beach will be gradual and it may be difficult to identify the cause of change as being directly related to global warming, especially where there has been significant human intervention along the coast. This is certainly the case along the south-east Fife coastline where human activities through the mining activities have radically altered the natural equilibrium.

Until more regional data are available one can only use the IPCC results available, which have been shown to be too general to be of much use to local sites. Given the uncertainty surrounding so many elements of predictions for climate change and sea level rise, there does not appear to be an increasing future threat along the south-east Fife coastline. Due to the coastal morphology along the south-east Fife coastline, East Wemyss and Panhall may become prone to increased flooding under extreme weather conditions.

6.8 Conclusions

This chapter has explored the theory relating to global warming and sea level rise. The focus of the investigation has been weighted towards the global predictions because these 'global' theories presently form the foundation upon which more regional predictions are made. The number of assumptions made in the generation of predicted sea level height changes means that the values are unreliable and as such it would be misleading to apply such estimations to the south-east Fife coastline in any form.

Schneider (1989) discusses in detail the problems of predicting CO_2 emissions highlighting the problems in quantifying the effects of feedback mechanisms (Mikolajwicz & Maier Reimer 1990). Such problems are further compounded when these CO_2 predictions are used to generate GCMs such as those reviewed by Kukla (1993). The majority of GCMs are inadequate at predicting correctly the effects of any change in climate (Kukla 1993). Furthermore, the links between regional and global environmental systems are not clearly understood with the effect that the GCMs are unreliable when attempting to quantify climate

change at a regional scale. Likewise the predictions generated from the IPCC have severe limitations attached to them (Whyte 1995). Results of current and future sea level changes generated from the use of other methods such as monitoring benchmark heights on the land surface (e.g. Gornitz 1982, Barnett (1984)) all show relatively similar results; however, this is no indication that the results are valid. Given that the data used in the majority of these research projects are the same is it any wonder that the results are similar. More importantly, the size and location of these data samples are so minute in comparison to the water bodies which are being monitored it raises the question of the validity of any of the results. Pirazzoli (1996) examined extensively the work carried out on monitoring and predicting future sea level rise. He concluded that while no scientist presumes that global sea level has been dropping, despite the increasing concentration of greenhouse gases, no evidence can yet be found for an acceleration of MSL rise. (Pirazzoli 1996, p149, Woodworth 1990, Douglas 1992).

This chapter has highlighted fundamental weaknesses in CO_2 predictions and variability in the sea level change estimations to such an extent that it is the opinion of the author that to apply any sea level predictions in any form to a regional area such as Fife would be unreliable and ambiguous. The present predicted global rates of sea level change are shrouded in uncertainty; applying such values at a regional level will merely compound any error. The use of the Brunn rule (Brunn 1962, 1988), a 2D theory applied to a 3D problem combined with the potentially inaccurate sea level predictions could generate extremely misleading results. Therefore, at this stage one can merely hypothesise about the impact of a given rise in sea level in the south-east Fife coastal zone. At present there remains insufficient evidence (Pirazzoli 1996) to suggest that there will be a significant rise in sea level along the Fife coastline.

Chapter 7. Analysis of relationship between coastal changes and mining subsidence

7.1 Introduction

Independent investigations into the different processes known to have influenced the coastline have been explored in this thesis. In this chapter the findings from Chapter 3 and 5 (coastal changes and mining subsidence) are drawn together and the relationships between the two resulting data sets are analysed.

This final analysis required revisitation of the co-ordinates collected in Chapter 3 when the coastal movements were recorded. For every co-ordinate documented in the Smallworld GIS system (where a measurement in the HWM was made) a similar measurement was taken in the IDRISI GIS system where a value of cumulative subsidence was recorded. This process was repeated for the three time periods: 1894-1914, 1894-1960, 1894-1994. Hence, results for total subsidence for the given time period could be directly compared with total recorded movements of the HWM and LWM for the identical location. (All the results are held in Appendix 12, documenting the movements in the water marks with the actual recorded subsidence values for the same co-ordinates). Age breaks for the time periods of 1914-1960 and 1960-1994 were not used due to data anomalies as discussed in section 7.3.

The results from this analysis were then used to generate dual axes graphs (Figures 7.1-7.18) illustrating the mining subsidence values against movements in the water marks, for each point along the coastal strip. Correlation coefficients were calculated for segments of the coastal strip between Buckhaven and Dysart (points 1-102) quantifying the relationship between coastal changes and mining subsidence. As in Chapter 3, the coastline has been subdivided into segments taking into account the effects of the coastal morphology. The coefficients have been calculated using 1894 as the baseline so as to avoid including errors relating to data sampling (see section 7.3 for more details).

Table 7.1: The correlation coefficients between mining subsidence and the migration of the HWM and LWM, calculated for segments of the coast between Buckhaven and Dysart.

	1894-1914		1894-1960		1894-1994	
Points	HWM	LWM	HWM	LWM	HWM	LWM
1-13: Methil to Buckhaven	0.7	0.1	0.7	0.7	0.8	0.6
14-23: Shore Street	0.2	0.6	0.3	-0.2	0.6	N/A
24-50: West Sands to Michael headland	0.7	-0.2	-0.3	0.7	0.5	0.6
51-73: Michael headland to West Wemyss	-0.1	-0.3	-0.2	0.3	N/A	N/A

74-85: West Wemyss to Blair Point	0.2	-0.1	0.4	-0.2	0.5	-0.1
86-102: Blair Point to Dysart Harbour	0.5	-0.1	0.5	-0.2	0.6	0.5

Table 7.1 shows that for the period between 1894 and 1914 there is a varying range in the correlation calculated between the movement in the water mark and the mining subsidence. The low values of correlation equate to those areas where subsidence had not occurred, in particular points 13-23, 51-73 and 74-85. This pattern is equally true at LWM, where only a limited amount of coal had been worked by 1914. By 1960, virtually the entire coastline had been undermined by the coal mining activities, but the correlation coefficients remain low, because the increase in sediment along the beach from the mines had the effect of disguising the relationship between the subsidence and watermark movements. The results produced for the time period between 1894 and 1994 are most important as this time period encompasses the total effects of the mining activities on the coastal environment. Correlation coefficients have not been calculated for the section between the Michael Headland and West Wemyss for the period from 1894-1994 because the 1994 OS plans for this coastal stretch clearly state that the coastline was not resurveyed after 1960 for the latest production of the OS sheets, thus rendering any correlation coefficient for the period 1894-1994 as meaningless.

Volumetric changes in sediment within coastal cells for the Methil to Dysart coastline were also estimated using the digitised HWMs held in Smallworld GIS. The results from these calculations were used to reinforce the evidence that there was a significant build up of sediment along the coastline between Methil and Dysart. These calculations were based on the assumptions that a tidal range of 5m remained constant over the 100 years and that the build up of sediment on the beach did not exceed further than the HWM; thus the beach effectively shifted seawards or landwards. Errors encountered were estimated to be within 20% as a result of possible changes in the beach slope and changes in the height of the beach above HWM. The data were collected by calculating the areas between the digitised HWMs held in Smallworld GIS for the years 1894 to 1914, 1914 to 1960 and 1960 to 1994. The area between the respective high water marks, for the respective editions of the O.S. plans, were converted to square metres and multiplied by the tidal range to give a volume of sediment change for the coastal section. See Table 7.2 for results.

Time Period	**Volumetric change m^3**
1894-1914	$4.3x10^6$
1914-1960	$6.5x10^6$
1960-1994	$3.1x10^6$

Table 7.2 Estimated volumetric changes of sediment for the coastal stretch between Methil Docks and Dysart Harbour.

Further analysis of the results is divided into three sections: Methil to Buckhaven, West Sands to West Wemyss and West Wemyss to Dysart. All reference to points where measurements are taken refer to those co-ordinates used in Chapter 3 (Appendices 2 & 3).

7.2 Methil to Buckhaven (points 1-23)

A significant correlation coefficient of 0.7 was calculated for the section of coast encompassing Methil and Buckhaven (points 1-13) for the relationship between the HWM and the mining subsidence during the 1894-1914 period (Figure 7.1). There was an initial exploitation of coal beneath the coastal zone at Methil, in the Chemiss (panels O, N, P, Q) and Barncraig (panels F and G) seams; all were worked before 1914 (Plate 7.1). These panels generated up to 1.4m of subsidence at HWM (point 4) and 1.8m of subsidence at the LWM (point 4) (see Appendices 11 & 12).

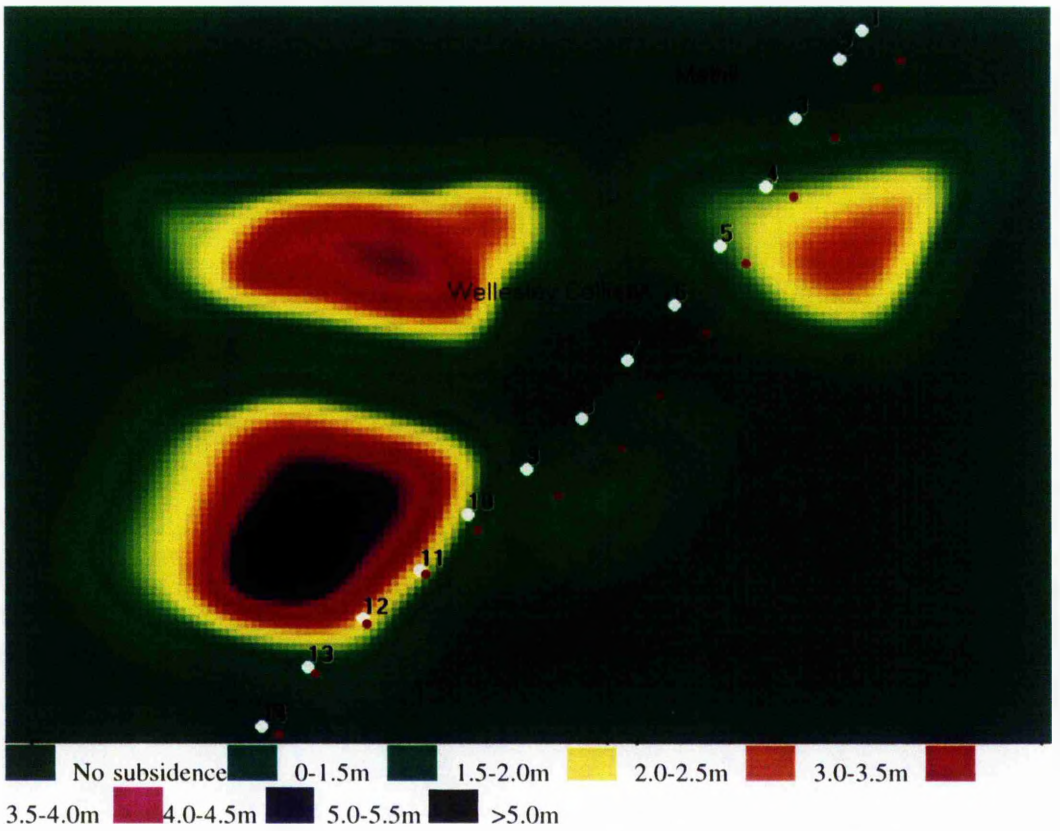

Plate 7.1 Panels worked prior to 1914 in the Methil area. The white dots indicate the 1914 HWM, and the red dots indicate the location of the 1914 LWM. The black areas of the subsidence troughs illustrate maximum subsidence of up to 4m. The plate clearly shows that the coastal zones between points 3-6 and 7-14 were affected by mining subsidence.

The relationship between the LWM and mining subsidence shown in the graph (Figure 7.2) for the period until 1914 is much weaker. However it is important to note that in the early 1900s the Methil docks were being constructed and the coastal dynamics affected by this major construction, may have influenced the changing position of the LWM. This third

unquantifiable variable, in the form of human interference, makes the anticipated explanation for the relationship between mining subsidence and the movement of the LWM difficult to prove.

Towards Shore Street (points 13-22), no coal was mined during this early phase of coal extraction, and thus the coast was affected only by the increase in sediment from the colliery. In chapter 3, for the points 16-23, no unusual movements in the HWM or LWM were recorded for this initial phase; this corresponds with the low correlation coefficient calculated for this coastal stretch.

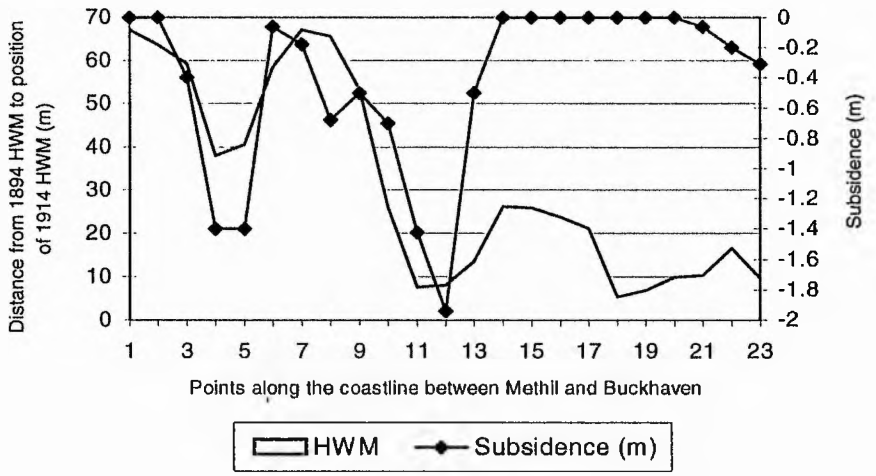

Figure 7.1 Movements in the HWM between 1894 and 1914, between Methil and Buckhaven. There is a strong relationship visible between the position of the sediment build up and the amount of subsidence which occurred in the same place. The site of the Wellesley bing is illustrated between points 7-8 where there has been the greatest build up of colliery waste on the beach. The build up of material towards Shore Street (17-23) is significantly less, and it clear that no coal had been extracted along this coastal stretch up until 1914.

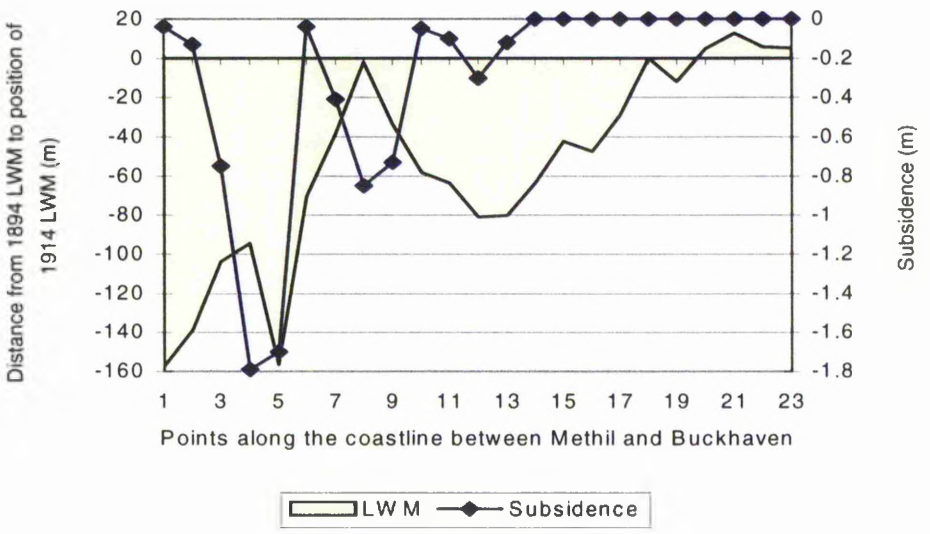

Figure 7.2 Movements of the LWM between 1894 and 1914 compared to the mining subsidence for the same points. The erosion of the LWM between points 4 and 6 is concordant with the subsidence at the same location. Towards Shore Street, (points 17-23) the coastline is more stable, signified by no subsidence recorded at this location and the more stable LWM.

After 1914, to the north of the Wellesley, no further coal was extracted in the coastal zone (Plate 7.2). The review of the process of mining subsidence in Chapter 5 indicates that the residual subsidence would have occurred by the 1960s, so it can be assumed that the subsidence troughs from these workings would have been fully developed and that the land surface would have been lowered. However, it is difficult to assess whether the shoreline would have fully reacted to these changes. The weak correlation between the coastal changes and subsidence at HWM and LWM of 0.3 and -0.2 respectively (for the period 1894-1960) is to be expected and can be explained by a significant increase in colliery waste being dumped on the shoreline. At HWM the supply of sediment flowing into the coastal environment via the bings, and being reworked along the shoreline, caused the beach to build forward significantly. The LWM, also migrated landwards between 1914 and 1960.

Only one small pocket of subsidence was recorded in the Shore Street area, caused by the working of the coal from the Barncraig seam. Panels D and E were small narrow panels which ran parallel to the Shore Street coastline, and generated subsidence values up to 1.94m at the HWM (point 17) and 1.89m at the LWM (point 18) (Figure 7.3, 7.4) (Plate 7.2) (Appendix 12); the results described in Chapter 3, indicate that the HWM did not react significantly to the subsidence, but the LWM migrated significantly landward by between 18 and 49m.

After 1960, no more coal was worked in the Methil to Shore Street coastal zone. The total changes in the coastline recorded between 1894 and 1994, plotted against the total mining subsidence, show that the areas of no subsidence correlate with the positions of greatest deposition (points 6-16) (Figures 7.5, 7.6). The area to the west of the Wellesley Colliery had been converted into the RDL yard. During this period, however, the mining subsidence was insignificant in affecting the coastal changes, and it is probable that erosion along the coast was triggered by the construction of the riprap to protect the Wellesley bing. The supply of sediment down shore was halted and consequently the sea defences had to be extended to protect the housing scheme at Shore Street. The erosion experienced at Shore Street, Buckhaven (points 16-23) in the 1970s which removed the excess sediment along the beaches was predominantly caused by the cessation of the supply of colliery waste, and to a lesser extent by the mining subsidence; this is because only a limited amount of coal had been worked along this stretch. When the coastal erosion began, the rapid removal of material (estimated rates of >10m/year, FRC Report 1977) was due to the nature of the deposited unconsolidated detritus coupled with high energy wave dynamics of the North Sea.

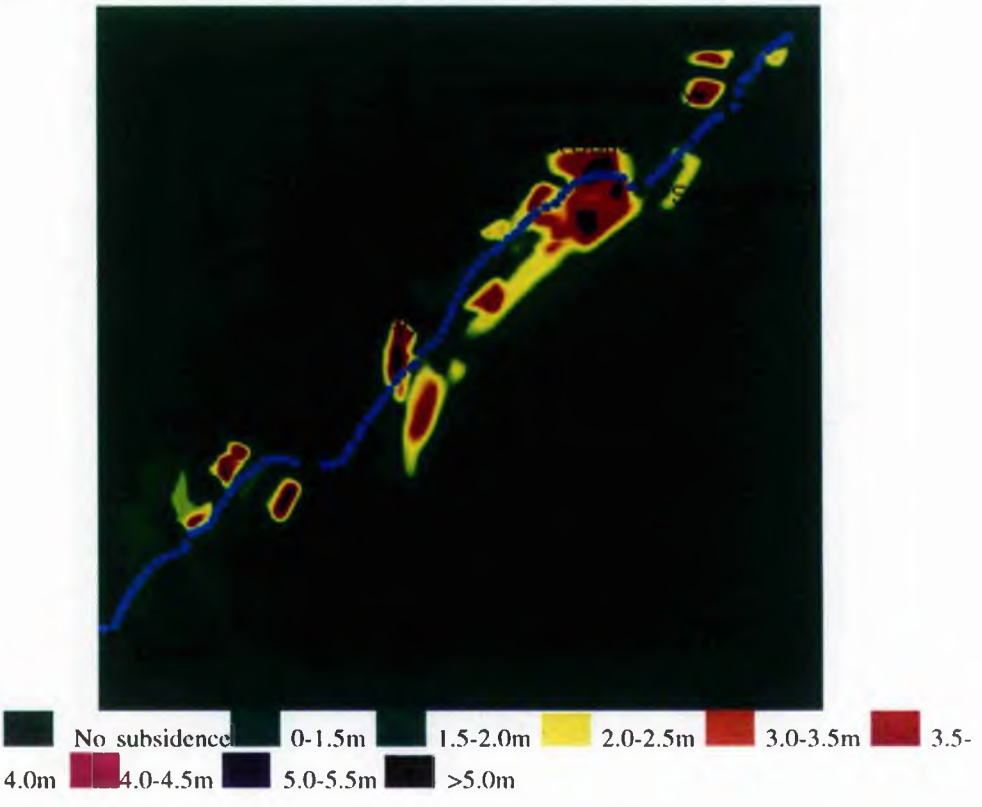

Plate 7.2 Buckhaven to Dysart coastline. The total amount of subsidence generated from coal mining until 1945. Note how no more coal has been extracted in the Methil area, but at Shore Street subsidence from a small panel has occurred.

Riprap protection was constructed before the sea was able to retreat to its former position of 1894 documented on the OS plans (1894) (Plate 2.19, p.24). The limited subsidence

recorded at this site (~0.2m) however, suggests that the coastline could have stabilised once the redd had been naturally removed. Mining subsidence appears to have played a significantly less important role during the entire 100 year period at Shore Street with the human activities, viz the creation of the Methil Docks and increase in sediment supply to the coast via the Wellesley bing, remaining the underlying cause for the recorded changes in the coastal equilibrium. The most recent protection constructed at Shore Street has now stabilised this coastal stretch.

Over the 100 year period the beach at Shore Street has shifted seaward with an estimated total volumetric increase of $4.2x10^5m^3$ of sediment present along this stretch of coastline (Coastal stretch encompassing Shore Street to Buckhaven Harbour points 17-23). In comparison the mining subsidence appears to have been insignificant in altering the equilibrium of this coastal stretch despite values of up to 1.8m of subsidence occurring in the Methil zone (points 4-5). The sediment input from the bings has dominated the changing characteristics of this stretch of coastline.

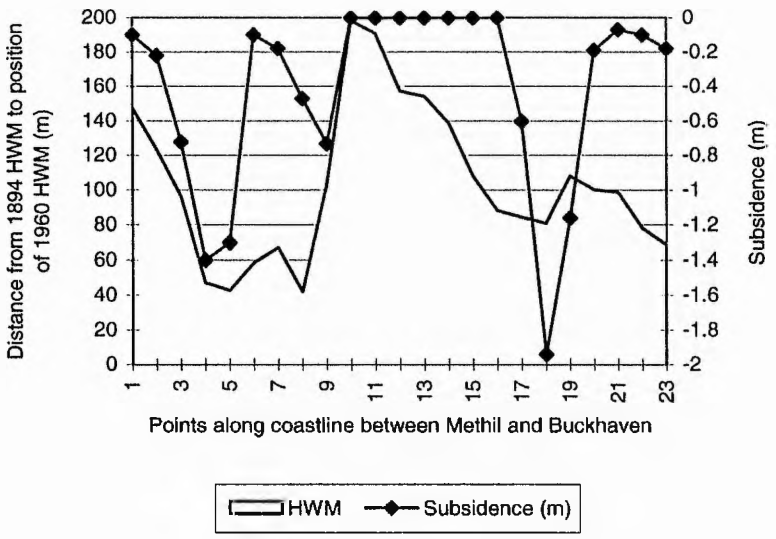

Figure 7.3 Movement in the HWM for the period 1894-1960, between Methil and Buckhaven. The entire coastline has experienced deposition at the HWM, although, the amount of deposition varies significantly along the coastline. Those areas which have experienced least deposition are concordant with those locations of maximum subsidence.

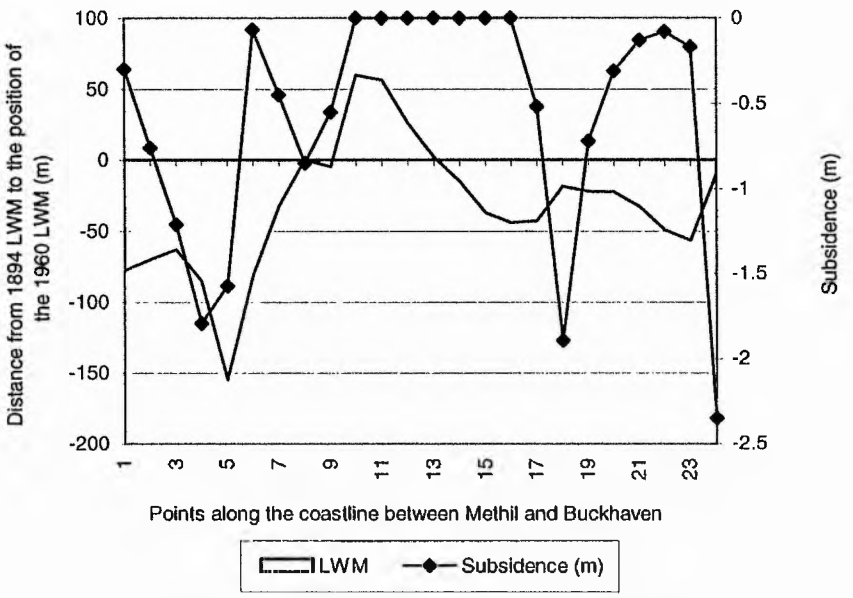

Figure 7.4 Movement of the LWM for the period 1894-1960, between Methil and Buckhaven. The Wellesley bing protrudes beyond the LWM at points 10-13. Elsewhere the LWM has shifted landward, although the movements in the LWM do not appear to relate to the values of subsidence at the same points.

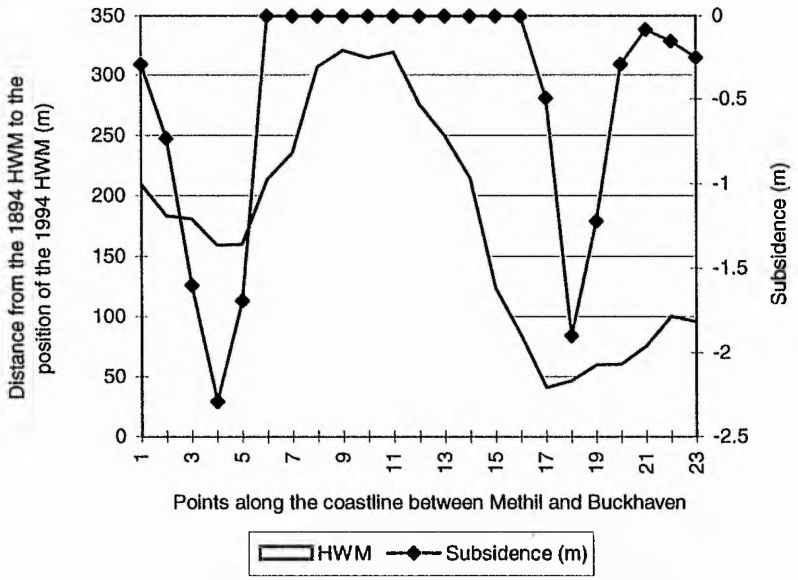

Figure 7.5 Movements in the HWM and subsidence values, for the period 1894-1994, between Methil and Buckhaven. The waste from the Wellesley bing has completely dominated this entire coastal stretch. Overall, less deposition has occurred where subsidence has been recorded, specifically at points 4 and 18.

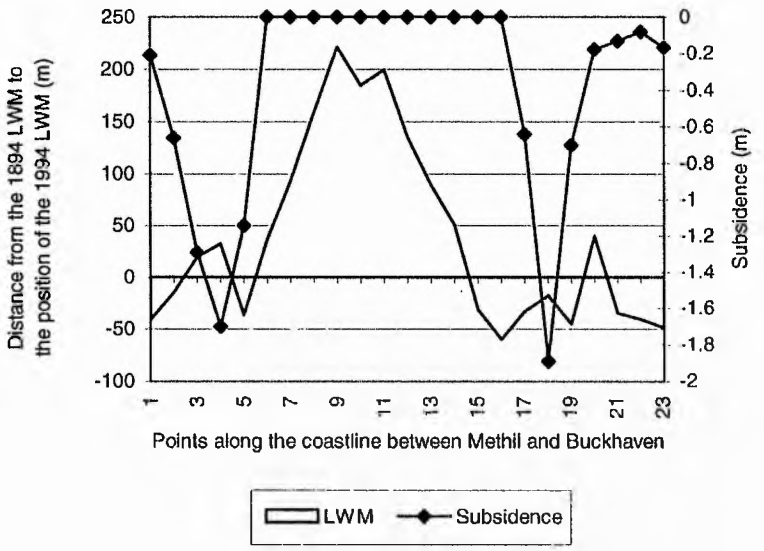

Figure 7.6 Movements in the LWM and subsidence values, for the period 1894-1994, between Methil and Buckhaven. Once more the Wellesley bing has dominated the coastal activities along this coastal stretch, specifically between points 6 and 15. To both the east and west of these areas subsidence troughs have caused a landward migration of the LWM at points 4 and 18, although, only a limited amount of subsidence has affected this coastal stretch.

7.3 West Sands to West Wemyss (points 24-73)

The sheltered nature of the West Sands Bay (points 24-30) complicates the relationships between erosion, deposition and mining subsidence. The working of the Chemiss seam, prior to 1910 (panel A) (Appendix 11) (Plate 7.3), undermined the coastal zone at West Sands and may have caused the immediate landward migration of the HWM at the points 24 and 31, for the period 1894-1914 (Figure 7.7) as up to 2m of subsidence were generated from this mine panel. For the same period, the LWM did not change position significantly, despite the effects of subsidence (>1.3m) from the panel extending into the Forth Estuary (Figure 7.8) (Plate 7.3). Beyond point 31, although erosion was recorded, no subsidence is documented as having occurred. However, on closer inspection of the results, this divergence between the data sets is probably caused by a systematic error in the analysis. Along this coastal stretch, a coal panel, panel A of the Barncraig seam, was excluded from the analysis because it was being worked during the cut off point of 1913; in all probability it had already caused subsidence. This suspected subsidence is reinforced by the recorded negative movements of the HWM (Figure 7.7). Such discrepancies between the comparison of water movements and subsidence results highlight an inherent problem in dealing with historical data sets. The 1914 OS plans document the movements of the HWM and LWM until 1913 (when the coast was re-surveyed); hence for a consistent comparison of data, only coal panels worked out completely by this date were included. The graph (Figure 7.7) clearly illustrates the misalliance between the two data sets, caused by setting the arbitrary

cut off point; there is a landward movement of the watermark but no subsidence is recorded at the given location and date. However, if extra data from the Barncraig A panel (worked between 1910 and 1928 see Appendix 11) are included, the correlation coefficient is improved. Here, for example the partial extraction of the Barncraig A panel should have been included. Such an anomaly can only be identified in hindsight. Information supplied on the plans for each panel tends to be restricted to start date of extraction and end date of extraction; in some cases covering more than one calendar year in time. An estimation of the position of the face during that period is impossible to make with reasonable confidence as there is no way of knowing if the panel was worked consistently during that time period. This example illustrates how mine panels appear to have had an impact upon the coastal zone almost immediately. Thus the interpretation of the results requires an in-depth knowledge of the data sources used.

Just beyond the Dovecot (point 43-50) as far as the Michael Colliery, there was very little change in either the HWM or the LWM. Likewise there had been no coal extracted in this area. The coastline appears to have remained stable (Figure 7.7). This relationship highlighted between the mine workings and coastal stability further explains the anomaly identified in Chapter 3, where it was demonstrated that at point 43, at the HWM, between 1894 and 1914, there was a sudden shift in the HWM. The mining subsidence results which were collected independently, show that point 43 (0.5m subsidence recorded), represents the edge of some mine panels and thus a sudden reduction in subsidence beyond that point occurred (0.1m subsidence recorded at point 44).

From the Michael Colliery towards West Wemyss (points 50-73) in 1914, subsidence generated was coupled with a reduction in sediment deposition at the HWM. The panel of coal worked out beneath the Glass Cave (points 58-59) was probably the direct cause for the collapse of this cave in the early 1900s. Again the irregular shift in the HWM, noted at point 58 of the HWM between 1894 and 1914, can be directly linked to subsidence troughs from the Barncraig and Chemiss seams (Panels K and J respectively) at the same locations where up to 1.9m subsidence occurred. Beyond point 63, towards West Wemyss, the HWM was recorded as being stable; this is coupled with no subsidence recorded for this coastal stretch. The influx of sediment along the coastline at point 68, can be accounted for by the groyne which encouraged the natural deposition of sediment in that vicinity.

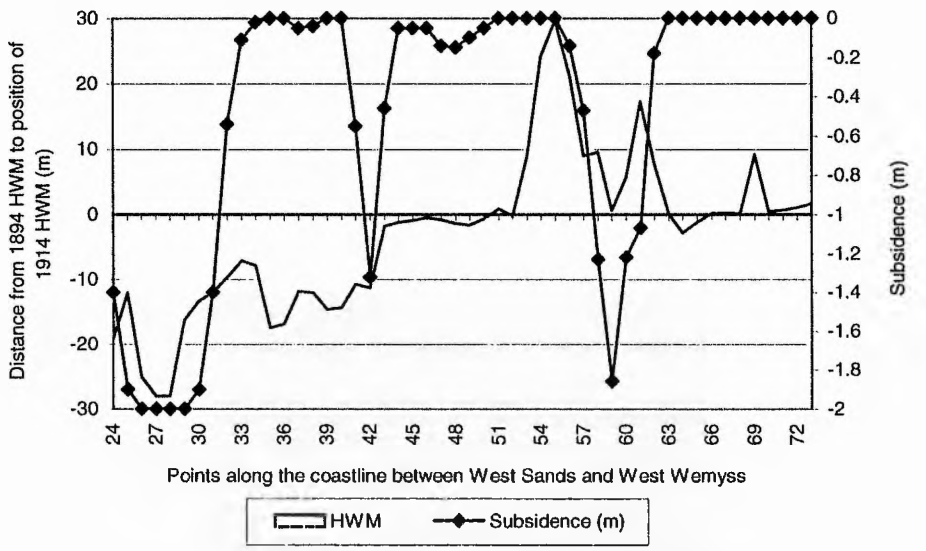

Figure 7.7 Movements in the HWM for the period 1894-1914, between West Sands and West Wemyss. The subsidence at West Sands and the erosion for this coastal section correlate well. The misalliance of the data is clearly visible between points 31 and 42. Along the coastline, at points 43-53, the stability of the coastline is reflected in the lack of coal which has been mined at the same points. The Michael bing protrudes, at point 54, where it has caused the seaward migration of the HWM. The subsidence at points 58-59 also correlates with the erosion documented at the same points.

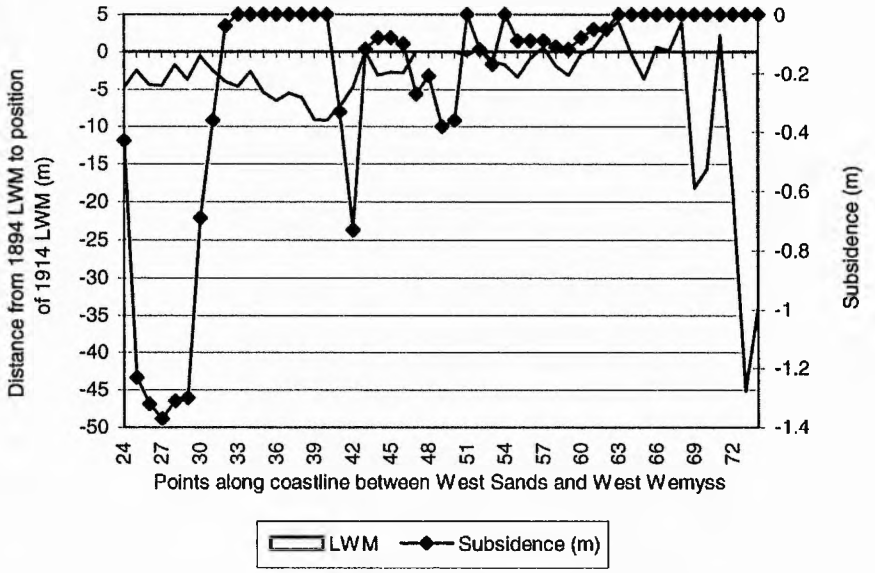

Figure 7.8 Movements of the LWM and subsidence values, for the period 1894-1914, between West Sands and West Wemyss. The subsidence recorded in the West Sands Bay does not correlate as well with the erosion recorded at the same points. Similarly, beyond point 67, over 45m of erosion has been recorded, although no subsidence has been calculated for the same location.

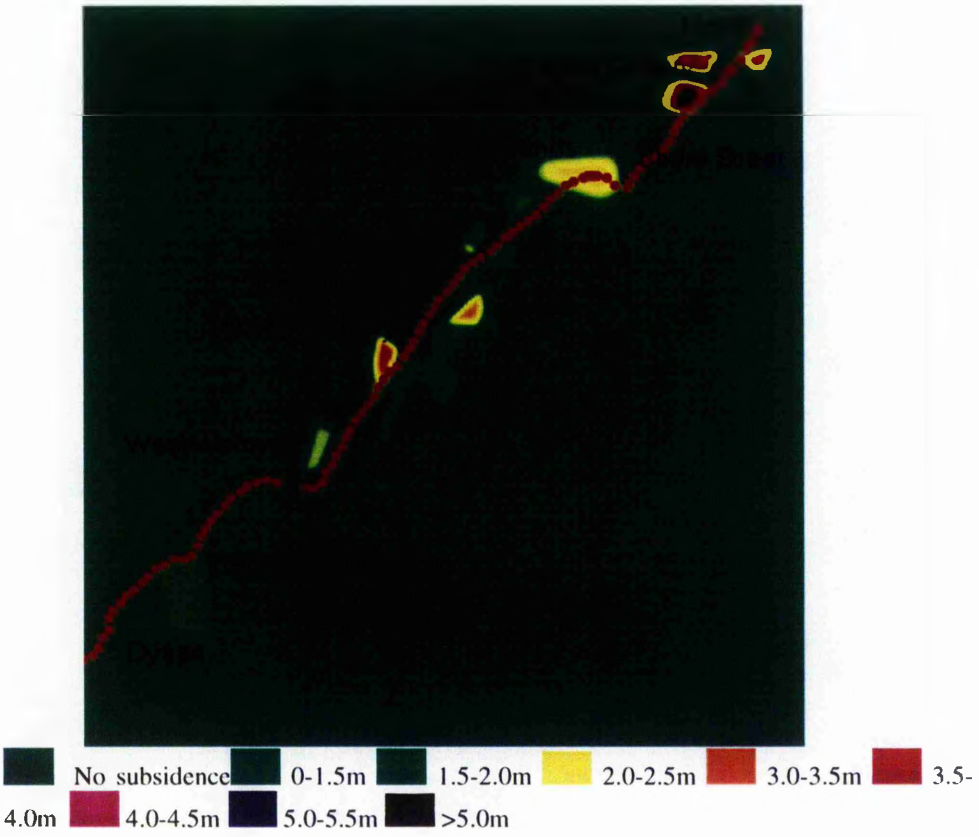

Plate 7.3 Mining subsidence from coal working out up until 1910, between the Buckhaven to Dysart coastline. Coal worked in the West Sands area has produced a large subsidence trough, and pockets of subsidence can be seen along the East Wemyss coastline. The red dots show the 1914 coastline at 100m intervals where coastal changes were measured.

The LWM is recorded as having migrated landward significantly during this period (1894-1914). Coal had been mined along this coastal stretch prior to 1894 (Plate 5.4, p.123-124). By the time the coastline was surveyed in 1894 the HWM may have already retreated as a result of the subsidence. Given that the LWM at West Sands did not appear to react immediately to the lowering of the land surface by subsidence, it is feasible that a delayed reaction of the LWM was experienced here too. It is also extremely likely that those panels were dipping, (which is consistent with all the other seams in the area) which would have the effect of deflecting the subsidence in the seaward direction beyond the HWM, towards the LWM. Thus, it is proposed, that the erosion experienced at the LWM between 1894 and 1914 is due to the older workings mined from Victoria and Lady Pit prior to 1894 (Plate 5.4, p.123) which caused subsidence beneath the position of the LWM.

Between 1914 and 1960, there was extensive working of all the coal seams along the south-east Fife coast. In the vicinity of West Sands (for point 31), subsidence movements between 1914 and 1960 increased from 2m to almost 4.5m across the entire coastal zone, due to the further working of panels from the Bowhouse and Dysart Main seams (Appendix 11). This additional subsidence however, was coupled with an estimated $3.5 \times 10^5 m^3$ of sediment

deposition within the bay (Figure 7.9). These trends suggest that the coastal morphology, together with the large influx in sediment, influenced the changing coastal equilibrium. This was illustrated more towards the back of the beach where its sheltered aspect encouraged greater deposition of material, forcing the HWM seaward. Towards the back of the beach the subsidence generated (up to 4.5m subsidence) from the mining appears to have been merely filled with material as it is estimated that between 1914-1960 $3.5x10^6m^3$ of sediment was deposited along this coastal stretch in front of the Michael Colliery (from the loom factory to West Wemyss). To the west of the Michael Colliery, coal was worked extensively as far as point 63, causing subsidence in the coastal zone of up to 3m. Beyond point 63 along the coastline, there was a reduction in the amount of coal worked, although extensive workings continued offshore far into the Forth Estuary, in many of the seams. At the LWM, where the coast is more exposed, the subsidence had a greater influence on the coastal changes and the LWM was forced to migrate landwards as the land surface subsided (between points 24-38 values of 2.3-4.5m of subsidence occurred). By 1960, the new landward position of the LWM appears to be strongly influenced by the subsidence generated along the shore (Figure 7.10).

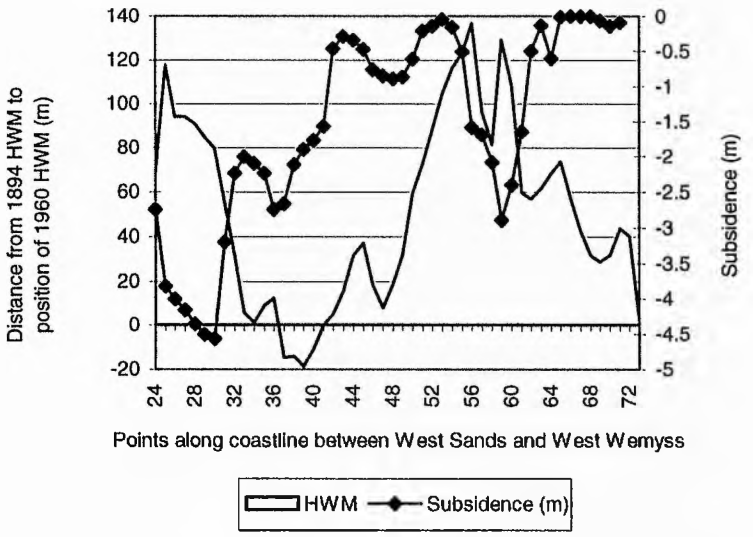

Figure 7.9 Movements in the HWM and subsidence values for the period 1894-1960, between West Sands and West Wemyss. The deposition in the West Sands region of over 100m, clearly disguises the subsidence trough generated at the same location. The build up of colliery waste dominates the graph, especially at the points 52-62, the site of the Michael bing. The sediment build up tapers off towards West Wemyss. There is only a very weak relationship between subsidence and HWM change.

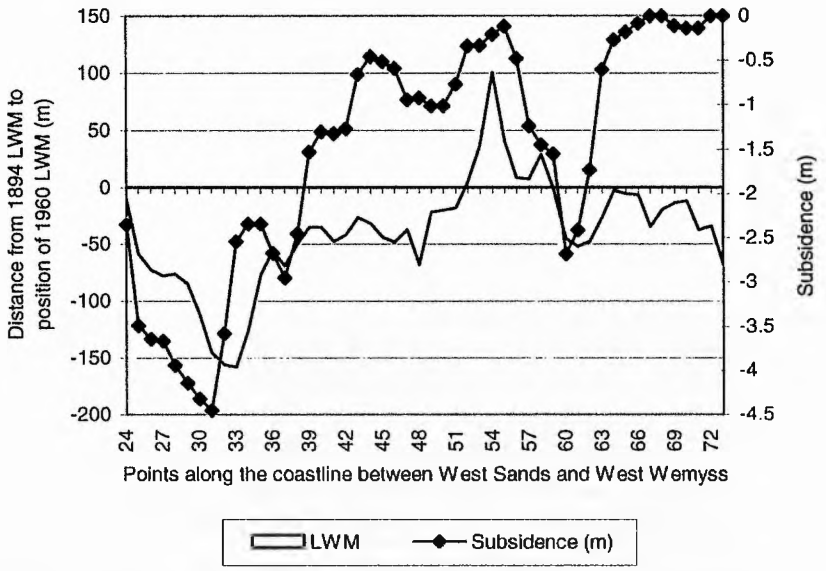

Figure 7.10 Movements in the LWM and subsidence values, for the period 1894-1960, between West Sands and West Wemyss. The erosion of the LWM at West Sands (points 24-34) relate well to the subsidence values calculated for the same location. Likewise, where there has been less subsidence at East Wemyss (points 48-51), the amount of erosion at those points is reduced. Beyond the Michael Colliery, no subsidence is recorded, and similarly, the recorded landward migration of the LWM is lower.

Comparing results of the total subsidence and the total coastal changes for the whole period from 1894 to 1994, for the West Sands to Michael Colliery area, eliminates any problems of including or excluding particular workings based on the dates they were extracted. The redd on the coastal foreshore has disappeared, with only a limited amount of redd remaining at the back of the beaches. Since 1894, between points 30-40, the negative movement of the HWM (17-25m) (Figure 7.11) correlates with the subsidence values (>5m) generated from the Dysart Main, Chemiss, Barncraig, Bowhouse, Coxtool and Branxton seams. Beyond point 40, deposition is the dominant process recorded at HWM which correlates with less subsidence estimated at the same points (See Appendix 12). The recorded changes in the position of the LWM and subsidence values also correlate well (Figure 7.12). Between 2.4-3.0m of subsidence occurred in front of the Wemyss Caves (points 38-42), compared to 0.3-0.9m of subsidence which occurred in the area fronting the loom factory (point 48) (Figure 7.11); this variation in subsidence correlates with the current differential rates of erosion currently occurring along this coastal stretch. This finding confirms the proposal that the areas which are experiencing erosion today are related to mining subsidence. As described in Chapter 2, riprap protection was constructed along only segments of the coast, including a section from the caves to the front of the East Wemyss village. This abrupt ending of the coastal protection scheme just before the loom factory may generate new problems; the area which is now protected may prevent the movement of material along the coast, which in turn could initiate a new phase of erosive activity, specifically at the loom factory. The mining subsidence has clearly caused a significant change in the coastal equilibrium along this

coastal stretch, and human interference is now attempting to prevent any further erosion along the East Wemyss section of coast which has been severely undermined.

In the sheltered bay at West Sands, despite the fact that subsidence has occurred in this area, there still exists a large deposit of colliery waste, which has been maintained due to the coastal morphology, protecting the bay from severe coastal erosion. Given that this sediment build up is man-made and that the supply of the material from further up coast has halted, it is predicted that between the points of 29-34, more erosion of the coastline will be experienced before the coast stabilises. The effects of the subsidence behind the water mark are visible in Plate 7.5 compared to Plate 7.4.

Comparing results of the total subsidence and the total coastal changes for the whole period from 1894 to 1994, for the West Sands to Michael Colliery area, eliminates any problems of including or excluding particular workings based on the dates they were extracted. The redd on the coastal foreshore has disappeared, with only a limited amount of redd remaining at the back of the beaches. Since 1894, between points 30-40, the negative movement of the HWM (17-25m) (Figure 7.11) correlates with the subsidence values (>5m) generated from the Dysart Main, Chemiss, Barncraig, Bowhouse, Coxtool and Branxton seams. Beyond point 40, deposition is the dominant process recorded at HWM which correlates with less subsidence estimated at the same points (See Appendix 12). The recorded changes in the position of the LWM and subsidence values, also correlate well (Figure 7.12). Between 2.4-3.0m of subsidence occurred in front of the Wemyss Caves (points 38-42), compared to 0.3-0.9m of subsidence which occurred in the area fronting the loom factory (point 48) (Figure 7.11); this variation in subsidence correlates with the current differential rates of erosion currently occurring along this coastal stretch. This finding confirms the proposal that the areas which are experiencing erosion today are related to mining subsidence. As described in Chapter 2, riprap protection was constructed along only segments of the coast, including a section from the caves to the front of the East Wemyss village. This abrupt ending of the coastal protection scheme just before the loom factory may generate new problems; the area which is now protected may prevent the movement of material along the coast, which in turn could initiate a new phase of erosive activity, specifically at the loom factory. The mining subsidence has clearly caused a significant change in the coastal equilibrium along this coastal stretch, and human interference is now attempting to prevent any further erosion along the East Wemyss section of coast which has been severely undermined.

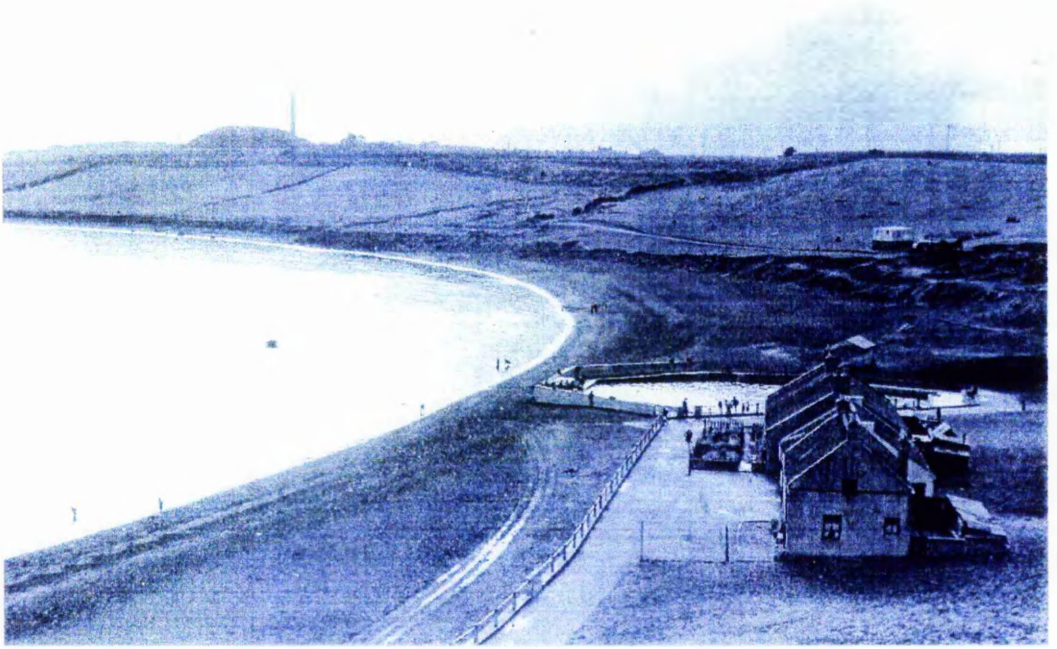

Plate 7.4 The tidal swimming pool at West Sands, Buckhaven, in the mid 1920s. Note the smooth sloping topography of the land area at the back of the picture.

Plate 7.5 The West Sands bay area in 1997, the topography in the back of the picture has become noticeably more 'hummocky' over the past 90 years compared to Plate 7.4. There is no remaining evidence that a tidally linked swimming pool was sited here less than 100 years ago.

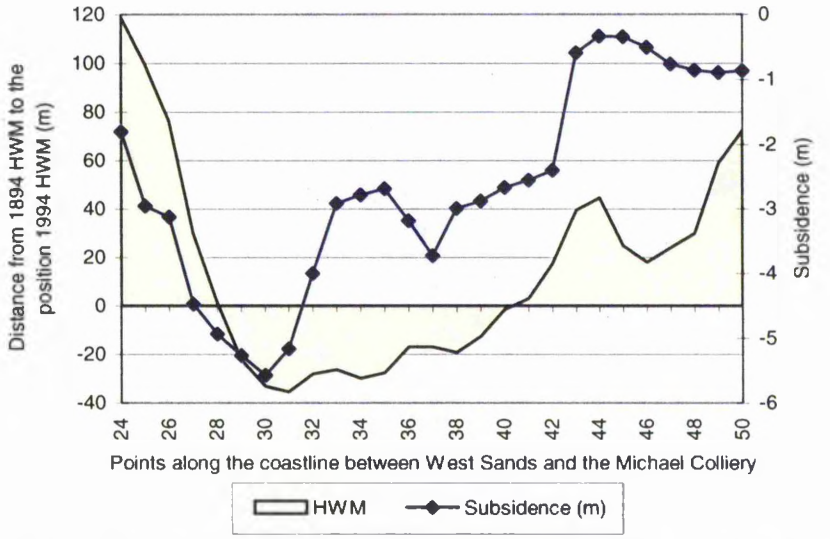

Figure 7.11 Movement in the HWM and subsidence values for the period 1894-1994, between West Sands and the Michael Colliery. Erosion dominates the coastal section between points 29 and 40, subsidence between these points ranges from between 2.5 and 6.0m. The area fronting the loom factory (point 48) has experienced <1m of subsidence. For this period 1894-1994 the graph shows points 24-50 only because the OS 1994 editions were the same as those generated for the 1960 maps thus any comparison of coastal changes against mining subsidence would be incorrect.

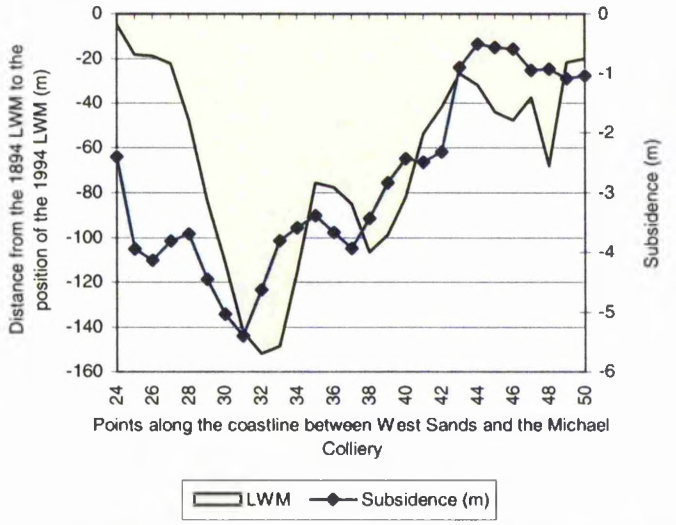

Figure 7.12 Movement in the LWM and subsidence values, for the period 1894-1994, between West Sands and the Michael Colliery. The LWM has migrated landward along the entire coastal stretch, and similarly, subsidence between 1-5m has been experienced. The movement of the LWM, and the subsidence troughs generated between the points 24-50, correlate well. In the West Sand bay, the relationship between the two variables, is less good, but is to be expected, due to the sheltered nature of the coast at the points 24-29. For this period 1894-1994 the graph shows points 24-50 only because the OS 1994 editions were the same as those generated for the 1960 maps thus any comparison of coastal changes against mining subsidence would be incorrect.

7.4 West Wemyss to Dysart (points 74-102)

Between West Wemyss and Dysart, for the period 1894 - 1994, weak correlation coefficients were calculated between mining subsidence and the changing positions of the HWM and LWM. Likewise the graphs produced for this coastal section (points 77-102) show virtually no correlation between the movements of HWM or LWM to subsidence.

Only one coal panel (Dysart Main panel I) was worked beneath the coastal zone between 1894 and 1914 causing only 2.3m of subsidence, although older workings from Lady Pit and Victoria Pit are known to have been worked earlier. The erosion encountered in Chapel Bay (points 75-84) (Figure 7.13) at the HWM had been caused either by the earlier workings taken out via Lady Pit, of which at least two panels have been sited as directly underlying points 74 to 81 (Plate 5.4, p.123-124), or from a natural phase of erosion occurring independently of the mining activities. It is proposed that the recorded erosion at Chapel Bay was caused by mining subsidence at these points because it was noted in Chapter 3 that the free transfer of sediment by longshore drift from adjacent sections of the coast would be inhibited here, and as such, given the correlation of subsidence to erosion along the coastline elsewhere, it is more likely that the erosion was as a result of subsidence rather than from the effect of the Wemyss Harbour or sediment throughput form the east.

Beyond the Frances Colliery (points 93-98) the recorded deposition of sediment may have been as a result of the small bings created from the older pits at Panhall. Once again subsidence prior to 1894 is known to have occurred along this coastal stretch (Knox 1954), making any comparison with the estimated subsidence results for this early period difficult. At Dysart (points 91-102) where no subsidence was recorded, a significant amount of erosion at LWM was measured between 1894 and 1914 (Figure 7.14). It is difficult to make any further comment on this observation as mining activities prior to 1894 are known to have occurred but details of extraction are not documented.

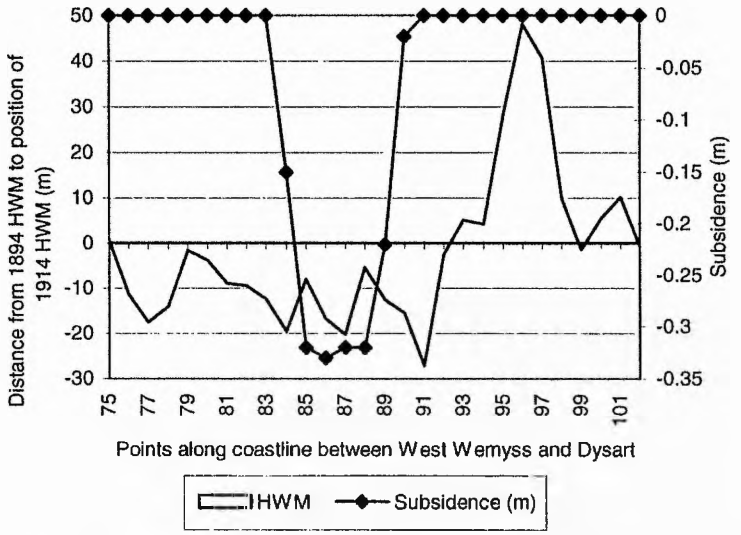

Figure 7.13 Movements in the HWM and subsidence for the period 1894-1914, between West Wemyss and Dysart. No relationship between subsidence and coastal erosion is evident for this coastal stretch. Data exist for only one panel, extracted before 1914, between the points 84-90, although, more coal was undoubtedly taken out during this period.

During the 1914 to 1960 period there was extensive working of the coal in the Sandwell and Dysart Lower seams from the Frances Colliery (See Appendix 11). Although erosion continued along this coastal stretch, in the Chapel Bay area (points 77-88), the effects of the subsidence (>1m subsidence recorded) on the coastal equilibrium made an insignificant impact along the coast (Figures 7.15, 7.16). The massive influx of sediment from the Frances bing into the coastal system counteracted any possible attack of erosion of the HWM caused by subsidence. Likewise, in front of the bing (point 90), any subsidence (~0.3m) has been concealed by the deposition of the colliery waste. The coastal morphology has reduced the effect of erosion; the headland of Blair Point has provided protection in the bay areas of Chapel Bay and Dubbie Bay. The Frances bing, by 1960, extruded over 100 metres into the Forth Estuary; only at this location between West Wemyss and Dysart was the LWM forced seawards. There appears to be little relationship between the coastal changes and mining subsidence; the combination of the sediment influx and coastal morphology appears to have masked any relationship between the coastal changes and mining subsidence (Figures 7.17, 7.18). For the LWM there appears to be a stronger relationship present between subsidence and the movement in the water marks as illustrated in Figure 7.18.

Since 1994, erosion of the coastline has occurred, and the LWM is now sited landward of its former position in 1894 in the Chapel Bay area and at Dysart. The erosion being experienced at Dysart today (points 93-102) is coincident with the location of subsidence (-0.5m) recorded along this section of coast. Although, because only a limited amount of

subsidence has been recorded in this area, the rapid erosion may be equally due to the reduction in the supply of material from the France bing, since the closure of the colliery in 1984. Given that subsidence has occurred between these points, the erosion is likely to continue despite the fact that the HWM has reached its former position of 1894.

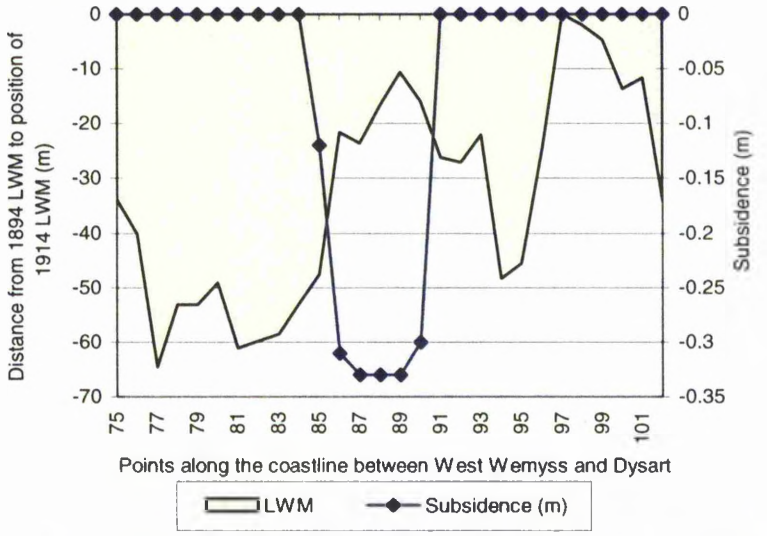

Figure 7.14 Movement in the LWM and subsidence values, for the period 1894-1914, between West Wemyss and Dysart. The landward movement of the LWM dominated this early period, although, this graph indicates that the erosion was not due to the coal mining in the area. Only one panel has been extracted, and only a small amount of subsidence was generated from that panel, <0.35m. This section of coastline, is again hindered by the lack of data available for the old panels extracted.

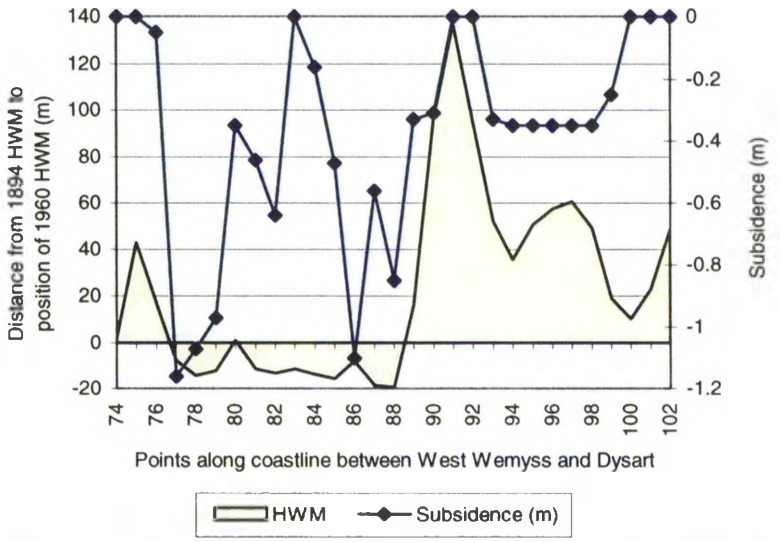

Figure 7.15 Movements in the HWM and subsidence values, for the period 1894-1960, between West Wemyss and Dysart. Extremely erratic subsidence troughs were generated along this coastal stretch due to the irregular working of the coal in this local region. Very limited erosion has been generated as a result of the subsidence between points 74-88. However, beyond point 90, the waste from the Frances bing dominates the activities within the coastal zone.

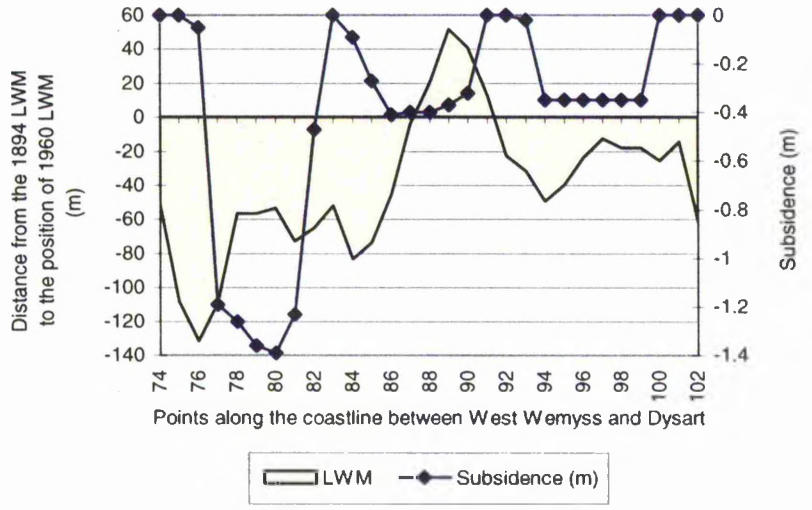

Figure 7.16 Movements in the LWM and subsidence values, for the period 1894-1960, between West Wemyss and Dysart. Again, the trends in the movement of the LWM and the subsidence along the coast do not correlate well. The LWM has migrated landwards, everywhere, except for the area directly fronting the Frances bing. The subsidence troughs which have occurred along this coastal stretch do not appear to relate to the movements of the LWM in any way.

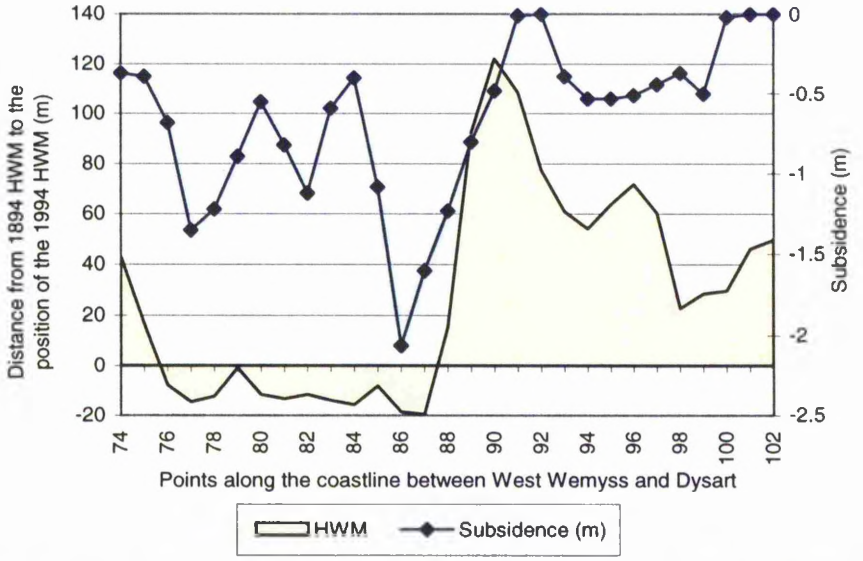

Figure 7.17 Movements in the HWM and subsidence values, for the period 1894-1994, between West Wemyss and Dysart. The Frances bing, has clearly dominated the coastal activity in this coastal stretch over the 100 years; with deposition of waste on the coastline being the main feature, between points 88 and 102. Although up to 2m of subsidence has occurred along this coastal stretch (point 86), it has not triggered a severe phase of erosion.

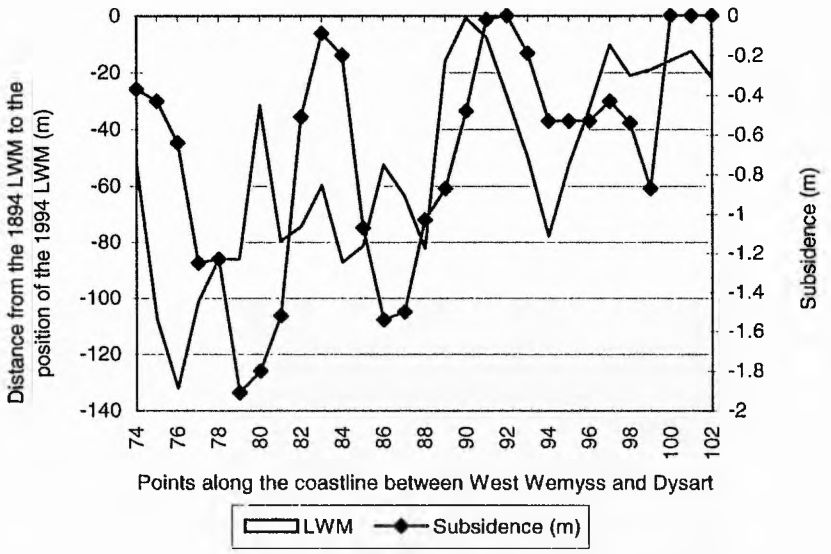

Figure 7.18 Movements in the LWM and subsidence values, for the period 1894-1994, between West Wemyss and Dysart. The erratic movement of the LWM is reflected in similar erratic subsidence troughs along this coastal stretch. These data sets have been produced independently of each other, and yet they appear to follow almost the identical movements. The subsidence troughs are deflected to the right, compared to the erosion produced along the coastline. This may be due to production errors in calculating the deflection of the steeply dipping seams.

7.5 Conclusion

The evidence provided in this analysis chapter suggests that the mining along the coastal stretch of south-east Fife has influenced the coastal changes documented in Chapter 3. Most significant is the landward movement of the LWM in the West Sands bay area of up to 150m on rock platform. This landward migration, documented in Chapter 3, was considered to be accurate and now with the evidence that subsidence of up to 5.4m did occur at this same confirms suggests that the mining activities did in fact cause coastal erosion along this coastal stretch. The total volumetric increase in sediment of $1.0x10^7m^3$ calculated for the entire Buckhaven to Dysart zone between 1894 and 1994 does not detract from the hypothesis that mining subsidence affected this coastline. Indeed simultaneous influx of sediment from the mines on the land surface via the bings has been proved to disguise the effects of the mining subsidence, thus explaining why some of the correlation coefficients for the period 1894-1960 are so weak. It is only in the later years after the mines closed and when there has been extensive removal of sediment along this coastline estimated to be greater than $1.5x10^4m^3$ that the full extent of the mining subsidence has become apparent. The calculated volumetric removal of sediment of $1.5x10^4m^3$ between 1960 and 1994 is likely to significantly underestimate the amount of sediment which was removed because of the problems with the editions of the O.S. plans using the same HWM and LWM data for the years 1960 and 1994.

An inherent limitation of working with the OS plans and mining subsidence data sets is the impossibility of dating the exact timing of certain coal extractions and movements in the water marks, thus making direct comparison of results (water marks to subsidence values) less reliable. As a result of the static nature of the data sets used, the comparison of results was restricted to the start date of 1894 and in this way the number of panels in the process of being worked was significantly reduced. Likewise by 1960 many of the panels had been completely worked out and the major coal extraction was occurring further out under the Forth. The correlation co-efficient for the 1894-1914 period are subject to the limitation that other seams may have already contributed to the slumping of the land but were not included in the subsidence value calculated.

Such limitations are caused by the static nature of the historical data sets used but they do not weaken the argument that mining subsidence has been the major contributor to the coastal erosion recorded along this stretch of coastline.

Chapter 8. Conclusions

This thesis has investigated in detail the coastal zone of East Fife between Buckhaven and Dysart to determine the impact of mining activities, especially subsidence and spoil disposal, on the development of that zone over the last 100 years. These changes experienced by the coastline are exemplified by the landward and seaward migration of the High Water and Low Water datum recorded on Ordnance Survey maps. Rigorous GIS techniques have been used in the thesis to ensure accurate registration between the data sets derived from different topographic surveys and mine plans. This provides confidence that the correlations calculated between mining activity and coastal changes confirm causal mechanisms. Mining subsidence is now seen to be a major factor in the degradation of the coastal zone. This degradation is now serious, threatening properties and amenities; this has only become apparent following the cessation of spoil dumping on to the beaches.

Integration of data relating to coastal changes through the use of GIS methods is a considerable methodological improvement over simple 'analogue' methods of superimposing maps from different surveys to determine planform changes. However, the setting up of the systems has been extremely time consuming, although the ability to maintain a high level of accuracy has ensured reliability of results. Of course, the selection of the best GIS system is fundamental to obtaining maximum performance from the system. Unfortunately in this thesis the advantage of Smallworld, a UNIX based system, in creating vector images, proved inappropriate for the investigations required for the subsidence data, where a raster based GIS system was the most appropriate tool to use. The incompatibility of IDRISI and Smallworld meant that a significant amount of time was consumed manually transferring data between the two GIS systems. Despite its limitations the GIS system did allow for the precise overlaying of mining subsidence troughs onto the coastal changes data sets; a combination of data sources never attempted before. In further research investigating subsidence in a coastal location, the incompatibility noted above between the two GIS systems would not prove to be a barrier as new programs, such as ArcView, which are able to deal comprehensively with both raster and vector data sets are now available.

The SDPS software package used to calculate the mining subsidence, although requiring a significant amount of preparation of the mine plans, was capable of producing detailed and accurate results for the coastal zone. Limitations lay in the maximum spatial distribution of the points at which subsidence was being calculated, a feature dependent on the capacity of the computer. The PC used restricted the size of the panels for which subsidence was being generated, whereas a more powerful computer would have allowed more detailed analysis to be performed. SDPS was sufficiently flexible to permit the adjustment of the program to replicate the characteristics of the British coalfields. Furthermore, if site specific data on subsidence troughs generated in the south-east Fife area had been available, the calibration

of the SDPS could have been made more accurate. This approach would have eliminated the 10% confidence limited imposed by the SEH data set.

The methods established in this thesis could be applied to other investigations of other coastal areas where mining has taken place directly under the coastal zone. The creation of an iconic model, by using GIS, together with other detailed coastal information can be used as a predictive tool to identify those areas which will be at greatest risk. The use of the correlation coefficients has provided statistical evidence of a strong relationship between coastal movements and mining subsidence. The dual-axis graphs demonstrated the spatial relationships which exist between these two variables (HWM/LWM and subsidence values). It would be of value to extend further the data set to other areas of the country where similar processes have occurred. From such investigations it may be possible to enhance and develop a more sophisticated and reliable method for predicting the effects of subsidence where only a limited amount of data exists. The independent evidence collected for the benchmark evaluation further reinforced the relationship between mining subsidence and recorded land slumping.

Despite the emphasis placed upon the use of reliable map sources used in this thesis, other sources of data must be also be investigated in order to develop an understanding of the history of the area in question. Thus, photographic evidence still remains one of the most important data sources for any thesis which is exploring changes which have occurred over a given time period.

During the past 100 year period mining subsidence has proved to have played a significant role in altering the coastal equilibrium of the south-east Fife coastline. Evidence collected, concerning the movement of water marks, benchmark evaluations and the calculation of subsidence values, has shown that there is a strong relationship between coastal erosion and land slumping through mining subsidence. It is clear from the investigations of relative sea-level in Chapter 4 that the effects of isostatic uplift over the last few thousand years have had minimal effect upon sea-level changes around East Fife over the last 100 years. The current prediction of 1-2mm/yr land uplift is clearly insignificant with respect to the coastal changes occurring today. The work by Shennan (1989) in the Forth area could be refined by a detailed analysis of all tidal records in the Forth estuary area, but even if there were a doubling of Shennan's estimates this would not affect the conclusions regarding the impact of isostasy on coastal processes in the area.

The investigations in Chapter 6 suggest that it is not yet possible to quantify either the mechanisms or the extent of sea level change associated with possible global warming. Changes of sea level due to this cause over the past 100 years and predictions for the future vary widely, depending upon the data base and the analytical procedures used (Pirazzoli 1998). However, the findings of chapter 6 suggest that further research in this field is

required to enable the environmental impacts of global warming on the coastal zone to be explored. The effects of extreme weather conditions, experienced in the form of high tides and storm surges, as predicted by some investigations into global climatic change, may also further threaten those areas of coastline which have been rendered unstable by the mining activities..

This historical investigation has highlighted the long term effects that coal mining can have on the coastal environment. Presently, the mining of coal beneath residential or commercial settlements is treated with care, in an attempt to reduce the effects of subsidence on the land surface. This thesis has shown that the coastline should also be treated with as much respect, since the consequences of working extensively under the coastal zone have been shown to be manifested in both the immediate erosion of the coast, as well as threatening developments adjacent to the shore. It is worth highlighting here that many of the coastal land features between Buckhaven and Dysart have disappeared, the dovecot, gasworks, swimming pool - all victims of the mining era.

The volumes of sediment mobilised and transported in the coastal zone of East Fife during and after recent mining activities are very considerable. The data demonstrate the extent of the power available for coastal modification even in a relatively sheltered environment where wave heights rarely exceed 1.5metres at the break point (Miller 1996). The large scale movements can be attributed not only to the fact that the dumping of spoil represents a disruption of the natural equilibrium but also that much of the spoil was erratic in terms of both size and density compared to the natural beach material. The study by Miller (1996) showed that coal and sandstone from the bings was transported greater distances over a tidal cycle compared to quartz and ironstone debris of similar size. Significantly some materials were transported in opposite directions under the same wave conditions. The exposures of spoil in today's eroding bings show substantial amounts of fine material which are not represented on the beaches and are clearly rapidly lost from the beach zone.

The net movement of material in the coastal zone as exemplified by the migrations of the Low Water and High Water marks, underestimates the gross movements in the shore zone. It would be of interest, and worthy of a detailed research investigation, but beyond the scope of this thesis, to study the pathways and destinations of the exotic material introduced to the beaches of east Fife. Commination of the softer rocks must take place during transport along the coastal fringe and the recession of the present shoreline indicated that material is being lost from the intertidal areas. The location of the sinks of material in the offshore zone are not clear. If the material is localised, the shoaling would be sufficient, considering the volumes involved, to be identifiable in an offshore bathymetric survey and thus warrants further research.

It is the opinion of the author that the problems of coastal erosion will continue where the coastal areas have been found to coincide with past mining subsidence. Presently, in some areas the HWM continues to migrate landwards. Where little subsidence or no subsidence has occurred the HWM is predicted to stabilise once it has reached its former position in 1894. This will not be the case along those coastal segments where over 0.5m of subsidence has occurred. Segments of the coastline which have not been disturbed by the coal extraction include the site of the Wellesley pit-head (points 6-9), along Shore Street at Buckhaven (points 14-17), the Michael outbuildings (points 53-54), and the site of the Frances pit-head (points 90-91). The lack of coal worked out underneath the colliery pitheads ensured the stability of the land surface at these points. The control site at Kinghorn illustrates how these changes which occurred between Buckhaven and Dysart are unique to this coastline where mining activities have dominated the environment.

The consequences of future sea level rises must be considered not only in terms of those areas threatened by coastal inundation, but also in relation to the effects of the rise in the water table. This could have the effect of raising the water level in old stoop and room workings located just beyond the coastal zone. A reduction in the stability of the remaining pillars through corrosion, could cause further subsidence. However, mining activities, which include the dumping of waste on the beaches and mining subsidence, have strongly influenced the changing face of this coastal landscape. Although the sediment scarred the landscape during the mining era, the subsidence will have a longer lasting effect on the coast, altering the natural equilibrium forever. The potential rising sea-levels combined with the subsidence are a combination which will accentuate any problems of erosion along this coastal stretch.

References

Allen, K. (1992). *Personal communication.* Fife Council Department of Engineering (Water and Drainage Division).

Arrol, T. (24.10.96). *Warning of coastal erosion problems.* The Courier, Dundee.

Ballantyne, C. K. (1984). The late Devensian periglaciation of upland Scotland. *Quat. Sci. Rev.*, 3, 311-343.

Barnett T.P. (1983). Recent changes in sea level and their possible causes. *Climate Change,* 5, 15-38.

Barnett, T.P. (1984). The estimation of global sea level change: a problem of uniqueness. *J. Geophys. Res.,* 89 (C5), 7980-7988.

Barnet, T.P. (1988). Global sea level change. In *NCPO climate variations over the past century and the greenhouse effect.* A report based on the first climate trend workshop, 7-9 Sept. 1988, Washington DC, National Climate Program Office/ NOAA, Roxville, Maryland.

Bernharsden, T. (1992). *Geographical Information Systems.* Viak IT, Norway.

Bird, E.C.F. (1993). *Submerged coasts: the effects of a rising sea level on coastal environments.* Wiley, Chichester and New York.

Boulton, G.S, Jones, A.S., Clayton, K.M. & Kenning, M.J. (1977). A British ice-sheet model and patterns of glacial erosion and deposition in Britain, in *British Quaternary Studies: Recent Advances,* pp. 231-246, ed. Shotton, R.W., Clarendon Press, Oxford.

Burrough, P.A. (1986). *Principles of Geographical Information Systems for Land Resources Assessment*, Clarendon Press, Oxford.

Bowen, D. Q., Rose, J., McCabe, A.M. & Sutherland, D.G. (1986). Correlation of Quaternary glaciation in England, Ireland, Scotland and Wales. *Quat. Sci. Rev.,* 5, 229-340.

Brauner, G. (1973). Subsidence due to underground mining. Pt 1. Theory and practices in predicting surface deformation. *US Dept. of the Interior. Bureau of Mines.*

Bristler, C. (1972). *This is my kingdom.* David Winter and Son, Dundee.

Browne, M. A. E. (1980). Late Devensian marine limits and the pattern of deglaciation of the Strathearn area, Tayside. *Scot. J. Geol.* , 16, 221-230.

Brunn, P. (1962). Sea-level rise as a cause of shore erosion. *Proc. Am. Soc. Civil Engineers. Journal Waterways & Harbours Division,* 88, 117-130.

Brunn, P. & Schwartz, M.L. (1985). Analytical predictions of beach profile change in response to a sea level rise. *Zeitschrift fur Geomorphologie* , 57, 33-50.

Brunn, P. (1988). The Brunn rule of erosion by sea-level rise: a discussion on large-scale two- and three- dimensional usages. *Journal of Coastal Research*, 4(4), 627-648.

Budd, W. F., & Smith, I.N. (1987). Conditions for growth and retreat of Laurentide ice sheet. *Geographic Phys. Quat.*, 41, 229-290.

Cairns, C. (10.10.96). *Nitty-gritty of shifting sands.* Scotsman.

Carey, W.S. (1981). Causes of sea-level oscillations. *Proc. Roy. Soc. Vict.*, 92, 13-17.

Cathles, L.M. (1980). Interpretation of postglacial isostatic adjustment phenomena in terms of mantle rheology. In *Earth Rheology, Isostasy and Eustasy,* N.-A. Mörner (ed.) Wiley, Chichester and New York, 11-43.

CCIRG (1986). *Review of the potential effects of climate change in the United Kingdom.* Prepared for the Dept. of the Environment, HMSO, London.

Clark, J.A., Farrell, W.E. & Peltier, W.R. (1978). Global changes in postglacial sea level; a numerical calculation. *Quater. Res.*, 9, 265-298.

Chamberlain, T.C. (1897). The method of multiple working hypotheses. *Journal of Geology*, 5, 837-848.

Chappell, J. (1974). Geology of coral terraces, Huon peninsula New Guinea: a study of Quaternary tectonic movements and sea-level changes. *Bull. Geol. Soc. Am.*, 85, 553-570.

Cunningham, A.S. (1905) *Rambles in the parishes of Scoonie and Wemyss.* Leven Advertiser and Wemyss Gazette.

Cunningham, A.S. (1912) *Dysart, past and present: and Pathead, Sinclairtown and Gallatown.* L.E. & H. Russell, Leven.

Cunningham, A.S. (1913) *Mining in the 'Kingdom' of Fife: history of the industry.* Leven Advertiser and Wemyss Gazette.

Cunningham, A.S. (1922) *Fife Coal Company Limited: the Jubilee year, 1872-1922.* Leven Advertiser and Wemyss Gazette.

Cullingford, R.A. & Smith, D.E. (1966). Late-glacial shorelines in eastern Fife. *Trans. Inst. Brit. Geogr.*, 39, 31-51.

Cullingford, R.A. Smith, D.E. (1980). Late Devensian raised shorelines in Angus and Kincardineshire, Scotland. *Boreas,* 9, 21-38.

Davis, R.A. (1971). Beach and nearshore zone. In Davis, R.A. (ed). *Coastal Sedimentary Environments.* 237-280. Springer-Verlag.

Denton, G.H. & Hughes, T.J. (eds) (1981). *The Last Great Ice Sheet.* John Wiley, New York.

Devoy, R.J.N. (1987). First principles and the scope of sea-surface studies. In Devoy, R.J.N. (ed) *Sea Surface Studies: A Global View.* Croom Helm, London,1-30.

Donald, T. (23.10.96). *Coastal Scheme Targets Wemyss.* Fife Free Mail.

Duckham, F. (1970). *A history of the Scottish coal industry. Vol.1 1700-1815.* David and Charles: Newton Abbot.

Emery, K.O. and Aubrey, D.G (1991). *Sea levels, land levels and tide gauges.* Springer, Berlin, 237.

Fairbridge, R.W. (1983). Isostasy and eustasy. In Smith, D.E. & Dawson, A.G. (eds). *Shorelines and Isostasy.* Academic Press, New York , 3-28.

Fairbridge, R.W. & Jelgersma, S. (1990). Sea level. In *Greenhouse Effect, Sea Level and Drought.* Paepe, R., Fairbridge, R.W. & Jelgersma,S. (eds). Kluwer Academic Pulishers, Netherlands. 117-143.

Fife Regional Council (1977). *Coastal Erosion at Buckhaven.* Department of Engineering Drainage Division.

Firth, C.R., Collins, P.E.F. & Smith, D.E. (1995). *Focus on Firths. Coastal landforms, processes and management options. IV The Firth of Forth.* Unpublished Report, Scottish National Heritage.

Flemming, N. C. (1982). Multiple regression analysis of earth movements and eustatic sea-level changes in the UK in the past 9000 years. *Proceedings of the Geologists' Association,* 93, 113-125.

Forth River Purification Board (1988). *Hydrographic survey off East Wemyss and West Wemyss in connection with proposed sewage outfalls.* Tidal Water Section Report No. TW 11/88.

Frank, A.V. & Egenhofer, M.J. (1992). Computer cartography for GIS- an object oriented view on the display. *Computers and Geosciences,*.18, 975-987.

Franks, C.A.M. & Geddes, J.D. (1986). Subsidence on steep slopes due to longwall mining. *International Journal of Mining and Geological Engineering,* 4, 291-301.

Goodwin, R. (1959). Some physical and social factors in the evolution of a mining landscape. *Scottish Geographical Magazine,* 75, 1-17.

Gornitz, V. & Lebedeff, S. (1987). Global sea level changes during the past century. In *Sea Level Fluctuations and Coastal Evolution.* Nummedal, D., Pilkey, O.H., & Howard, J.D. (eds). SEPM Special Publication. 141, 3-16.

Gornitz, V. (1995). Sea level rise: a review of recent, past and near-future trends. *Earth Surface Processes and Landforms*, 20, 7-20.

Gowans, I.A.T. (1994). *Dysart and East Wemyss coastal protection study.* Report by R.H. Cuthbertson & Partners, in association with H.R. Wallingford, for Fife Regional Council Engineering Department (Water and Drainage Division).

Gray, J.M. & Lowe, J.J. (1977). *The Scottish Lateglacial Environment: a Synthesis, in Studies in the Scottish Lateglacial Environment* 163-182. (eds) Gray, J.M. & Lowe, J.J., Pergamon, Oxford.

Gribbin, J. & Gribbin, M. (1996, July). The greenhouse effect. *New Scientist,* 192, July 6th 1996.

Groger, M. & Plag, H., (1992). Estimations of a global sea level trend: limitations from the structure of the PSMSL global sea level data set. *Submitted to Global and Planetary Change.*

Haines-Young, R.H. & Petch, J.R. (1983). Multiple working hypotheses: Equifinality and the study of landforms. *Trans. Inst. Brit. Geogr.,* 8, 458-66.

Halliday, R.S. (1990). *The disappearing Scottish colliery.* Scottish Academic Press.

Hansen, J., Lacis, A., Rind, D., Russell, G., Store, P., Find, I., Ruedy, R., and Lern, J. (1984). Climate sensitivity: analysis of feedback mechanisms. In Hansen, J.E. & Takahashi, T.,(eds.). *Climate processes and climate sensitivity.* Washington DC. Geophys. Monogr. Ser. 130-163.

Hasselmann, K., Suassen, E., Maier-Reimer, E. & Voss, R. (1993). On the cold start problem with coupled ocean atmosphere models. *Clim. Dyn.,* 9, 53-61.

Hindman, C.A. & Treworgy, C. (1989). Use of a geographic information system to evaluate the potential for damage from subsidence of underground mines in Illinois. *Auto Cartography 9: International Symposium on Computer-Assisted Cartography,* 94, 483-492.

Hoffman, J.S. (1984). Estimates of future sea level rise. In *Greenhouse Effect and Sea Level Rise: A Challenge for this Generation.* Barth, M.C. &. Titus, J.J. (eds), Van Nostrand Reinhold, New York, 79-103.

Huddart, D., Tooley, M.J. & Carter, P.A. (1977). The coasts of Northwest England, in *The Quaternary History of the Irish Sea.* Kidson, C. & Tooley, M.J. (eds), Seel House Press, Liverpool, 120-154.

Hughes, T.J., (1981). Numerical reconstruction of paleo-ice sheets. In: *The Last Great Ice Sheets.* 222-261, (eds) Denton, G.H. & Hughes, T.J., Wiley, New York.

Inglis, R.M. (1951). *A geographical study of the Dysart-Wemyss coalfield.* Unpublished undergraduate dissertation, University of St.Andrews.

IPCC, (1990). *Climate change, The IPCC Scientific Assessment,* Houghton, J.T., Jenkins, G.J., and Ephraums, J.H. (eds), Cambridge University Press, Cambridge.

IPCC, (1992). *Climate change 1992: The supplementary report to the IPCC Scientific Assessment.* Houghton, Callander, B.A., & Varney (eds), Cambridge University Press, Cambridge.

IPCC WG1, (1995). *Climate change 1995 - The science of climate change: contribution of Woking Group 1 to the second assessment report of the intergovernmental panel on climate change.* Houghton, J.T., Meira Filho, L.G., Callander, B.A., Harris, N., & Maskell, K. (eds), Cambridge University Press, Cambridge.

IPCC WG1, (1995). *Climate change 1995 - The science of climate change: Summary for policy makers and technical summary of the Working Group 1 report.* Houghton, J.T., Meira Filho, L.G., Callander, B.A., Harris, N., & Maskell, K. (eds), Cambridge University Press, Cambridge.

Karmis, M., Jarosz, A. & Agioutantis, Z. (1989). Predicting subsidence with a computer. *Coal*, 26, 12, 54-61.

Karmis, M., Haycocks, C. & Agioutantis, Z. (1989). The prediction of ground movements caused by mining. *34rd subsidence workshop due to underground mining*. 1-9.

Knothe, S. (1957). Observations of surface movements under influence of mining and the theoretical interpretation. *Proceedings, European Congress on Ground Movements,* University of Leeds, April.

Knox, J. (1954). *The economic geology of the Fife coalfields. Area III, Markinch, Dysart and Leven.* HMSO, Edinburgh.

Kratzch, H.(1983). *Mining Subsidence Engineer.* Springer Verlag. Berlin.

Kuhn, M. (1993). Possible future contributions to sea level change from small glaciers. In *Climate and sea level change observations, projections and implications.* Warrick, R.A., Barrow, E.M. & Wigley, T.M.L. (eds). Cambridge University Press, Cambridge.

Kukla, G. (1990). Present, past and future precipitation: can we trust the models? In *Greenhouse Effect, Sea Level and Drought.* R.Paepe *et al.*(eds), Kluwer Academic Publishers, 109-114.

Komar, P.D.(1975) *Beach processes and sedimentation.* Prentice-Hall Inc.

Lambeck, K. (1990). Glacial rebound, sea-level change and mantle viscosity. *Quat. J. Roy. Astr. Soc.*, 31, 1-30.

Lambeck, K. (1991). Glacial rebound and sea-level change in the British Isles. *Terra Nova*, 383-392.

Lambeck, K. (1993a). Glacial rebound of the British Isles-I. Preliminary model results. *Geophys. J. Int.*, 115, 941-959.

Lambeck, K. (1993b). Glacial rebound of the British Isles-II. A high resolution, high-precision model. *Geophys. J. Int.*, 115, 960-990.

Lambeck, K. & Nakada, M. (1985). Holocene fluctuations in sea-level constraints on mantle viscosity and meltwater sources. In *Proc. Fifth Int. Coral Reef Congr., Tahiti*, vol. 3, 79-84.

Law, F.M. (1990). The greenhouse effect on low lying land in Britain. In *The greenhouse effect and rising sea levels in the UK.* Doornkampf, J.C. (ed), Nottingham, M.Press, 95-107.

Levenberger, M. & Seigenthaler, U. (1992). Ice age atmospheric composition of nitrous oxide from an Antarctic ice core. *Nature*,360, 449-51.

Lironi, B. (9.9.96). *Call for cash to save historic caves.* The Scotsman.

McManus, J. (1990). *Assessment of sediment movement along the coast at East Wemyss, Fife.* Consultant report to Fife Regional Council.

Malcolm, J. (1990). *Personal Communication..* Head of Subsidence Engineering, International Mining Consultants Ltd., Sutton-in-Ashfield, Nottinghamshire..

Marr, J. (1996). The application of the zone area system to the prediction of mining subsidence. *The Mining Engineer*, October 1975, 53-61.

Marsh, J.G. & Martin, T.V. (1982). The seasat altimeter mean sea surface model. *J. Geophys. Res.*, 87, C5 3269-80.

Melillo, J.M., Prentice, I.C., Farquhar, G.D., Schulz, E.D. & Sala, O.E., (1996). Terrestrial biotic responses to environmental change and feedbacks to climate. In IPCC WG1, (1995). *Climate change 1995 - The science of climate change: contribution of Woking Group 1 to the second assessment report of the intergovernmental panel on climate change.* Houghton, J.T., Meira Filho, L.G., Callander, B.A., Harris, N., & Maskell, K. (eds), Cambridge University Press, Cambridge.

Mikolajewicz, U., Santer, B.D. & Maier-Reimer, E. (1990). Ocean response to greenhouse warming. *Nature*, 345, 589-93.

Mörner, N.-A. (1969). Eustatic changes during the last 20 000 years and a method of separating the isostatic and eustatic factors in an uplifted area. *Palaeogeography, Palaeoclimatol., Palaeocol.*, 9, 153-81.

Mörner, N -A. (1976). Eustasy and geoid changes. *J. Geol.*, 84, 123-51.

Mörner, N.-A., (1987a). Models of global sea-level changes. In *Sea Level Changes,* Tooley, M.J. & Shennan I. (eds). Oxford: Basil Blackwell Ltd., 332-55.

Mörner, N.-A. (1987b). Pre-Quaternary long term changes in sea level. In *Sea Surface Studies: A Global View,* Devoy, R.J.N. (ed). Croom Helm, London. 233-241.

NCB (1975). *The Subsidence Engineer's Handbook.* The National Coal Board.

NCB Records. Mining Records Office, Bretby Business Park, Staffordshire.

National Environmental Research Council (1992). United Kingdom Digital Marine Atlas. Version 2.0 NERC/BODC, Birkenhead.

Oerlemans, J. (1993). Possible changes in the mass balance of the Greenland and Antarctic ice sheets and their effects on sea level. In *Climate and sea level change observations, projections, and implications.* Warrick, R.A., Barrow, E.M., & Wigley, T.M.L. (eds), Cambridge Unversity Press, Cambridge.

Oliver, R. (1993) *Ordnance survey maps: a concise guide for historians.* The Charles Close Society.

Ove Arup & Partners, Scotland (1991). *Wemyss Caves. East Wemyss - Study of coastal protection measures.* Job No.42168, Feb. 1991.

Paren, J.G., Doake, C.S.M. & Peel, D.A. (1993). The Antarctic peninsula contribution to future sea level rise. In *Climate and sea level change observations, projections, and implications.* Warrick, R.A., Barrow, E.M., & Wigley, T.M.L. (eds), Cambridge Unversity Press, Cambridge.

Paterson, I. B., Armstrong, M. & Browne, M. A. E. (1981). Quaternary estuarine deposits in the Tay-Earn area, Scotland,. *Inst. Geol. Sci. Rep.,* 81/7.

Pearman, G.I. (1986). Climate change and coastal management. *Planner,* 2(4), 11-13.

Peltier, W.R. (1982). Dynamics of an ice age earth. *Adv. Geophys.,* 24, 1-146.

Peltier, W.R. (1987). Mechanisms of relative sea-level change and the geophysical responses to ice water loading. In Devoy, R.J.N. (ed) *Sea Surface Studies: A Global View.* Croom Helm. London, 57-94.

Peltier, W.R. & Andrews, J.T. (1966). Glaical isostatic adjustment-1: The forward problem. *Geophys. J.Roy. Astr. Soc.,* 46, 605-646.

Peltier, W.R., and Tushingham, A.M. (1989). Global sea level rise and greenhouse effect: might they be connected?. *Science,* 244, 806-810.

Peltier, W.R., and Tushingham, A.M. (1990). The influence of glacial isostatic adjustment on tide gauge measurements of secular sea level. *J. Geophys. Res.,* 96, 6779-6796.

Pirazzoli, P.A. (1986). Secular trends of relative sea level (RSL) changes indicated by tide gauge records. *Journal of Coastal Research,* Special Issue, 1, 1-26.

Pirazzoli, P.A. (1989). Present and near future global sea level changes. *Palaeogeogr. Paleoclimatol.,* Global and Planetary Change Section, 75, 241-258.

Pirazzoli, P.A. (1996). *Sea-level changes. The last 20 000 years.* John Wiley & Sons. Chichester.

Plag, H.P. (1992). The sea level rise problem: an assessment of methods and data. *Proc. Int. Coastal Congress,* 714-732.

Plassche, O. van de (1982). Sea level change and water-level movements in the Netherlands during the Holocene. *Mededelingen. Rijks Geologische. Dienst,* 36, 1-93.

Price, R. J., (1983). *Scotland's Environment during the last 30 000 years.* Scottish Academic Press, Edinburgh.

Ramanathan, V. (1988). The greenhouse theory of climate change: a test by an inadvertant global experiment. *Science*, 240, 293-299.

Rankin, F. (1989). *Guide to the Wemyss Caves.* Wemyss Environmental Education, Fife.

Rankin, F. (9.9.96). *Pictish art at mercy of the sea.* Herald.

Ren, G., Reddish, D.J., & Whittaker, R.N. (1987). Mining subsidence and adjustment prediction using the influence function. *Mining Science Technology,* 5, 89-104.

Ren, G., Reddish, D.J., & Whittaker, R.N. (1987b). Mining subsidence and displacement prediction using the influence function methods for steep seams. *Mining Science Technology,* 8, 235-282.

Ritchie, W. (1979). *Beaches of Fife.* University of Aberdeen.

Rossiter, J. R. (1962). Long term variations in sea level. In Hill, M.N. (ed) *The Sea, Vol 1.* London: Wiley Interscience, p. 590-610.

Rossiter, J.R. (1967). An analysis of annual mean sea level variations in European waters. *Geophysical J. Roy. Astr. Soc.,* 12, 259-299.

Saiu, E. (1992). *Destabilisation of coastal equilibrium by industrial growth and decline in eastern Scotland.* Unpublished undergraduate dissertation, University of St. Andrews.

Schlesinger, M.E. & Mitchell, J.F.B. (1985). Model projections of the equilibrium climate response to increased carbon dioxide. In *Projecting the Climate Effects of Increasing Carbon Dioxide.* MacCracken, M.C. & Luther, F.M. (eds). (DOE/ER-0237) Washington, D.C. US Dept. of Energy.

Schlesinger, M.E. & Zhao, Z.C. (1989). Seasonal climatic changes induced by doubled CO_2 as simulated by the OSU atmospheric GCM/mixed layer ocean model. *Journal of Climate* 2.

Schumm, S.A. & Lichty, R. W. (1965). Time space and causality in geomorphology. *American Journal of Science,* 236, 110-119.

Schumm, S.A. (1991). *To interpret the earth.* Cambridge University Press.

SDPS (Surface Deformation Prediction System) Version 4 (1994). *Prediction of ground movements due to underground mining in Eastern United States.* Department of Mining and Minerals Engineering, Virginia Polytechnic Institute and State University, Blaksburg, Virginia.

Shennan, I. (1987). Global analysis and correlation of sea-level data. In Devoy, R. J. N., (ed) *Sea Surface Studies: A Global View.* Croom Helm. London, p. 198-232.

Shennan, I. (1988). Holocene sea level changes and crustal movements in the North Sea region: An experiment with regional eustasy. In Scott, D.B. et al. (eds). *Late Quaternary Sea-Level Correlation and Applications,* Kluwer Academic Publishers, 1-25.

Shennan, I. (1989). Holocene crustal movements and sea-level changes in Great Britain. *Journal of Quaternary Science,* 4 (1) 77-89.

Shennan, I. (1992). Late Quaternary sea level changes and crustal movements in eastern England and eastern Scotland: An assessment of models of coastal evolution. *Quaternary International,* 15/16, 161-173.

Shennan, I. (1993). Geographic information systems and future sea level rise. In Warrick, R.A., Barrow, E.M., & Wigley, T.M.L. (eds). *Climate and sea level change observations, projections and implications.* Cambridge University Press, Cambridge.

Shennan, I. & Pirazzoli, P. (comps) (1984). *Directory of Sea Level Research,* printed for IGCP-200 by Mörner, N.-A., Geol. Inst., Stockholm University.

Sissons, J. B., (1966). Relative sea-level changes between 10 300 and 8300 BP in part of the Carse of Stirling. *Trans. Inst. Brit. Geogr.,* 39, 19-29.

Sissons, J. B. (1966b). Late glacial shorelines in eastern Fife. *Trans. Inst. Brit. Geogr.,* 39, 31-51.

Sissons, J.B., (1967). *The evolution of Scotland's Scenery.* Oliver & Boyd. Edinburgh.

Sissons, J.B. (1974). The Quaternary in Scotland: a review, *Scot. J. Geol.,* 10, 311-337.

Sissons, J. B. (1983). Shorelines and isostasy in Scotland. In Smith, D.E. & Dawson, A.G., (eds). *Shorelines and Isostasy.* Academic Press, 209-225.

Sissons, J.B. & Brooks, C.L. (1971). Dating of early post-glacial land and sea level changes in the western Forth valley. *Nature Physical Science,* 234, 124-127.

Sissons, J.B., Smith, D.E. & Cullingford, R.A. (1966). Late glacial and post-glacial shorelines in SE Scotland. *Trans. Inst. Brit. Geogr.,* 39, 9-18.

Smith, D. E. (1968). Post-glacial displaced shorelines in the surface of the carse clay on the north bank of the River Forth, in Scotland. *Zeitschrift fur Geomorphologie,* 12, 388-408.

Smith, D.E., Sissons, J.B. & Cullingford, R.A., (1969). Isobases for the Main Perth raised shoreline in SE Scotland as determined by trend surface analysis. *Trans. Inst. Brit. Geogr.* , 46, 45-52.

Smith, D.I. (1993). Greenhouse climatic change and flood damages: the implications. *Climatic Change,* 25, 319-333.

Sutherland, D.G. (1984). The Quaternary deposits and landforms of Scotland and the neighbouring shelves: a review. *Quat. Sci. Rev.,* 157-254.

Titus, J.G. (1987). The greenhouse effect, rising sea level changes and society's response. In *Sea surface studies: a global view,* Devoy, R.J.N. (ed). Croon Helm, London.

Tooley, M.J. (1982a). Introduction: IGCP project No. 61 in the UK, *Proc. Geol. Ass.,* 93, 3-6.

Tooley, M.J. (1982b). Sea-level changes in northern England. *Proc. Geol. Ass.,* 93, 43-51.

Tooley, M.J. (1987). Sea-level studies. In M.J. Tooley & I. Shennan (eds). *Sea-Level Changes.* Oxford: Basil Blackwell Ltd., 1-24.

Tooley, M.J. (1993). Long-term changes in eustatic sea level. In *Climate and sea level change observations, projections and implications.* Warrick, R.A., Barrow, E.M., & Wigley, T.M.L. (eds). Cambridge University Press, Cambridge.

Van der Veen, C.J. (1988). Projecting future sea level. *Surveys in Geophysics,* 9, 389-418. Kluwer Academic Publishers.

Walcott, R.I. (1980). Rheological models and observational data of glacio-isostatic rebound. In *Earth Rheology, Isostasy and Eustasy,* N.-A. Mörner (ed.) Wiley, Chichester and New York, 3-10.

Wallingford, H.R. (1993). *Setting Forth - Second Forth road bridge and associated road bridge and associated links: hydrodynamic investigatory studies of proposed estuary crossing.* Report No. Ex 2885, December 1993.

Warrick, R.A. & Jones P.D. (1988). The greenhouse effect: impacts and policies. *Forum for Applied research and Public Policy.* 48-62.

Warrick, R.A. & Oerlemans. J. (1990). Sea level rise. In Houghton, J.T., Jenkins, G.J., and Ephraums, J.J. (eds.) *Climate change, The IPCC scientific assessment.* Cambridge University Press, Cambridge, 257-281.

Warrick, R.A., Provost, C.Le., Meier, M.P., Oerlemans, J., & Woodworth, P.L (1996). Changes in sea level. IPCC WG1, (1995). *Climate change 1995 - The science of climate change: contribution of Woking Group 1 to the second assessment report of the intergovernmental panel on climate change.* In Houghton, J.T., Meira Filho, L.G., Callander, B.A., Harris, N., & Maskell, K. (eds), Cambridge University Press, Cambridge.

Warrick, R.A. (1993). Climate and sea level change: a synthesis. In *Climate and sea level change observations, projections and implications.* Warrick, R.A., Barrow, E.M., & Wigley, T.M.L. (eds). Cambridge University Press, Cambridge.

Wetherald, R.T. & Manabe, S. (1986). An investigation of cloud cover in response to thermal forcing. *Climate Change*, 8, 5-23.

Wemyss Coal Company. (1908). *Wemyss collieries.* Fife.

Wemyss Estate Records. Wemyss Estates Office, Red House, East Wemyss, Fife.

Wilson, I. (1990). *Subsidence prediction over room and pillar mining systems.* Royal Institution of Chartered Surveyors, Thesis, June 1990.

Wilson, C.A. & Mitchell, J.F.B. (1987). Simulated climate and CO_2 induced climate change over western Europe. *Climate Change,* 10, 11-42.

Whitaker, B.N. & Reddish, D.J. (1989). *Subsidence - Occurrence, Prediction, and Control.* Elsevier.

Whittington, G., Fallick, A., Edwards, K.J., (1996). Stable oxygen isotope and pollen records from eastern Scotland and a consideration of late- glacial and early Holocene climate change for Europe, *Journal of Quaternary Science,* 11 (4), 327-340.

Whyte, I.D. (1995). *Climate Change and Human Society.* Arnold.

Woodworth, P.L. (1985). The interannual correlation between sea level air pressure and rainfall in the British Isles-North Sea region. Weather, 40, 285-292.

Woodworth, P.L. (1987). Trends in UK mean sea level. *Marine Geodesy,* 11, 57-87.

Woodworth, P.L. (1990). Measuring and predicting long term sea level changes. Reprinted from NERC News, October 1990.

Yao, X.L., Reddish, D.J. & Whittaker, B.N. (1991). Evaluation of subsidence parameters for inclined seams in UK coalfields. *10th International Conference on Ground Control in Mining.* Proceedings, 1991, 36, 225-232.

OS Sheet Numbers 1:2500 Plans				
1894 & 1914			**1956/1960**	
28 8			NT3295, NT3395	
28 11			NT3476	
28 12			NT3698	
28 14			NT3698	
28 15			NT3396	
35 12			NT3396	
35 16			NT3497, NT3597	
36 2			NT3496	
36 5			NT3697	
36 6			NT3294	
36 9			NT3294	
40 4			NT3093, NT3193	
40 8			NT3092	
			NT3094, NT3194	

NCB 1:2500 Mine Records were used in the analysis.
A list of the the sheets numbers used together with the number of seams covered by each sheet is listed below:

Sheet Number		**No. seams covered by each sheet**		
NT3699		8 Seams		
NT3698		8 Seams		
NT3697		7 Seams		
NT3497		11 Seams		
NT3496		8 Seams		
NT3296		11 Seams		
NT3295		13 Seams		
NT3294		13 Seams		
NT3094		8 Seams		
NT3093		8 Seams		

Provides information on the co-ordinates for inidiviual OS 1:2500 plans used to 'snap' into the real world (in the Smallworld GIS). The average displacement for each sheet is also provided.					
Year	Sheet Ref at Fife Council	Location	Average Displacement	Relevelling Dates	Survey Dates
1896	1	Methil Docks	0.04		
1896	2	Buckhaven	0.05		
1894	3	Coaltown Wemyss	0.1		
1894	4	East Wemyss	0.11		
1894	5	Wemyss Caves	0.01		
1894	6	West Wemyss	0.04		
1896	7	Dysart, Kirkcaldy			
1896	8	Frances Colliery	0.04		
1894	11	Tyrie Works	0.03		
1894	12	Seafield	0.02		
1894	13	Kinghorn	0.01		
1914	285	Wemyss Castle	0.85	1894	1911
1914	286	East Wemyss	0.17	1893	1911
1914	272	Buckhaven	0.76	1893	1911
1914	273	Buckhaven	0.77	1893	1911
1914	261	Methil Docks	0.28	1893	1911
1914	301	West Wemyss	0.13	1894	1913
1914	315	Dysart, Kirkcaldy	0.19	1894	1913
1914	375	Kinghorn	0.05		
1914	360	Seafield	0.01		
	NT3295, NT3395			1943	1955/59
	NT3476	East Wemyss		1943	1955/59
	NT3698	Wellesley Colliery		1943	
	NT3698	Buckhaven		1943	
	NT3396	Michael Colliery		1943	1955/59
	NT3396	East Wemyss		1943	1955/59
1961	NT3497, NT3597	East Wemyss		1943	1948/59
1959	NT3496	East Wemyss		1943	1955/59
	NT3697	Buckhaven		1943	
	NT3294	West Wemyss		1966	1966
1959	NT3294	West Wemyss		1943	1955/59
1962	NT3093, NT3193	Dysart		1942/49	1959/60
	NT3092	Panhall		1943	
1961	NT3094, NT3194	West Wemyss		1943/49	1955/59

The co-ordinates from which measurements were taken from the OS plans.					
Point	Year	HWM Co-ordinates		LWM Co-ordinates	
1	1894	337077.3	699248.1	337299.2	699068.3
	1914	337129.4	699205.7	337176.6	699167.8
	1960	337191.9	699155.4	337238.9	699117.3
	1994	337238.2	699117.9	337267.1	699094.4
2	1894	337047.6	699208.0	337244.4	699055.5
	1914	337097.9	699168.9	337134.5	699140.6
	1960	337145.0	699132.5	337189.2	699098.1
	1994	337192.3	699095.7	337232.7	699064.4
3	1984	336987.9	699127.7	337169.4	699032.7
	1914	337040.3	699100.3	337077.4	699080.9
	1956	337073.1	699083.2	337113.7	699062.0
	1994	337147.8	699044.2	337186.9	699023.8
4	1894	336950.7	699034.9	337111.1	698974.9
	1914	336986.2	699021.6	337022.6	699008.0
	1956	336994.9	699018.4	337031.3	699004.7
	1994	337098.9	698979.5	337141.4	698963.6
5	1894	336888.9	698953.9	337090.4	698822.5
	1914	336922.8	698931.7	336959.2	698908.1
	1960	336923.8	698931.1	336957.4	698909.2
	1994	337022.7	698866.6	337056.6	698844.6
6	1894	336826.9	698875.5	336955.2	698753.7
	1914	336869.2	698835.3	336904.0	698802.3
	1960	336869.2	698835.3	336896.3	698809.5
	1994	336981.8	698728.4		
7	1894	336761.8	698799.5	336868.8	698686.8
	1914	336807.9	698750.8	336842.3	698714.6
	1960	336807.9	698750.9	336838.0	698719.2
	1994	336924.2	698628.5		
8	1894	336701.3	698719.9	336794.6	698647.5
	1914	336753.1	698679.7	336793.1	698648.7
	1960	336734.3	698694.3	336794.8	698647.2
	1994	336919.8	698550.2		
9	1894	336628.2	698651.7	336730.5	698559.9
	1914	336667.8	698616.2	336705.5	698582.3
	1960	336704.9	698582.8	336727.0	698563.1
	1994	336867.0	698437.5	336895.0	698412.4
10	1894	336547.3	698592.8	336627.6	698463.9
	1914	336561.1	698570.8	336596.8	698513.4
	1960	336652.2	698424.5	336659.2	698413.3
	1994	336713.7	698325.6	336725.1	698307.3
11	1894	336484.4	698515.2	336612.8	698446.4
	1914	336490.9	698511.7	336556.5	698476.3
	1960	336652.3	698424.8	336662.4	698419.4

	1994	336765.0	698363.6	336788.1	698351.2
12	1894	336408.4	698450.1	336504.7	698322.8
	1914	336413.3	698443.7	336455.8	698387.4
	1960	336503.1	698324.8	336520.3	698302.0
	1994	336574.5	698230.4	336586.0	698215.2
13	1894	336334.0	698383.4	336465.1	698259.4
	1914	336343.8	698374.0	336385.0	698335.0
	1960	336445.9	698277.4	336467.4	698256.9
	1994	336515.0	698212.1	336530.6	698197.3
14	1894	336272.7	698304.3	336431.7	698208.0
	1914	336295.1	698290.7	336377.2	698241.1
	1960	336391.3	698232.5	336419.0	698215.7
	1994	336456.2	698193.1	336475.0	698181.8
15	1894	336225.3	698216.2	336379.9	698132.9
	1914	336248.1	698204.0	336342.7	698153.0
	1960	336320.3	698165.1	336347.5	698150.5
	1994	336334.2	698157.7	336352.7	698147.7
16	1894	336185.1	698124.7	336333.7	698059.5
	1914	336206.9	698115.1	336290.3	698078.5
	1960	336265.8	698089.3	336293.4	698077.1
	1994	336262.8	698090.6	336279.5	698083.2
17	1894	336128.4	698042.3	336260.6	697951.4
	1914	336145.7	698030.4	336236.8	697967.8
	1960	336197.9	697994.5	336225.4	697975.7
	1994	336161.6	698019.5	336233.8	697969.9
18	1894	336055.2	697974.2	336152.8	697869.2
	1914	336058.9	697970.3	336152.8	697869.2
	1960	336110.2	697915.1	336140.4	697882.5
	1994	336086.9	697940.2	336140.8	697882.1
19	1894	335965.5	697930.0	336071.9	697791.4
	1914	335969.6	697924.6	336072.6	697790.0
	1960	336031.2	697844.3	336062.6	697803.4
	1994	336001.7	697882.8	336048.6	697821.7
20	1894	335900.8	697853.8	336029.4	697732.2
	1914	335907.9	697847.1	336033.0	697728.8
	1960	335973.5	697785.1	336013.3	697747.4
	1994	335944.2	697812.7	336000.4	697759.7
21	1894	335834.2	697779.2	335974.2	697656.5
	1914	335841.9	697772.3	335983.6	697648.2
	1960	335908.2	697714.3	335949.6	697678.1
	1994	335890.7	697729.6	335948.1	697679.4
22	1894	335781.1	697694.4	335924.4	697604.4
	1914	335795.1	697685.7	335929.2	697601.5
	1960	335847.2	697653.0	335882.8	697630.6
	1994	335828.4	697664.8	335890.0	697626.1

23	1894	335757.9	697657.5	335892.8	697572.4
	1914	335766.0	697652.4	335897.2	697569.8
	1960	335815.9	697621.0	335845.0	697602.5
	1994	335793.1	697635.3	335851.8	697598.4
24	1894	335635.7	697685.6	335594.8	697507.9
	1914	335640.1	697704.5	335595.9	697512.9
	1960	335609.2	697570.9	335596.9	697517.6
	1994	335608.9	697569.6	335595.7	697512.5
25	1894	335563.5	697754.8	335494.8	697562.9
	1914	335567.5	697766.1	335495.6	697565.3
	1960	335531.7	697666.1	335514.4	697617.8
	1994	335529.9	697661.2	335500.7	697580.3
26	1894	335465.5	697774.4	335462.6	697573.0
	1914	335465.8	697799.3	335462.6	697577.4
	1960	335464.1	697680.2	335463.6	697645.4
	1994	335464.3	697698.2	335462.9	697591.8
27	1894	335415.5	697774.6	335424.5	697582.8
	1914	335414.1	697802.8	335424.5	697587.3
	1960	335419.7	697683.9	335420.8	697660.2
	1994	335416.8	697744.8	335423.4	697605.1
28	1894	335365.8	697769.2	335385.5	697584.3
	1914	335362.7	697797.4	335385.2	697586.0
	1960	335374.8	697684.8	335377.4	697659.9
	1994	335365.8	697768.1	335380.4	697631.8
29	1894	335316.9	697758.8	335357.1	697571.3
	1914	335313.4	697774.7	335356.2	697574.9
	1960	335333.5	697680.7	335339.3	697654.0
	1994	335312.1	697780.4	335339.0	697654.9
30	1894	335223.7	697722.5	335314.8	697545.9
	1914	335217.6	697734.3	335314.5	697546.4
	1960	335249.0	697673.5	335263.8	697644.6
	1994	335208.5	697751.9	335263.8	697644.8
31	1894	335139.1	697669.1	335267.3	697507.9
	1914	335131.7	697678.5	335265.7	697509.9
	1960	335158.8	697644.3	335176.9	697621.6
	1994	335117.1	697696.7	335178.9	697619.2
32	1894	335060.9	697606.8	335180.1	697457.2
	1914	335054.9	697614.4	335177.6	697460.3
	1960	335064.5	697602.3	335083.0	697578.9
	1994	335043.3	697628.9	335085.4	697575.9
33	1894	334987.0	697539.4	335123.2	697415.5
	1914	334981.7	697544.3	335119.8	697418.5
	1960	334987.9	697538.6	335006.4	697521.8
	1994	334967.5	697557.2	335013.5	697515.6

34	1894	334920.7	697464.6	335043.5	694359.7
	1914	334914.7	697469.7	335041.5	697361.4
	1960	334927.5	697458.7	334947.6	697441.6
	1994	334898.1	697483.9	334955.5	697434.8
35	1894	334850.0	697393.9	334942.6	697292.1
	1914	334838.2	697406.8	334939.0	697296.1
	1960	334858.2	697384.8	334890.6	697349.2
	1994	334831.4	697417.3	334891.7	697348.0
36	1894	334771.9	697331.4	334850.2	697222.8
	1914	334762.0	697345.1	334846.5	697228.0
	1960	334763.3	697343.3	334817.8	697267.8
	1994	334762.0	697345.2	334804.7	697285.9
37	1894	334686.8	697278.9	334799.4	697183.7
	1914	334677.8	697286.5	334795.3	697187.2
	1960	334676.0	697288.0	334747.0	697228.0
	1994	334673.9	697289.8	334734.6	697238.4
38	1894	334614.0	697210.3	334695.7	697106.8
	1914	334606.5	697219.8	334692.0	697111.6
	1960	334602.5	697224.9	334664.9	697145.8
	1994	334602.0	697225.5	334629.7	697190.5
39	1894	334573.0	697181.6	334649.0	697071.5
	1914	334564.7	697193.7	334643.9	697078.9
	1960	334566.9	697190.5	334629.1	697100.3
	1994	334565.8	697192.1	334593.0	697152.7
40	1894	334531.9	697153.2	334613.0	697044.1
	1914	334523.3	697164.7	334607.5	697051.4
	1960	334532.0	697153.1	334591.9	697072.4
	1994	334530.9	697154.5	334564.1	697109.9
41	1894	334461.2	697082.5	334540.0	697020.7
	1914	334452.8	697089.1	334534.2	697025.1
	1960	334465.2	697079.4	334502.4	697050.2
	1994	334463.6	697080.6	334497.6	697053.9
42	1894	334383.6	697019.4	334454.6	696929.8
	1914	334376.6	697028.2	334451.7	696933.5
	1960	334393.1	697007.4	334428.6	696962.6
	1994	334394.5	697005.7	334428.3	696963.0
43	1894	334301.3	696962.6	334363.8	696862.7
	1914	334300.3	696964.2	334363.4	696863.6
	1960	334318.0	696935.9	334349.2	696886.3
	1994	334322.3	696929.2	334349.3	696886.1
44	1894	334225.4	696897.5	334311.0	696811.6
	1914	334224.5	696898.4	334308.8	696813.9
	1960	334251.7	696871.1	334288.4	696834.3
	1994	334256.8	696866.0	334288.8	696833.9
45	1894	334145.4	696837.5	334228.4	696726.9

	1914	334144.9	696838.2	334226.8	696729.0
	1960	334156.4	696822.8	334202.0	696762.1
	1994	334160.3	696817.6	334201.7	696762.5
46	1894	334086.9	696756.4	334183.5	696671.2
	1914	334086.5	696756.7	334181.4	696673.0
	1960	334092.8	696751.2	334147.6	696702.8
	1994	334100.4	696744.5	334147.3	696703.2
47	1894	334020.0	696682.0	334145.4	696569.6
	1914	334019.4	696682.6	334144.9	696570.0
	1960	334034.1	696669.4	334117.0	696595.0
	1994	334037.9	696666.0	334116.7	696595.3
48	1894	333958.4	696603.3	334055.8	696493.2
	1914	333957.5	696604.2	334056.1	696492.8
	1960	333979.5	696579.4	334010.9	696544.0
	1994	333978.2	696580.9	334010.3	696544.6
49	1894	333887.6	696532.7	334023.4	696440.7
	1914	333886.3	696533.6	334023.7	696440.5
	1960	333936.7	696499.3	334005.4	696452.8
	1994	333936.5	696499.6	334005.2	696453.0
50	1894	333835.9	696447.0	333981.0	696378.8
	1914	333835.4	696447.3	333980.0	696379.3
	1960	333901.7	696416.1	333938.9	696398.6
	1994	333901.6	696416.2	333939.3	696398.4
51	1894	333778.9	696364.9	333902.0	686267.0
	1914	333779.6	696364.4	333901.5	696267.2
	1960	333848.5	696309.4	333887.5	696278.4
52	1894	333720.9	696283.4	333859.5	696206.3
	1914	333720.8	696283.5	333859.8	696206.1
	1960	333812.2	696232.2	333863.3	696204.1
53	1894	333680.7	696191.8	333807.5	696131.4
	1914	333688.9	696188.0	333806.4	696132.0
	1960	333785.8	696142.1	333840.4	696116.4
54	1894	333633.5	696103.7	333739.9	696033.9
	1914	333656.6	696090.5	333738.5	696034.9
	1960	333736.5	696036.2	333823.7	695979.1
55	1894	333574.5	696022.9	333681.0	695944.7
	1914	333598.5	696005.3	333678.2	695946.8
	1960	333684.7	695941.9	333714.3	695920.2
56	1894	333519.3	695939.5	333630.1	695866.2
	1914	333537.0	695927.8	333629.3	695866.7
	1960	333599.8	695886.3	333637.0	695861.6
57	1894	333463.0	695856.9	333563.7	695788.2
	1914	333470.4	695851.8	333564.1	695787.9
	1960	333530.2	695811.0	333569.7	695784.0

58	1894	333385.5	695793.6	333478.6	695682.9
	1914	333391.7	695786.3	333477.3	695684.2
	1960	333468.5	695694.8	333496.9	695660.9
59	1894	333327.0	695712.6	333447.9	695634.2
	1914	333327.5	695712.2	333445.3	695635.9
	1960	333418.0	695653.6	333447.2	695634.7
60	1894	333276.4	695626.3	333374.9	695544.6
	1914	333280.8	695622.7	333374.6	695544.8
	1960	333322.2	695588.3	333340.3	695573.3
61	1894	333222.9	695541.8	333341.3	695473.6
	1914	333229.2	695538.2	333341.7	695473.3
	1960	333263.5	695518.4	333296.4	695499.5
62	1894	333167.4	695458.6	333284.4	695380.7
	1914	333173.8	695454.4	333286.6	695379.1
	1960	333218.6	695424.5	333244.9	695407.0
63	1894	333109.4	695377.2	333205.4	695279.5
	1914	333109.5	695377.1	333208.3	695276.6
	1960	333157.2	695328.6	333187.3	695298.0
64	1894	333047.5	695298.6	333144.0	695224.9
	1914	33045.3	695300.4	333143.7	695225.1
	1960	333106.0	695253.9	333141.7	695226.6
65	1894	333002.4	695209.4	333116.0	695151.9
	1914	3333001.4	695209.9	333112.7	695153.7
	1960	333053.2	695183.8	333110.8	695154.6
66	1894	332957.4	695120.1	333058.7	695059.2
	1914	332957.5	695120.0	333059.2	695058.9
	1960	332993.6	695098.4	333053.0	695062.7
67	1894	332911.0	695031.5	333005.6	694985.2
	1914	332911.3	695031.4	333005.5	694985.2
	1960	332939.4	695017.6	332974.2	695000.5
68	1894	332861.0	694944.9	332944.7	694883.2
	1914	332861.2	694944.8	332947.9	694880.8
	1960	332884.2	694927.8	332928.7	694895.0
69	1894	332808.3	694859.9	332896.3	694803.9
	1914	332816.1	694855.0	332881.0	694813.7
	1960	332835.3	694842.8	332884.6	694811.3
70	1894	332763.4	694770.6	332857.0	694723.5
	1914	332763.8	694770.3	3328843.0	694730.5
	1960	332802.5	694751.1	332846.1	694729.1
71	1894	332708.2	694687.2	332800.6	694616.3
	1914	332708.8	694686.7	332798.9	694617.6
	1960	332740.1	694662.7	332767.5	694641.7

72	1894	332640.8	694613.3	332646.8	694522.9
	1914	332640.9	694612.2	332645.6	694541.7
	1960	332641.0	694611.4	332644.7	694557.0
73	1894	332566.2	694620.5	332558.9	694513.4
	1914	332566.1	694618.8	332561.9	694558.4
	1960	332566.1	694618.6	332563.5	694581.1
74	1894	332263.2	694687.8	332247.0	694527.6
	1914	332263.7	694692.1	332250.4	694561.3
	1960	332258.9	694645.3	332251.9	694578.3
	1994	332258.9	694645.0	332251.6	694577.5
75	1894	332163.5	694695.1	332145.0	694530.9
	1914	332163.4	694694.4	332148.9	694564.6
	1960	332161.6	694678.4	332157.1	694638.6
	1994	332161.6	694678.0	332157.1	694637.9
76	1894	332064.7	694679.5	332123.6	694530.1
	1914	332060.5	694690.0	332109.2	694567.6
	1960	332061.8	694686.7	332075.4	694652.7
	1994	332061.6	694687.2	332075.3	694653.0
77	1894	331973.3	694639.0	332039.3	694512.2
	1914	331965.3	694654.6	332009.4	694569.5
	1960	331966.5	694651.9	331988.6	694609.2
	1994	331966.0	694652.9	331992.4	694602.0
78	1894	331898.5	694572.4	331992.1	694487.6
	1914	331888.2	694581.8	331949.1	694526.6
	1960	331889.4	694580.7	331938.2	694536.4
	1994	331888.7	694581.3	331939.1	694535.6
79	1894	331816.8	694514.8	331899.9	694410.4
	1914	331815.8	694516.1	331867.1	694452.2
	1960	331817.3	694514.1	331864.6	694454.6
	1994	331816.8	694514.7	331846.3	694477.7
80	1894	331742.2	694448.1	331842.1	694352.1
	1914	331739.5	694450.8	331806.2	694386.6
	1960	331733.9	694456.2	331803.7	694389.0
	1994	331733.5	694456.6	331788.1	694404.1
81	1894	331676.6	694372.7	331786.6	694294.0
	1914	331669.4	694377.9	331736.7	694329.3
	1960	331665.8	694380.5	331727.3	694336.1
	1994	331665.3	694380.9	331721.7	694340.1
82	1894	331612.8	694295.7	331710.7	694210.2
	1914	331605.6	694301.9	331665.7	694249.5
	1960	331604.1	694303.3	331661.8	694253.0
	1994	331603.3	694304.0	331654.6	694259.0
83	1894	331555.5	694213.7	331666.7	694151.6
	1914	331544.6	694219.8	331615.6	694180.1

	1960	331543.3	694220.6	331651.3	694176.9
	1994	331542.6	694220.9	331614.6	694180.8
84	1894	331510.9	694124.2	331614.9	694075.7
	1914	331493.1	694132.6	331566.9	694098.1
	1960	331496.7	694130.9	331539.6	694110.9
	1994	331495.6	694131.4	331535.9	694112.6
85	1894	331465.4	694035.2	331555.3	693989.1
	1914	331459.0	694038.5	331513.0	694010.9
	1960	331458.8	694038.6	331490.0	694022.6
	1994	331457.5	694039.3	331483.0	694026.2
86	1894	331417.4	693947.5	331471.1	693892.0
	1914	331405.7	693959.6	331456.1	693907.5
	1960	331404.6	693960.9	331439.7	693924.7
	1994	331404.5	693961.0	331434.7	693929.8
87	1894	331332.4	693894.8	331378.9	693819.5
	1914	3313321.7	693912.0	331366.6	693839.7
	1960	331322.1	693911.4	331376.9	693822.9
	1994	331321.9	693911.8	331345.6	693873.4
88	1894	331232.4	693895.2	331277.0	693883.1
	1914	331230.4	693900.3	331270.8	693798.6
	1960	331238.4	693880.2	331284.4	693764.4
	1994	331238.1	693881.0	331246.6	693859.4
89	1894	331144.4	693847.8	331190.9	693733.6
	1914	331139.6	693859.4	331186.8	693743.4
	1960	331180.9	693758.7	331210.7	693685.7
	1994	331179.3	693762.6	331185.1	693748.4
90	1894	331058.1	693797.3	331146.5	693698.3
	1914	331047.7	693808.9	331135.8	693710.2
	1960	331149.6	693695.1	331173.9	693667.9
	1994	331139.5	693706.4	331146.1	693699.0
91	1894	330985.9	693728.0	331076.5	693636.1
	1914	330966.8	693747.4	331058.1	693654.8
	1960	331052.7	693660.4	331085.5	693627.2
	1994	331062.1	693650.9	331071.3	693641.6
92	1894	330914.7	693657.8	331001.7	693569.5
	1914	330912.9	693659.7	330982.7	693588.8
	1960	330951.3	693620.8	330985.9	693585.7
	1994	330969.0	693602.7	330981.8	693589.8
93	1894	330845.8	693585.4	330957.8	693522.7
	1914	330850.3	693582.8	330938.3	693533.6
	1960	330876.6	693568.1	330930.2	693538.2
	1994	330898.9	693555.7	330914.3	693547.1
94	1894	330768.5	693521.9	330868.8	693399.9
	1914	330771.2	693518.7	330838.0	693437.2
	1960	330800.5	693482.9	330837.4	693437.9

	1994	330802.7	693480.2	330819.3	693460.0
95	1894	330698.7	693450.3	330808.2	693343.4
	1914	330718.7	693430.8	330775.6	693375.2
	1960	330739.8	693410.2	330779.8	693371.1
	1994	330744.3	693405.8	330770.7	693380.0
96	1894	330631.7	693376.0	330758.9	693299.3
	1914	330673.0	693351.1	330738.1	693311.9
	1960	330686.9	693342.7	330738.7	693311.5
	1994	330693.1	693339.0	330730.8	693316.3
97	1894	330587.2	693286.5	330695.7	693232.6
	1914	330623.7	693268.4	330695.7	693232.6
	1960	330631.2	693264.6	330684.4	693238.2
	1994	330641.1	693259.7	330686.5	693237.2
98	1894	330576.9	693187.0	330653.9	693148.8
	1914	330585.7	693182.6	330652.1	693149.7
	1960	330594.0	693178.5	330637.7	693156.8
	1994	330597.3	693176.9	330635.1	693158.1
99	1894	330533.6	693096.9	330608.5	693053.6
	1914	330532.3	693097.6	330604.4	693055.9
	1960	330542.5	693091.7	330592.9	693062.6
	1994	330558.2	693082.6	330592.0	693063.2
100	1894	330488.5	693007.6	330561.9	692951.5
	1914	330492.9	693004.3	330550.9	692959.8
	1960	330506.8	692993.7	330541.5	692967.1
	1994	330514.0	692989.6	330549.5	692961.1
101	1894	330414.5	692930.8	330510.5	692859.1
	1914	330432.3	692924.3	330501.5	692866.6
	1960	330461.8	692899.7	330499.5	692868.3
	1994	330459.8	692901.3	330500.9	692867.1
102	1894	330332.9	692890.7	330415.1	692777.1
	1914	330332.4	692891.3	330395.1	692804.7
	1960	330357.1	692857.3	330379.3	692826.6
	1994	330363.1	692849.0	330386.2	692817.1
103	1894	330267.5	692815.0	330359.0	692736.1
	1914	330265.1	692817.1	330337.8	692754.3
	1960	330294.5	692791.8	330328.4	692762.5
	1994	330307.2	692780.8	330336.7	692755.3
104	1894	330136.7	692713.7	330202.1	692579.3
	1914	330137.4	692712.3	330181.9	692620.9
	1960	330141.9	692702.9	330177.7	692629.5
	1994	330155.1	692675.8	330187.5	692609.5
105	1894	330066.4	692642.6	330184.3	692558.5
	1914	330066.1	692642.8	330171.9	692567.2
	1960	330073.2	692637.7	330121.2	692603.6
	1994	330074.6	692636.7	330120.8	692603.8

106	1894	329967.9	692659.9	329968.2	692525.0
	1914	329967.9	692661.8	329968.0	692532.2
	1960	329967.9	692647.6	329967.9	692609.0
	1994	329967.9	692649.1	329967.9	692607.5
107	1894	329873.1	692627.8	329990.8	692529.6
	1914	329868.6	692631.6	329981.3	692537.5
	1960	329880.0	692622.1	329931.5	692580.0
	1994	329882.7	692619.8	329931.7	692578.8
108	1894	329796.2	692563.9	329873.1	692492.1
	1914	329794.5	692565.5	329784.3	692491.0
	1960	329815.5	692545.9	329861.5	692503.1
	1994	329815.9	692545.6	329857.5	692506.8
109	1894	329756.2	692472.3	329820.0	692444.4
	1914	329753.4	692473.5	329796.1	692454.8
	1960	329763.1	692469.3	329768.8	692466.8
	1994	329764.7	692468.5	329803.5	692451.6
110	1894	329660.4	692419.2	329653.2	692347.1
	1914	329659.2	692407.5	329656.1	692375.9
	1960	329658.3	692398.2	329656.1	692376.2
	1994	329658.6	692401.4	329653.6	692350.9
111	1894	329570.5	692403.4	329584.3	692324.7
	1914	329570.6	692402.5	329581.1	692342.8
	1960	329571.3	692398.7	329577.3	692364.9
	1994	329571.3	692398.4	329579.0	692354.7
112	1894	329437.9	692403.5	329375.6	692250.8
	1914	329438.7	692405.5	329397.5	692304.5
	1960	329437.9	692403.5	329408.5	692331.4
	1994	329438.4	692404.6	329401.0	692313.0
113	1894	329369.6	692476.5	329303.5	692266.9
	1914	329370.6	692479.6	329312.8	692296.3
	1960	329364.7	692461.2	329324.0	692331.7
	1994	329362.1	692462.9	329318.3	692312.5
114	1894	329275.3	692509.9	329232.7	692268.5
	1914	329275.6	692511.2	329238.7	692303.5
	1960	329274.5	692505.4	329244.6	692335.8
	1994	329268.9	692473.7	329235.9	692286.4
115	1894	329175.5	692504.4	329217.4	692269.0
	1960	329175.3	692505.1	329209.6	692312.5
	1960	329178.5	692487.1	329205.3	692336.3
	1994	329183.3	692460.2	329216.3	692274.8
116	1894	329091.3	692439.7	329188.1	692269.8
	1914	329091.3	692439.7	329169.9	692301.7
	1960	329103.5	692418.3	329158.4	692322.0
	1994	329105.7	692414.3	329193.3	692260.6

117	1894	328991.4	692443.9	329017.3	692268.0
	1914	328993.2	692431.5	329022.8	692231.8
	1960	328998.9	692392.9	329024.9	692218.0
	1994	329008.9	692325.2	329034.3	692153.3
118	1894	328897.3	692409.8	328972.9	692236.7
	1914	328907.8	692385.9	328987.3	692204.0
	1960	328926.7	692343.5	328992.3	692191.8
	1994	328954.9	692277.9	329014.5	692141.4
119	1894	328811.3	692358.8	328936.1	692193.7
	1914	328826.5	692338.8	328952.3	692172.7
	1960	328854.7	692301.5	328958.4	692164.6
	1994	328908.0	692231.0	328986.8	692126.8
120	1894	328736.9	692292.1	328875.3	692118.1
	1914	328738.6	692289.9	328882.1	692109.9
	1960	328760.7	692262.1	328892.2	692096.9
	1994	328841.8	692160.3	328910.2	692074.3
121	1894	328696.5	692263.0	328839.7	692068.7
	1914	328695.2	692264.7	328844.3	692062.4
	1960	328711.1	692243.1	328859.6	692042.1
	1994	328804.2	692117.0	328868.2	692030.7
122	1894	328349.7	691776.2	328544.8	691647.2
	1914	328357.6	691770.9	328557.1	691638.9
	1960	328365.1	691766.0	328483.6	691687.5
	1994	328364.6	691766.3	328497.1	691677.2
123	1894	328269.6	691593.0	328460.6	691509.7
	1914	328275.8	691590.2	328472.7	691504.2
	1960	328292.0	691583.2	328432.2	691521.9
	1994	328292.1	691583.1	328434.5	691520.9
124	1894	328206.3	691403.2	328393.0	691341.2
	1914	328209.2	691402.3	328396.3	691340.1
	1960	328224.9	691397.0	328348.4	691355.9
	1994	328224.8	691397.1	328369.5	691348.9
125	1894	328157.2	691209.4	328365.7	691176.8
	1914	328162.3	691208.6	328369.8	691176.1
	1960	328175.5	691206.5	328306.5	691186.0
	1994	328175.8	691206.4	328337.3	691181.2
126	1894	328115.7	691013.7	328329.7	690932.4
	1914	328121.9	691011.3	328332.7	690931.4
	1960	328123.0	691010.9	328258.2	690959.6
	1994	328123.3	691010.8	328252.1	690961.9
127	1894	328059.8	690821.7	328287.2	690744.6
	1914	328066.3	690819.5	328280.1	690747.1
	1960	328064.5	690820.1	328190.0	690777.6
	1994	328064.5	690820.1	328240.2	690760.6
128	1894	328008.8	690628.3	328253.7	690563.6

	1914	328009.5	690628.1	328208.7	690575.5
	1960	328012.0	690627.4	328150.4	690590.9
	1994	328012.2	690627.4	328172.9	690584.9
129	1894	327971.0	690431.9	328235.2	690381.0
	1914	327968.6	690432.3	328186.0	690390.6
	1960	327962.1	690433.6	328130.7	690401.1
	1994	327959.5	690434.1	328131.6	690401.0
130	1894	327934.3	690033.6	328181.5	690034.4
	1914	327945.8	690033.6	328156.3	690034.3
	1960	327943.8	690033.6	328063.9	690034.0
	1994	327948.5	690033.6	328063.1	690034.0
131	1894	327927.1	689833.7	328139.2	689825.9
	1914	327939.3	689833.2	328134.4	689826.2
	1960	327933.3	689833.5	328097.3	689827.5
	1994	327933.1	689833.5	328098.4	689827.4
132	1894	327943.1	689634.3	328132.5	689620.6
	1914	327927.2	689635.5	328110.7	689622.0
	1960	327903.9	689637.2	328107.0	689622.3
	1994	327917.0	689636.2	328107.1	689622.3
133	1894	327908.2	689437.4	328133.9	689386.1
	1914	327899.4	689439.4	328102.8	689393.0
	1960	327888.9	689441.8	328070.6	689400.5
	1994	327895.4	689440.3	328070.6	689400.5
134	1894	327952.4	689242.4	328105.0	689242.4
	1914	327949.7	689242.4	328081.6	389242.4
	1960	327947.8	389242.4	328042.3	389242.3
	1994	327949.5	389242.4	328042.7	389242.4
135	1894	327977.5	688943.4	328163.7	688959.1
	1914	327977.5	688943.4	328153.1	388958.2
	1960	327981.0	688943.7	328121.3	688955.5
	1994	327980.7	688943.7	328120.3	688955.4
136	1894	327974.5	688743.4	328140.4	688740.9
	1914	327975.1	688743.4	328117.1	688741.2
	1960	327988.3	688743.2	328104.0	688741.4
	1994	327989.5	688743.2	328103.7	688741.5
137	1894	327968.0	688543.5	328092.2	688479.4
	1914	327967.7	688543.7	328088.8	688481.3
	1960	327975.2	688539.8	328089.4	688481.0
	1994	327975.7	688539.5	328089.0	688481.1
138	1894	327903.0	688354.4	328001.5	688320.4
	1914	327890.8	688358.6	328004.4	688319.5
	1960	327898.8	688355..81	327988.1	688325.1
	1994	327898.1	688356.1	327988.5	688325.0
139	1894	327824.3	688170.5	327895.9	688097.7
	1914	327823.9	688170.9	327897.0	688096.5

	1960	327826.4	688168.4	327882.7	688111.1
	1994	327825.7	688169.0	327882.7	688111.1
140	1894	327729.6	687994.5	327811.6	687994.5
	1914	327726.5	687994.5	327809.8	687994.5
	1960	327732.7	687994.5	327794.2	687994.5
	1994	327733.6	687994.5	327794.4	687994.5
141	1894	327657.6	687807.9	327754.0	687794.0
	1914	327656.4	687808.1	327751.8	687794.4
	1960	327665.3	687807.0	327741.4	687796.1
	1994	327665.7	687807.0	327742.3	687796.0
142	1894	327623.9	687610.8	327704.6	687610.8
	1914	327621.8	687610.8	327703.0	687610.8
	1960	327624.2	687610.8	327719.3	687610.8
	1994	327624.8	687610.8	327720.7	687610.8
143	1894	327521.9	687438.8	327609.8	687412.2
	1914	327519.0	687439.6	327606.0	687413.4
	1960	327522.6	687438.5	327597.7	687415.9
	1994	327523.5	687438.3	327599.4	687415.4
144	1894	327418.6	687267.5	327417.4	687129.1
	1914	327418.7	687270.8	327417.5	687164.3
	1960	327418.6	687257.9	327418.0	387200.1
	1994	327418.6	687258.5	327417.9	687199.9
145	1894	327311.3	687098.7	327370.1	687061.3
	1914	327307.7	687101.0	327353.8	387071.7
	1960	327308.4	687100.6	327349.7	687074.2
	1994	327310.1	687099.5	327349.4	687074.4
146	1894	327092.3	686893.7	327239.5	686736.4
	1914	327091.1	686895.0	327221.1	686756.0
	1960	327094.4	686891.5	327231.2	686745.3
	1994	327091.2	686894.9	327229.8	686746.8
147	1894	327010.4	686711.2	327219.4	686708.3
	1914	327009.6	686711.2	627195.1	686708.5
	1960	327010.9	686711.2	327179.9	686708.8
	1994	327010.9	686711.2	327177.1	686708.9
148	1894	327019.0	686511.4	327159.1	686503.7
	1914	327019.4	686511.4	327126.8	686505.4
	1960	327019.9	686511.4	327121.6	656505.7
	1994	327019.5	686511.4	327120.0	686505.8
149	1894	327033.7	686311.9	327105.8	686311.9
	1914	327038.3	686311.9	327107.6	686311.9
	1960	327043.7	686311.9	327109.0	686311.9
	1994	327040.9	686311.9	327108.0	686311.9
150	1894	326908.1	686156.3	326885.6	686112.5
	1914	326908.4	686157.0	326858.0	686058.5
	1960	326907.2	686154.6	326825.0	685993.9

	1994	326907.4	686155.0		
151	1894	326658.6	686140.4	326641.7	686034.6
	1914	326657.6	686134.3	326641.4	686033.0
	1960	326657.2	686131.8	326642.4	686039.0
	1994	326657.4	686132.7	326641.5	686033.9
152	1894	326444.3	686269.1	326306.0	686039.2
	1914	326448.5	686269.5	326305.7	686038.2
	1960	326448.0	686275.3	326313.3	686051.1
	1994	326445.0	686270.3	326316.1	686055.7
153	1894	326252.5	686325.8	326398.3	686029.5
	1914	326257.1	686316.5	326397.4	686030.8
	1960	326256.6	686317.5	326382.7	686061.6
	1994	326259.2	686312.2	326381.3	686064.0
154	1894	326068.3	686247.9	326068.2	686056.6
	1914	326068.3	686246.1	326068.3	686053.1
	1960	326068.3	686259.6	326068.2	686023.4
	1994	326068.3	686261.1	326068.3	686023.9

1996 Co-ordinates and coastal changes.					
Number	Location	x co-ordinate	y co-ordinate	x co-ordinate	y co-ordinate
		1894	1894	1996	1996
1	West			335607	697612
2	Sands to			335660	697634
3	Michael			335558	697650
4	Colliery			335482	697700
5				335440	697726
6				335390	697748
7				335336	697754
8				335278	697760
9				335200	697742
10				335130	697788
11				335076	697654
12				335025	697608
13				334960	697575
14				334925	697524
15				334894	697485
16				334850	697430
17				334813	697395
18				334795	697360
19				334762	697336
20				334675	697295
21				334635	697268
22				334596	697235
23				334592	697205
24				334535	697182
25				334487	697122
26				334426	697055
27				334370	697002
28				334330	696960
29	South of	333902.6	696555.2	333925	696541
30	Michael	333686.8	696504	333898	696486
31	Colliery	333843.7	696464.1	333868	696452
32	to as far	333815.6	696416.8	333836	696404
33	as West	333756.5	696335.6	333822	696358
34	Wemyss	333721	696282.3	333785	696313
35		333698.8	696230.6	333770	696258
36		333680.1	696190.4	333757	696206
37		333685.7	696145.3	333704	696156
38		333628	696095.2	333683	696106
39		333601.6	696057.9	333644	696025
40		333564.5	696008.5	333586	696025
41		333535.7	695965.9	333540	695994
42		333495.3	695908.9	333491	695963
43		333461.5	695854.7	333446	695912
44		333424.3	695820.8	333420	695868
45		333368.7	695779.2	333372	695825
46		333347.4	695744.6	333362	695733
47		333309.1	694676.6	333296	695687
48		333252.7	695596.4	333245	695602
49		333208	695514	333208	695514
50		333174.7	695471.8	333182	695466
51		333132.4	695397	333120	695406

52		333078.9	695342.8	333085	695336
53		333045.7	695297.2	333062	695285
54		333015	695234.1	333036	695220
55		332990.1	695185.3	333006	695176
56		332960.5	695124.9	332962	695124
57		332927.9	695071.1	332931	695070
58		332900.5	695017.6	332906	695014
59		332865.1	694971.8	332880	694962
60		332844.5	694920.5	332860	694910
61		332799.7	694841.3	332816	694830
62		332758.5	694763.3	332770	694755
63	Frances	331034.8	693774.4	331085	693714
64	Colliery to	330951.8	693693.5	330975	693671
65	Dysart	330925.2	693667.9	330936	693658
66		330910.9	693652.5	330906	693635
67		330867.6	693611.9	330876	693604
68		330844	693581	330844	693581
69		693561		693561	330822
70		330795	693539.3	330794	693540
71		330761.8	693513.3	330760	693516
72		330728.7	693491	330735	693485
73		330688	693445.5	330700	693435
74		330652.5	693413.9	330674	693394
75		330628.9	693372.8	330650	693355
76		330603.8	693320.6	330628	693310
77		330579.4	693269.9	330616	693258
78		330587.4	693227.1	330591	693225
79		330577	693189.2	330575	693190
80		330556	693150	330556	693150
81		330570.6	693113	330550	693120
82		330528	693084	330528	693084
83		330504.8	693037.9	330509	693035

Recorded movements of the HWM 1894 and 1994							
Location	Point	1894-1914	1914-1960	1960-1994	1894-1960	1894-1994	1914-1994
Methil	1	67.0	80.4	62.1	147.4	209.6	142.5
	2	63.7	59.5	59.9	123.2	183.1	119.5
	3	59.1	37.0	84.3	96.1	180.4	121.3
	4	37.9	9.2	111.7	47.2	158.9	120.9
	5	40.6	1.2	118.1	41.7	159.8	119.3
	6	58.3	0.0	155.2	58.3	213.6	155.2
	Mean	**54.4**	**31.2**	**98.6**	**85.7**	**184.2**	**129.8**
Wellesley	7	67.1	-0.1	168.8	67.0	235.8	168.7
Bing	8	65.6	-23.8	264.9	41.8	306.7	241.1
	9	53.2	49.8	217.7	103.1	320.8	267.6
	10	26.0	172.3	116.5	198.3	314.8	288.8
	11	7.4	183.3	128.3	190.7	319.0	311.6
	12	8.1	149.0	118.4	157.1	275.5	267.4
	13	13.6	140.6	95.0	154.2	249.2	235.6
	14	26.2	112.4	75.9	138.6	214.5	188.4
	15	25.9	82.0	15.7	107.9	123.6	97.8
	Mean	**32.6**	**96.2**	**133.5**	**128.7**	**262.2**	**229.6**
Shore St.	16	23.8	64.3	-3.3	88.1	84.8	61.1
Buckhaven	17	21.0	63.3	-44.0	84.3	40.3	19.3
	18	5.4	75.3	-34.3	80.7	46.4	41.1
	19	6.8	101.2	-48.5	108.0	59.5	52.7
	20	9.9	90.2	-40.3	100.1	59.8	50.0
	21	10.3	88.1	-23.3	98.5	75.2	64.9
	22	16.5	61.5	22.2	78.0	100.2	83.7
	23	9.6	59.0	26.8	68.6	95.4	85.8
	Mean	**12.9**	**75.4**	**-18.1**	**88.3**	**70.2**	**57.3**
West	24	-19.3	137.1	1.3	117.8	119.1	138.4
Sands	25	-12.0	106.2	5.2	94.2	99.4	111.4
	26	-24.9	119.2	-18.0	94.3	76.3	101.2
	27	-28.2	119.0	-60.9	90.8	29.9	58.1
	28	-28.3	113.2	-83.7	84.9	1.2	29.5
	29	-16.3	96.1	-102.0	79.8	-22.2	-5.9
	30	-13.3	68.4	-88.3	55.2	-33.1	-19.8
	31	-12.0	43.7	-67.0	31.7	-35.4	-23.3
	32	-9.6	15.4	-34.0	5.8	-28.2	-18.6
	33	-7.2	8.5	-27.6	1.3	-26.3	-19.2
	34	-7.8	16.8	-38.7	9.0	-29.8	-21.9
	Mean	**-16.3**	**76.7**	**-46.7**	**60.4**	**13.7**	**30.0**
Gasworks,	35	-17.4	29.7	-39.9	12.3	-27.6	-10.2
Wemyss	36	-16.9	2.3	-2.4	-14.6	-17.0	-0.1
Caves to	37	-11.8	-2.3	-2.8	-14.1	-16.9	-5.1
East	38	-12.0	-6.5	-0.8	-18.5	-19.4	-7.3
Wemyss	39	-14.6	3.8	-1.8	-10.8	-12.7	2.0
	40	-14.3	14.5	-1.8	0.2	-1.6	12.7
	41	-10.7	15.7	-2.1	5.1	3.0	13.7
	42	-11.3	26.6	2.2	15.3	17.5	28.8
	43	-1.8	33.4	8.0	31.5	39.5	41.3
	44	-1.2	38.5	7.3	37.3	44.6	45.8
	45	-0.9	19.3	6.5	18.3	24.8	25.8
	46	-0.5	8.4	10.1	7.9	18.0	18.5
	47	-0.8	19.7	5.2	18.9	24.1	24.9
	48	-1.3	33.2	-2.0	31.8	29.8	31.1
	49	-1.6	61.0	-0.3	59.4	59.1	60.6

	50	-0.7	73.4	-0.2	72.7	72.5	73.2
	51	0.9	87.2		88.1		
		-6.9	**26.9**	**-0.9**	**20.1**	**14.9**	**22.2**
Micheal	52	-0.2	104.8		104.6		
Colliery	53	9.0	107.2		116.2		
	54	24.1	99.1		123.2		
	55	29.8	106.9		136.7		
	56	21.2	75.3		96.5		
	57	9.0	72.3		81.3		
	58	9.5	119.5		129.1		
	59	0.7	107.8		108.4		
	60	5.7	53.8		59.5		
	Mean	**12.1**	**94.1**		**106.2**		
Michael	61	17.3	39.6		56.8		
Colliery to	62	7.7	53.8		61.5		
West	63	0.1	68.1		68.2		
Wemyss.	64	-2.8	76.5		73.7		
	65	-1.2	58.1		56.9		
	66	0.2	42.1		42.2		
	67	0.3	31.3		31.6		
	68	0.2	28.6		28.8		
	69	9.2	22.8		32.0		
	70	0.5	43.1		43.6		
	71	0.7	39.5		40.3		
	72	1.1	0.7		1.9		
	73	1.7	0.2		1.9		
		2.7	**38.8**		**41.5**		
West	74	-4.3	47.0	0.4	42.7	43.1	47.3
Wemyss	75	0.7	16.1	0.4	16.8	17.2	16.5
along to	76	-11.4	3.5	-0.5	-7.8	-8.3	3.1
Chapel	77	-17.6	3.1	-1.1	-14.6	-15.7	2.0
Gardens.	78	-14.0	1.7	-0.9	-12.4	-13.2	0.8
	79	-1.6	2.5	-0.8	0.9	0.1	1.7
	80	-3.8	-7.8	-0.6	-11.6	-12.2	-8.4
	81	-9.0	-4.4	-0.7	-13.3	-14.0	-5.1
	82	-9.5	-2.1	-1.1	-11.6	-12.6	-3.2
	83	-12.4	-1.5	-0.8	-13.9	-14.8	-2.4
	84	-19.7	4.0	-1.2	-15.7	-16.9	2.8
	85	-7.9	-0.3	-1.5	-8.2	-9.7	-1.8
	86	-16.8	-1.8	-0.1	-18.6	-18.7	-1.9
	87	-20.3	0.8	0.5	-19.5	-19.0	1.3
	Mean	**-10.5**	**4.3**	**-0.6**	**-6.2**	**-6.8**	**3.8**
Blair Point	88	-5.5	21.6	-0.8	16.1	15.4	20.8
to Frances	89	-12.5	108.8	-4.2	96.3	92.1	104.7
Colliery.	90	-15.6	152.8	-15.2	137.2	122.0	137.6
	91	-27.2	122.3	13.4	95.1	108.4	135.6
	92	-2.6	54.6	25.3	52.0	77.3	80.0
	93	5.2	30.2	25.5	35.4	60.9	55.7
	Mean	**-9.7**	**81.7**	**7.3**	**72.0**	**79.4**	**89.1**
Panhall to	94	4.1	46.3	3.5	50.4	53.9	49.8
Dysart	95	27.9	29.4	6.3	57.4	63.7	35.7
harbour.	96	48.1	16.3	7.3	64.4	71.7	23.6
	97	40.7	8.4	11.1	49.1	60.2	19.5
	98	9.8	9.2	3.7	19.0	22.7	12.9

	99	-1.5	11.8	18.2	10.3	28.5	30.0
	100	5.5	17.4	6.6	23.0	29.6	24.1
	101	10.1	38.4	-2.5	48.5	46.0	35.9
	102	-0.8	40.0	10.3	39.3	49.5	50.3
	Mean	**16.0**	**24.2**	**7.2**	**40.2**	**47.3**	**31.3**
West of	103	-3.2	38.8	16.8	35.6	52.4	55.6
Dysart	104	1.6	10.5	30.1	12.1	42.2	40.6
harbour.	105	-0.3	8.7	1.8	8.4	10.1	10.4
	106	-1.9	14.2	-1.5	12.3	10.8	12.7
	107	-5.9	14.7	3.6	8.9	12.5	18.4
	108	-2.3	28.7	0.5	26.4	26.9	29.2
	109	-3.1	10.7	1.8	7.6	9.4	12.4
	110	11.8	9.3	-3.2	21.2	18.0	6.1
	111	0.8	3.9	0.3	4.6	5.0	4.2
	Mean	**-0.3**	**15.5**	**5.6**	**15.2**	**20.8**	**21.1**
Ravencraig	112	-2.6	2.6	-1.3	0.0	-1.3	1.3
Sands	113	-3.3	19.3	8.8	16.0	24.8	28.1
	114	-1.4	6.0	32.2	4.6	36.7	38.1
	115	-0.7	18.2	27.3	17.5	44.8	45.5
	116	0.0	24.7	4.5	24.7	29.2	29.2
	117	12.5	39.1	68.4	51.6	119.9	107.4
	118	26.2	47.3	70.5	73.5	144.0	117.8
	119	25.2	46.8	88.4	71.9	160.3	135.1
	120	2.8	35.5	130.1	38.3	168.4	165.7
	121	2.1	26.8	156.7	28.9	185.7	183.6
	Mean	**6.1**	**26.6**	**58.6**	**32.7**	**91.3**	**85.2**
S. Kirkcaldy	122	9.5	8.9	-0.5	18.4	17.9	8.4
harbour	123	6.8	17.7	0.2	24.4	24.6	17.9
	124	3.1	16.5	-0.1	19.6	19.4	16.4
	125	5.1	13.4	0.3	18.6	18.8	13.7
	126	6.6	1.2	0.4	7.8	8.2	1.5
	127	6.8	-1.8	0.0	5.0	5.0	-1.8
	128	0.7	2.5	0.3	3.2	3.5	2.8
	129	2.4	-6.6	-2.7	-4.2	-6.9	-9.3
	Mean	**5.1**	**6.5**	**-0.3**	**11.6**	**11.3**	**6.2**
Tyrie Works	130	11.5	-2.1	4.7	9.4	14.2	2.7
	131	12.2	-6.0	-0.2	6.2	5.9	-6.3
	132	-16.0	-23.4	13.2	-39.4	-26.2	-10.2
	133	-9.1	-10.7	6.7	-19.8	-13.1	-4.1
	134	-2.8	-1.9	1.7	-4.6	-2.9	-0.2
	135	-0.1	3.6	-0.3	3.5	3.2	3.2
	Mean	**-0.7**	**-6.8**	**4.3**	**-7.5**	**-3.2**	**-2.5**
South of	136	0.6	13.2	1.2	13.9	15.0	14.4
Tyrie	137	0.3	8.4	0.6	8.7	9.4	9.1
Works to	138	-12.9	8.5	-0.8	-4.4	-5.1	7.8
Kinghorn.	139	-0.6	3.6	0.9	3.0	3.9	4.5
	140	-3.1	6.2	0.9	3.1	4.0	7.1
	141	-1.3	9.0	0.4	7.7	8.1	9.4
	142	-2.1	2.4	0.6	0.3	0.9	3.0
	143	3.1	3.8	0.9	6.9	7.8	4.8
	144	-3.3	12.9	-0.5	9.5	9.0	12.4

	145	-4.3	0.8	2.1	-3.5	-1.4	2.9
	146	-1.8	4.8	-4.7	3.0	-1.7	0.1
	147	-0.8	1.3	0.0	0.5	0.5	1.3
	148	0.4	0.5	0.4	0.9	1.2	0.8
	149	4.7	5.4	-2.8	10.0	7.2	2.6
	150	-0.8	2.7	-0.4	1.9	1.5	2.3
	151	6.2	2.5	-0.9	8.7	7.8	1.6
	Mean	**-1.0**	**5.4**	**-0.1**	**4.4**	**4.3**	**5.2**
Kinghorn.	152	0.5	6.8	5.8	7.2	13.0	12.6
	153	10.4	-1.1	5.9	9.3	15.1	4.7
	154	1.8	-13.4	1.5	-11.6	-10.1	-11.9
	Mean	**4.2**	**-2.6**	**4.4**	**1.6**	**6.0**	**1.8**

Recorded movements of the LWM 1894 and 1994							
	Point	1894-1914	1914-1960	1960-1994	1894-1960	1894-1994	1914-1994
Location	1	-157.9	80.3	36.3	-77.6	-41.4	116.5
Methil	2	-139.0	69.3	55.1	-69.7	-14.7	124.4
	3	-103.8	40.9	82.6	-63.0	19.6	123.5
	4	-94.4	9.3	117.5	-85.2	32.4	126.8
	5	-156.7	2.1	118.4	-154.6	-36.2	120.5
	6	-70.5	-10.5	117.8	-81.1	36.7	107.2
	Mean	**-120.4**	**31.9**	**87.9**	**-88.5**	**-0.6**	**119.8**
Wellesley	7	-38.5	6.3	125.1	-32.2	92.9	131.3
Bing	8	-1.9	2.3	158.2	0.3	158.5	160.4
	9	-33.6	28.8	225.8	-4.8	221.0	254.6
	10	-58.3	118.0	124.9	59.6	184.5	242.8
	11	-63.8	120.3	143.1	56.5	199.6	263.4
	12	-81.0	107.0	108.9	26.0	134.9	215.9
	13	-80.1	82.3	86.9	2.3	89.2	169.3
	14	-63.8	48.9	65.5	-14.9	50.6	114.4
	15	-42.3	5.4	5.9	-36.9	-31.0	11.3
	Mean	**-81.6**	**46.4**	**103.7**	**-35.2**	**68.5**	**150.1**
Shore St.	16	-47.4	3.5	-15.8	-43.9	-59.7	-12.4
Buckhaven	17	-28.8	-13.9	10.1	-42.7	-32.5	-3.7
	18	0.0	-18.2	0.6	-18.2	-17.6	-17.6
	19	-12.0	-10.0	-23.2	-22.0	-45.2	-33.1
	20	4.9	-27.1	-17.8	-22.2	-40.0	-44.9
	21	12.5	-45.2	-2.0	-32.7	-34.7	-47.2
	22	5.6	-54.7	8.5	-49.1	-40.7	-46.3
	23	5.1	-61.6	7.9	-56.5	-48.6	-53.7
	Mean	**-7.5**	**-28.4**	**-4.0**	**-35.9**	**-39.9**	**-32.4**
West	24	-4.8	-5.2	5.2	-9.9	-4.7	0.0
Sands	25	-2.5	-55.8	40.0	-58.3	-18.4	-15.9
	26	-4.4	-68.0	53.6	-72.4	-18.8	-14.4
	27	-4.5	-73.0	55.2	-77.5	-22.3	-17.8
	28	-1.8	-74.3	28.3	-76.1	-47.8	-46.1
	29	-3.7	-80.8	1.0	-84.5	-83.6	-79.9
	30	-0.6	-110.5	0.2	-111.1	-110.9	-110.3
	31	-2.5	-142.7	3.0	-145.2	-142.2	-139.7
	32	-4.0	-151.7	3.8	-155.7	-151.8	-147.8
	33	-4.6	-153.3	9.4	-157.9	-148.5	-143.9
	34	-2.6	-123.4	10.4	-126.1	-115.7	-113.0
	Mean	**-3.3**	**-94.4**	**19.1**	**-97.7**	**-78.6**	**-75.3**
Gasworks,	35	-5.5	-71.8	1.6	-77.3	-75.7	-70.2
Wemyss	36	-6.5	-49.0	-22.4	-55.5	-77.9	-71.4
Caves to	37	-5.5	-63.8	-15.6	-69.3	-85.0	-84.9
East	38	-6.0	-43.6	-56.9	-49.6	-106.6	-106.5
Wemyss	39	-9.0	-26.0	-63.5	-35.0	-98.6	-98.5
	40	-9.1	-26.2	-46.7	-35.3	-82.0	-82.0
	41	-7.3	-40.5	-6.1	-47.8	-53.9	-53.9
	42	-4.8	-37.1	0.0	-41.9	-41.9	-41.9
	43	0.0	-26.8	0.0	-26.8	-26.8	-26.8
	44	-3.1	-28.9	0.0	-32.0	-32.0	-32.0
	45	-2.7	-41.4	0.0	-44.1	-44.1	-44.1
	46	-2.8	-45.1	0.0	-47.9	-47.9	-47.9
	47	0.0	-37.5	0.0	-37.5	-37.5	-37.5
	48	0.0	-68.3	0.0	-68.3	-68.3	-68.3
	49	0.0	-21.8	0.0	-21.8	-21.8	-21.8
	50	0.0					

	51	-0.5	-17.9				
Micheal	52	0.4	4.0		4.4		
Colliery	53	-1.3	37.4		36.1		
	54	-1.7	101.9		100.2		
	55	-3.4	44.8		41.4		
	56	-0.9	9.2		8.3		
	57	0.6	6.8		7.4		
	58	-1.9	30.5		28.6		
	59	-3.1	2.3		-0.9		
	60	-0.4	-44.6		-45.0		
	Mean	**-1.3**	**21.4**		**20.1**		
Michael	61	0.5	-52.4		-51.9		
Colliery to	62	2.8	-50.2		-47.4		
West	63	4.0	-30.0		-26.0		
Wemyss.	64	-0.3	-2.5		-2.8		
	65	-3.7	-2.1		-5.8		
	66	0.6	-7.3		-6.7		
	67	0.2	-34.8		-34.6		
	68	4.1	-23.9		-19.9		
	69	-18.2	4.3		-13.8		
	70	-15.6	3.4		-12.3		
	71	2.2	-39.6		-37.4		
	72	-18.8	-15.3		-34.1		
	73	-45.1	-22.8		-67.9		
	Mean	**-6.7**	**-21.0**		**-27.7**		
West	74	-33.8	-17.1	-0.9	-51.0	-51.9	-18.0
Wemyss	75	-33.8	-74.5	0.7	-108.3	-107.6	-73.8
along to	76	-40.2	-91.7	-0.3	-131.8	-132.1	-91.9
Chapel	77	-64.6	-44.8	8.2	-109.5	-101.3	-36.7
Gardens.	78	-53.2	-3.4	-29.4	-56.7	-86.1	-32.9
	79	-53.2	-3.4	-29.4	-56.7	-86.1	-32.9
	80	-49.8	-3.5	21.7	-53.3	-31.6	18.2
	81	-61.1	-11.7	-6.9	-72.8	-79.6	-18.5
	82	-59.8	-5.2	-9.4	-65.0	-74.4	-14.6
	83	-58.5	6.6	-7.8	-52.0	-59.7	-1.2
	84	-52.9	-30.2	-4.0	-83.2	-87.1	-34.2
	85	-47.6	-25.9	-7.8	-73.4	-81.3	-33.7
	86	-21.6	-23.7	-7.1	-45.3	-52.5	-30.8
	87	-23.7	19.7	-59.4	-4.0	-63.4	-39.7
	Mean	**-46.7**	**-22.1**	**-9.4**	**-68.8**	**-78.2**	**-31.5**
Blair Point	88	-16.7	36.9	-102.3	20.1	-82.2	-65.4
to Frances	89	-10.6	62.5	-67.8	51.9	-15.9	-5.3
Colliery.	90	-16.0	57.0	-41.8	41.0	-0.8	15.2
	91	-26.3	38.8	-20.3	12.6	-7.7	18.6
	92	-27.1	4.5	-5.8	-22.7	-28.5	-1.3
	93	-22.1	-9.5	-18.2	-31.6	-49.8	-27.7
	Mean	**-19.8**	**31.7**	**-42.7**	**11.9**	**-30.8**	**-11.0**
Panhall to	94	-48.4	-0.9	-28.6	-49.3	-77.9	-29.5
Dysart	95	-45.5	5.9	-12.8	-39.7	-52.4	-6.9
harbour.	96	-24.4	0.8	-9.2	-23.7	-32.9	-8.5
	97	0.0	-12.6	2.3	-12.7	-10.3	-10.3
	98	-2.0	-16.0	-3.0	-18.0	-21.0	-19.0
	99	-4.7	-13.4	-1.0	-18.1	-19.1	-14.4
	100	-13.7	-11.9	9.9	-25.6	-15.7	-2.0
	101	-11.7	-2.6	1.8	-14.3	-12.5	-0.8
	102	-34.1	-27.1	39.3	-61.1	-21.8	12.3

	Mean	**-20.5**	**-8.7**	**-0.1**	**-29.2**	**-29.3**	**-8.8**
West of	103	-28.0	-12.5	11.1	-40.5	-29.4	-1.4
Dysart	104	-46.2	-9.6	22.2	-55.8	-33.6	12.7
harbour.	105	-15.1	-62.5	-0.4	-77.6	-78.0	-62.9
	106	-7.2	-76.8	1.5	-84.0	-82.5	-75.3
	107	-12.4	-64.8	0.2	-77.1	-76.9	-64.6
	108	1.6	-17.6	-5.5	-16.0	-21.5	-23.1
	109	-26.0	-29.8	37.8	-55.9	-18.0	8.0
	110	-28.9	-0.4	25.4	-29.3	-3.8	25.1
	111	-18.4	-22.4	10.3	-40.8	-30.5	-12.0
	Mean	**-20.1**	**-32.9**	**11.4**	**-53.0**	**-41.6**	**-21.5**
Ravencraig	112	-58.0	-29.0	19.8	-87.0	-67.2	-9.2
Sands	113	-30.9	-37.2	20.1	-68.0	-47.9	-17.1
	114	-35.5	-32.8	50.1	-68.3	-18.2	17.3
	115	-44.3	-24.2	62.5	-68.5	-6.0	38.3
	116	-36.8	-23.3	70.7	-60.1	10.6	47.4
	117	36.6	14.0	65.4	50.6	116.0	79.3
	118	35.7	13.2	55.1	48.9	104.0	68.3
	119	26.6	10.1	47.3	36.7	84.0	57.4
	120	10.7	16.4	28.9	27.1	56.0	45.3
	121	7.7	25.5	14.3	33.2	47.5	39.8
	Mean	**-5.9**	**-4.7**	**43.3**	**-10.6**	**32.7**	**38.6**
S. Kirkcaldy	122	14.8	-88.2	17.0	-73.3	-56.4	-71.2
harbour	123	13.3	-44.2	2.5	-30.9	-28.4	-41.7
	124	3.5	-50.4	22.2	-47.0	-24.8	-28.2
	125	4.2	-64.0	31.1	-59.8	-28.7	-32.9
	126	3.2	-79.7	-6.5	-76.5	-83.0	-86.2
	127	-7.5	-95.2	53.1	-102.7	-49.6	-42.1
	128	-46.6	-60.3	23.3	-106.8	-83.6	-37.0
	129	-50.2	-56.3	0.9	-106.5	-105.6	-55.4
	Mean	**-8.2**	**-67.3**	**17.9**	**-75.4**	**-57.5**	**-49.3**
Tyrie Works	130	-25.3	-92.4	-0.8	-117.6	-118.4	-93.2
	131	-4.9	-37.1	1.2	-42.0	-40.8	-36.0
	132	-21.9	-3.7	0.0	-25.6	-25.5	-3.6
	133	-31.8	-33.0	-0.1	-64.9	-64.9	-33.1
	134	-10.7	-39.2	-1.0	-49.9	-50.9	-40.3
	135	-10.7	-32.0	-1.0	-42.6	-43.6	-33.0
	Mean	**-17.5**	**-39.6**	**-0.3**	**-57.1**	**-57.4**	**-39.9**
South Tyrie	136	-23.3	-13.1	-0.3	-36.4	-36.7	-13.4
Works to	137	-3.8	0.6	-0.5	-3.2	-3.6	0.2
Kinghorn.	138	3.0	-17.3	0.4	-14.2	-13.8	-16.8
	139	1.7	-20.4	0.0	-18.8	-18.8	-20.4
	140	-1.9	-15.6	0.1	-17.4	-17.3	-15.4
	141	-2.3	-10.6	0.9	-12.9	-12.0	-9.7
	142	-1.6	16.3	1.5	14.6	16.1	17.7
	143	-3.7	-8.6	1.7	-12.3	-10.6	-6.9
	144	-35.2	-35.9	0.3	-71.1	-70.8	-35.6
	145	-19.3	-4.8	-0.4	-24.1	-24.4	-5.1
	146	26.9	14.8	-2.1	41.7	39.6	12.7
	147	-24.4	-15.1	-2.8	-39.5	-42.3	-18.0
	148	-32.3	-5.2	-1.6	-37.5	-39.1	-6.7
	149	1.8	1.4	-1.0	3.2	2.2	0.4
	150	60.7	72.5		133.2	133.2	72.5
	151	1.6	-6.1	5.2	-4.5	0.7	-0.9
	Mean	**-3.3**	**-2.9**	**0.1**	**-6.2**	**-6.1**	**-2.8**
Kinghorn.	152	1.1	-15.0	-5.4	-13.9	-19.3	-20.4

	153	-1.6	-34.1	-2.9	-35.7	-38.6	-37.0
	154	3.5	29.7	-0.5	33.2	32.7	29.2
	Mean	**1.0**	**-6.5**	**-2.9**	**-5.5**	**-8.4**	**-9.4**

Appendix 4: Benchmark and spot height data								
				Heights in (m) from OS plans.				
ID	Location	x co-ordinate	y co-ordinate	1894	1914	1960	1994	Change in height (m)
1	Wellesely	335870.6	697828.6		6.3	6.1		-0.2
2	colliery	335882.4	697874.5	9.2		8.2		-1
3		335963.3	698023.8	25.1	25.1			0
4		336002.4	698034.9			23.2	23.2	0
5		336047.2	698046.8	18.9		18.9		0
6		336138.7	698148.5	12.8	12.5	13.7		0.9
7		336184.7	698216.3	7.9	7.7			-0.2
8		336226.3	698284.9	6.4	6.1			-0.3
9		336280.6	698369.0	5.2	5.2			0
10	West Sands	335684.8	697846.0	26.6		25.9		-0.7
11	Buckhaven	335715.2	697829.9	25.3	25.2	24.7		-0.6
12		335718.3	697807.5	23.5		23.2		-0.3
13		335818.2	697788.5	7.4	6.7			-0.7
14		335793.9	697769.8			6.7		
15		335742.1	697729.7			6.4		
16		335698.3	697712.4		7.4	7.3	7.0	-0.4
17		335685.5	697700.3	8.4	8.2			-0.2
18		335650.8	697736.7			4.3		
19		335549.7	697771.5			4.0		
20		335477.3	697812.1			4.3		
21		335448.0	697836.7			4.9		
22		335388.4	697836.9			6.1		
23		335354.9	697838.9			8.8		
24		335316.9	697823.6			9.1		
25		335353.9	697794.1			10.7		
26		335188.8	697746.9			7.9		
27		335158.6	697735.6			8.8		
28		335122.1	697707.8			7.3		
29		335075.5	697673.0			6.4		
30		335060.7	697660.1			8.2		
31		335024.4	697621.4			7.0		
32		334974.6	697569.7			6.4		
33		334936.8	697525.3			4.6		
34		334778.5	697364.7			5.7		
35		334757.2	697348.8			5.2		
36		334686.0	697315.0			4.9		
37		334558.1	697200.3			6.1		
38		334521.9	697179.6			4.9		
39		334462.0	697119.8			5.2		
40		334424.8	697060.9			4.7		
41		334328.3	696998.9			2.7		
42		334187.7	696913.7			9.8		
43		334143.1	696903.8			9.8		
44		334050.1	696790.7			3.7		
45		334050.1	696790.7			6.1		
46		333989.0	696780.8			7.9		
47		333986.9	696732.2			6.7		
48		333932.7	696600.8			5.2		
49		333856.4	696501.2			5.7	5.6	-0.1
50		333506.7	695951.0			8.2	7.4	-0.8
51		333173.2	695671.4		30.2	28.2		-2.2
52		333262.1	695603.5		4.6			

53		333218.6	695537.5		5.5			
54		333165.5	695452.1		5.8			
55		333145.8	695473.7			7.6		
56		333091.6	695354.5		5.3	5.5		0.2
57		332995.7	695406.7			28.5	28.2	-0.3
58		333025.3	695277.9			4.3	4.1	-0.2
59		333010.0	695263.3			6.6	6.4	-0.2
60		332988.5	695205.7			4.9		
61		332979.2	695169.1	2.7				
62		332969.7	695159.8			4.0		
63		332937.8	695095.3			4.0		
64		332922.2	695063.1	2.2				
65		332899.6	695031.6			3.7		
66		332795.1	694878.9	6.0	5.9	5.6	5.4	-0.6
67		332755.7	694821.2	5.1	4.9	4.9	4.6	-0.5
68	West	332670.3	694702.5	7.7	7.6	7.3	7.5	-0.2
69	Wemyss	332594.6	694662.9	9.8	9.8			0
70		332526.4	694654.7	7.3		7.6	7.4	-0.1
71		332464.3	694708.6	16.5	14.1	14.3	14.3	-2.2
72		332422.3	694786.5		22.3	21.0		-1.3
73	Frances	330802.8	693714.9			42.1	43.6	1.5
74	Colliery	330701.5	693608.9			43.6	43.0	-0.6
75		330673.7	693539.6			38.1	38.4	0.3
76		330595.3	693464.2			31.7	31.4	-0.3
77		330547.6	693318.8			22.6	22.6	0
78		330534.5	693223.7			21.4	21.3	-0.1
79		330530.7	693183.4			19.2	19.2	0

Appendix 5

Correction graph for limited face advance (NCB 1975, p.11).

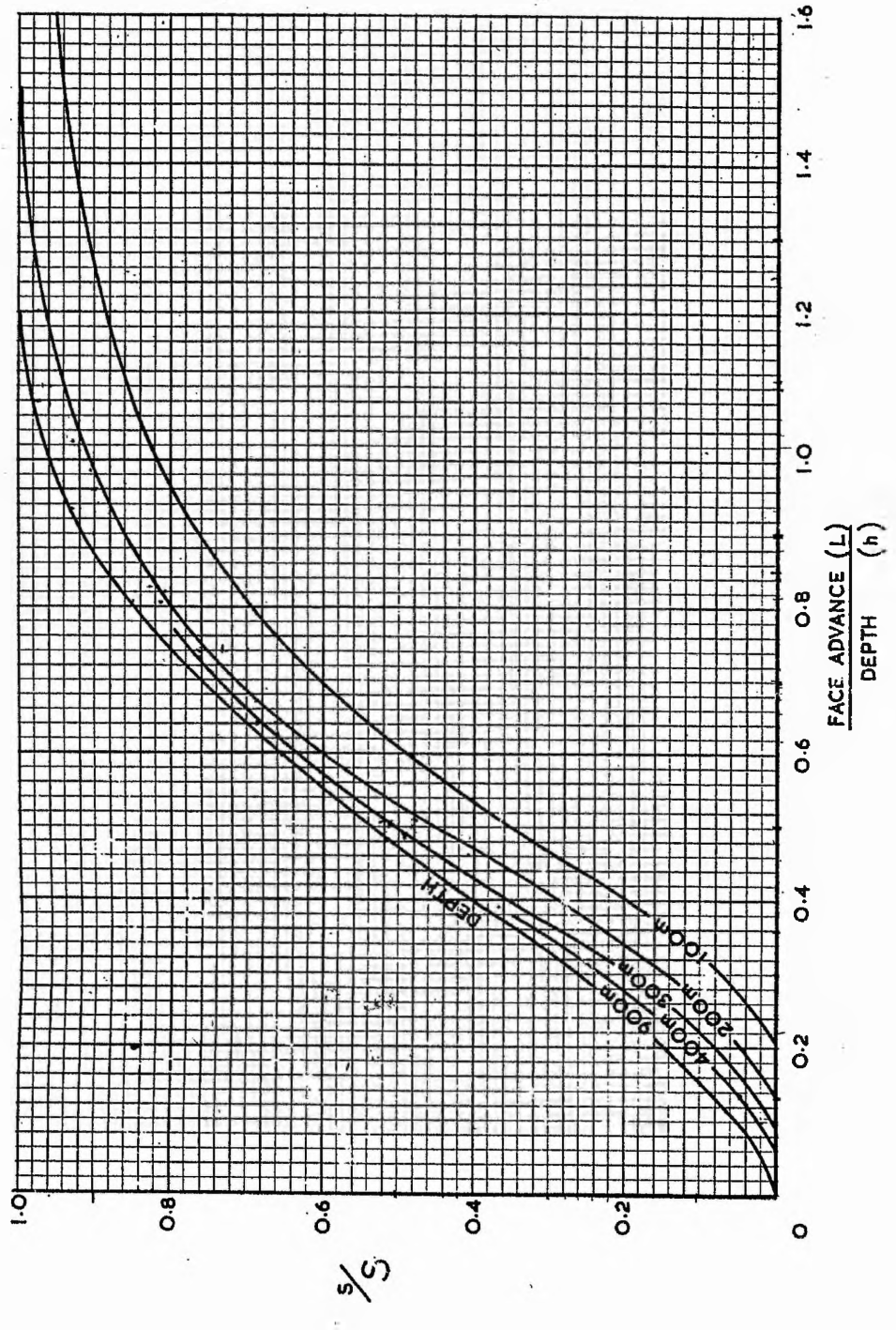

Appendix 6

Relationship of subsidence to the width and depth of the panel (NCB 1975, p.9).

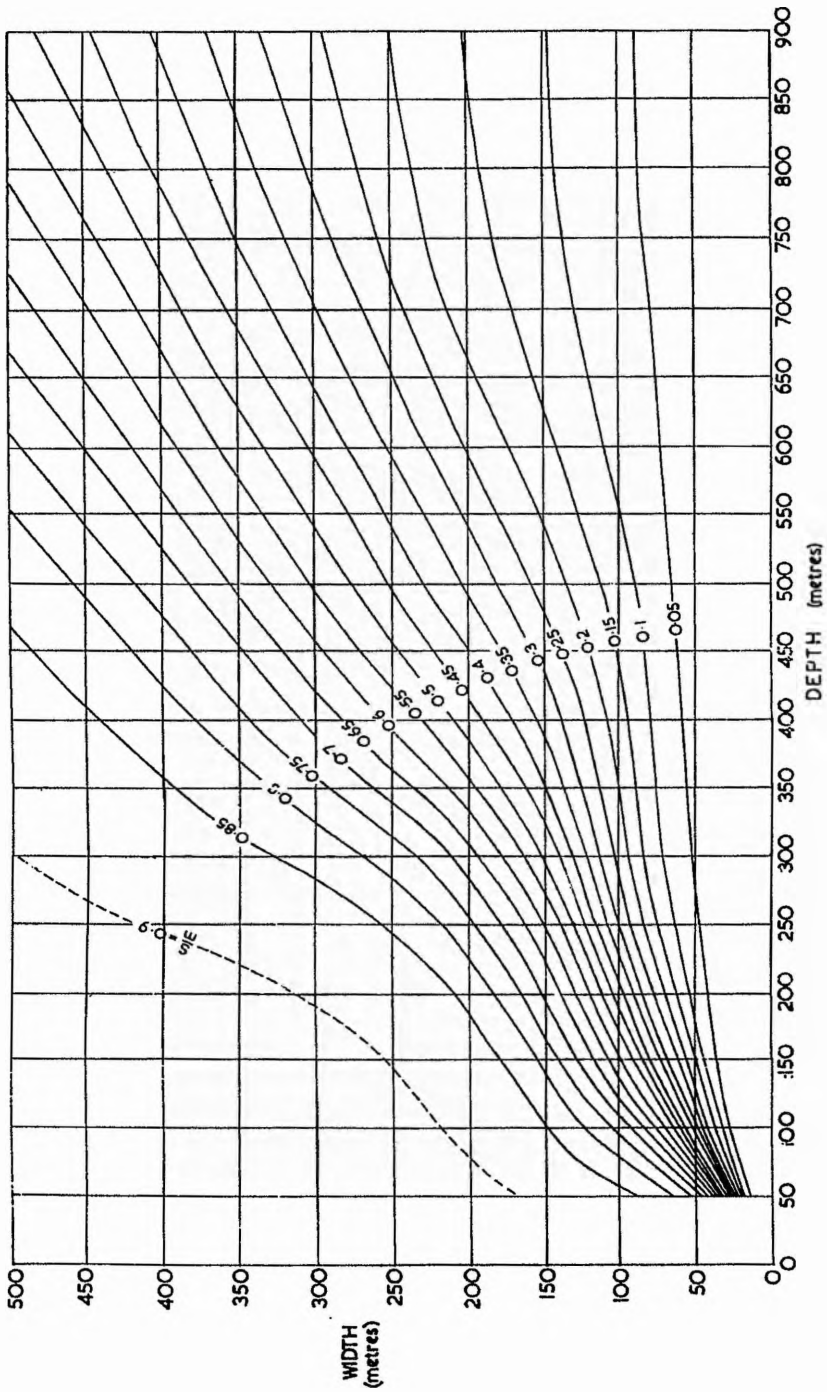

Appendix 7

Table 1 from (NCB 1975 p.14) . Relationship between w/h and d/h for points along a subsidence profile.

Values of s/S	0	0.05	0.10	0.20	0.30	0.40	0.50	0.60	0.70	0.80	0.90	0.95	1.00
w/h RATIO OF PANEL	DISTANCES FROM PANEL CENTRE IN TERMS OF DEPTH												
2.6	2.00	1.51	1.39	1.29	1.24	1.19	1.16	1.12	1.08	1.03	0.95	0.87	0.41
2.4	1.90	1.41	1.29	1.19	1.14	1.10	1.06	1.02	0.98	0.93	0.85	0.77	0.31
2.2	1.80	1.31	1.19	1.09	1.04	1.00	0.96	0.92	0.88	0.83	0.75	0.67	0.23
2.0	1.70	1.21	1.09	0.99	0.94	0.90	0.86	0.82	0.78	0.73	0.65	0.57	0.16
1.8	1.60	1.11	1.00	0.90	0.84	0.80	0.76	0.72	0.68	0.63	0.55	0.47	0.10
1.6	1.50	1.01	0.90	0.80	0.74	0.70	0.66	0.62	0.58	0.53	0.45	0.37	0.06
1.4	1.40	0.91	0.80	0.70	0.64	0.60	0.56	0.52	0.48	0.43	0.35	0.27	0.01
1.3	1.35	0.86	0.75	0.65	0.59	0.55	0.51	0.47	0.43	0.38	0.30	0.23	0
1.2	1.30	0.81	0.70	0.60	0.54	0.50	0.46	0.42	0.38	0.33	0.25	0.19	0
1.1	1.25	0.77	0.65	0.55	0.50	0.45	0.42	0.38	0.34	0.29	0.21	0.16	0
1.00	1.20	0.72	0.61	0.51	0.45	0.41	0.37	0.33	0.29	0.24	0.18	0.13	0
0.98	1.19	0.71	0.60	0.50	0.44	0.40	0.36	0.33	0.28	0.24	0.17	0.12	0
0.96	1.18	0.70	0.59	0.49	0.43	0.39	0.35	0.32	0.27	0.23	0.16	0.11	0
0.94	1.17	0.69	0.58	0.48	0.42	0.38	0.34	0.31	0.26	0.22	0.16	0.11	0
0.92	1.16	0.68	0.57	0.47	0.41	0.37	0.33	0.30	0.26	0.21	0.15	0.10	0
0.90	1.15	0.68	0.57	0.46	0.40	0.36	0.32	0.29	0.25	0.20	0.14	0.10	0
0.88	1.14	0.67	0.56	0.45	0.40	0.36	0.32	0.28	0.24	0.20	0.13	0.10	0
0.86	1.13	0.66	0.55	0.45	0.39	0.35	0.31	0.27	0.23	0.19	0.13	0.09	0
0.84	1.12	0.65	0.54	0.44	0.38	0.34	0.30	0.26	0.22	0.18	0.12	0.09	0
0.82	1.11	0.64	0.53	0.43	0.37	0.33	0.29	0.26	0.21	0.17	0.12	0.08	0
0.80	1.10	0.63	0.52	0.42	0.36	0.32	0.28	0.25	0.21	0.17	0.11	0.08	0
0.78	1.09	0.63	0.52	0.42	0.36	0.32	0.28	0.24	0.20	0.16	0.11	0.08	0
0.76	1.08	0.62	0.51	0.41	0.35	0.31	0.27	0.23	0.20	0.16	0.11	0.07	0
0.74	1.07	0.61	0.50	0.40	0.34	0.30	0.26	0.23	0.19	0.15	0.10	0.07	0
0.72	1.06	0.61	0.50	0.39	0.34	0.30	0.26	0.22	0.18	0.15	0.10	0.07	0
0.70	1.05	0.60	0.49	0.39	0.33	0.29	0.25	0.21	0.18	0.14	0.10	0.07	0
0.68	1.04	0.60	0.49	0.38	0.32	0.28	0.24	0.21	0.17	0.14	0.10	0.07	0
0.66	1.03	0.60	0.48	0.38	0.32	0.28	0.24	0.20	0.17	0.14	0.09	0.06	0
0.64	1.02	0.59	0.48	0.37	0.31	0.27	0.23	0.20	0.17	0.13	0.09	0.06	0
0.62	1.01	0.59	0.47	0.37	0.31	0.27	0.23	0.19	0.16	0.13	0.09	0.06	0
0.60	1.00	0.59	0.47	0.36	0.30	0.26	0.22	0.19	0.16	0.13	0.09	0.06	0
0.58	0.99	0.59	0.47	0.35	0.30	0.26	0.22	0.18	0.16	0.13	0.09	0.06	0
0.56	0.98	0.59	0.47	0.36	0.29	0.25	0.21	0.18	0.15	0.12	0.08	0.06	0
0.54	0.97	0.59	0.47	0.34	0.29	0.25	0.21	0.18	0.15	0.12	0.08	0.06	0
0.52	0.96	0.59	0.47	0.34	0.28	0.24	0.21	0.17	0.15	0.12	0.08	0.06	0
0.50	0.95	0.59	0.47	0.34	0.28	0.24	0.21	0.17	0.15	0.12	0.08	0.06	0
0.48	0.94	0.59	0.47	0.33	0.28	0.23	0.20	0.17	0.15	0.12	0.08	0.06	0
0.46	0.93	0.59	0.47	0.33	0.28	0.23	0.20	0.17	0.15	0.12	0.08	0.06	0
0.44	0.92	0.59	0.47	0.33	0.28	0.23	0.20	0.17	0.15	0.12	0.08	0.06	0
0.42	0.91	0.59	0.47	0.34	0.28	0.24	0.20	0.17	0.15	0.12	0.08	0.06	0
0.40	0.90	0.59	0.47	0.34	0.28	0.24	0.21	0.18	0.15	0.12	0.08	0.06	0
0.38	0.89	0.60	0.48	0.35	0.29	0.24	0.21	0.18	0.15	0.12	0.08	0.06	0
0.36	0.88	0.60	0.48	0.35	0.29	0.25	0.21	0.18	0.15	0.12	0.08	0.06	0
0.34	0.87	0.60	0.49	0.36	0.30	0.25	0.22	0.19	0.16	0.12	0.08	0.06	0
0.32	0.86	0.60	0.49	0.37	0.31	0.26	0.22	0.20	0.16	0.13	0.09	0.06	0
0.30	0.85	0.61	0.50	0.38	0.32	0.27	0.23	0.20	0.17	0.13	0.09	0.06	0
0.28	0.84	0.61	0.51	0.39	0.33	0.28	0.24	0.21	0.18	0.14	0.09	0.07	0
0.26	0.83	0.62	0.52	0.41	0.35	0.30	0.26	0.22	0.19	0.15	0.10	0.07	0
0.24	0.82	0.62	0.53	0.43	0.36	0.32	0.28	0.24	0.20	0.16	0.11	0.07	0
0.22	0.81	0.63	0.55	0.46	0.39	0.34	0.30	0.26	0.21	0.17	0.11	0.08	0
0.20	0.80	0.64	0.57	0.48	0.41	0.37	0.32	0.28	0.23	0.19	0.13	0.08	0

Appendix 8

Empirical tables designed by Wilson (1990) to estimate the effects of mining subsidence on stoop and room workings.

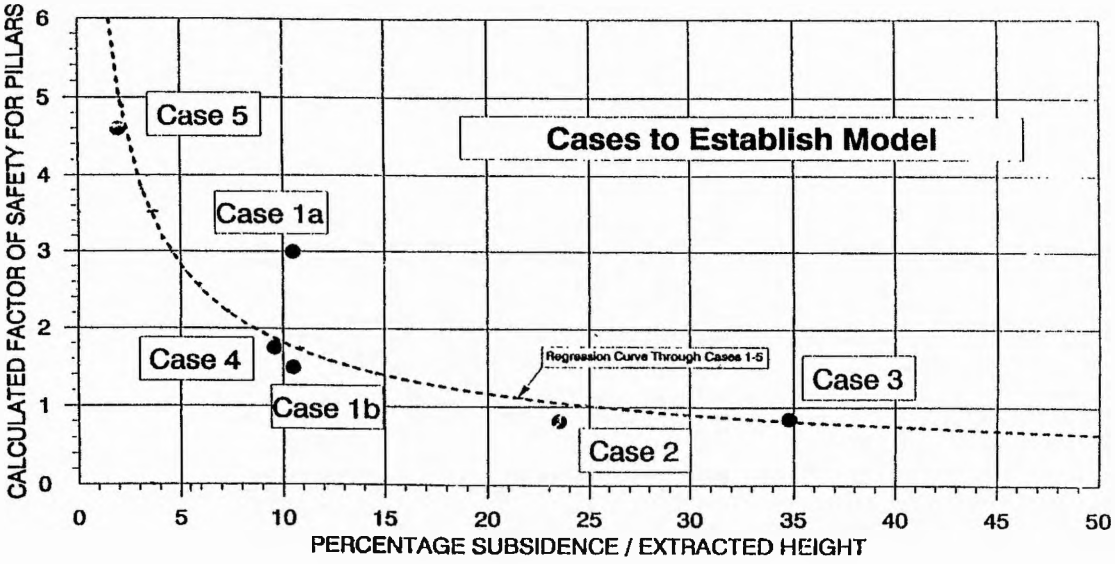

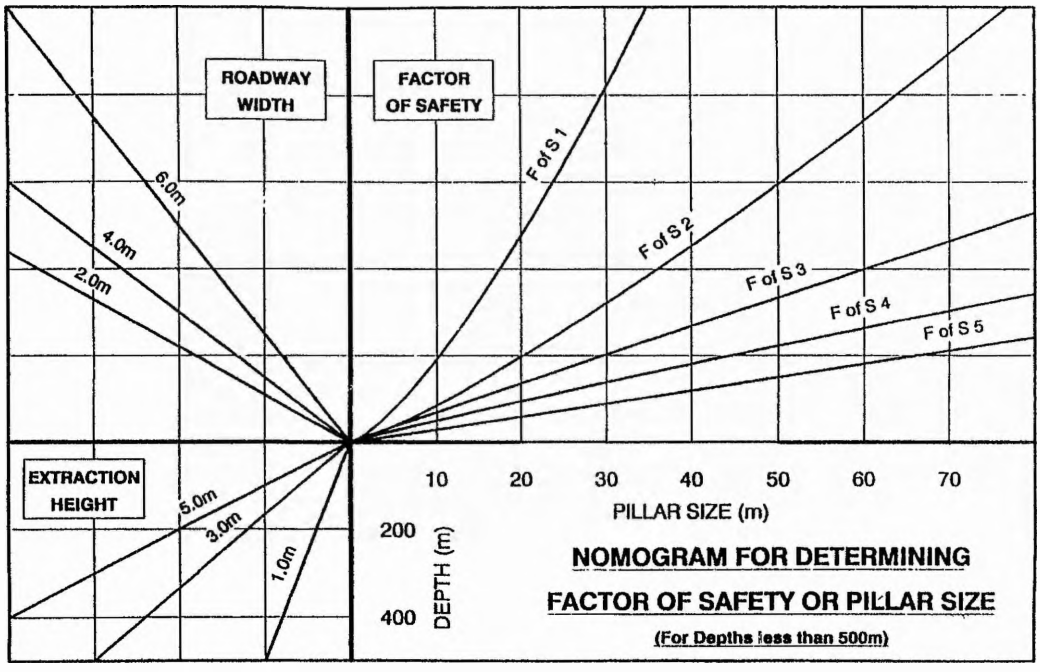

Appendix 9: Estimating subsidence using both SEH formulae and SDPS

The dimensions of the panels and the preparation required in order to use the SDPS software is outlined for each of the panel types.

Example 1. Subcritical Panel:

Length	200
Depth	150
Width	135
Thickness coal	3.0m
tan influence angle	3.1
Maximum Subsidence	0.67

The edge effect occurs at half maximum subsidence, which with reference to the table is 48m from the centre of the panel, which translates to 19.5m inside the original ribside. Hence the panel dimensions are adjusted as follows:

	Panel dimensions	Adjusted dimensions
west border	-67.5	-48
east border	+67.5	48
south border	-100	-80.5
north border	+100	+80.5

Relationship of subsidence values to to points on subsidence profile for subcritical panel.

No.	s/S	S(m)	Distance (h)	Distance (m)
1	0	-0	1.15	172.5
2	0.05	-0.1	0.68	102
3	0.1	-0.201	0.57	85.5
4	0.2	-0.402	0.46	69
5	0.3	-0.603	0.4	60
6	0.4	-0.804	0.36	54
7	0.5	-1.005	0.32	48
8	0.6	-1.206	0.29	43.5
9	0.7	-1.407	0.25	37.5
10	0.8	-1.608	0.2	30
11	0.9	-1.809	0.14	21
12	0.95	-1.909	0.1	15
13	1.0	-2.01	0	0

Example 2:Stoop and Room Panel

Width (w)	360m
Length (L)	300m
Depth (h)	360m
Thickness (m)	3m

Pillar Width 25m
Road Width 5m
From Nomogram (Appendix 8)- Factor of Safety = 1.5
S_{max} = 15%
S_{max} = 0.45m
w/h ratio = 1.2 (See Appendix 7)
Half maximum subsidence occurs 138m from panel centre.

No.	s/S	S(m)	Distance (h)	Distance (m)
1	0	0	1.3	390
2	0.05	-0.0225	0.81	243
3	0.1	-0.045	0.7	210
4	0.2	-0.09	0.6	180
5	0.3	-0.135	0.54	162
6	0.4	-0.18	0.5	150
7	0.5	-0.225	0.46	138
8	0.6	-0.27	0.42	126
9	0.7	-0.315	0.38	114
10	0.8	-0.36	0.33	99
11	0.9	-0.405	0.25	75
12	0.95	-0.4275	0.19	57
13	1.0	-0.45	0	0

The relationship of subsidence values to points along a subsidenc profile, using the SEH method.

Example 3: Critical Panel:

Length	600m
Depth	300m
Width	420m
Thickness coal	1.9m
S/m =0.87	

The edge effect occurs at 42m inside the rib,. The adjusted dimensions are:

	Panel Dimensions	Adjusted Dimensions
west border	-210	-168
east border	+210	+168
south border	-300	-258
north border	+300	+258

The relationship of subsidence values to points along a subsidence profile, using the SEH method.

No.	s/S	S(m)	Distance (h)	Distance (m)
1	0	0	1.4	420
2	0.05	-0.083	0.91	273
3	0.1	-0.0165	0.8	240
4	0.2	-0.3306	0.7	210
5	0.3	-0.4959	0.64	192
6	0.4	-0.6612	0.6	180
7	0.5	-0.8265	0.56	168
8	0.6	-0.9918	0.52	156
9	0.7	-1.157	0.48	144
10	0.8	-1.3224	0.43	129
11	0.9	-1.4877	0.35	105
12	0.95	-1.5703	0.27	81
13	1.0	-1.653	0.01	3

Example 4:Supercritical Panel:

depth	250m
width	135m
length	200m
coal extracted	2.0m
S/m=0.895	

The edge effects occurs at 35m inside the rib.
The adjusted panel dimensions are listed below:

	Panel dimensions	Adjusted dimensions
west border	-200	-165
east border	200	165
south border	-350	-315
north border	300	315

The relationship of subsidence values to points along a subsidence profile, using the SEH method.

No.	s/S	S(m)	Distance (h)	Distance (m)
1	0	0	1.5	375
2	0.05	-0.0895	1.01	252.5
3	0.1	-0.179	0.9	225
4	0.2	-0.358	0.8	200
5	0.3	-0.537	0.74	185
6	0.4	-0.716	0.7	175
7	0.5	-0.895	0.66	165
8	0.6	-1.074	0.62	155
9	0.7	-1.253	0.58	145
10	0.8	-1.432	0.53	132.5
11	0.9	-1.611	0.45	122.5
12	0.95	-1.7	0.37	92.5
13	1.0	-1.79	0.05	12.5

Appendix 10: Summary of coal panels identified along the south-east Fife coastline

The summary includes information on the year the coal was worked, the type of working, the depth of the panel, the dip and thickness of the coal extracted, this is summary compliments the information held in Appendix 10.

Pilkembare

Name of Panel	Year Worked	Type working	Depth	Dip	Thickness
A	1923	Subcritical	91-172.3	1 in 4	1.2

Barncraig

Name of Panel	Year Worked	Type working	Depth	Dip	Thickness
A	1928	supercritical	227	1 in 6	1.3
B	1925	supercritical	149-279	1 in 4	1.0
C	1905	supercritical	133-172	1 in 6	1.2
D	1929	subcritical	300-302	1 in 6	1.4
E	1931	subcritical	289-353	1 in 4, 1 in 5	1.2
F	1906	subcritical	212-288	1 in 5	1.3
G	1906	subcritical	237-288	1 in 4	1.4
H	1851	stoop & room	NO DATA: Too old		
I	1910	stoop & room	209-270	1 in 4	1.7
J	1911	subcritical	133-179	1 in 6	1.3
K	1910	supercritical	165	level	1.6
L	1911	stoop & room	171-262	1 in 2.5/ 1 in 4	1.5
M	1912	stoop & room	125-174	1 in 4	1.7
N	1900	supercritical	110-235	1 in 5	1.5
O	1899	supercritical	83-192	1 in 5	1.6
P	1896	subcritical	144-212	1 in 5	1.6

Coxtool

Name of Panel	Year Worked	Type working	Depth	Dip	Thickness
A	1936-40	supercritical	151-332	1 in 4	0.5-0.8
B	1914	subcritical	124-184	1 in 4	0.8-1.2
C	1915	supercritical	119-188	1 in 4	0.7-1.0
D	1945	supercritical	177-324	1 in 4	1.5-2.3
E	1917	subcritical	203-243	1 in 8	1.3-1.7

Chemiss

Name of Panel	Year Worked	Type working	Depth	Dip	Thickness

A	1905	supercritical	321-487	1 in 5	1.7-2.4
B	1915	supercritical	160-323	1 in 4, 1 in 8	0.9-2.5
C	1909	stoop & room	328-358	1 in 4.5, 1 in 7	1.6
D	1904	subcritical	185-246	1 in 4	0.9-1.3
E	1907	subcritical	246-288	1 in 4	2.5
F	1909	subcritical	239-315	1 in 3	1.2-1.3
G	1911	subcritical	271-362	1 in 3	2.4
H (3 leaves)	1913	subcritical	285-408	1 in 3	0.9-1.8
I	1908-12	subcritical	212-436	1 in 3	1.4-1.6
J	1907	supercritical	134-254	1 in 3	1.1
L	1906	stoop & room	194-254	1 in 4	1.7
M	1914-18	subcritical	373-427	1 in 4, 1 in 5	1.2-3.0
N	1902	subcritical	313-342	1 in 6	2.5-2.7
O (2 leaves)	1889	supercritical/ subcritical	205-276	1 in 6	1.9-2.8
P	1906	subcritical	245-353	1 in 4	1.3-2.5
Q (2 leaves)	1903-4	subcritical	276	1 in 5	1.0-1.8

Bowhouse

Name of Panel	Year Worked	Type working	Depth	Dip	Thickness
A	1937	subcritical	309-401	1 in 3	1.4
B	1958	subcritical	365-540	1 in 3	0.9-1.7
C	1941	subcritical	370-483	1 in 3	1.2-1.8
D	1958	subcritical	266-361	1 in 4	1.3-2.7
E	1920	subcritical	326-458	1 in 5	1.-1.3
F	1924-34	subcritical	240-318	1 in 3	1.2-1.4
G	1891	supercritical	138-203	1 in 3	1.6-1.7
H	1895	stoop & room	159-214	1 in 3	1.6-1.9

One vector panel - I.

Branxton:

Name of Panel	Year Worked	Type working	Depth	Dip	Thickness
A	1962-1963	subcritical	345-376	1 in 5	1.4-3.6
B	1941	subcritical	254-395	1 in 4	0.9-1.5
C	1953	subcritical	414-540	1 in 3.3	1.4-1.8
D	1949	subcritical	429-538	1 in 25	0.9-1.5
E	1873-75	stoop & room	No data		

Boreland

Name of Panel	Year Worked	Type working	Depth	Dip	Thickness
A	1960	subcritical	491-538	1 in 3	0.9-1.0
B	1960	subcritical	385-537	1 in 4	0.8-1.4
C	1925-26	supercritical	236	1 in 2, 1 in 5	0.9

Sandwell

Name of Panel	Year Worked	Type working	Depth	Dip	Thickness
A	1923-39	supercritical	69-146	1 in 2.5	0.9-1.2
B	1924	supercritical	27-83	1 in 8	0.6-1.0
C	no date	no data	no data	no data	no data

Dysart Main

Name of Panel	Year Worked	Type working	Depth	Dip	Thickness
A	1960-61	subcritical	491-526	1 in 4	2.6-3.9
B	1932-46	subcritical	575-512	1 in 5	1.1-1.8
C	1966-67	subcritical	639-553	1 in 4	2.4-4.0
D	1952	stoop & room	504-464	1 in 4	3.9
E	1952	stoop & room	540-443	1 in 4.4	3.2
F	abandoned		too narrow		
G	1943-57	stoop & room	346-468	1 in 7	2.1
H	1881-1893	stoop & room	109-173	1 in 9.75	2.6
I	1900-1907	stoop & room	179-255	1 in 5.5	2.5
J	1931-36	stoop & room	256-223	1 in 4.7, 1 in 7	5.8
K	1934-53	stoop & room	272-338	1 in 4	5.2
L (3 leaves)	1923-36	super/subcrit./subcritical	173-216	1 in 5, 1 in 7.4	3.0
M	1930	subcritical	173-210	1 in 6.8	2.6
N	1940	subcritical	434-446	1 in 7	2.5-2.6
O	1964	subcritical	378-425	1 in 4	3.3

Lower Dysart

Name of Panel	Year Worked	Type working	Depth	Dip	Thickness
A	1948	stoop & room	155-265	1 in 4.5	1.9-2.3
B	1948	stoop & room	161-239	1 in 7	1.6-2.0
C	1915	stoop & room	234-276	1 in 4	1.6-1.9
D	1953-55	subcritical	182-267	1 in 6.6	1.2-1.0
E	1953-55	subcritical	182-267	1 in 6.6	1.2-1.0
F	1953-55	subcritical	182-267	1 in 6.6	1.2-1.0

G (2 leaves)	1958	subcritical	279-320	1 in 5	1.0-2.3
H	1956-60	subcritical	307-373	1 in 3.2	0.7-1.1
I	1957	stoop & room	506-556	1 in 2, 1 in 5	2.3-2.6
J	1941-43	subcritical	207-237	1 in 8	1.1-1.7
K	1941	subcritical	210-236	1 in 8	1.1-1.8

Lethemwell

Name of Panel	**Year Worked**	**Type working**	**Depth**	**Dip**	**Thickness**
A	1965-67	subcritical	316-484	1 in 3, 1 in 5	1.3-2.5
B	1968	subcritical	294-484	1 in 6	2.1-2.8
C	1964	subcritical	334-376	1 in 6	2.4-3.0
D	1964	subcritical	278-376	1 in 6	3.2-2.0
E	1968	subcritical	356-428	1 in 5, 1in 3.6	1.4-2.7
F	1968	subcritical	277-428	1 in 5	2.5-3.0

Appendix 11

Preparatory calculations of subsidence panels for processing within SDPS

All information on each panel is provided including the depth, width, thickness of coal extracted and the edge effect calculated using Appendix 7. The new co-ordinates are also documented.

Pilkembare A: Worked out by 1923. Smax=70%, (-0.818m)

Location: South of Michael Colliery.

Prediction Points: (333100-334000), (695150-696110)

Point	Depth(m)	Width(m)	E.Effect(m)	Dip(m)	Coal(m)	x co-ordinate	y co-ordinate
A1	162.0	100.6	-13.0	58.0	.9	333315.5	695267.9
A2	167.0	240.8	-23.6	55.6	1.4	333414.7	695620.5
A3	172.7	45.7	22.0	57.6	1.2	333597.1	695828.2
A4	156.9	76.2	-6.0	31.4	1.2	333536.9	695896.0
A5	156.9	76.2	-6.7	25.0	1.2	333501.3	695883.7
A6	163.0	45.7	16.3	54.3	1.1	333517.8	695834.8
A7	151.0	61.0	1.2	44.0	1.2	333456.2	695779.5
A8	117.3	176.8	-16.4	34.5	1.1	333338.0	695825.1
A9	91.0	259.0	-14.8	27.6	1.0	333257.9	695850.3
A10	94.0	216.0	-30.5	31.5	1.3	333210.6	695640.1
A11	132.6	107.0	-15.5	44.2	1.1	333301.0	695555.5
A12	126.5	100.6	-14.9	42.0	1.1	333231.1	695334.1

Barncraig A: Worked between 1910 - 1928. Smax = 90%, (-1.327m)

Location: West Sands, Buckhaven.

Prediction Points: (334500-336000), (697200-697970)

Point	Depth(m)	Width(m)	E.Effect(m)	Dip(m)	Coal(m)	x co-ordinate	y co-ordinate
A1	269.0	570.0	-32.0	45.0	1.1	335547.3	697398.9
A2	269.0	570.0	-32.0	45.0	1.6	335672.8	697521.8
A3	237.0	424.0	-36.6	39.5	1.4	335487.4	697569.9
A4	237.0	426.7	-33.0	39.5	1.7	335552.6	697641.8
A5	206.0	283.0	-12.6	25.7	1.7	335441.5	697732.4
A6	182.0	424.0	-18.2	45.5	1.7	335516.7	697999.3
A7	194.0	424.0	-25.7	24.3	1.7	334664.1	697997.7
A8	227.0	424.0	-36.6	70.6	1.5	334775.6	697697.6
A9	217.0	570.0	-32.0	45.0	1.5	335064.9	697670.2
A10	217.0	270.0	-32.0	45.0	1.3	335056.3	697549.4
A11	217.0	570.0	-32.0	45.0	1.3	335053.6	697492.7
A12	217.0	570.0	-32.0	45.0	1.3	335169.3	697448.2

Barncraig B: Worked by 1925, Smax = 90%, (-0.898).

Location: Offshore at gaswork, large panel.

Prediction Points: (334300-335600), (696800-697590)

Point	Depth(m)	Width(m)	E.Effect(m)	Dip(m)	Coal(m)	x co-ordinate	y co-ordinate
B1	270.7	313.9	-37.0	67.6	.9	334843.7	696849.9
B2	279.2	457.2	-38.7	69.8	.9	335339.3	697115.2
B3	197.5	457.2	-38.7	49.4	.8	334989.3	697433.9
B4	179.3	524.3	-54.2	90.0	.8	334846.5	697424.4
B5	164.0	435.8	-27.7	32.8	1.2	334859.2	697448.0
B6	194.5	426.7	-28.6	38.9	.9	334878.4	697295.5
B7	167.4	533.4	-22.4	50.0	.9	334621.7	697241.0
B8	164.3	30.5	37.3	27.9	1.2	334709.6	697344.5
B9	148.8	30.5	32.4	24.8	1.2	334667.5	697407.4
B10	151.8	502.9	-25.5	50.8	1.2	334576.2	697218.0
B11	194.5	335.3	-29.5	48.6	.9	334698.8	697115.4

B12	209.7	152.4	-21.7	41.9	1.0	334636.2	697001.2
B13	230.7	101.6	-12.2	41.9	1.0	334593.0	696904.1
Barncraig C: Worked by 1905, Smax = 90%, (-1.111m)							
Location: Small panel landward of coastline, between gasworks and West Sands.							
Prediction Points: (334500-335000), (697150-697750)							
Point	Depth(m)	Width(m)	E.Effect(m)	Dip(m)	Coal(m)	x co-ordinate	y co-ordinate
C1	149.0	30.5	80.8	25.0	1.7	334564.6	697234.7
C2	149.0	176.8	-32.3	25.0	1.2	334710.2	697403.7
C3	149.0	198.1	-20.8	25.0	1.2	334784.6	697475.1
C4	171.6	271.3	-25.8	28.6	1.2	334944.4	697548.6
C5	133.5	271.3	20.8	22.3	1.1	334739.8	697628.6
C6	133.5	198.1	80.1	22.3	1.1	334621.2	697584.5
Barncraig D: Worked by 1929. Smax=3.5%, (-0.042m).							
Location: Small narrow panel, Shore Street.							
Prediction Points: (335700-336300), (697500-697900)							
Point	Depth(m)	Width(m)	E.Effect(m)	Dip(m)	Coal(m)	x co-ordinate	y co-ordinate
D1	300	30.5	80.8	50.0	1.3	335909.2	697609.5
D2	302	61.0	66.1	50.3	1.4	336047.4	697598.4
D3	302	61.0	66.1	50.3	1.4	336080.4	697759.8
D4	289	76.2	37.0	50.0	1.4	335915.3	697712.3
D5	300	30.5	80.8	50.0	1.4	335875.5	697615.1
Barncraig E: Worked by 1931. Smax=24.3%, (-0.126m).							
Location: Near Shore Street (parrallel to coast).							
Prediction Points: (335500-336700), (697300-698500)							
Point	Depth(m)	Width(m)	E.Effect(m)	Dip(m)	Coal(m)	x co-ordinate	y co-ordinate
E1	334.6	182.9	-21.2	83.7	1.1	336170.0	697637.9
E2	338.0	168.0	-16.4	51.2	1.4	336245.0	697813.1
E3	354.5	228.6	-32.8	88.6	1.4	336332.6	697782.7
E4	354.5	228.6	-32.8	88.6	1.1	336373.3	697902.6
E5	289.0	228.6	-21.2	83.6	1.1	336266.7	697848.2
Barncraig F: Worked by 1906. Smax=46.8%, (-0.548).							
Location: Wellsley Pit Area.							
Prediction Points: (336600-337400), (698400-699210)							
Point	Depth(m)	Width(m)	E.Effect(m)	Dip(m)	Coal(m)	x co-ordinate	y co-ordinate
F1	264.0	185.9	-26.9	52.8	1.3	336829.8	698622.9
F2	264.2	137.0	-13.0	52.8	1.3	336896.3	698727.3
F3	238.7	137.0	-17.2	47.7	1.3	336770.8	698739.3
F4	238.7	137.0	-17.2	47.7	1.3	336721.1	698661.7
F5	211.7	207.0	-44.2	42.4	1.3	336657.0	698648.0
F6	243.0	91.4	5.3	48.6	1.3	336662.9	698527.5
Barncraig G: Worked by 1906 Smax = 67.5%, (-0.942m).							
Location: Wellesley Pit Area.							
Prediction Points: (336600-337400), 698810-699210)							
Point	Depth(m)	Width(m)	E.Effect(m)	Dip(m)	Coal(m)	x co-ordinate	y co-ordinate
G1	287.6	173.7	-23.6	71.9	1.4	337119.1	698811.3
G2	287.6	182.9	-25.4	46.5	1.5	337199.7	699064.9
G3	236.9	305.0	-86.2	145.0	1.4	336944.3	698968.6
G4	264.0	173.7	-23.5	66.0	1.4	337000.0	698835.2
Barncraig H: Vector Polygon. No data. Worked by 1851.							

Stoop and room workings over West Wemyss. Extremely large pillars remain.							
Point						x co-ordinate	y co-ordinate
H1						332544.9	694000.8
H2						332746.6	694143.0
H3						333050.0	694793.0
H4						333006.9	694826.6
H5						333072.4	695084.3
H6						332965.6	695050.7
H7						332533.7	694098.2
Barncraig Z No data. Vector Polygon.							
Location: West Wemyss area.							
Point						x co-ordinate	y co-ordinate
Z1						332484.6	694095.6
Z2						332582.0	694225.8
Z3						332747.5	694555.1
Z4						332914.7	694942.1
Z5						333018.1	695221.3
Z6						332994.9	695241.2
Z7						333017.3	695371.3
Z8						332975.4	695341.8
Z9						332915.6	695105.0
Z10						332846.6	694922.2
Z11						332719.0	694796.4
Z12						332590.6	694615.4
Z13						332619.1	694464.6
Z14						332475.1	694195.8
Barncraig I: Worked by 1910. Stoop and room workings. Smax=3.0-7.5%, (-0.093m).							
Location: Offshore, to south of Michael Colliery (parrallel to beach).							
Prediction Points: (333000-333900), (694700-696060)							
Point	Depth(m)	Width(m)	E.Effect(m)	Dip(m)	Coal(m)	x co-ordinate	y co-ordinate
I1	270.0	244.0	-35.6	90.0	1.9	333275.8	694825.0
I2	254.5	244.0	-35.6	67.5	1.5	333540.4	695491.8
I3	262.0	210.0	-31.6	.0	1.6	333782.0	695903.6
I4	254.5	210.0	-30.0	.0	1.6	333607.7	695937.0
I5	208.7	271.0	-29.5	41.7	1.5	333449.7	695753.5
I6	208.7	183.0	-24.7	61.4	1.9	333267.3	695256.9
	P. Width	Rd Width	F. Safety	S. Max			
I1	18.3	4.6	2.1	7.5			
I2	23.0	5.2	3.5	3.5			
I3	24.0	3.7	2.6	6.0			
I4	24.0	3.7	4.0	6.0			
I5	18.3	3.0	4.0	3.0			
I6	18.3	4.6	2.1	7.5			
Barncraig J: Worked by 1911. Smax = 72.5%, (-0.921m)							
Location: Landward of gasworks, East Wemyss.							
Prediction Points: (3338000-334800), (696850-697520)							
Point	Depth(m)	Width(m)	E.Effect(m)	Dip(m)	Coal(m)	x co-ordinate	y co-ordinate
J1	179.0	189.0	-28.3	29.8	1.3	334321.9	696967.0
J2	179.0	183.0	-25.3	29.8	1.3	334502.8	697121.1
J3	133.5	57.9	-2.3	26.7	1.3	334527.8	697297.6
J4	133.5	57.9	-2.3	26.7	1.3	334488.7	697315.2
J5	133.5	189.0	-19.7	42.0	1.3	334020.0	697095.2

Barncraig K: Worked by 1910. Smax = 90%, (-1.436m).
Location: Michael Colliery.
Prediction Points: (333050-333700), (695350-696370)

Point	Depth(m)	Width(m)	E.Effect(m)	Dip(m)	Coal(m)	x co-ordinate	y co-ordinate
K1	164.7	85.3	-8.1	.0	.9	333222.6	695444.9
K2	164.7	304.8	-27.3	.0	2.3	333480.0	696026.8
K3	164.7	304.8	-27.3	.0	2.3	333277.9	696204.1
K4	164.7	85.3	-8.1	.0	.9	333174.1	695509.5

Barncraig L: Worked by 1911. Smax=3.0-4.5%, (-0.057m).
Location: Offshore at Michael Colliery, Stoop and Room Workings.
Prediction Points: (333400-335100), (695850-697150)

Point	Depth(m)	Width(m)	E.Effect(m)	Dip(m)	Coal(m)	x co-ordinate	y co-ordinate
L1	262.0	312.3	-33.4	105.0	1.2	333973.0	695949.3
L2	224.0	225.6	-30.0	56.0	1.6	334690.0	696798.7
L3	170.6	225.6	-26.1	42.6	1.6	334552.8	696957.3
L4	175.0	213.4	-26.2	70.0	1.5	333781.4	696119.9

	P. Width	Rd Width	F. Safety	S. Max
L1	20.4	4.6	3.5	3.5
L2	15.2	3.7	3.0	4.5
L3	15.2	3.7	3.0	4.5
L4	18.3	5.2	3.8	3.0

Barncraig M: Worked by 1912. Smax=2.0-3.5%, (-0.046m).
Location: East Wemyss. Stoop & Room workings. 1 Non-active panel.
Prediction Points: (333000-334850), (696200-697300)

Point	Depth(m)	Width(m)	E.Effect(m)	Dip(m)	Coal(m)	x co-ordinate	y co-ordinate
M1	174.3	241.0	-23.0	38.7	1.5	333788.9	696294.8
M2	163.0	91.0	-14.3	40.8	1.5	334637.3	697107.4
M3	138.6	91.0	-12.2	34.7	1.5	334582.0	697149.0
M4	148.0	341.4	-21.2	37.0	1.8	334352.1	696928.0
M5	94.0	549.0		23.5	2.0	334129.7	696945.6
M6	124.7	241.0	-19.5	27.7	1.6	333604.8	696429.2

	P.Width	Rd Width	F. Safety	S. Max
M1	21.0	3.3	5.0	2.0
M2	18.3	6.1	3.5	3.5
M3	18.3	6.1	3.5	3.5
M4	18.3	4.6	3.5	3.5
M5	21.0	4.6	4.9	2.0
M6	21.0	3.3	5.0	2.0

Non Active Panel:

Point	x co-ordinate	y co-ordinate
1	334088.0	696700.0
2	334126.9	696745.0
3	3340823.0	696846.6
4	334034.1	696869.6
5	333952.8	696788.9

Barncraig N: Worked by 1900. Smax = 90%, (-1.377m).
Location: South of Wellesley behind LWM (1945).
Prediction Points: (335950-336700), (698350-698850)

Point	Depth(m)	Width(m)	E.Effect(m)	Dip(m)	Coal(m)	x co-ordinate	y co-ordinate

N1	234.8	256.0	-29.4	42.7	1.4	336495.8	698501.3
N2	234.8	283.5	-29.4	42.7	1.6	336589.9	698689.3
N3	110.1	283.5	-24.3	24.3	1.8	336132.8	698754.3
N4	119.2	283.5	-19.0	21.7	1.8	336023.8	698529.3
N5	143.3	377.9	-22.7	26.1	1.2	336105.6	698431.8
N6	189.3	323.1	-27.2	47.3	1.5	336347.9	698453.8
N7	192.4	240.8	-27.1	38.5	1.5	336398.2	698528.3
Barncraig O: Worked by 1899. Smax = 90%, (-1.470m).							
Location North, landward of Wellesley Colliery.							
Prediction Points: (336000-336700), (698700-699200)							
Point	Depth(m)	Width(m)	E.Effect(m)	Dip(m)	Coal(m)	x co-ordinate	y co-ordinate
O1	192.1	95.5	-8.4	38.4	1.9	336572.8	698800.2
O2	192.1	95.5	-8.4	32.0	1.5	336605.2	698871.1
O3	143.3	253.0	-24.8	28.7	1.7	336435.6	699041.6
O4	82.7	185.9	-1.2	16.5	1.6	336085.0	699035.8
O5	110.1	185.9	-14.8	22.0	1.6	336133.0	698876.9
Barncraig P: Worked by 1896. Smax=40.2%, (-0.639m).							
Location: North of Wellesley Colliery.							
Prediction Points: (336300-336900), (698770-699220)							
Point	Depth(m)	Width(m)	E.Effect(m)	Dip(m)	Coal(m)	x co-ordinate	y co-ordinate
P1	211.8	118.9	-15.0	42.4	1.6	336697.6	698848.3
P2	211.8	118.9	-15.0	53.0	1.6	336756.3	698928.7
P3	170.8	149.4	-20.9	34.2	1.6	336617.7	699060.2
P4	143.7	67.1	-4.8	28.7	1.6	336474.9	699037.0
Coxtool A: Worked between 1936-1940. Smax = 90%, (-0.625m).							
Location: Large Panel offshore at East Wemyss.							
Prediction Points: (333600-335350), (695790-697870)							
Point	Depth(m)	Width(m)	E.Effect(m)	Dip(m)	Coal(m)	x co-ordinate	y co-ordinate
A1	331.5	176.8	-18.8	82.9	.7	334031.4	695904.5
A2	314.8	719.3	-44.9	78.7	.8	334904.3	696775.8
A3	279.7	592.8	-40.5	69.9	.7	334828.0	696878.5
A4	278.4	643.1	-40.4	69.6	.8	334917.8	696955.8
A5	166.9	131.1	-18.9	41.7	.5	334789.9	697604.3
A6	165.4	129.5	-18.5	41.4	.5	334828.3	697668.2
A7	157.6	129.5	-19.1	39.4	.5	334736.6	697719.1
A8	151.4	659.9	-20.0	37.9	.8	334251.4	697081.7
A9	217.9	442.0	-33.6	54.5	.8	334403.5	696872.8
A10	229.7	378.0	-31.7	57.4	.8	333888.1	696286.0
A11	252.6	378.0	-34.9	63.2	.7	333967.1	696213.5
A12	267.5	785.0	-34.0	66.9	.7	333928.1	696122.8
A13	282.8	239.3	-34.9	70.7	.7	333987.5	696088.9
A14	281.1	176.8	-23.7	70.3	.8	333877.7	696002.8
Coxtool B: Worked by 1914. Smax = 66%, (-0.688m).							
Location: Offshore at West Sands, Buckhaven.							
Prediction Points: (333050-333650), (695600-696200)							
Point	Depth(m)	Width(m)	E.Effect(m)	Dip(m)	Coal(m)	x co-ordinate	y co-ordinate
B1	150.0	61.0	.0	43.0	.8	333244.5	695766.2
B2	184.2	240.8	-25.5	46.0	1.3	333476.4	696022.0
B3	124.0	240.8	-17.4	31.0	1.2	333271.2	696125.9
B4	144.0	61.0	.0	41.0	.8	333214.1	695784.2
Coxtool C: Worked by 1915. Smax = 90%, (-0.830m).							

Location: Landward behind the Michael Colliery.							
Prediction Points: (333300-333900), (696200-696700)							
Point	Depth(m)	Width(m)	E.Effect(m)	Dip(m)	Coal(m)	x co-ordinate	y co-ordinate
C1	188.2	280.4	-26.3	44.3	1.0	333627.2	696248.1
C2	188.2	326.0	-26.6	41.8	.7	333746.8	696407.0
C3	118.8	326.0	-11.0	29.7	1.0	333495.8	696592.0
C4	125.9	280.4	-17.4	28.0	1.0	333410.4	696444.0
Coxtool D: Worked by 1945. Smax = 90%, (-1.642).							
Location: Landward of the Michael Colliery.							
Prediction Points: (334800-336100), (696800-697910)							
Point	Depth(m)	Width(m)	E.Effect(m)	Dip(m)	Coal(m)	x co-ordinate	y co-ordinate
D1	323.7		-26.1	73.6	1.2	335128.2	696853.7
D2	321.8		60.0	80.5	2.3	335893.1	697489.9
D3	302.9		47.0	75.7	2.3	335786.7	697541.4
D4	279.5		-39.6	69.9	2.3	335602.2	697447.1
D5	262.5		-37.3	65.6	1.8	335527.1	697511.7
D6	260.8		20.4	65.2	1.8	335605.9	697635.1
D7	244.6		14.2	61.2	1.8	335511.5	697668.1
D8	244.5		-34.6	38.8	1.6	335322.9	697473.0
D9	201.8		-28.6	33.6	1.9	335194.0	697799.4
D10	197.2		-26.4	32.9	1.8	335067.8	697654.5
D11	177.4		-22.8	29.6	1.8	334965.3	697676.5
D12	194.2		-27.0	32.4	1.5	334955.4	697510.4
NON ACTIVE PANEL							
Point	Depth					x co-ordinate	y co-ordinate
D1	298.0					335423.2	697224.4
D2	295.0					335489.4	697291.6
D3	243.2					335348.3	697504.4
D4	240.1					335258.7	697433.9
Coxtool E: Worked by 1917. Smax=75%, (-1.120).							
Location: East of Gasworks.							
Prediction Points: (335100-335700), (697500-698000)							
Point	Depth(m)	Width(m)	E.Effect(m)	Dip(m)	Coal(m)	x co-ordinate	y co-ordinate
E1	239.9	289.6	-33.2	30.0	1.3	335305.0	697586.7
E2	243.0	289.6	-34.0	30.4	1.8	335477.2	697726.6
E3	232.3	149.4	-21.3	29.0	1.6	335431.4	697931.3
E4	203.3	289.6	-31.0	20.3	1.0	335190.0	697841.6
Chemiss A: Worked by 1905, 1 non-active panel. Smax = 90%, (-1.998m).							
Location: West Sands.							
Prediction Points: (334600-335920), (697400-698100)							
Point	Depth(m)	Width(m)	E.Effect(m)	Dip(m)	Coal(m)	x co-ordinate	y co-ordinate
A1	321.0	792.5	-44.7	64.2	2.2	335504.2	697504.4
A2	321.0	792.5	-44.7	64.2	1.7	335714.5	697659.0
A3	321.0	792.5	-44.7	64.2	2.5	335638.9	698027.5
A4	487.0	821.0	-69.5	97.4	2.3	334871.6	697969.8
A5	487.0	792.5	-67.6	97.4	2.4	334806.5	697752.1
Non Active Pillar							
Point						x co-ordinate	y co-ordinate
1						335361.8	697523.9
2						335423.2	697588.4
3						335416.0	697622.2

4						335407.3	697632.0
5						335391.3	697583.9
6						335337.1	697535.3
Chemiss B Worked by 1915. Smax = 90%, (-1.608m).							
Location : Large panel offshore, West Sands/ Gasworks.							
Prediction Points: (334200-335500), (697000-697800)							
Point	Depth(m)	Width(m)	E.Effect(m)	Dip(m)	Coal(m)	x co-ordinate	y co-ordinate
B1	323.0	280.0	-38.3	80.8	1.4	334898.7	697011.8
B2	323.0	762.0	-54.8	80.8	2.5	335378.0	697318.4
B3	160.0	762.0	-54.8	20.0	2.0	334724.1	697627.0
B4	184.7	219.4	-24.7	46.0	2.0	334419.6	697345.6
B5	227.7	219.4	-30.0	45.5	2.6	334577.7	697269.5
B6	227.8	85.3	7.5	56.9	.9	334459.2	697138.6
B7	245.6	85.3	11.4	61.4	.9	334453.4	697010.4
B8	245.6	85.3	11.4	61.4	.9	334574.8	697100.8
B9	288.0	231.6	-35.2	57.6	2.5	334685.1	697089.0
B10	288.0	582.0	-43.3	57.6	2.6	334781.9	697156.8
B11	321.0	152.4	-12.0	80.3	1.4	334812.7	697003.6
Non Active Panel							
Point						x co-ordinate	y co-ordinate
1						334505.8	697110.5
2						334778.2	697254.0
3						334825.8	697259.2
4						334888.8	697364.1
5						334852.8	697407.9
6						334607.4	697179.6
7						334623.7	697165.3
8						334594.4	697137.5
9						334550.8	697182.1
10						334527.1	697160.7
11						334567.6	697110.1
Chemiss C: Worked by 1909. Smax=4.5-5.5%, (-0.078m).							
Location: Shore Street, Buckhaven. Stoop & Room Working.							
Prediction Points: (335400-336200), (697200-698100)							
Point	Depth(m)	Width(m)	E.Effect(m)	Dip(m)	Coal(m)	x co-ordinate	y co-ordinate
C1	358.0	137.0	6.7	79.6	1.6	335711.6	697365.9
C2	358.0	231.6	-31.8	51.0	1.6	335943.9	697770.4
C3	358.0	204.0	-25.0	79.6	1.6	335998.8	697888.2
C4	327.5	204.0	-27.0	46.0	1.6	335803.3	697888.4
C5	327.5	137.0	-3.0	72.8	1.6	335590.5	697432.9
Point	P. Width	Rd Width	F. Safety	S. Max			
C1	21.0	3.1	3.0	4.5			
C2	21.0	3.6	2.7	5.4			
C3	21.0	3.6	2.7	5.4			
C4	21.0	3.6	2.7	5.4			
C5	21.0	3.6	2.7	5.4			
Chemiss D: Worked by 1904. Smax=85.3%, (-1.476m).							
Location: 4 smaller panels overlie this large working.							
Prediction Points: (333900-334600), (696800-697300)							
Point	Depth(m)	Width(m)	E.Effect(m)	Dip(m)	Coal(m)	x co-ordinate	y co-ordinate
D1	245.6	283.5	8.3	61.4	.9	334340.1	696953.1

D2	245.6	292.6	-33.3	61.4	.9	334422.1	697014.7
D3	227.7	292.6	-30.3	57.0	1.0	334348.3	697085.4
D4	227.3	168.0	-25.0	45.5	1.0	334380.0	697155.3
D5	184.7	168.0	-19.0	36.9	1.0	334300.1	697274.8
D6	184.7	195.0	-29.2	41.0	1.3	334058.3	697081.8
D7	227.3	195.0	-27.0	50.5	1.3	334170.9	696967.3
D8	227.3	289.6	-28.8	56.8	1.3	334323.3	697037.5
Non Active Panel							
Point						x co-ordinate	y co-ordinate
1						334236.9	697095.7
2						334191.9	697164.9
3						334166.7	697183.4
4						334143	697167.9
5						334152.7	697127.2
6						334223	697095
Leaf D1: Smax= 5.1%.							
Point	Depth(m)	Width(m)	E.Effect(m)	Dip(m)	Coal(m)	x co-ordinate	y co-ordinate
1	245.6	48.8	54.0	61.4	1.3	334336.0	696904.4
2	245.6	79.2	14.4	61.4	1.3	334455.3	697034.9
3	227.4	79.2	9.3	56.9	1.3	334381.2	697098.1
4	228.0	48.8	46.3	57.0	1.3	334284.5	696997.7
Leaf D2: Smax = 5.3%.							
Point	Depth(m)	Width(m)	E.Effect(m)	Dip(m)	Coal(m)	x co-ordinate	y co-ordinate
1	225.0	39.6	56.7	56.3	1.3	334328.9	697019.9
2	225.0	67.1	18.2	56.3	1.3	334430.1	697148.2
3	209.7	67.1	12.6	52.4	1.3	334356.6	697206.5
4	208.7	85.3	2.1	52.1	1.3	334326.6	697188.6
Leaf D3: Smax = 20.3%.							
Point	Depth(m)	Width(m)	E.Effect(m)	Dip(m)	Coal(m)	x co-ordinate	y co-ordinate
1	209.7	118.9	-14.4	52.4	.5	334272.1	697128.8
2	195.4	70.1	7.9	48.9	.5	334324.5	697199.1
3	188.1	39.6	38.5	47.0	.5	334296.7	697184.2
4	200.9	36.6	49.0	50.3	.5	334316.0	697188.1
5	200.0	79.2	2.4	50.0	.5	334347.6	697208.2
6	176.2	82.3	-5.9	44.1	.5	334321.4	697299.5
7	176.2	118.9	-17.2	44.1	.5	334187.9	697185.7
Leaf D4: Smax = 49.2%.							
Point	Depth(m)	Width(m)	E.Effect(m)	Dip(m)	Coal(m)	x co-ordinate	y co-ordinate
1	227.3	195.0	-27.0	50.5	1.3	334159.2	696963.4
2	227.3	227.3	-27.0	50.5	1.3	334250.6	697022.9
3	176.2	192.0	-22.0	39.2	1.3	334154.1	697108.1
4	176.2	195.0	-22.0	39.2	1.3	334078.3	697063.9
Chemiss E: Worked out by 1907. Smax = 40%, (-0.746m).							
Location: Panel close to HWM at East Wemyss, includes non-active panel.							
Prediction Points: (334200-334800), (696700-697300)							
Point	Depth(m)	Width(m)	E.Effect(m)	Dip(m)	Coal(m)	x co-ordinate	y co-ordinate
E1	288.0	116.0	2.5	72.0	2.5	334455.3	696831.6
E2	288.0	106.7	2.5	72.0	2.5	334635.7	696996.6
E3	245.6	116.0	-4.3	61.4	2.5	334511.1	697034.7

E4	245.6	116.0	-9.0	61.4	2.5	334378.3	696927.7
E5	267.0	116.0	-4.6	66.7	2.5	334389.8	696872.9
Non Active Panel							
Ppints						x co-ordinate	y co-ordinate
1						334534.2	696965.0
2						334500.0	697024.5
3						334470.8	696999.2
4						334499.3	696966.0
Chemiss F: Worked by 1909. Smax= 46.9%, (-0.549m).							
Location: Offshore at Michael Colliery.							
Prediction Points: (333700-334200), (695900-696360).							
Point	Depth(m)	Width(m)	E.Effect(m)	Dip(m)	Coal(m)	x co-ordinate	y co-ordinate
F1	315.4	103.6	17.6	105.1	1.2	333904.5	695929.6
F2	315.4	91.4	28.4	100.0	1.2	334161.9	696199.9
F3	254.5	219.5	-30.9	84.8	1.2	333843.1	696183.8
F4	239.2	240.8	-31.9	79.7	1.2	333788.2	696157.3
F5	284.9	240.8	-33.5	95.0	1.3	333904.1	696072.5
F6	292.6	88.4	23.0	97.5	1.3	333831.8	695981.1
Chemiss G: Worked by 1911. Smax = 89%, (-2.089m).							
Location: Offshore at Michael Colliery. 2 Non-active panels.							
Prediction Points: (333800-334700), (696100-696910)							
Point	Depth(m)	Width(m)	E.Effect(m)	Dip(m)	Coal(m)	x co-ordinate	y co-ordinate
G1	362.0	256.0	-37.5	120.7	2.4	334258.5	696262.8
G2	331.6	183.0	-21.9	110.5	2.4	334318.3	696434.9
G3	271.0	183.0	-34.5	90.3	2.4	334286.0	696645.5
G4	271.0	256.0	-36.0	90.3	2.4	333903.3	696276.7
Non-active Panels:							
Point						x co-ordinate	y co-ordinate
1						334173.6	696355.1
2						334188.3	696370.8
3						334108.3	696460.4
4						334094.2	696445.0
1						334181.2	696229.4
2						334190.4	696321.1
3						334094.3	696234.6
Chemiss H: Worked by 1913. Smax = 90%, (-1.279m).							
Location: Offshore to south of Michael Colliery. 3 Leaves and 1 non-active panel.							
Prediction Points: (333000-333900), (694200-696030)							
Point	Depth(m)	Width(m)	E.Effect(m)	Dip(m)	Coal(m)	x co-ordinate	y co-ordinate
1	391.6	70.0	98.0	156.6	1.5	333376.2	694294.4
2	391.6	91.4	70.0	156.6	1.2	333507.4	694507.6
3	408.0	104.0	58.2	136.0	1.2	333494.5	694671.8
4	391.6	347.5	-50.5	112.0	1.3	333720.4	695409.3
5	285.0	347.5	-42.7	95.0	1.0	333589.2	695834.2
6	285.0	350.5	-40.3	81.4	.9	333413.1	695459.1
7	331.6	151.0	-9.2	110.5	1.3	333318.6	694828.8
Non-Active Pillar							
Point						x co-ordinate	y co-ordinate
1						333608.2	694992.9

2						333635.9	695040.3
3						333475.9	695144.7
4						333456.1	695079.0
Chemiss H Leaf 2: Worked by 1909. Smax = 41.9%.							
Point	Depth(m)	Width(m)	E.Effect(m)	Dip(m)	Coal(m)	x co-ordinate	y co-ordinate
H1	323.1	131.1	3.9	92.3	.4	333528.0	695470.9
H2	408.0	207.3	-29.2	110.3	.4	333670.4	6956829.0
H3	262.1	207.3	-30.3	87.4	.4	333590.9	695845.0
H4	262.1	131.1	-10.5	74.9	.4	333421.8	695582.2
Chemiss H: Leaf: 3. Worked by 1909. Smax = 44.1%.							
Location: Offshore at Michael Colliery.							
Point	Depth(m)	Width(m)	E.Effect(m)	Dip(m)	Coal(m)	x co-ordinate	y co-ordinate
H1	388.6	189.0	-14.8	155.4	.4	333660.7	695041.5
H2	388.6	164.6	-4.6	110.0	.4	333724.6	695311.7
H3	376.4	118.9	23.4	107.5	.4	333647.5	695297.3
H4	376.4	118.9	23.4	107.5	.4	333713.1	695442.0
H5	333.7	79.2	53.8	95.3	.4	333702.5	695677.9
H6	330.7	189.0	23.4	110.4	.4	333416.3	695172.5
Chemiss I: Worked between 1908-1912. Smax = 59%, (-0.854m).							
Location: Offshore at Michael Headland. 1 Non-active panel.							
Prediction Points: (333600-334100), (695400-696100)							
Point	Depth(m)	Width(m)	E.Effect(m)	Dip(m)	Coal(m)	x co-ordinate	y co-ordinate
I1	435.6	143.0	24.5	145.0	1.6	333876.4	695439.1
I2	435.6	335.0	-55.5	145.0	1.6	334028.7	695712.3
I3	312.0	353.0	-30.5	70.7	1.4	333814.8	695881.1
I4	300.0	317.0	-38.5	100.0	1.4	333760.5	695848.5
Non-active panel							
Point						x co-ordinate	y co-ordinate
1						333795.0	6957010.9
2						333923.9	695837.3
3						333877.8	695866.4
Chemiss J: Worked by 1907. Smax = 90%, (-0.963m).							
Location: Landward, south of the Michael Colliery.							
Prediction Points: (333000-33750), (695500-696510)							
Point	Depth(m)	Width(m)	E.Effect(m)	Dip(m)	Coal(m)	x co-ordinate	y co-ordinate
J1	254.0	140.0	-16.7	84.7	1.1	333351.9	695575.9
J2	254.0	360.0	-38.0	84.7	1.1	333514.1	695973.2
J3	134.0	360.0	-25.0	44.7	1.1	333227.6	696170.4
J4	134.0	256.0	-19.5	44.7	1.1	333177.1	695887.8
Chemiss K: Worked between 1835-1837.							
Location: West Wemyss. Large stoop and room working. No data.							
Point						x co-ordinate	y co-ordinate
1						332687.7	694073.0
2						332869.3	694153.9
3						333055.6	694697.9
4						333094.2	695554.1
5						332937.1	695749.2
6						332514.7	694522.2
Chemiss L: Worked by 1906. Smax = 3.0-4.5%, (-0.058m).							

Location: Large stoop and room working, at East Wemyss close to Michael Colliery.							
1 Non-active Panel.							
Prediction Points: (333550-334500), (696300-697000)							
Point	Depth(m)	Width(m)	E.Effect(m)	Dip(m)	Coal(m)	x co-ordinate	y co-ordinate
L1	254.0	353.6	-34.8	63.5	1.7	333920.9	696415.2
L2	223.7	228.6	-29.0	56.0	1.7	334383.5	696832.6
L3	216.0	228.6	-28.0	54.0	1.7	334247.8	696971.1
L4	213.0	355.0	-25.1	53.2	1.7	334171.2	696917.5
L5	194.5	355.0	-37.5	48.6	1.7	334066.2	696972.8
L6	195.0	353.6	-28.8	48.7	1.7	333689.2	696638.5
Point	P. Width	Rd Width	F. Safety	S. Max			
L1	21.3	3.7	3.0	4.5			
L2	21.3	3.7	3.0	3.0			
L3	21.3	3.7	3.0	3.0			
L4	21.3	3.7	3.0	3.0			
L5	15.3	3.7	3.0	3.5			
L6	15.3	3.7	3.0	3.5			
Non-active panel							
Point						x co-ordinate	y co-ordinate
1						334299.7	696731.8
2						334334.9	69671.2
3						334315.2	696841.1
4						334240.1	696853.9
5						334163.0	696947.6
6						334086.1	696878.9
7						334162.5	696896.1
8						334196.5	696840.6
9						334156.0	696778.0
Chemiss M: Worked between 1914-1918. Smax = 90%, (-2.08m).							
Location: Offshore at Shore Street, Buckhaven.							
Prediction Points: (335600-336500), (697200-698090)							
Point	Depth(m)	Width(m)	E.Effect(m)	Dip(m)	Coal(m)	x co-ordinate	y co-ordinate
M1	427.4	234.7	-27.6	106.8	2.1	336017.3	697276.7
M2	425.8	256.0	-34.3	106.5	1.2	336271.5	697662.0
M3	415.2	326.0	-46.7	83.0	3.0	336361.5	697883.0
M4	372.5	61.0	103.6	74.5	3.0	336033.8	698060.7
M5	372.5	61.0	103.6	74.5	3.0	335945.1	697855.4
M6	377.0	228.6	-31.4	75.4	1.8	336155.3	697852.1
M7	372.5	265.2	-39.5	132.6	2.3	336055.2	697695.3
M8	372.5	207.3	-25.5	118.6	2.7	335947.6	697466.5
M9	372.5	234.7	-31.7	93.1	2.74	335822.4	697353.4
Non-active Panel							
Point						x co-ordinate	y co-ordinate
1						336000.0	697471.8
2						335965.9	697546.0
3						335924.3	697477.8
Chemiss N: Worked by 1902. Smax = 18.4%, (-0.410m).							
Location: Small Panel, offshore at Wellesley Colliery.							
Prediction Points: (336500-337000), (698500-698900)							
Point	Depth(m)	Width(m)	E.Effect(m)	Dip(m)	Coal(m)	x co-ordinate	y co-ordinate
N1	341.8	148.4	-6.3	68.4	2.7	336764.1	698523.3

N2	341.8	131.1	-6.7	57.0	2.5	336839.2	698628.2
N3	320.5	115.8	9.4	53.4	2.5	336781.0	698756.9
N4	313.4	149.4	-12.0	59.7	2.7	336630.7	698600.2
Chemiss O: Worked out by 1889. Smax = 90%, (-2.698m).							
Location: Landward, south of Wellesley Colliery. 2 Leaves.							
Prediction Points: (336000-336600), (698300-698900)							
Point	Depth(m)	Width(m)	E.Effect(m)	Dip(m)	Coal(m)	x co-ordinate	y co-ordinate
O1	276.5	256.0	-35.4	79.0	1.9	336404.8	698391.7
O2	276.5	356.6	-37.3	55.3	2.6	336569.4	697678.1
O3	205.2	356.6	-8.0	41.0	2.8	336261.3	698768.2
O4	219.6	256.0	-29.6	42.7	2.5	336167.7	698468.8
Chemiss O: Second Leaf. Smax = 55.5%							
Point	Depth(m)	Width(m)	E.Effect(m)	Dip(m)	Coal(m)	x co-ordinate	y co-ordinate
1	276.5	173.7	-23.3	79.0	.9	336413.1	698392.7
2	276.5	173.7	-23.3	79.0	.9	336467.8	698510.0
3	215.0	198.0	-28.1	47.8	1.2	336230.0	698603.7
4	215.0	198.0	-28.1	47.8	1.2	336190.6	698477.2
Chemiss P: Worked by 1906. Smax = 81%, (-1.493M).							
Location: Offshore to east of Wellesley Colliery.							
Prediction Points: (336600-337350), (698800-699300)							
Point	Depth(m)	Width(m)	E.Effect(m)	Dip(m)	Coal(m)	x co-ordinate	y co-ordinate
P1	352.7	359.7	-49.4	70.5	1.3	337116.4	698854.9
P2	352.7	359.7	-49.4	70.5	1.8	337260.8	699112.1
P3	244.7	182.9	-26.6	61.2	1.9	336763.6	699049.8
P4	290.0	280.4	-37.2	72.5	2.5	336927.1	698853.8
Chemiss Q: Worked by 1904. Smax = 84.5%, (-1.801m).							
Location: North of Wellesley Colliery. 2 Leaves.							
Prediction Points: (336100-336900), (698800-699250)							
Point	Depth(m)	Width(m)	E.Effect(m)	Dip(m)	Coal(m)	x co-ordinate	y co-ordinate
Q1	276.5	274.3	-36.2	55.3	1.6	336552.7	698834.1
Q2	276.5	274.3	-36.2	55.3	1.8	336692.7	699068.6
Q3	249.0	240.8	-32.0	49.8	1.0	336479.3	699040.1
Q4	212.4	158.5	-23.0	42.5	1.0	336272.1	698995.5
Q5	212.4	158.5	-23.0	35.4	1.6	336197.1	698894.0
Second Leaf:							
Point	Depth(m)	Width(m)	E.Effect(m)	Dip(m)	Coal(m)	x co-ordinate	y co-ordinate
1	276.5	106.7	4.6	55.3	1.2	336608.0	698892.4
2	276.5	106.7	4.6	55.3	1.2	336663.4	698981.3
3	282.1	195.1	-28.2	50.4	1.2	336560.2	699043.6
4	235.7	51.8	44.8	47.1	1.0	336432.8	698982.6
5	224.7	167.6	-24.3	45.0	.9	336377.9	699015.2
6	212.4	176.8	-25.7	42.5	.9	336277.2	698995.8
7	212.4	176.8	-25.7	35.4	1.2	336210.7	698873.4
8	224.7	167.6	-24.3	45.0	.9	336349.5	698949.4
9	255.8	182.9	-26.2	51.2	1.2	336420.1	698867.6
Wemyss Parrot A: Smax = 30%, (-0.518m).							
Location: West Wemyss.							
Prediction Points: (332600-333050), (694450-694950)							
Point	Depth(m)	Width(m)	E.Effect(m)	Dip(m)	Coal(m)	x co-ordinate	y co-ordinate
A1	255.3	103.6	2.0	102.0	.8	332794.6	694511.1

A2	255.3	103.6	2.0	102.0	.8	332934.7	694858.8
A3	216.8	103.6	2.0	97.0	.3	332814.8	694837.4
A4	216.8	103.6	2.0	102.0	.4	332708.9	694568.8
Wemyss Parrot B No data.							
Located at West Wemyss. Co-ordinates only.							
Point						x co-ordinate	y co-ordinate
1						332547.8	694141.2
2						332712.7	694390.2
3						332344.2	694663.3
4						332124.9	694697.8
5						332200.0	694427.8
6						332267.6	694184.7
7						332255.9	694066.4
Bowhouse A: Worked out by 1937. Smax=43.2%							
Located south of Michael Colliery, on the coast.							
Prediction Points: (333100-333600), (695200-695900)							
Point	Depth(m)	Width(m)	E.Effect(m)	Dip(m)	Coal(m)	x co-ordinate	y co-ordinate
A1	382.5	122.0	23.2	191.3	1.4	333363.7	695236.5
A2	400.8	259.0	-35.2	121.4	1.4	333484.6	695631.8
A3	321.4	259.0	-39.5	97.4	1.4	333296.1	695845.1
A4	309.5	122.0	19.3	155.0	1.4	333205.3	695317.5
Bowhouse B: Worked out by 1958. Smax = 66%, (-0.931m).							
Location: Offshore south of Michael Colliery, between East and West Wemyss.							
Prediction Points: (332900-334300), (694300-696040)							
Point	Depth(m)	Width(m)	E.Effect(m)	Dip(m)	Coal(m)	x co-ordinate	y co-ordinate
B1	526.0	323.0	-43.1	263.0	.9	333431.4	694461.5
B2	527.6	304.8	-36.4	240.0	1.5	333624.1	694947.6
B3	540.0	365.8	-53.3	196.4	1.4	333840.5	695410.0
B4	540.5	320.0	-41.0	180.0	1.4	334066.2	695646.4
B5	434.0	320.0	-47.2	144.7	1.7	333805.7	695808.0
B6	422.0	317.0	-46.7	156.3	1.3	333661.9	695599.9
B7	407.0	356.6	-48.0	148.0	1.3	333585.6	695589.4
B8	382.5	371.8	-50.0	159.4	1.5	333378.4	695247.2
B9	392.0	304.8	-42.4	178.2	1.5	333391.5	695154.5
B10	369.4	323.0	-45.1	184.7	1.5	333118.2	694499.2
Bowhouse C: Worked by 1941. Smax = 63%, (-0.891m).							
Location: Offshore at East Wemyss, north of Michael Colliery. 2 Non-active panels.							
Prediction Points: (333750-336000), (695800-697780)							
Point	Depth(m)	Width(m)	E.Effect(m)	Dip(m)	Coal(m)	x co-ordinate	y co-ordinate
C1	483.0	174.0	14.4	161.0	1.4	334037.3	695845.0
C2	471.6	317.0	-45.3	138.7	1.8	334674.4	696585.3
C3	463.0	431.3	-60.7	100.6	1.4	335446.0	697117.0
C4	450.8	164.6	12.4	118.6	1.2	335740.9	697343.5
C5	407.5	365.8	-52.5	107.0	1.2	335567.2	697400.8
C6	407.5	201.0	-17.0	81.5	1.2	335610.2	697477.5
C7	368.5	201.0	-23.1	73.7	1.2	335485.9	697602.9
C8	371.0	431.3	-51.0	80.6	1.3	335134.1	697309.4
C9	377.0	317.0	-45.4	111.0	1.4	334576.0	696824.5
C10	378.4	307.8	-48.0	126.0	1.8	334269.3	696517.2
C11	402.4	317.0	-45.8	134.0	1.8	334283.3	696442.0
C12	422.0	174.0		140.7	1.4	333877.4	695967.8

Non-active Pillar 1							
Point						x co-ordinate	y co-ordinate
1						334589.0	696532.4
2						334650.8	696576.3
3						334667.0	696574.4
4						334584.8	696742.4
5						334526.7	696724.7
6						334637.7	696589.0
Non-active Pillar 2							
Point						x co-ordinate	y co-ordinate
1						335147.6	697133.4
2						335306.1	697221.0
3						335502.3	697374.3
4						335175.3	697159.0
Bowhouse D: Worked out by 1958. Smax = 63%, (-1.045m).							
Location: East Wemyss to West Sands. 1 non-active panel.							
Prediction Points: (334200-335750), (696700-698130)							
Point	Depth(m)	Width(m)	E.Effect(m)	Dip(m)	Coal(m)	x co-ordinate	y co-ordinate
D1	356.2	157.0	-7.3	99.0	1.4	334433.9	696868.7
D2	347.0	171.0	-16.1	86.7	1.3	334632.2	697108.9
D3	358.0	304.8	-43.2	22.0	1.6	335384.3	697714.9
D4	361.7	369.3		22.6	1.4	335492.4	697891.0
D5	346.5	304.8	-41.5	21.6	1.6	335352.5	697758.3
D6	339.5	304.8	-43.8	21.0	2.6	335236.0	697923.0
D7	265.6	122.0	-7.9	66.4	1.2	334634.6	697575.7
D8	285.0	122.0	-12.6	36.6	1.4	334656.6	697527.7
D9	331.4	362.7	-43.9	66.3	2.3	334911.8	697423.7
D10	329.0	115.8	12.8	65.8	2.7	334805.7	697395.7
D11	308.3	180.0	-22.0	68.5	1.5	334731.9	697374.9
D12	304.1	176.8	-21.5	76.0	1.3	334556.6	697257.0
D13	313.3	157.0	-12.7	87.0	1.3	334333.1	696989.1
Non-active Panel:							
Point						x co-ordinate	y co-ordinate
1						335087.0	697630.6
2						335095.4	697636.7
3						334965.5	697820.3
4						334959.5	697816.0
Bowhouse E: Worked by 1920. Smax = 26.8%, (-0.295m).							
Location: Shore Street, Buckhaven.							
Prediction Points: (336000-336600), (698200-698700)							
Point	Depth(m)	Width(m)	E.Effect(m)	Dip(m)	Coal(m)	x co-ordinate	y co-ordinate
E1	378.0	311.0	-45.9	68.7	1.9	336378.2	698396.6
E2	374.5	106.7	-36.0	68.0	1.0	336417.9	698519.4
E3	457.6	106.7	-79.0	83.2	1.0	336337.0	698583.4
E4	326.5	289.6	-40.3	59.4	1.0	336239.1	698582.9
E5	326.5	82.3	-48.6	59.4	1.0	336354.3	698647.9
E6	308.2	82.3	36.0	56.0	1.0	336278.2	698697.0
E7	311.3	311.0	.0	56.6	1.3	336068.6	698408.3
Bowhouse F: Worked out by 1934. Smax = 88%, (-1.163m).							
Location: Landward, south of the Michael Colliery. 1 Non-active panel.							
Prediction Points: (332950-333700), (695200-696250)							

Point	Depth(m)	Width(m)	E.Effect(m)	Dip(m)	Coal(m)	x co-ordinate	y co-ordinate
F1	309.3	179.8	-21.9	154.7	1.4	333224.2	695404.8
F2	316.8	228.6	-31.9	-105.6	1.4	333329.4	696001.1
F3	318.5	253.0	-37.3	86.1	1.4	333422.0	696129.7
F4	254.5	253.0	-33.6	68.8	1.3	333207.0	696207.3
F5	239.2	204.2	-29.1	108.7	1.2	333112.3	695830.8
F6	224.0	115.8	-10.9	106.7	1.4	333003.6	695371.6
F7	278.9	115.8	-2.1	132.8	1.4	333133.0	695344.2
F8	278.9	182.9	-24.5	139.5	1.4	333150.2	695417.9
1 Non-active Panel							
Point						x co-ordinate	y co-ordinate
1						333224.3	695766.6
2						333258.1	696038.9
3						333197.5	696280.3
4						333213.0	696261.3
5						333246.0	696033.4
Bowhouse G: Worked by 1891. Smax = 90%, (-1.425m).							
Location: West Wemyss, towards Michael Colliery.							
Prediction Points: (332500-332950), (694600-695400).							
Point	Depth(m)	Width(m)	E.Effect(m)	Dip(m)	Coal(m)	x co-ordinate	y co-ordinate
G1	143.7	204.2	-20.2	47.9	1.7	332497.3	694738.5
G2	202.6	204.2	-27.1	67.5	1.6	332692.5	694810.1
G3	197.0	216.4	-25.5	54.7	1.6	332847.6	695209.8
G4	137.6	216.4	-19.5	38.2	1.6	332649.1	695282.0
Bowhouse H: Insufficient data. Stoop and Room workings.							
Point						x co-ordinate	y co-ordinate
1						332554.3	694501.5
2						332680.4	694838.1
3						332366.5	694734.8
4						332372.2	694504.4
Point						x co-ordinate	y co-ordinate
1						331454.8	694229.3
2						331504.0	694289.3
3						331525.1	694370.8
4						331444.0	694412.1
5						331428.3	694353.0
6						331420.5	694281.8
7						331408.5	694259.9
Bowhouse I: Insufficient data. Co-ordinates only.							
Point						x co-ordinate	y co-ordinate
1						331772.9	694107.3
2						332017.8	694367.0
3						332221.6	694754.3
4						332397.3	695082.6
5						332001.0	695098.7
6						331865.8	694849.5
7						331852.1	694703.8
8						331819.3	694651.0
9						331742.1	694632.9
10						331751.8	694534.9
11						331795.1	694563.4
12						331753.9	694420.9
13						331692.6	694375.5

14						331678.8	694282.0
Branxton A: Worked by 1962-63. Smax = 45%, (-0.599m).							
Location: West Sands, Buckhaven.							
Prediction Points: (334800-335500), (697350-697850).							
Point	Depth(m)	Width(m)	E.Effect(m)	Dip(m)	Coal(m)	x co-ordinate	y co-ordinate
A1	365.0	131.0	11.2	73.0	2.3	335016.5	697398.2
A2	365.0	131.0	11.2	52.0	1.4	335230.9	697562.3
A3	376.4	271.3	-37.8	43.8	3.6	335276.6	697343.1
A4	365.0	186.0	-16.2	40.6	2.9	335318.4	697620.8
A5	345.0	186.0	-2.6	40.6	2.4	335211.1	697790.2
A6	345.0	186.0	-2.6	40.6	3.0	335147.8	697755.1
A7	345.0	131.0	7.4	49.6	3.2	335172.2	697714.7
A8	339.0	131.0	11.2	67.8	1.9	334944.4	697547.8
Branxton B: Worked by 1941. Smax = 84%, (-1.029m).							
Location: Landward, south of Michael Colliery.							
Prediction Points: (333000-333450), (695250-696000).							
Point	Depth(m)	Width(m)	E.Effect(m)	Dip(m)	Coal(m)	x co-ordinate	y co-ordinate
B1	387.0	51.8	.0	193.0	.9	333343.2	695303.7
B2	395.0	610.0	-56.0	98.7	1.5	333329.0	695721.1
B3	254.5	610.0	-254.1	98.7	1.5	333125.7	695936.2
B4	248.0	283.5	-37.6	124.0	1.3	333098.0	695597.7
B5	329.2	283.5	-39.8	165.0	1.5	333292.4	695531.2
B6	360.0	51.8	.0	180.0	.9	333288.2	695333.8
Branxton C: Worked by 1953. Smax = 40%, (-0.609m).							
Location: Offshore, to the south of the Michael Colliery.							
Prediction Points: (333150-334250), (694700-695920).							
Point	Depth(m)	Width(m)	E.Effect(m)	Dip(m)	Coal(m)	x co-ordinate	y co-ordinate
C1	523.0	210.0	5.0	261.5	1.8	333540.9	694782.2
C2	540.0	243.8	-14.0	163.6	1.4	333977.2	695643.9
C3	468.0	243.8	-24.0	142.0	1.4	333767.9	695760.1
C4	414.0	210.0	-18.0	207.0	1.8	333310.4	694889.6
Branxton D: Worked by 1949. Smax = 60%, (-0.771m).							
Location: Parrallel to the coastline, offshore, north of the Michael Colliery.							
Prediction Points: (333800-336200), (695900-697600).							
Point	Depth(m)	Width(m)	E.Effect(m)	Dip(m)	Coal(m)	x co-ordinate	y co-ordinate
D1	538.0	296.0	-35.0	179.0	1.4	334269.7	695942.1
D2	500.0	305.0	-40.0	125.0	.9	335889.5	697290.3
D3	429.0	305.0	-43.5	107.3	1.1	335588.7	697365.7
D4	538.0	360.0	-51.0	21.4	1.4	334588.7	696841.8
D5	437.0	335.0	-49.5	146.0	1.5	334068.1	696171.3
D6	441.0	296.0	-42.0	179.0	1.5	334035.6	696043.8
Branxton E: Worked by 1875. No data.							
Location: West Wemyss area. Co-ordinates only.							
Point						x co-ordinate	y co-ordinate
E1						331204.9	694351.9
E2						332355.4	694808.6
E3						332264.4	694795.5
E4						332172.2	694671.9
E5						332156.2	694625.7
E6						332188.9	694591.6
E7						332131.2	694536.2

E8						332096.7	694563.0
E9						332052.1	694524.9
Boreland A: Worked out by 1960. Smax = 64.2%, (-0.544m).							
Location: West of Michael Colliery.							
Prediction Points: (333300-334100), (695100-695910).							
Point	Depth(m)	Width(m)	E.Effect(m)	Dip(m)	Coal(m)	x co-ordinate	y co-ordinate
A1	538.0	134.0	78.0	179.0	.9	333633.4	695209.3
A2	353.0	134.0	78.0	178.0	.9	333925.0	695663.2
A3	495.0	134.0	56.7	165.0	.9	333743.7	695780.3
A4	491.0	134.0	55.7	163.7	1.0	333463.9	695385.6
Boreland B: Worked by 1960. Smax=90%, (-0.769m).							
Location: East Wemyss, large panel parrallel to coastline.							
Prediction Points: (333600-335600), (695700-697190).							
Point	Depth(m)	Width(m)	E.Effect(m)	Dip(m)	Coal(m)	x co-ordinate	y co-ordinate
B1	523.3	128.0	82.5	130.8	1.3	334004.2	695863.5
B2	536.3	320.0	-42.0	149.0	.8	334544.8	696408.4
B3	513.5	234.7	-14.7	147.0	.8	3334530.7	696482.0
B4	513.5	280.4	-32.2	128.0	1.1	3334594.9	696575.1
B5	537.0	362.7	-52.4	134.0	1.3	334660.5	696542.6
B6	522.0	134.0	68.7	104.4	.9	335364.0	696966.5
B7	495.0	134.0	56.7	99.0	.9	335191.6	697075.6
B8	513.0	576.0	-68.4	142.5	.9	334820.7	696633.8
B9	387.7	576.0	-55.4	107.7	.9	334514.5	697030.2
B10	385.5	548.6	-54.6	149.0	.9	334436.5	696928.9
B11	440.4	280.4	-38.9	149.0	1.4	334468.6	696779.8
B12	446.5	320.0	-44.0	124.0	.8	334412.3	696670.4
B13	483.0	213.4	-10.1	130.9	1.2	334438.8	696573.3
B14	483.0	213.4	-10.1	130.9	1.2	334375.2	696524.5
B15	511.9	213.4	113.5	128.0	.8	334449.2	696464.1
B16	492.5	128.0	73.9	123.0	.9	333864.0	696068.1
Boreland C: Worked by 1926. Smax =90%, (-0.819m).							
Location: Frances Colliery.							
Prediction Points: (330550-331600), (693800-694820).							
Point	Depth(m)	Width(m)	E.Effect(m)	Dip(m)	Coal(m)	x co-ordinate	y co-ordinate
C1	236.6	297.0	-32.7	118.0	.9	331386.0	693896.7
C2	122.9	88.4	-12.3	61.5	.9	331468.7	6942401.0
C3	122.9	88.4	-12.3	61.5	.9	331399.6	694271.3
C4	100.0	88.4	-12.2	50.0	.9	331354.8	694183.9
C5	87.8	673.6	-12.2	44.0	.9	331268.4	694187.7
C6	55.8	503.0		47.0	.9	331188.8	691739.7
C7	27.0	420.6		2.0	.9	330692.5	694596.7
C8	54.6	420.6		4.0	.9	330861.6	694081.1
C9	62.0	420.6		4.4	.9	330970.0	694232.7
C10	72.6	265.0		13.2	.9	330970.0	694095.6
C11	74.6	297.0		37.8	.9	331045.8	694010.3
Sandwell A: Worked by 1923/39. Smax =90%, (-0.915m).							
Location: Frances Colliery.							
Prediction Points: (330900-331800), (693750-694560)							
Point	Depth(m)	Width(m)	E.Effect(m)	Dip(m)	Coal(m)	x co-ordinate	y co-ordinate
A1	173.7	173.7	-21.8	51.0	1.2	331239.6	693908.8
A2	320.0	320.0	-18.5	51.0	1.1	331302.3	694019.9

A3	136.6	76.2	-9.4	54.6	1.1	331349.4	693922.5
A4	146.0	360.0	-22.3	58.4	1.1	331417.8	693969.7
A5	139.6	463.3	-20.0	15.5	1.0	331458.8	694222.5
A6	112.5	463.3	-20.0	12.5	.9	331216.4	694244.6
A7	68.7	457.0	.0	7.6	.9	331160.7	694684.7
A8	75.6	457.0	.0	50.8	.9	331003.6	694268.1
Sandwell B: Worked out by 1924. Smax = (-0.756m).							
Location: Frances Colliery.							
Prediction Points: (330350-331200), (693600-694400).							
Point	Depth(m)	Width(m)	E.Effect(m)	Dip(m)	Coal(m)	x co-ordinate	y co-ordinate
B1	83.0	457.0		10.4	.9	330888.1	693719.2
B2	72.6	400.0		9.0	.9	330888.6	693971.1
B3	41.7	457.0		5.0	1.0	330791.3	694256.5
B4	30.0	457.0		3.7	.8	330602.3	694177.7
B5	27.0	450.0		3.4	.6	330449.2	693851.2
Sandwell C: Given Pit. No data given with the outline of this working.							
Location: To south of Frances Colliery, at Panhall.							
Point						x co-ordinate	y co-ordinate
C1						330628.1	693404.2
C2						330644.2	693583.4
C3						330676.4	693729.3
C4						330643.0	693730.5
C5						330562.1	693691.2
C6						330536.5	693656.6
C7						330543.0	693488.1
C8						330560.9	693435.1
C9						330588.3	693407.1
Dysart Main A: Worked out by 1961. Smax=16.7%, (-0.49m).							
Location: Parrallel to the coast at the gasworks.							
Prediction Points: (334400-335400), (696900-697610).							
Point	Depth(m)	Width(m)	E.Effect(m)	Dip(m)	Coal(m)	x co-ordinate	y co-ordinate
A1	526.4	140.2	61.5	131.6	3.3	334635.1	696927.5
A2	519.1	115.8	108.0	94.4	3.9	335221.2	697325.2
A3	498.7	115.8	86.7	90.7	3.0	335120.7	697537.5
A4	490.8	140.2	45.2	122.7	2.6	334555.0	697156.2
Dysart Main B: Worked by 1946.							
Location: Offshore West Sands. 2 leaves, Smax=24% & 11.5% respectively (-0.4m).							
Prediction Points: (334900-335800), (696800-697700).							
Point	Depth(m)	Width(m)	E.Effect(m)	Dip(m)	Coal(m)	x co-ordinate	y co-ordinate
B1	575.5	137.2	92.5	143.9	1.3	335116.5	696906.8
B2	552.6	210.3	10.9	110.5	1.1	335652.3	697456.2
B3	511.5	210.3	.0	102.3	1.2	335483.7	697606.5
B4	529.8	192.0	15.3	132.5	1.3	335132.3	697260.6
2nd Leaf:							
Point	Depth(m)	Width(m)	E.Effect(m)	Dip(m)	Coal(m)	x co-ordinate	y co-ordinate
B1	548.1	210.3	10.0	109.6	1.1	335487.4	697370.9
B2	552.6	210.3	10.9	110.5	1.8	335636.1	697468.0
B3	511.5	210.3	.0	102.3	1.8	335485.2	697598.0
B4	511.5	210.3	.0	102.3	1.8	335293.0	697470.1
Dysart Main C: Worked out by 1966.							
Location: Offshore east of Michael Colliery. 2 leaves. Smax=17.4% & 13.6% (-0.7m).							

Prediction Points: (334000-334900), (696000-696920).							
Point	Depth(m)	Width(m)	E.Effect(m)	Dip(m)	Coal(m)	x co-ordinate	y co-ordinate
C1	639.0	283.5	-14.0	193.6	3.3	334272.6	696013.7
C2	625.8	262.1	-5.9	189.6	4.0	334651.6	696376.8
C3	577.6	262.1	-15.6	175.0	3.2	334509.5	696483.6
C4	579.2	137.2	93.6	144.8	3.4	334763.4	696635.9
C5	543.2	137.2	78.1	135.8	2.4	334587.6	696807.6
C6	553.2	283.5	-25.6	167.0	2.7	334080.1	696222.0
2nd Leaf:							
Point	Depth(m)	Width(m)	E.Effect(m)	Dip(m)	Coal(m)	x co-ordinate	y co-ordinate
C1	637.0	265.2	-5.2	182.0	1.3	334267.0	696051.9
C2	626.3	219.5	25.0	189.8	1.5	334642.3	696368.7
C3	559.3	219.5	7.7	169.5	1.5	334434.6	696537.1
C4	560.5	265.2	-20.5	160.1	1.3	334090.3	696248.6
Dysart Main D: Worked out by 1952. Smax=21.5%, (-0.79m)							
Location: Small panel landwards, east of Michael Colliery. Stoop & room working.							
Prediction Points: (333600-334400), (696100-696810).							
Point	Depth(m)	Width(m)	E.Effect(m)	Dip(m)	Coal(m)	x co-ordinate	y co-ordinate
D1	504.2	97.5	112.6	126	3.9	333886.4	696236.3
D2	491.4	97.5	108.5	140.4	3.9	334237.4	696598.6
D3	463.9	97.5	99.7	132.5	3.9	334045.7	696782.6
D4	479.8	97.5	104.8	120	3.9	333713.1	696379.4
Point	P. Width	Rd Width	F. Safety	S.Max%			
D1	36.6	6.0	1.1	21.5			
D2	36.6	6.0	1.1	21.5			
D3	36.6	6.0	1.1	21.5			
D4	36.6	6.0	1.1	21.5			
Dysart Main E: Worked out by 1952. Smax=13.5%, (-0.35m).							
Location: Landward, south of Macduff Castle. Stoop & room working.							
Prediction Points: (334050-334600), (696500-697100).							
Point	Depth(m)	Width(m)	E.Effect(m)	Dip(m)	Coal(m)	x co-ordinate	y co-ordinate
E1	510.3	243.8	-19.8	116.0	3.2	334222.6	696655.7
E2	504.2	91.4	125.7	114.6	3.2	334568.1	696811.1
E3	485.9	91.4	114.6	110.4	3.2	334374.6	696993.3
E4	485.9	213.4	-9.5	97.2	3.2	334295.7	696806.4
E5	443.2	213.4	-18.1	100.7	3.2	334195.5	696880.4
E6	443.2	243.8	-28.8	100.7	3.2	334059.8	696799.7
Point	P.width(m)	Rd width(m	F. Safety	S. Max			
E1	39.6	6.0	1.5	13.5			
E2	39.6	6.0	1.5	13.5			
E3	39.6	6.0	1.5	13.5			
E4	39.6	6.0	1.5	13.5			
E5	39.6	6.0	1.5	13.5			
E6	39.6	6.0	1.5	13.5			
Dysart Main F: Workings abandoned in 1953. Subsidence generated = negligible.							
Dysart Main G:Worked out by 1957.							
Location: Landward, west of Michael Colliery. Stoop & room working.							
Prediction Points: (332900-333500), (695170-695800).							
Point	Depth(m)	Width(m)	E.Effect(m)	Dip(m)	Coal(m)	x co-ordinate	y co-ordinate
G1	467.6	204.2	-8.6	275.0	2.1	333266.5	695279.1

G2	467.6	204.2	-8.6	275.0	2.1	333307.2	695423.1
G3	345.7	85.3	50.7	203.4	2.1	333058.8	695681.1
G4	345.7	204.2	-26.0	203.4	2.1	333051.4	695408.1
Points G1, G2, Smax=10.5%, Points G3, G4 Smax = 22%.							
Point	P. Width	Rd Width	F. Safety	S. Max			
G1	24.4	3.7	1.8	10.5			
G2	24.4	3.7	1.8	10.5			
G3	16.8	5.2	1.1	22.0			
G4	16.8	5.2	1.1	22.0			
Dysart Main H: Worked out by 1893. Smax=13.5%, (-0.35m).							
Location: South of Frances Colliery, parrallel to coastline. Stoop & room working.							
Prediction Points: (330300-331200), (692900-694110).							
Point	Depth(m)	Width(m)	E.Effect(m)	Dip(m)	Coal(m)	x co-ordinate	y co-ordinate
H1	146.3	323.1	-21.3	13.3	2.6	330802.8	6963011.8
H2	172.6	362.7	-24.3	17.7	2.6	330970.0	693871.6
H3	109.1	362.7	-16.6	11.2	2.6	330636.6	693920.3
H4	116.3	323.1	-15.1	11.9	2.6	330521.0	693004.6
Point	P. Width	Rd Width	F. Safety	S. Max			
H1	14.0	6.0	1.5	13.5			
H2	14.0	6.0	1.5	13.5			
H3	14.0	6.0	1.5	13.5			
H4	14.0	6.0	1.5	13.5			
Dysart Main I: Worked out by 1907. Smax=13%, (-0.33m).							
Location: North of Frances Collliery. Stoop & room working.							
Prediction Points: (330800-331900), (692900-694350).							
Point	Depth(m)	Width(m)	E.Effect(m)	Dip(m)	Coal(m)	x co-ordinate	y co-ordinate
I1	255.2	204.2	-30.6	46.4	2.5	331189.0	693206.8
I2	252.6	353.6	-35.3	45.9	2.5	331588.0	693890.2
I3	228.0	353.6	-32.0	41.5	2.5	331492.6	693991.9
I4	228.0	222.5	-29.2	41.5	2.5	331545.9	694079.3
I5	179.4	222.5	-25.1	32.6	2.5	331412.6	694212.7
I6	179.4	222.5	-25.1	32.6	2.5	331084.5	693826.1
Point	P. Width	Rd Width	F. Safety	S. Max			
I1	21.5	5.5	1.7	13.0			
I2	21.5	5.5	1.7	13.0			
I3	21.5	5.5	1.7	13.0			
I4	21.5	5.5	1.7	13.0			
I5	21.5	5.5	1.7	13.0			
I6	21.5	5.5	1.7	13.0			
Dysart Main J: Worked out by 1936. Smax=25%, (-1.4m).							
Location: Chapel House, West Wemyss. Stoop & room working.							
Prediction Points: (331600-332100), (694100-694800).							
Point	Depth(m)	Width(m)	E.Effect(m)	Dip(m)	Coal(m)	x co-ordinate	y co-ordinate
J1	256.4	158.5	-20.3	54.6	5.8	331744.4	694188.4
J2	252.4	128.0	-11.0	36.1	5.8	332042.4	694650.6
J3	234.0	128.0	-14.9	33.4	5.8	331943.9	694699.9
J4	223.4	161.5	-22.7	54.6	5.8	331813.2	694523.3
J5	222.9	158.5	-31.3	47.4	5.8	331649.7	694282.2

Point	P. Width	Rd Width	F. Safety	S. Max			
J1	24.4	5.5	1.0	25.0			
J2	24.4	5.5	1.0	25.0			
J3	24.4	5.5	1.0	25.0			
J4	24.4	5.5	1.0	25.0			
J5	24.4	5.5	1.0	25.0			
Dysart Main K: Worked out by 1935. Smax=36%, (-1.87m).							
Location: Offshore close to Chapel House, West Wemyss. Stoop & room working.							
Prediction Points: (331900-332400), (694000-694650).							
Point	Depth(m)	Width(m)	E.Effect(m)	Dip(m)	Coal(m)	x co-ordinate	y co-ordinate
K1	334.7	265.2	-38.9	83.7	5.2	332111.1	694033.8
K2	337.7	256.0	-36.8	84.4	5.2	332343.1	694418.6
K3	276.8	256.0	-36.7	69.2	5.2	332161.4	694540.9
K4	271.8	265.2	-34.8	68.0	5.2	331916.5	694171.0
Point	P. Width	Rd Width	F. Safety	S. Max			
K1	24.4	6.0	.8	36.0			
K2	24.4	6.0	.8	36.0			
K3	24.4	6.0	.8	36.0			
K4	24.4	6.0	.8	36.0			
Dysart Main L: Worked out by 1936.							
Location: Close to Chapel House, West Wemyss (landwards). Consisting of 1 large							
panel and 2 smaller leaves. Smax= 90%, 25.4% and 15.5%, respectively, (-2.95m).							
Prediction Points: (331250-332000), (694250-695060).							
Point	Depth(m)	Width(m)	E.Effect(m)	Dip(m)	Coal(m)	x co-ordinate	y co-ordinate
L1	212.8	91.4	-3.1	28.8	3.0	331542.0	694358.8
L2	215.8	222.5	-19.6	43.2	3.0	331853.0	694777.8
L3	173.2	292.6	-24.7	34.6	3.0	331681.0	694872.9
L4	173.2	265.0	-24.2	23.4	3.0	331359.2	694550.0
L5	197.5	265.2	-27.9	49.4	3.0	331537.0	694468.1
2nd Leaf:							
Point	Depth(m)	Width(m)	E.Effect(m)	Dip(m)	Coal(m)	x co-ordinate	y co-ordinate
LL1	212.8	198.1	-27.8	26.6	2.0	331584.7	694431.8
LL2	212.8	114.3	-12.5	26.6	2.0	331624.4	694479.2
LL3	197.5	114.3	-13.7	24.7	2.0	331541.0	694531.3
LL4	188.4	198.1	-24.7	23.5	2.0	331445.3	694527.4
LL5	188.4	198.1	-24.7	23.5	2.0	331446.8	694515.9
3rd Leaf:							
Point	Depth(m)	Width(m)	E.Effect(m)	Dip(m)	Coal(m)	x co-ordinate	y co-ordinate
LLL1	215.8	85.3	2.7	45.9	2.0	331672.3	694492.9
LLL2	214.3	70.0	12.0	45.6	2.0	331762.9	694624.2
LLL3	197.5	70.0	7.5	42.0	2.0	331688.8	694657.2
LLL4	197.5	85.3	-3.2	42.0	2.0	331599.7	694544.9
Dysart Main M: Worked out by 1930. Smax=57.6%, (-1.426m).							
Location:South of Chapel House, West Wemyss, landwards.							
Prediction Points: (331250-331550), (694270-694540).							
Point	Depth(m)	Width(m)	E.Effect(m)	Dip(m)	Coal(m)	x co-ordinate	y co-ordinate
M1	209.7	213.4	-27.0	30.8	2.6	331495.3	694332.2
M2	209.7	259.1	-28.9	30.8	2.6	331500.4	694356.2
M3	200.6	201.2	-26.4	29.5	2.6	331472.9	694419.5
M4	173.2	234.7	-23.9	25.5	2.6	331321.8	694503.5
M5	188.4	183.0	-66.9	27.7	2.6	331349.6	694360.3

Dysart Main N: Worked out by 1940. Smax=10.7%, (-0.266m).
Location: West Sands, Buckhaven (landwards).
Prediction Points: (334600-335500), (697300-698110).

Point	Depth(m)	Width(m)	E.Effect(m)	Dip(m)	Coal(m)	x co-ordinate	y co-ordinate
N1	434.9	48.8	63.5	62.1	2.6	334811.2	697460.5
N2	445.6	57.9	72.9	63.7	2.6	335275.7	697837.8
N3	434.3	57.9	69.7	62.0	2.6	335188.2	697953.0
N4	406.9	219.5	-24.3	58.1	2.5	334878.5	697864.4

Dysart Main O: Worked out by 1964. Smax=6.7%, (-0.175m).
Location: Macduff Castle, East Wemyss (landward).
Prediction Points: (333900-334900), (696900-697520).

Point	Depth(m)	Width(m)	E.Effect(m)	Dip(m)	Coal(m)	x co-ordinate	y co-ordinate
O1	399.9	91.4	70.3	100.0	2.9	334161.6	697043.9
O2	425.2	97.5	74.6	125.1	3.3	334662.7	697313.4
O3	396.8	97.5	58.4	116.7	3.0	334532.0	697429.1
O4	377.6	91.4	60.0	94.4	2.6	334067.7	697173.6

Lower Dysart A: Worked out by 1948. Smax=16.0-8.5%, (-0.922m).
Location: South of Frances Colliery. Stoop & room working.
Prediction Points: (330400-331300), (692900-693300).

Point	Depth(m)	Width(m)	E.Effect(m)	Dip(m)	Coal(m)	x co-ordinate	y co-ordinate
A1	264.6	176.8	-24.9	58.8	1.9	330924.7	692962.9
A2	265.8	176.8	-24.6	59.1	1.9	331021.1	693099.6
A3	154.9	176.8	-20.9	34.4	2.3	330581.6	693143.9
A4	160.4	176.8	-21.0	35.6	2.3	330586.7	693015.6

Point	P. Width	Rd Width	F. Safety	S. Max
A1	18.3	6.1	1.3	16.0
A2	18.3	6.1	1.3	16.0
A3	18.3	6.0	2.0	8.5
A4	18.3	6.0	2.0	8.5

Lower Dysart B: Worked out by 1948. Smax=14.5-4.5%, (-0.186m).
Location: Frances Colliery. Stoop & room working.
Prediction Points: (330500-331120), (693200-693800)

Point	Depth(m)	Width(m)	E.Effect(m)	Dip(m)	Coal(m)	x co-ordinate	y co-ordinate
B1	239.0	408.4	-33.3	53.1	1.9	330992.3	693191.3
B2	191.8	97.5	-8.5	27.4	2.0	330895.9	693718.7
B3	177.3	97.5	-11.6	25.3	2.0	330809.0	693728.5
B4	161.0	408.5	-22.3	35.8	1.3	330622.5	693242.7

Point	P. Width	Rd Width	F. Safety	S. Max
B1	15.2	6.0	1.4	14.5
B2	15.2	6.0	1.8	10.5
B3	15.2	6.0	1.8	10.0
B4	15.2	6.0	3.0	4.5

Lower Dysart C: Worked out by 1915. Smax=4.5%, (-0.079m).
Location: Frances Colliery. Stoop & room working.
Prediction Points: (331000-331900), (693200-694320).

Point	Depth(m)	Width(m)	E.Effect(m)	Dip(m)	Coal(m)	x co-ordinate	y co-ordinate
C1	267.6	121.9	-7.5	66.9	1.6	331198.3	693341.2
C2	276.2	225.6	-32.7	69.1	1.6	331452.3	693730.5
C3	270.1	134.1	-10.4	67.5	1.9	331624.1	694076.9

C4	250.6	134.1	-14.5	62.7	1.9	331524.5	694097.7
C5	234.0	225.6	-30.9	58.5	1.7	331282.0	693791.7
Point	P. Width	Rd Width	F. Safety	S. Max			
C1	36.6	6.1	3.0	4.5			
C2	36.6	6.1	3.0	4.5			
C3	36.6	6.1	3.0	4.5			
C4	36.6	6.1	3.0	4.5			
C5	36.6	6.1	3.0	4.5			
Lower Dysart D: Worked out by 1954.							
Location: Chapel Gardens, West Wemyss. 2 leaves, Smax=65% (-1.3m).							
Prediction Points: (331500-331900), (694200-695100).							
Point	Depth(m)	Width(m)	E.Effect(m)	Dip(m)	Coal(m)	x co-ordinate	y co-ordinate
D1	255.5	155.4	-20.2	38.7	1.0	331652.2	694296.9
D2	211.0	162.0	-23.0	32.0	1.3	331605.8	694717.9
D3	197.5	162.0	-23.7	30.0	1.2	331478.6	694701.3
D4	243.3	155.4	-21.7	36.7	1.3	331537.1	694300.2
2nd Leaf:							
Point	Depth(m)	Width(m)	E.Effect(m)	Dip(m)	Coal(m)	x co-ordinate	y co-ordinate
DD1	257.9	137.2	-14.4	39.1	1.0	331638.6	694304.8
DD2	209.7	137.2	-19.3	31.8	1.1	331592.3	694727.3
DD3	194.5	137.2	-20.0	29.5	1.0	331483.3	694723.7
DD4	237.8	137.2	-16.3	36.0	.8	331534.9	694308.5
Lower Dysart E: Worked out by 1955. Smax=24.3%.							
Location: South of West Wemyss.							
Prediction Points: (331500-331900), (694200-695100).							
Point	Depth(m)	Width(m)	E.Effect(m)	Dip(m)	Coal(m)	x co-ordinate	y co-ordinate
E1	250.3	106.7	-3.3	36.8	1.0	331766.3	694469.6
E2	237.8	112.8	-8.8	35.0	1.0	331767.7	694638.6
E3	266.5	112.8	-3.1	39.2	1.0	331668.4	694653.4
E4	244.8	106.7	-4.4	36.0	1.0	331666.4	694460.9
Lower Dysart F: Worked out by 1955.							
Location: South of West Wemyss. 2 leaves, Smax=65.5%							
Prediction Points: (331700-332200), (694000-694700)							
Point	Depth(m)	Width(m)	E.Effect(m)	Dip(m)	Coal(m)	x co-ordinate	y co-ordinate
F1	241.1	167.7	-23.5	40.2	1.0	331794.3	694653.6
F2	225.0	167.7	-25.3	37.5	1.0	331775.1	694798.4
F3	181.7	170.7	-23.6	30.3	1.2	331540.0	694945.9
F4	181.7	-170.7	-23.6	30.3	1.1	331543.3	694819.3
2nd Leaf:							
Point	Depth(m)	Width(m)	E.Effect(m)	Dip(m)	Coal(m)	x co-ordinate	y co-ordinate
F1	240.2	134.1	-16.6	40.0	1.0	331793.3	694674.7
F2	222.8	134.1	-18.0	37.1	1.0	331777.2	694787.7
F3	185.3	140.2	-20.1	30.9	1.0	331509.2	694953.9
F4	186.9	140.2	-20.6	31.2	1.0	331544.4	694835.6
Lower Dysart G: Worked out by 1958.							
Location: South of West Wemyss. 2 leaves, Smax=90%, (-1.0m).							
Prediction Points: (331700-332200) (694000-694700).							
Point	Depth(m)	Width(m)	E.Effect(m)	Dip(m)	Coal(m)	x co-ordinate	y co-ordinate
G1	319.5	167.6	-16.7	61.4	1.1	331927.8	694095.4
G2	301.4	126.5	-3.0	57.9	1.1	332116.5	694473.7
G3	278.6	126.5	-7.5	53.6	1.0	332010.1	694530.6

G4	281.3	128.0	-7.7	54.1	1.0	331974.8	694451.8
G5	279.8	179.8	-25.5	53.8	1.0	331849.0	694300.4
G6	281.4	167.6	-21.9	54.1	1.1	331796.6	694174.2
2nd Leaf:(worked out by 1960).							
Point	Depth(m)	Width(m)	E.Effect(m)	Dip(m)	Coal(m)	x co-ordinate	y co-ordinate
G1	319.5	158.5	-12.2	61.4	2.3	331925.1	694113.4
G2	269.6	88.4	24.0	57.0	.8	332126.3	694541.3
G3	278.9	88.4	17.2	36.4	.8	332024.9	694612.4
G4	281.3	128.0	-7.7	54.1	1.2	331976.1	694432.8
G5	282.5	143.3	-12.3	53.8	1.0	331871.2	694286.6
G6	282.9	158.5	-19.8	54.4	2.3	331809.2	694180.9
Lower Dysart H: Worked out by 1956/1960.							
Location: South of West Wemyss. 2 leaves, Smax=77.4%, (-1.316m).							
Prediction Points: (331750-332600), (693800-694610).							
Point	Depth(m)	Width(m)	E.Effect(m)	Dip(m)	Coal(m)	x co-ordinate	y co-ordinate
H1	372.7	158.5	-4.7	116.5	.7	332154.9	693975.4
H2	354.2	146.3	3.0	110.7	1.1	332336.3	694366.3
H3	315.5	146.3	-10.1	98.6	1.0	332192.7	694420.3
H4	328.6	158.5	-13.5	102.7	1.0	332011.4	694035.3
2nd Leaf:							
Point	Depth(m)	Width(m)	E.Effect(m)	Dip(m)	Coal(m)	x co-ordinate	y co-ordinate
H1	373.0	179.8	-15.3	116.6	1.0	332164.8	693978.4
H2	355.7	164.6	-11.1	111.2	.8	332337.2	694360.4
H3	306.8	164.6	-17.9	95.9	.8	332191.8	694431.2
H4	320.7	179.8	-22.6	100.2	.9	332001.6	694031.4
Lower Dysart I: Worked out by 1957. Smax=13-35%, (-0.582m).							
Location: West Wemyss. Stoop & room working.							
Prediction Points: (332800-334000), (694700-696250).							
Point	Depth(m)	Width(m)	E.Effect(m)	Dip(m)	Coal(m)	x co-ordinate	y co-ordinate
I1	555.9	97.5	140.3	278.0	2.3	33364.4	694904.8
I2	552.7	106.7	129.0	110.5	2.4	333661.2	695958.2
I3	516.6	106.7	122.3	103.3	2.4	333210.7	695535.6
I4	511.5	118.9	88.9	196.7	2.6	333210.7	695535.6
I5	505.9	97.5	123.4	253.0	2.3	33103.2	695000.1
Point	P. Width	Rd Width	F. Safety	S. Max			
I1	18.3	5.2	0.9	34.5			
I2	30.5	6.1	1.1	21.5			
I3	30.5	6.1	1.3	15			
I4	30.5	5.2	1.5	13			
I5	18.5	5.2	0.9	35			
Lower Dysart J: Worked out by 1943.							
Location: North of Frances Colliery (behind HWM). 2 leaves, Smax=48%, (-1.334m).							
Prediction Points: (331000-331500), (693800-694300).							
Point	Depth(m)	Width(m)	E.Effect(m)	Dip(m)	Coal(m)	x co-ordinate	y co-ordinate
J1	227.0	146.3	-21.0	28.4	1.2	331236.2	693889.3
J2	236.8	88.4	5.5	39.5	1.1	331413.3	694114.3
J3	207.0	164.6	-24.3	29.6	1.1	331197.2	694054.6
J4	206.7	143.3	-21.0	25.8	1.2	331134.0	693942.3
J5	214.3	76.2	6.9	26.8	1.2	331133.6	693896.5
J6	214.3	76.2	9.0	27.4	1.2	331161.4	693862.7
J7	218.9	146.3	-20.6	27.4	1.2	331184.4	693930.4
2nd Leaf:							

Point	Depth(m)	Width(m)	E.Effect(m)	Dip(m)	Coal(m)	x co-ordinate	y co-ordinate
J1	228.0	85.3	5.2	27.1	1.7	331221.9	693826.7
J2	234.7	121.9	-11.7	39.1	1.7	331362.6	694097.4
J3	212.6	121.9	-15.2	35.4	1.7	331225.5	694072.0
J4	211.9	128.0	-17.4	30.3	1.7	331173.3	693993.0
J5	217.8	85.3	3.1	25.9	1.7	331154.7	693879.0
Lower Dysart K: Worked out by 1941.							
Location: North of Frances Colliery (behind HWM). 2 Leaves, Smax=16%, (-0.349m).							
Prediction Points: (331200-331500), (694000-694400).							
Point	Depth(m)	Width(m)	E.Effect(m)	Dip(m)	Coal(m)	x co-ordinate	y co-ordinate
K1	235.6	134.1	-33.6	29.5	1.1	331388.4	694198.3
K2	225.9	121.9	-13.5	30.1	1.1	331401.6	694253.9
K3	209.7	121.9	-14.8	28.0	1.1	331298.5	694269.1
K4	219.2	134.1	-17.7	27.4	1.1	331304.9	694164.6
2nd Leaf:							
Point	Depth(m)	Width(m)	E.Effect(m)	Dip(m)	Coal(m)	x co-ordinate	y co-ordinate
K1	235.4	94.5	2.2	30.6	1.8	331406.7	694174.7
K2	225.9	73.2	13.0	18.5	1.8	331434.4	694268.2
K3	219.9	73.2	11.8	18.0	1.8	331328.9	694292.5
K4	223.1	94.5	-2.6	29.0	1.8	331331.2	694164.5
Lethemwell A: Worked out by 1967. Smax=39%, (-0.635m).							
Location: Offshore at Frances Colliery. 1 non-active panel.							
Prediction Points: (331000-332350), (693360-694150)							
Point	Depth(m)	Width(m)	E.Effect(m)	Dip(m)	Coal(m)	x co-ordinate	y co-ordinate
A1	402.2	388.6	-51.5	89.4	1.3	331440.1	693288.7
A2	483.8	329.2	-48.5	161.3	1.3	332074.0	693733.1
A3	375.0	329.2	-44.6	125.0	2.3	331754.9	693876.4
A4	350.0	344.4	-46.2	87.5	2.5	331548.2	693726.3
A5	334.7	385.6	-45.5	83.7	2.5	331440.5	693695.3
A6	316.0	388.6	-44.2	70.2	2.1	331264.8	693576.1
Lethemwell B: Worked out by March 1968. Smax=45%.							
Location: Frances Colliery (under HWM and LWM).							
Prediction Points: (331000-332350), (693360-694150)							
Point	Depth(m)	Width(m)	E.Effect(m)	Dip(m)	Coal(m)	x co-ordinate	y co-ordinate
B1	319.7	158.5	-13.7	53.3	2.1	331217.0	693622.8
B2	361.4	259.0	-35.5	72.2	2.3	331623.7	693952.9
B3	310.6	259.0	-37.9	62.0	2.8	331467.9	694064.9
B4	301.2	231.6	-33.0	50.2	2.8	331312.8	693963.2
B5	298.0	152.4	-13.6	59.6	2.6	331239.4	693813.6
B6	293.9	158.5	-17.6	66.6	2.6	331157.6	693756.9
Lethemwell C: Worked out by 1964. Smax=39.4%, (-0.957m).							
Location: Blair Point, Dysart.							
Prediction Points: (331200-332300), (693900-694980).							
Point	Depth(m)	Width(m)	E.Effect(m)	Dip(m)	Coal(m)	x co-ordinate	y co-ordinate
C1	376.2	181.4	-15.5	75.2	3.0	331816.7	694085.7
C2	364.3	181.4	-14.2	60.7	2.4	331986.4	694445.7
C3	333.8	181.4	-20.6	55.6	2.5	331836.5	694507.4
C4	340.8	181.4	-19.1	68.2	2.6	331670.3	694164.6
Lethemwell D: Worked out by 1964.							
Location: Blair Point, Dysart. Smax=34.2%							
Prediction Points: (331200-332300), (693900-694980).							

Point	Depth(m)	Width(m)	E.Effect(m)	Dip(m)	Coal(m)	x co-ordinate	y co-ordinate
D1	322.5	277.4	-38.7	53.8	3.2	331518.7	694131.1
D2	316.1	186.0	-23.5	52.7	2.7	331857.9	694760.8
D3	286.0	186.0	-25.8	47.7	2.5	331715.1	694817.5
D4	287.2	265.2	-37.5	49.5	3.1	331488.0	694373.0
D5	281.6	265.2	-36.9	46.9	2.0	331409.7	694413.9
D6	278.0	277.4	-35.7	46.0	3.2	331309.6	694228.2
Lethemwell E: Worked out by 1968. Smax=18.9%, (-0.635m).							
Location: West Wemyss.							
Prediction Points: (331800-332700), (694500-695620).							
Point	Depth(m)	Width(m)	E.Effect(m)	Dip(m)	Coal(m)	x co-ordinate	y co-ordinate
E1	427.7	179.8	-4.4	85.5	2.6	332349.7	694498.9
E2	406.5	179.8	3.6	113.0	1.4	332513.8	694989.7
E3	356.2	179.8	-15.1	98.9	2.7	332321.3	694993.1
E4	392.6	179.8	-1.4	78.5	2.7	332189.8	694548.1
Lethemwell F: Worked out by 1968.							
Location: West Wemyss. Smax=24.5%							
Prediction Points: (331800-332700), (694500-695620).							
Point	Depth(m)	Width(m)	E.Effect(m)	Dip(m)	Coal(m)	x co-ordinate	y co-ordinate
F1	392.6	179.8	-1.4	78.5	2.7	332173.6	694553.7
F2	381.6	256.0	-36.2	76.3	2.7	332219.4	694585.4
F3	367.3	256.0	-36.2	109.7	2.7	332158.4	694601.0
F4	337.7	181.4	-19.8	67.5	2.6	332242.4	695176.0
F5	313.2	181.4	-21.8	62.6	3.0	332257.2	695543.6
F6	277.4	181.4	-25.5	55.5	2.5	332104.2	695537.6
F7	303.0	181.4	-24.0	60.6	2.4	332091.7	695150.0
F8	331.7	173.7	-17.2	66.3	2.7	331981.4	694721.4
F9	333.1	256.0	-36.4	66.6	2.7	331938.1	694651.5

Movements in the HWM and LWM and subsidence values at the same points, 1894-1960				
Point aong coast	Movement in HWM (m)	Subsidence (m)	Movement in LWM (m)	Subsidence (m)
1	67.00	0.00	-157.88	-0.04
2	63.60	0.00	-139	-0.13
3	59.10	-0.40	-103.84	-0.75
4	37.90	-1.40	-94.44	-1.79
5	40.50	-1.40	-156.66	-1.7
6	58.30	-0.06	-70.53	-0.04
7	67.00	-0.18	-38.46	-0.41
8	65.60	-0.68	-1.93	-0.85
9	53.20	-0.50	-33.6	-0.73
10	26.00	-0.70	-58.32	-0.05
11	7.70	-1.42	-63.78	-0.1
12	8.00	-1.94	-81	-0.3
13	13.60	-0.50	-80.06	-0.12
14	26.20	0.00	-63.78	0
15	25.90	0.00	-42.28	0
16	23.80	0.00	-47.35	0
17	21.00	0.00	-28.82	0
18	5.40	0.00	0	0
19	6.80	0.00	-12.03	0
20	9.90	0.00	4.91	0
21	10.30	-0.06	12.47	0
22	16.50	-0.20	5.59	0
23	9.60	-0.31	5.12	0
24	-19.30	-1.40	-4.75	-0.43
25	-12.00	-1.90	-2.51	-1.23
26	-25.00	-2.00	-4.37	-1.32
27	-28.00	-2.00	-4.51	-1.37
28	-28.00	-2.00	-1.77	-1.31
29	-16.30	-2.00	-3.72	-1.3
30	-13.30	424.00	-0.61	-0.69
31	-12.02	-1.40	-2.51	-0.36
32	-9.64	-0.54	-3.99	-0.04
33	-7.15	-0.11	-4.59	0
34	-7.84	-0.02	-2.63	0
35	-17.44	0.00	-5.45	0
36	-16.88	0.00	-6.48	0
37	-11.80	-0.05	-5.5	0
38	-12.01	-0.04	-6.08	0
39	-14.60	0.00	-9.04	0
40	-14.30	0.00	-9.11	0
41	-10.70	-0.55	-7.31	-0.33
42	-11.30	-1.32	-4.78	-0.73
43	-1.84	-0.46	0	-0.12
44	-1.20	-0.05	-3.13	-0.08
45	-0.90	-0.05	-2.69	-0.08
46	-0.47	-0.05	-2.8	-0.1
47	-0.78	-0.14	0	-0.27
48	-1.32	-0.15	0	-0.21
49	-1.58	-0.10	0	-0.38
50	-0.66	-0.05	0	-0.36
51	0.90	0.00	-0.53	0
52	-0.20	0.00	0.38	-0.12

53	8.97	0.00	-1.25	-0.17
54	24.13	0.00	-1.71	0
55	29.77	0.00	-3.4	-0.09
56	21.18	-0.14	-0.93	-0.09
57	8.98	-0.47	0.59	-0.09
58	9.54	-1.23	-1.9	-0.11
59	0.67	-1.86	-3.13	-0.12
60	5.70	-1.22	-0.36	-0.08
61	17.26	-1.07	0.47	-0.05
62	7.73	-0.18	2.77	-0.05
63	0.12	0.00	4.04	0
64	-2.83	0.00	-0.34	0
65	-1.19	0.00	-3.67	0
66	0.16	0.00	0.61	0
67	0.30	0.00	0.16	0
68	0.16	0.00	4.05	0
69	9.21	0.00	-18.15	0
70	0.50	0.00	-15.64	0
71	0.74	0.00	2.18	0
72	1.11	0.00	-18.82	0
73	1.67	0.00	-45.11	0
74	-4.27	0.00	-33.82	0
75	0.67	0.00	-33.84	0
76	-11.37	0.00	-40.16	0
77	-17.62	0.00	-64.63	0
78	-14.04	0.00	-53.21	0
79	-1.57	0.00	-53.21	0
80	-3.83	0.00	-49.11	0
81	-8.97	0.00	-61.11	0
82	-9.49	0.00	-59.79	0
83	-12.41	0.00	-58.53	0
84	-19.65	-0.15	-52.93	0
85	-7.91	-0.32	-47.59	-0.12
86	-16.81	-0.33	-21.62	-0.31
87	-20.28	-0.32	-23.69	-0.33
88	-5.47	-0.32	-16.74	-0.33
89	-12.52	-0.22	-10.64	-0.33
90	-15.58	-0.02	-15.98	-0.3
91	-27.17	0.00	-26.25	0
92	-2.62	0.00	-27.14	0
93	5.20	0.00	-22.12	0
94	4.13	0.00	-48.35	0
95	27.93	0.00	-45.53	0
96	48.14	0.00	-24.41	0
97	40.70	0.00	-0.04	0
98	9.82	0.00	-2	0
99	-1.52	0.00	-4.69	0
100	5.53	0.00	-13.7	0
101	10.11	0.00	-11.71	0
102	-0.78	0.00	-34.09	0

Movements in the HWM and LWM and subsidence values at the same points, 1894-1960				
Point along coast	Movement in HWM (m	Subsidence (m)	Movement in LWM (m)	Subsidence (m)
1	147.42	-0.1	-77.63	-0.3
2	123.19	-0.22	-69.72	-0.76
3	96.1	-0.72	-62.98	-1.21
4	47.18	-1.4	-85.15	-1.79
5	42.73	-1.3	-154.59	-1.57
6	58.32	-0.1	-81.05	-0.07
7	67	-0.18	-32.2	-0.45
8	41.78	-0.47	0.32	-0.85
9	103.05	-0.73	-4.81	-0.55
10	198.3	0	59.63	0
11	190.69	0	56.48	0
12	157.08	0	25.99	0
13	154.16	0	2.27	0
14	138.61	0	-14.89	0
15	107.88	0	-36.89	0
87	88.07	0	-43.9	0
17	84.33	-0.6	-42.67	-0.52
18	80.69	-1.94	-18.23	-1.89
19	107.99	-1.16	-22	-0.72
20	100.07	-0.19	-22.21	-0.31
21	98.48	-0.07	-32.69	-0.13
22	77.98	-0.1	-49.14	-0.08
23	68.58	-0.18	-56.46	-0.17
24	117.77	-1.57	-9.93	-2.35
25	94.21	-2.74	-58.33	-3.49
26	94.27	-3.81	-72.4	-3.64
27	90.76	-4	-77.5	-3.66
28	84.89	-4.15	-76.09	-3.94
29	79.8	-4.35	-84.53	-4.14
30	55.16	424	-111.14	-4.32
31	31.67	-4.56	-145.2	-4.45
32	5.79	-3.19	-155.65	-3.58
33	1.32	-2.23	-157.92	-2.54
34	8.97	-2	-126.06	-2.34
35	12.28	-2.09	-77.26	-2.34
36	-14.6	-2.23	-55.46	-2.67
37	-14.09	-2.74	-69.15	-2.95
38	-18.52	-2.66	-49.69	-2.45
39	-10.83	-2.11	-35.07	-1.53
40	0.17	-1.89	-35.35	-1.3
41	5.08	-1.76	-47.79	-1.32
42	15.33	-1.56	-41.86	-1.27
43	31.53	-0.46	-26.77	-0.66
44	37.28	-0.29	-31.98	-0.46
45	18.34	-0.34	-44.09	-0.51
46	7.92	-0.47	-47.9	-0.59
47	18.88	-0.76	-37.53	-0.94
48	31.83	-0.85	-68.3	-0.92
49	59.4	-0.89	-21.75	-1.01
50	72.72	-0.86	-20.29	-1.01
51	88.14	-0.61	-17.94	-0.77
52	104.64	-0.21	4.41	-0.34

53	116.2	-0.14	36.12	-0.33
54	123.21	-0.04	100.22	-0.21
55	136.7	-0.16	41.36	-0.12
56	96.5	-0.51	8.25	-0.48
57	81.32	-1.58	7.37	-1.24
58	129.07	-1.68	28.59	-1.45
59	108.44	-2.08	-0.88	-1.55
60	59.49	-2.89	-45	-2.68
61	56.81	-2.4	-51.9	-2.41
62	61.5	-1.64	-47.41	-1.73
63	68.18	-0.5	-25.96	-0.6
64	73.66	-0.13	-2.79	-0.27
65	56.88	-0.6	-5.8	-0.18
66	42.23	-0.01	-6.69	-0.08
67	31.55	0	-34.6	0
68	28.78	0	-19.85	0
69	31.97	0	-13.82	-0.11
70	43.63	-0.06	-12.29	-0.14
71	40.25	-0.14	-37.43	-0.14
72	1.85	-0.09	-34.11	0
73	1.9		-67.89	0
74	42.7	0	-50.96	0
75	16.78	0	-108.33	0
76	-7.83	-0.05	-131.83	-0.05
77	-14.56	-1.16	-109.47	-1.19
78	-12.38	-1.07	-56.65	-1.26
79	0.88	-0.97	-56.65	-1.36
80	-11.64	-0.35	-53.27	-1.39
81	-13.34	-0.46	-72.76	-1.23
82	-11.57	-0.64	-64.99	-0.47
83	-13.94	0	-51.95	0
84	-15.66	-0.16	-83.16	-0.09
85	-8.21	-0.47	-73.44	-0.27
86	-18.56	-1.1	-45.31	-0.41
87	-19.51	-0.56	-3.8	-0.4
88	16.12	-0.85	20.12	-0.4
89	96.32	-0.33	51.85	-0.37
90	137.17	-0.31	40.98	-0.32
91	95.08	0	12.56	0
92	52.02	0	-22.67	0
93	35.37	-0.33	-31.64	-0.02
94	50.44	-0.35	-49.27	-0.35
95	57.37	-0.35	-39.65	-0.35
96	60.42	-0.35	-23.66	-0.35
97	49.14	-0.35	-12.67	-0.35
98	19.03	-0.35	-18.01	-0.35
99	10.3	-0.25	-18.05	-0.35
100	22.97	0	-25.59	0
101	48.52	0	-14.31	0
102	37.25	0	-61.14	0

Movements in the HWM and LWM and subsidence values at the same points, 1894-1960				
Point along coast	Movement in HWM (m)	Subsidence (m)	Movement in LWM (m)	Subsidence (m)
1	209.56	-0.29	-41.36	-0.21
2	183.13	-0.73	-14.65	-0.66
3	180.39	-1.6	19.63	-1.29
4	158.86	-2.29	32.37	-1.7
5	159.84	-1.69	-36.21	-1.14
6	213.56	0	36.71	0
7	235.79	0	92.86	0
8	306.67	0	158.5	0
9	320.77	0	220.98	0
10	314.77	0	184.5	0
11	318.96	0	199.6	0
12	275.49	0	134.9	0
13	249.18	0	89.2	0
14	214.54	0	50.6	0
15	123.62	0	-31	0
16	84.82	0	-59.74	0
17	40.29	-0.49	-32.54	-0.64
18	46.44	-1.9	-17.6	-1.89
19	59.51	-1.22	-45.2	-0.7
20	59.81	-0.29	40	-0.18
21	75.19	-0.08	-34.7	-0.13
22	100.17	-0.15	-40.7	-0.08
23	95.42	-0.25	-48.6	-0.17
24	119.1	-1.8	-4.71	-2.4
25	99.44	-2.95	-18.4	-3.93
26	76.28	-3.12	-18.8	-4.13
27	29.85	-4.47	-22.3	-3.8
28	1.16	-4.94	-47.8	-3.68
29	-22.19	-5.27	-83.6	-4.44
30	-33.12	424	-110.9	-5.03
31	-35.36	-5.16	-142.2	-5.39
32	-28.21	-4	-151.82	-4.62
33	-26.3	-2.91	-148.51	-3.79
34	-29.75	-2.78	-115.65	-3.58
35	-27.63	-2.69	-75.66	-3.37
36	-16.95	-3.18	-77.88	-3.65
37	-16.9	-3.72	-85	-3.92
38	-19.35	-2.99	-106.6	-3.42
39	-12.66	-2.88	-98.6	-2.83
40	-1.6	-2.67	-82	-2.43
41	2.99	-2.55	-53.9	-2.49
42	17.5	-2.4	-41.9	-2.32
43	39.5	-0.59	-26.8	-0.89
44	44.56	-0.33	-32	-0.5
45	24.83	-0.34	-44.1	-0.56
46	18.01	-0.5	-47.9	-0.59
47	24.09	-0.76	-37.5	-0.94
48	29.82	-0.85	-68.3	-0.92
49	59.06	-0.89	-21.8	-1.08
50	72.52	-0.86	-20.2	-1.03
51				
52				

53				
54				
55				
56				
57				
58				
59				
60				
61				
62				
63				
64				
65				
66				
67				
68				
69				
70				
71				
72				
73				
74	43.06	-0.37	-51.85	-0.37
75	16.78	-0.39	-107.64	-0.43
76	-7.83	-0.68	-132.09	-0.64
77	-14.56	-1.35	-101.28	-1.25
78	-12.36	-1.22	-86.09	-1.23
79	-0.88	-0.89	-86.09	-1.91
80	-11.64	-0.55	-31.57	-1.8
81	-13.34	-0.82	-79.61	-1.52
82	-11.57	-1.12	-74.39	-0.51
83	-13.94	-0.59	-59.74	-0.09
84	-15.66	-0.4	-87.14	-0.2
85	-8.21	-1.08	-81.25	-1.07
86	-18.56	-2.06	-52.45	-1.54
87	-19.51	-1.6	-63.35	-1.5
88	15.36	-1.23	-82.18	-1.03
89	92.13	-0.8	-15.94	-0.87
90	122.02	-0.48	-0.79	-0.48
91	108.44	-0.01	-7.69	-0.02
92	77.33	0	-28.48	0
93	60.86	-0.39	-49.84	-0.19
94	53.94	-0.53	-77.88	-0.53
95	63.66	-0.53	-52.41	-0.53
96	71.71	-0.51	-32.88	-0.53
97	60.2	-0.44	-10.33	-0.43
98	22.68	-0.37	-20.97	-0.54
99	28.48	-0.5	-19.07	-0.87
100	29.61	-0.02	-15.66	0
101	46.01	0	-12.49	0
102	49.51	0	-21.82	0

Movements in the HWM and LWM and subsidence values at the same points, 1894-1960					
Location	Lcation	x co-ordinate	y co-ordinate	Movement	Subsidence
		1996	0	HWM(m)	(m)
1	West	335607	697612	78.42	-1.61
2	Sands to	335660	697634	99.19	-2.54
3	Michael	335558	697650	74.82	-2.96
4	Colliery	335482	697700	50.69	-3.91
5		335440	697726	24.5	-4.8
6		335390	697748	-10.03	-5.19
7		335336	697754	-13.4	-5.59
8		335278	697760	-28.11	-5.58
9		335200	697742	-20.55	-5.25
10		335130	697788	-27.6	-4.36
11		335076	697654	-25.5	-3.55
12		335025	697608	-43.24	-2.68
13		334960	697575	-35.28	-2.82
14		334925	697524	-35.5	-2.78
15		334894	697485	-33	-2.76
16		334850	697430	-30	-2.78
17		334813	697395	-30	-2.72
18		334795	697360	-29.53	-2.78
19		334762	697336	-4.9	-3.15
20	Wemyss	334675	697295	-17.3	-3.27
21	Caves	334635	697268	-26.3	-3.82
22		334596	697235	-30	-3.58
23		334592	697205	-5.42	-3.47
24	Jon. Cave	334535	697182	-20.9	-2.84
25	Wall Cave	334487	697122	-13.85	-3.76
26	Site Doocot	334426	697055	-0.8	-3.01
27		334370	697002	0.33	-2.99
28		334330	696960	16.5	-1.28
29	South of	424	696541	26.5	-0.81
30	Michael	333898	696486	35.3	-0.83
31	Colliery	333868	696452	26.5	-0.78
32	to as far	333836	696404	20	-0.76
33	as West	333822	696358	37.75	-0.66
34	Wemyss	333785	696313	55.42	-0.4
35		333770	696258	66.11	-0.05
36		333757	696206	61.45	-0.08
37		333704	696156	59.95	-0.03
38		333683	696106	66.4	-0.02
39		333644	696025	53.6	-0.3
40		333586	696025	25.9	-0.09
41		333540	695994	5.15	-0.28
42		333491	695963	-5.28	-0.56
43		333446	695912	-20.45	-1.08
44		333420	695868	-6.06	-1.39
45		333372	695825	4.6	-1.68
46		333362	695733	18.6	-3.2
47		333296	695687	-16.71	-3.3
48		333245	695602	-9.54	-4.42
49		333208	695514	0	-3.9
50		333182	695466	9.31	-2.65
51		333120	695406	-15.35	-1.86

52		333085	695336	9.09	-0.67
53		333062	695285	20.38	-0.14
54		333036	695220	25.3	-0.05
55		333006	695176	18.42	-0.03
56		332962	695124	1.8	-0.01
57		332931	695070	3.6	0
58		332906	695014	6.6	0
59		332880	694962	17.83	0
60		332860	694910	18.71	0
61		332816	694830	19.86	-0.08
62		332770	694755	14.18	-0.06
63	Frances	331085	693714	78.57	-0.08
64	Colliery to	330975	693671	32.31	0
65	Dysart	330936	693658	14.66	-0.12
66		330906	693635	-7.31	-0.36
67		330876	693604	11.56	-0.51
68		330844	693581	0	-0.53
69		330822	693561	0	-0.53
70		330794	693540	-1.2	-0.53
71		330760	693516	-3.23	-0.51
72		330735	693485	8.69	-0.5
73		330700	693435	15.95	-0.45
74		330674	693394	29.36	-0.4
75		330650	693355	27.62	-0.44
76		330628	693310	26.43	-0.42
77		330616	693258	38.46	-0.42
78		330591	693225	4.19	-0.39
79		330575	693190	-2.16	-0.35
80		330556	6931550	0	-0.35
81		330550	693120	-21.79	-0.3
82		330528	693084	0	-0.37
83		330509	693035	5.15	-0.03

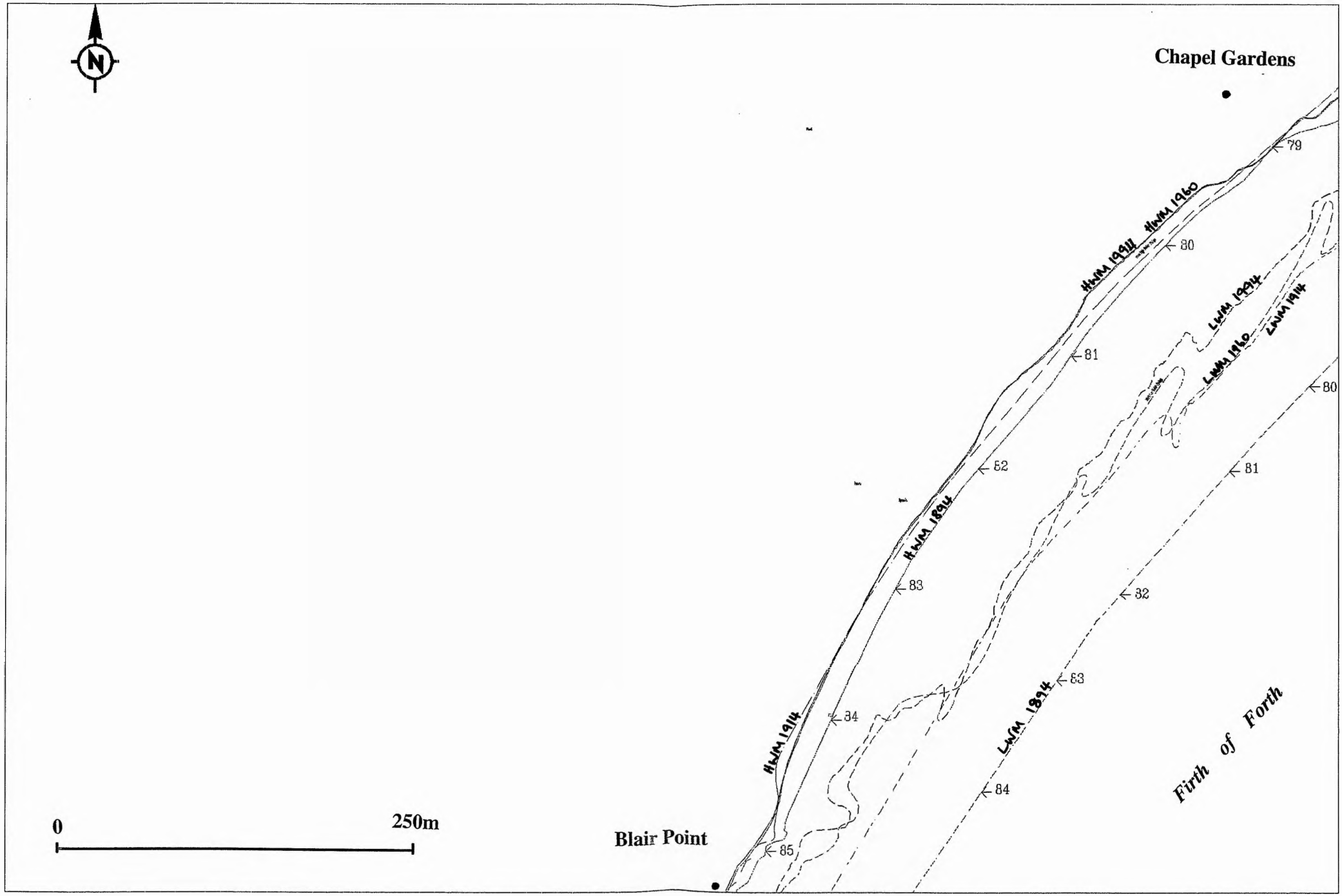

Figure 3.7 Coastal changes recorded to the south of West Wemyss towards Blair Point (1894-1994).

Fife Council
Planning Service
Fife House
Glenrothes KY7 5LT
Tel: 01592 414141

Title: West Wemyss
Coastal Changes 1894-1994
Scale: 1:2500 Date: 16/01/97

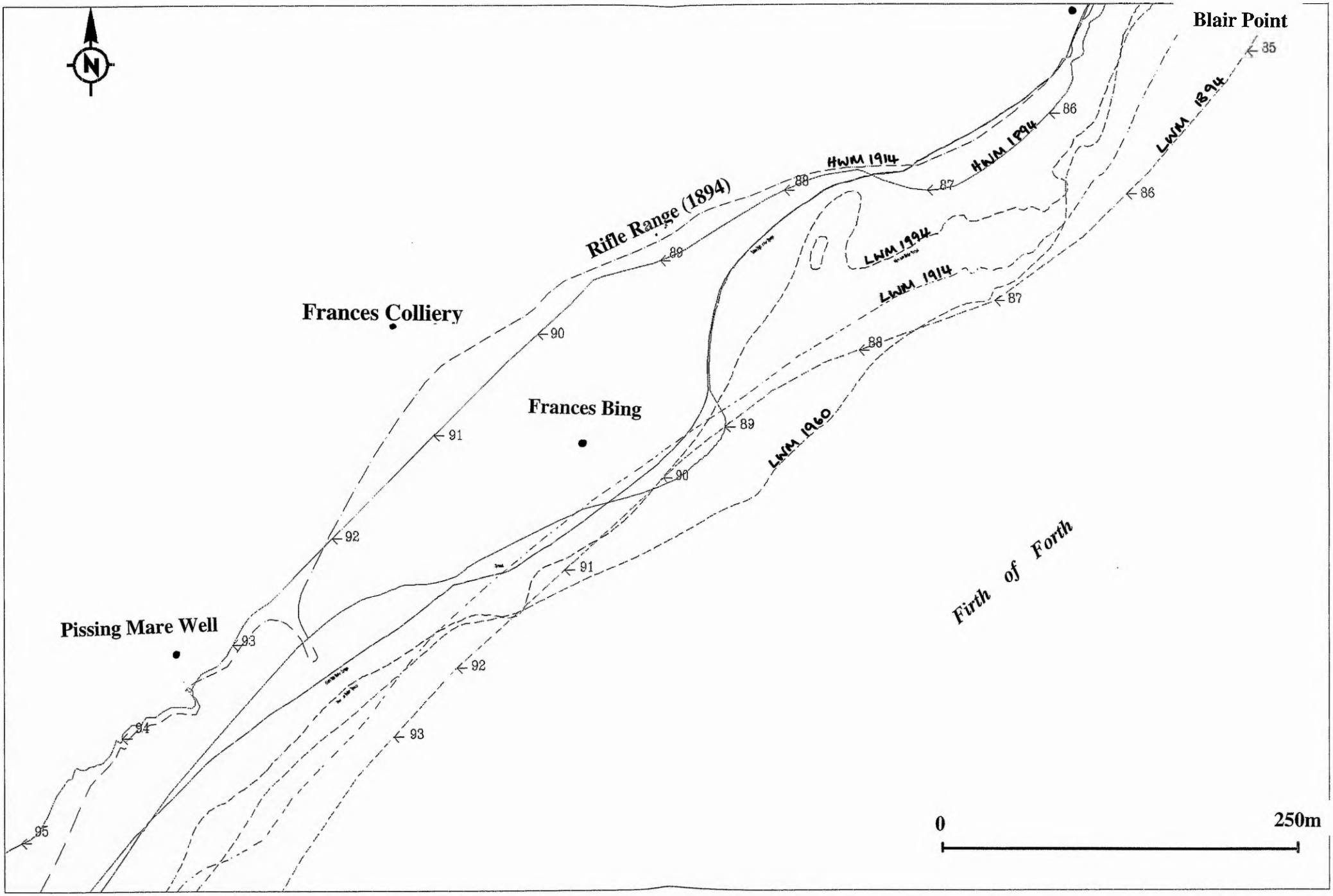

Figure 3.8 Coastal changes between Blair Point and the Frances Colliery (1894-1994). The points denoted along the coastline indicate the positions where measurements of the coastal changes were recorded. The original coastline has been significantly transformed especially between points 86-93.

Fife Council

Planning Service
Fife House
Glenrothes KY7 5LT
Tel: 01592 414141

Title: West Wemyss
Coastal Changes 1894–1994
Scale: 1:2500 Date: 16/01/97

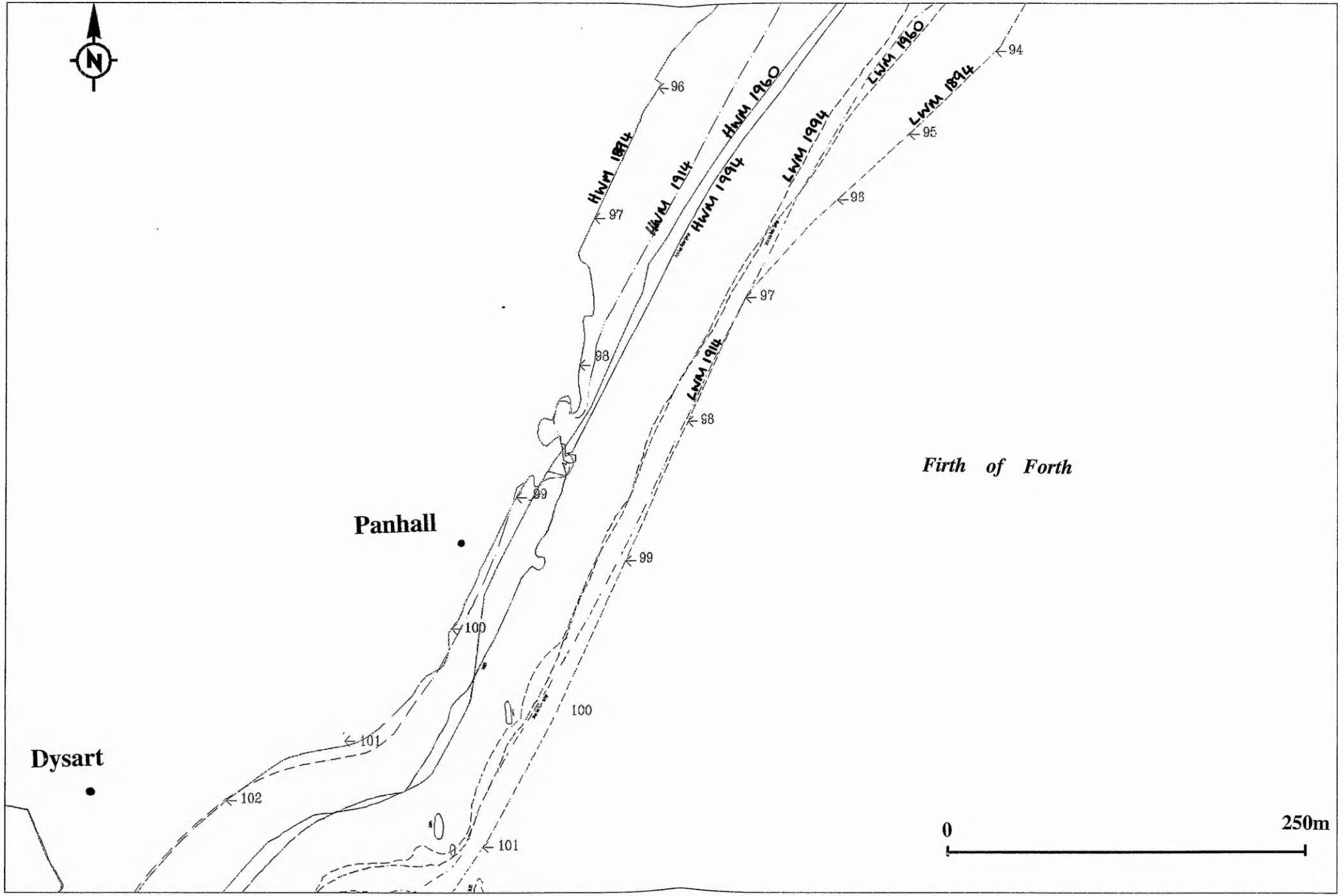

Fife Council	Planning Service Fife House Glenrothes KY7 5LT Tel: 01592 414141	Title: Frances Colliery, Dysart Coastal Changes 1894–1994 Scale: 1:2500 Date: 16/01/97

Figure 3.9 Coastal changes recorded to the south of the Frances Colliery (point 94) to Dysart.

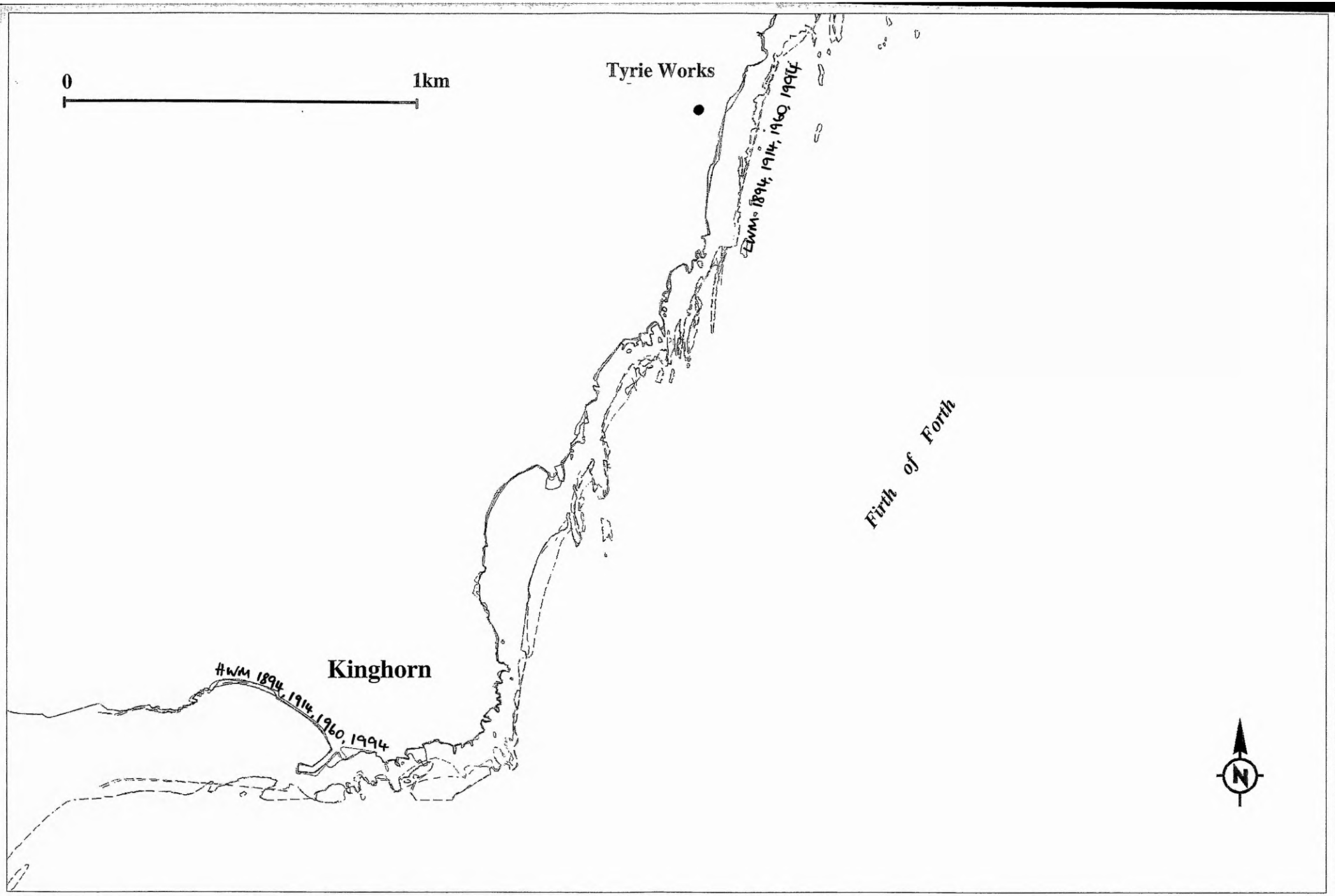

Fife Council	Planning Service Fife House Glenrothes KY7 5LT Tel: 01592 414141	Title: Kinghorn Coastal Changes 1894–1994 Scale: 1:10000 Date: 16/01/97

Figure 3.1 Coastal changes between Tyrie Works and Kinghorn (1894-1994). Note how the coastline has barely changed.

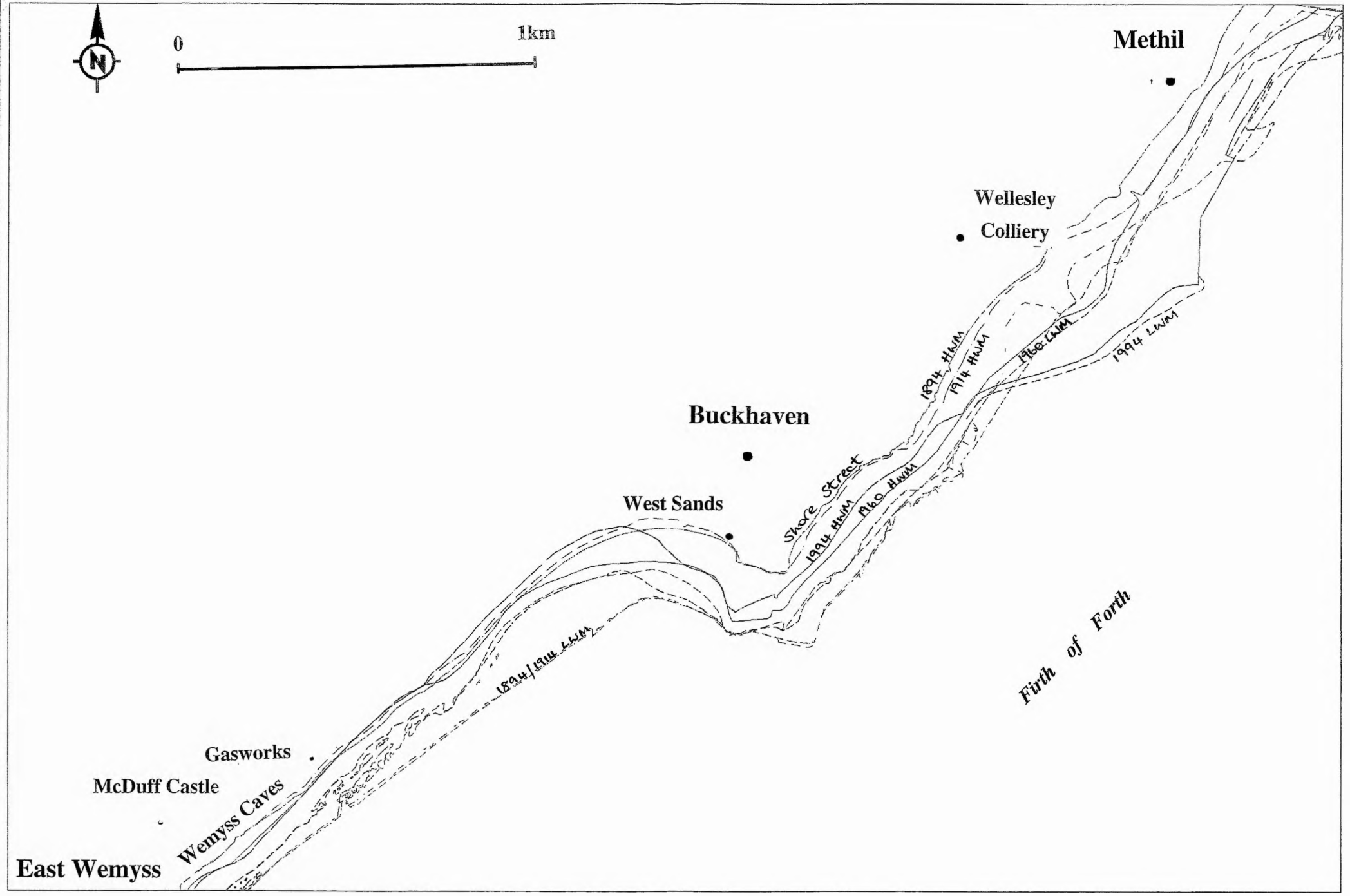

Figure 3.2 Coastal changes betweeen Methil and East Wemyss (1894-1994). The coastline has changed significantly around West Sands and at the Wellesley Colliery.

Fife Council Planning Service Fife House Glenrothes KY7 5LT Tel: 01592 414141	Title: Methil and Buckhaven Coastal Changes 1894–1994 Scale: 1:10000 Date: 16/01/97

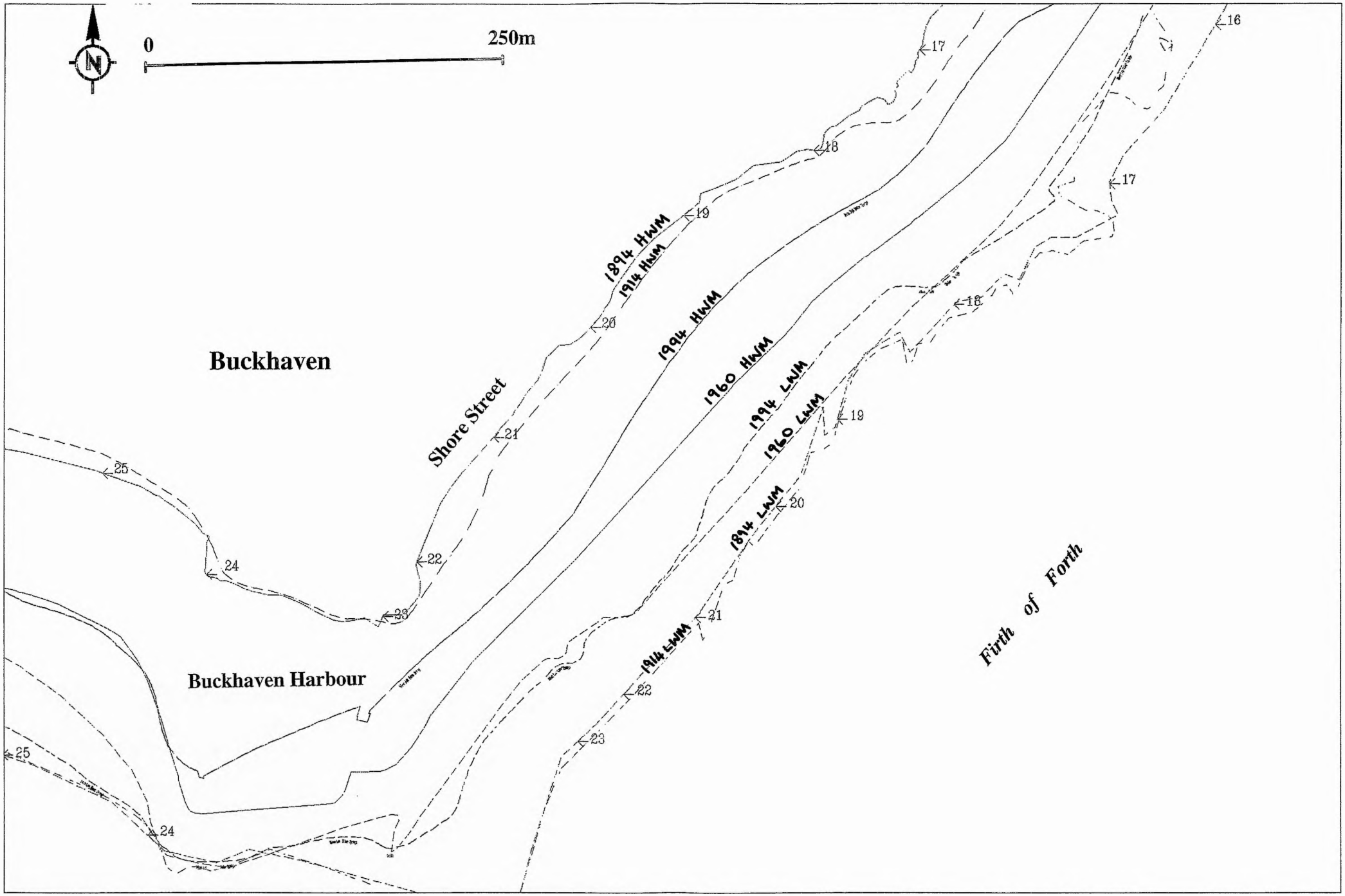

Figure 3.3 Movements in the HWM and LWM at Shore Street, Buckhaven.

Fife Council

Planning Service
Fife House
Glenrothes KY7 5LT
Tel: 01592 414141

Title: Buckhaven, Shore Street
Coastal Changes 1894–1994
Scale: 1:2500 Date: 16/01/97

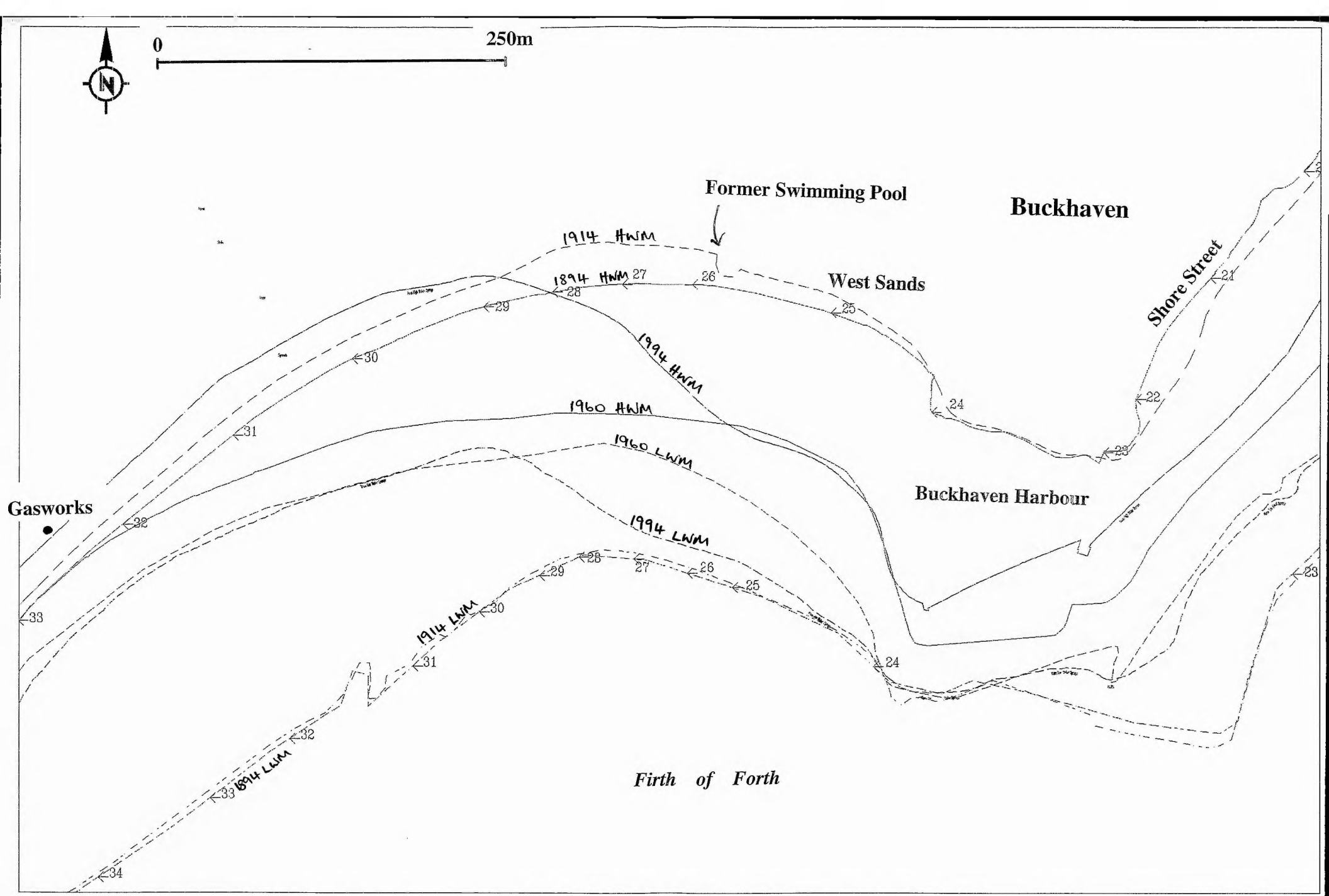

Fife Council	Planning Service Fife House Glenrothes KY7 5LT Tel: 01592 414141	Title: Silversands, Buckhaven Coastal Changes 1894–1994 Scale: 1:2500 Date: 16/01/97

Figure 3.4 Movements in the HWM and LWM at West Sands, Buckhaven.

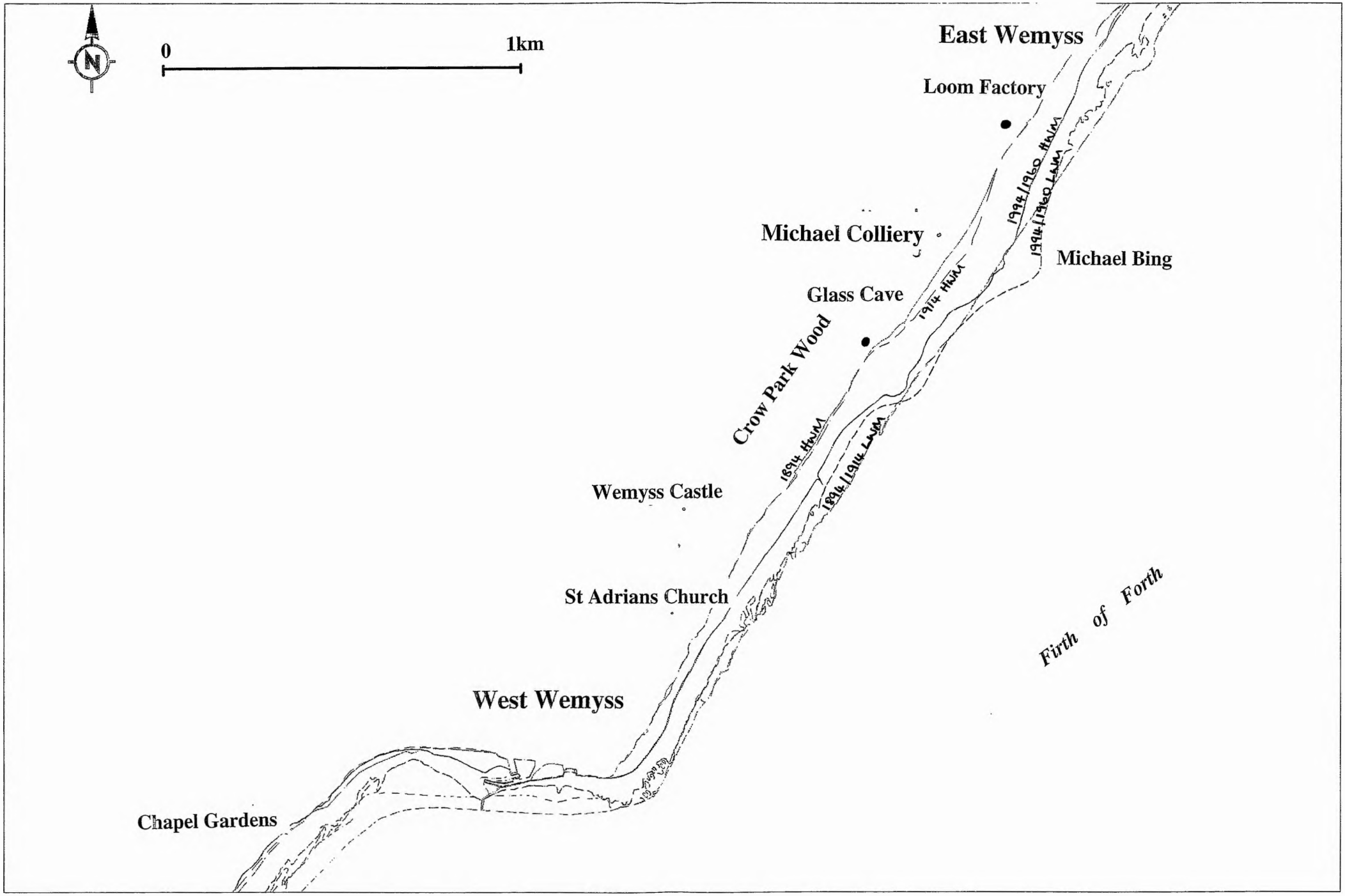

Figure 3.5 Coastal changes between East Wemyss and West Wemyss (1894-1994). Note how the coastline has built forward infront of the Michael Colliery during the mining era.

Fife Council Planning Service Fife House Glenrothes KY7 5LT Tel: 01592 414141	Title: East and West Wemyss Coastal Changes 1894–1994 Scale: 1:10000 Date: 16/01/97

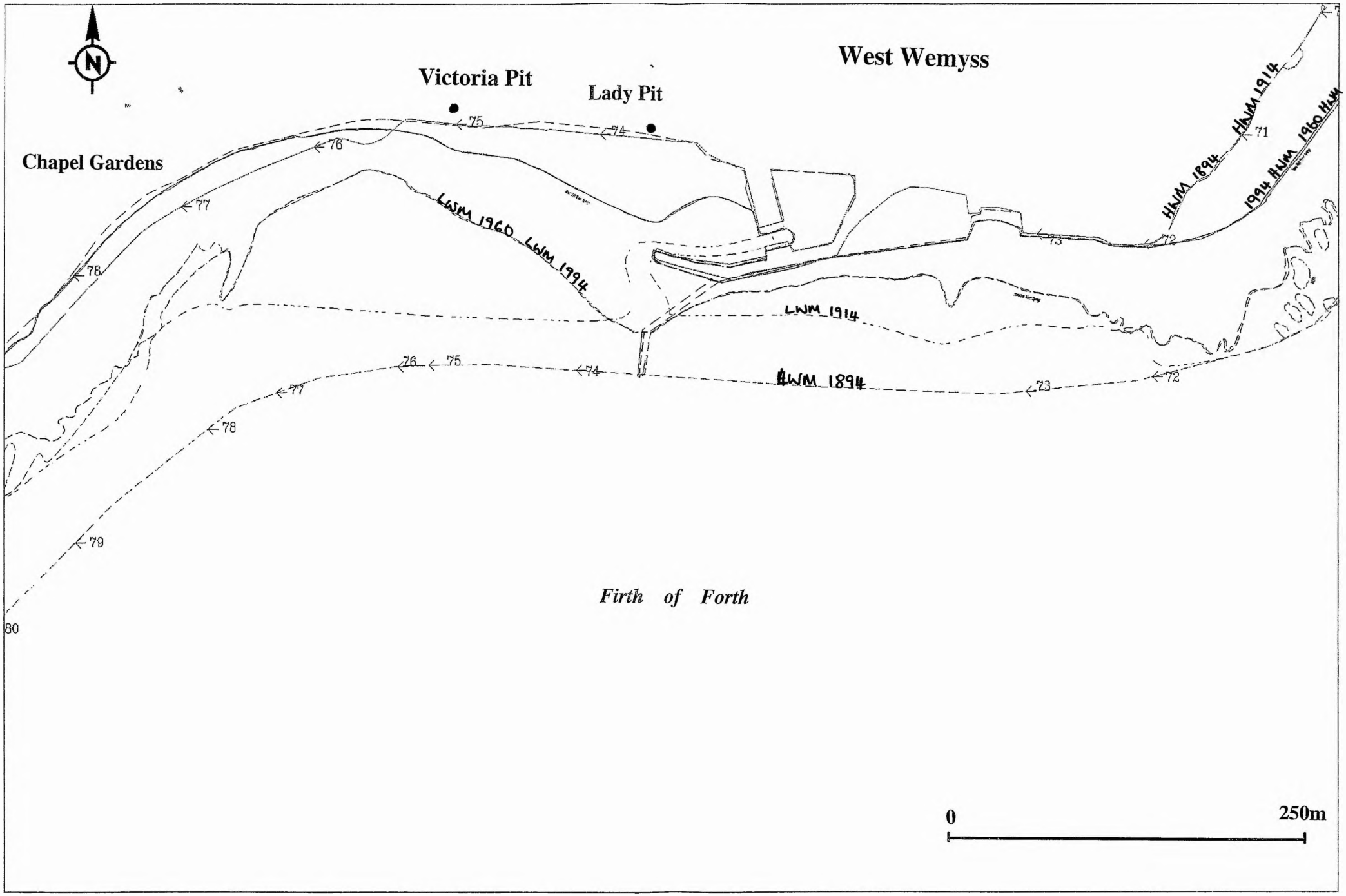

Figure 3.6 Coastal changes at West Wemyss (1894-1994).

Fife Council
Planning Service
Fife House
Glenrothes KY7 5LT
Tel: 01592 414141

Title: West Wemyss
Coastal Changes 1894–1994
Scale: 1:2500 Date: 16/01/97